MOL.20020603.0127

QA: QA

TDR-UDC-NU-000005 REV 00

May 2002

Summary Report of Code to Code Comparisons Performed for the Disposal Criticality Analysis Methodology

Prepared by:

Claude Mays

Prepared for:

U.S. Department of Energy
Yucca Mountain Site Characterization Office
P.O. Box 364629
North Las Vegas, Nevada 89036-8629

Prepared by:

Bechtel SAIC Company, LLC
1180 Town Center Drive
Las Vegas, Nevada 89144

Under Contract Number
DE-AC08-91RW00134

DISCLAIMER

This report was prepared as an account of work sponsored by an agency of the United States Government. Neither the United States Government nor any agency thereof, nor any of their employees, nor any of their contractors, subcontractors or their employees, makes any warranty, express or implied, or assumes any legal liability or responsibility for the accuracy, completeness, or any third party's use or the results of such use of any information, apparatus, product, or process disclosed, or represents that its use would not infringe privately owned rights. Reference herein to any specific commercial product, process, or service by trade name, trademark, manufacturer, or otherwise, does not necessarily constitute or imply its endorsement, recommendation, or favoring by the United States Government or any agency thereof or its contractors or subcontractors. The views and opinions of authors expressed herein do not necessarily state or reflect those of the United States Government or any agency thereof.

Summary Report of Code to Code Comparisons Performed for the Disposal Criticality Analysis Methodology

TDR-UDC-NU-000005 REV 00

May 2002

Prepared by:

Claude Mays — Date: 5/15/02

Checked by:

J. W. Harwell, Technical Checker — Date: 5/15/02

Dan Tunney, Quality Engineering Representative — Date: 5/21/2002

Approved by:

D.A. Brownson, Manager
Engineered Systems-Risk & Criticality — Date: 5/21/2002

INTENTIONALLY LEFT BLANK

CONTENTS

Page

ACRONYMS AND ABBREVIATIONS xiii

1. INTRODUCTION 1-1
   1.1 BACKGROUND 1-1
   1.2 OBJECTIVE 1-1
   1.3 SCOPE 1-1
   1.4 QUALITY ASSURANCE 1-1
   1.5 COMPUTER SOFTWARE 1-2

2. DESIGN INPUTS 2-1
   2.1 BWR ASSEMBLIES 2-1
      2.1.1 BWR Control Blades 2-5
   2.2 PWR ASSEMBLIES 2-6
      2.2.1 Integral Burnable Absorbers 2-7
      2.2.2 Burnable Poison Rods 2-9
      2.2.3 Control Rods 2-10
      2.2.4 PWR Chemical Assay Input 2-10
      2.2.5 Assumptions 2-12

3. DESCRIPTION OF THE CALCULATIONS 3-1
   3.1 BWR LATTICE ENRICHMENT SMEARING 3-1
   3.2 BWR STANDARD GADOLINIA ROD PATTERNS 3-1
   3.3 PWR BURNABLE POISON EFFECTS 3-2
   3.4 PWR FISSION PRODUCT WORTH 3-3
      3.4.1 GRCASMO3 Depletion 3-3
      3.4.2 MCNP Reactivity Calculations 3-5
      3.4.3 Reaction Rate Calculations 3-6
   3.5 CODE-TO-CODE COMPARISONS 3-8
      3.5.1 BWR Control Blade Refinements in SAS2H 3-8
      3.5.2 BWR Assembly Burnup Comparisons 3-14
      3.5.3 PWR Radio-Chemical Assay Comparisons 3-18

4. RESULTS 4-1
   4.1 LATTICE ENRICHMENT SMEARING RESULTS 4-1
   4.2 BWR STANDARD GADOLINIA ROD PATTERN RESULTS 4-21
   4.3 PWR BURNABLE POISON EFFECTS RESULTS 4-29
   4.4 PWR FISSION PRODUCT WORTH RESULTS 4-37
   4.5 CODE-TO-CODE COMPARISON RESULTS 4-40
      4.5.1 SAS2H BWR Control Blade Case Refinements 4-40
      4.5.2 BWR Assembly Burnup Results 4-51
      4.5.3 PWR Radio-Chemical Assay Comparison Results 4-57

5. SUMMARY & CONCLUSIONS 5-1

6. REFERENCES 6-1

6.1 SOURCE DATA, LISTED BY DATA TRACKING NUMBER 6-2

APPENDIX A INTEGRAL & REMOVABLE BURNABLE ABSORBER STUDY A-1

FIGURES

Page

Figure 2-1. Typical BWR Control Blade 2-6
Figure 2-2. Hypothetical 17x17 PWR Lattice with 8 Gd Rods 2-8
Figure 2-3. Hypothetical 17x17 PWR Lattice with 80 Erbia Rods 2-8
Figure 2-4. Hypothetical 17x17 PWR Lattice with 100 IFBA Rods 2-9
Figure 2-5. Hypothetical 16x16 PWR Lattice with12 B_4C-Alumina Rods 2-9
Figure 3-1. Lattice Map of Hypothetical 17x17 Assembly 3-5
Figure 3-2. 21-PWR Assembly Waste Package 3-6
Figure 3-4. Modified SAS2H 1-D model for YYYN4 3-14
Figure 4-1. Relative Difference (To Discrete) for Isotopic Concentrations at EOL, GUC 6x6 Fuel Assembly (2.40 wt% U^{235} avg. enr., no Gd) 4-3
Figure 4-2. Relative difference (to discrete) for isotopic concentrations at EOL, Cooper 7x7 Fuel Assembly (2.50 wt% U^{235} avg. enr., 3.4 wt% Gd) 4-4
Figure 4-3. Relative difference (to discrete) for isotopic concentrations at EOL,GG1-A 8x8 Fuel Assembly (2.99 wt% U^{235} avg. enr., 3.0 wt% Gd) 4-5
Figure 4-4. Relative difference (to discrete) for isotopic concentrations at EOL, GG1-M 9x9 Fuel Assembly (3.31 wt% U^{235} avg. enr., no Gd) 4-6
Figure 4-5. Relative difference (to discrete) for isotopic concentrations at EOL, GG1-M 9x9 Fuel Assembly (3.31 wt% U^{235} avg. enr., 3.5 wt% Gd) 4-7
Figure 4-6. Relative difference (to discrete) for isotopic concentrations at EOL, GG1-M 9x9 Fuel Assembly (3.31 wt% U^{235} avg. enr., 7.0 wt% Gd) 4-8
Figure 4-7. Relative difference (to discrete) for isotopic concentrations at EOL, GG1-M 9x9 Fuel Assembly (3.45 wt% U^{235} avg. enr., no Gd) 4-9
Figure 4-8. Relative difference (to discrete) for isotopic concentrations at EOL, GG1-M 9x9 Fuel Assembly (4.37 wt% U^{235} avg. enr., no Gd) 4-10
Figure 4-9. Relative difference (to discrete) for isotopic concentrations at EOL, GG1-M 9x9 Fuel Assembly (4.37 wt% U^{235} avg. enr., 3.5 wt% Gd) 4-11
Figure 4-10. Relative difference (to discrete) for isotopic concentrations at EOL, GG1-M 9x9 Fuel Assembly (4.37 wt% U^{235} avg. enr., 7.0 wt% Gd) 4-12
Figure 4-11. Relative difference (to discrete) for isotopic concentrations at EOL, GG1-M 9x9 Fuel Assembly (4.56 wt% U^{235} avg. enr., no Gd) 4-13
Figure 4-12. Relative difference (to discrete) for U^{235} at EOL 4-13
Figure 4-13. Relative difference (to discrete) for U^{235} at MOL (20 GWd/mtU) 4-14
Figure 4-14. Relative difference (to discrete) for U^{235} at BOL (0 GWd/mtU) 4-14
Figure 4-15. Δk_{inf} vs. BU for GUC 6x6 Fuel Assembly (2.40 wt% U^{235} avg. enr., no Gd) 4-15
Figure 4-16. Δk_{inf} vs. BU for Cooper 7x7 Fuel Assembly (2.50 wt% U^{235} avg. enr., 3.4 wt% Gd) 4-16
Figure 4-17. Δk_{inf} vs. BU for GG1-A 8x8 Fuel Assembly (2.99 wt% U^{235} avg. enr., 3.0 wt% Gd) 4-16
Figure 4-18. Δk_{inf} vs. BU for GG1-M 9x9 Fuel Assembly (3.31 wt% U^{235} avg. enr.) 4-17
Figure 4-19. Δk_{inf} vs. BU for GG1-M 9x9 Fuel Assembly (3.45 wt% U^{235} avg. enr., no Gd) . 4-18
Figure 4-20. Δk_{inf} vs. BU for GG1-M 9x9 Fuel Assembly (4.37 wt% U^{235} avg. enr.) 4-19
Figure 4-21. Δk_{inf} vs. BU for GG1-M 9x9 Fuel Assembly (4.56 wt% U^{235} avg. enr., no Gd) . 4-19
Figure 4-22. Difference between smeared and discrete k_{inf} values at BOL 4-20
Figure 4-23. Difference between smeared and discrete k_{inf} values at EOL 4-20

Figure 4-24. Standard Gadolinia Fuel Rod Lattice Map for 9x9-5 8Gd Fuel 4-21
Figure 4-25. Standard Gd fuel rod lattice map for 9x9-5 9 Gd fuel 4-22
Figure 4-26. Standard Gd fuel rod lattice map for 9x9-5 10 Gd fuel 4-22
Figure 4-27. Standard Gadolinia Fuel Rod Lattice Map for 8x8-4 7Gd Fuel 4-23
Figure 4-28. Standard Gadolinia Fuel Rod Lattice Map for 8x8-4 8Gd Fuel 4-23
Figure 4-29. Standard Gadolinia Fuel Rod Lattice Map for 8x8-4 9Gd Fuel 4-24
Figure 4-30. Standard Gadolinia Fuel Rod Lattice Map for 8x8-4 10Gd Fuel 4-24
Figure 4-31. Standard Gadolinia Fuel Rod Lattice Map for 8x8-4 11Gd Fuel 4-25
Figure 4-32. Standard Gadolinia Fuel Rod Lattice Map for 8x8-4 12Gd Fuel 4-25
Figure 4-33. GRCASMO3 Δk_{inf} Results for 7 Gadolinia Rod Lattice 4-26
Figure 4-34. GRCASMO3 Δk_{inf} Results for 9 Gadolinia Rod Lattice 4-26
Figure 4-35. GRCASMO3 k_{inf} Results for 12 Gadolinia Rod Lattice 4-27
Figure 4-36. GRCASMO3 Δk_{inf} Results for 7 Gadolinia Rod Lattice 4-27
Figure 4-37. Delta GRCASMO3 k_{inf} Results for 9 Gadolinia Rod Lattice 4-28
Figure 4-38. Delta GRCASMO3 k_{inf} Results for 12 Gadolinia Rod Lattice 4-28
Figure 4-39. GRCASMO3 k_{inf} Results for Gadolinia Integral BA Rods 4-30
Figure 4-40 Δk_{inf} Results for Gadolinia Integral BA Rods at Cold Cask Conditions 4-30
Figure 4-42. Δk_{inf} Results for Erbia Integral BA Rods at Cold Cask Conditions 4-31
Figure 4-43. GRCASMO3 k_{inf} Results for IFBA Integral BA Rods 4-32
Figure 4-44. ΔK_{inf} Results for IFBA Integral BA Rods at Cold Cask Conditions 4-32
Figure 4-45. GRCASMO3 k_{inf} Results for B_4C Integral BA Rods 4-33
Figure 4-46. Δk_{inf} Results for B_4C Integral BA Rods at Cold Cask Conditions 4-33
Figure 4-47. GRCASMO3 k_{inf} Results for Pyrex BPRs 4-34
Figure 4-48. Δk_{inf} Results for Pyrex BPRs at Cold Cask Conditions 4-34
Figure 4-48a. Δk_{inf} Results for Pyrex and WABAs at Cold Cask Conditions 4-35
Figure 4-49. GRCASMO3 k_{inf} Results for WABAs 4-35
Figure 4-50. Δk_{inf} Results for WABAs at Cold Cask Conditions 4-36
Figure 4-51. GRCASMO3 k_{inf} Results for a Lattice Controlled for Portions of its Depletion. 4-36
Figure 4-52. Δk_{inf} Results for a Lattice Controlled During Parts of its Depletion 4-37
Figure 4-53. Comparisons of Isotopic Concentrations for Pu^{239} 4-41
Figure 4-54. Comparisons of Isotopic Concentrations for U^{235} 4-42
Figure 4-55. Comparisons of Isotopic Concentrations for Np^{237} 4-43
Figure 4-56. Comparisons of Isotopic Concentrations for Am^{241} 4-44
Figure 4-57. Comparisons of Isotopic Concentrations for Pu^{241} 4-45
Figure 4-58. Comparisons of Isotopic Concentrations for Sm^{149} 4-46
Figure 4-59. Comparisons of Isotopic Concentrations for Sm^{151} 4-47
Figure 4-60. Comparisons of Isotopic Concentrations for Sm^{152} 4-47
Figure 4-61. Comparisons of Isotopic Concentrations for Nd^{143} 4-48
Figure 4-62. Comparisons of Isotopic Concentrations for Rh^{103} 4-48
Figure 4-63. Comparisons of Isotopic Concentrations for Eu^{153} 4-49
Figure 4-64. Comparisons of Isotopic Concentrations for Gd^{155} 4-49
Figure 4-65. Comparisons of Isotopic Concentrations for Ag^{109} 4-50
Figure 4-66. Comparisons of Flux Disadvantage Factor 4-50
Figure 4-67. Total Code-to-Code Differences in k_{inf} Using SAS2H and GRCASMO3 EOL Isotopics 4-57
Figure 4-68. Isotope Percentage Differences ((calc/meas-1)*100) for Calvert Cliffs Sample. 4-59

Figure 4-69. Isotope Percentage Differences ((calc/meas-1)*100) for Turkey Point Sample.. 4-59

Figures A-1 to A-4. Gd (2.00 wt%), U235 (4.19 wt%), B_4C (2.10 wt%)..... A-5
Figures A-5 to A-8. Gd (2.00 wt%), U235 (4.19 wt%), B_4C (2.10 wt%)..... A-6
Figures A-9 to A-12. Gd (2.00 wt%), U235 (3.60 wt%), B_4C (3.50 wt%)..... A-7
Figures A-13 to A-16. Gd (2.00 wt%), U235 (3.60 wt%), B_4C (3.50 wt%)..... A-8
Figures A-17 to A-20. Gd (2.00 wt%), U235 (3.60 wt%), B_4C (0.0 wt%)..... A-9
Figures A-21 to A-24. Gd (2.00 wt%), U235 (3.60 wt%), B_4C (0.0 wt%)..... A-10
Figures A-25 to A-28. Gd (2.00 wt%), U235 (4.19 wt%), B_4C (2.10 wt%)..... A-11
Figures A-29 to A-32. Gd (2.00 wt%), U235 (4.19 wt%), B_4C (2.10 wt%)..... A-12
Figures A-33 to A-36. Gd (6.08 wt%), U235 (3.40 wt%), B_4C (2.60 wt%)..... A-13
Figures A-37 to A-40. Gd (6.08 wt%), U235 (3.40 wt%), B_4C (2.60 wt%)..... A-14
Figures A-41 to A-44. Gd (3.01 wt%), U235 (3.99 wt%), B_4C (2.10 wt%)..... A-15
Figures A-45 to A-48. Gd (3.01 wt%), U235 (3.99 wt%), B_4C (2.10 wt%)..... A-16
Figures A-49 to A-52. Gd (3.01/8.17 wt%), U235 (3.99/2.87 wt%), B_4C (2.10 wt%) A-17
Figures A-53 to A-56. Gd (3.01/8.17 wt%), U235 (3.99/2.87 wt%), B_4C (2.10 wt%) A-18
Figure A-57. k-infinity Vs Burnup for Various BP Loading (Figures 01-04)..... A-21
Figure A-58. k-infinity Vs Burnup for Various BP Loading (Figures 05-08)..... A-24
Figure A-59. k-infinity Vs Burnup for Various BP Loading (Figures 09-12)..... A-27
Figure A-60. k-infinity Vs Burnup for Various BP Loading (Figures 13-16)..... A-30
Figure A-61. k-infinity Vs Burnup for Various BP Loading (Figures 17-20)..... A-33
Figure A-62. k-infinity Vs Burnup for Various BP Loading (Figures 21-24)..... A-36
Figure A-63. k-infinity Vs Burnup for Various BP Loading (Figures 25-28)..... A-39
Figure A-64. k-infinity Vs Burnup for Various BP Loading (Figures 29-32)..... A-42
Figure A-65. k-infinity Vs Burnup for Various BP Loading (Figures 33-36)..... A-45
Figure A-66. k-infinity Vs Burnup for Various BP Loading (Figures 37-40)..... A-48
Figure A-67. k-infinity Vs Burnup for Various BP Loading (Figures 41-44)..... A-51
Figure A-68. k-infinity Vs Burnup for Various BP Loading (Figures 45-48)..... A-54
Figure A-69. k-infinity Vs Burnup for Various BP Loading (Figures 49-52)..... A-57
Figure A-70. k-infinity Vs Burnup for Various BP Loading (Figures 53-56)..... A-60

INTENTIONALLY LEFT BLANK

TABLES

Page

2-1. Assembly Axial Region YYYN4: Typical Specifications for SAS2H Case (assumed values) 2-2
2-2. SAS2H Fuel Rod Cladding Material Specifications 2-2
2-3. Assembly Node YYYN4 Depletion History 2-3
2-4. Fuel Density for QC2 Assemblies for SAS2H Cases 2-4
2-5. Fuel Density for GG1 Assemblies for the SAS2H Cases 2-5
2-6. GRCASMO3 Case Control Blade Design Specifications 2-5
2-7. Fuel Design Specifications for Calvert Cliffs and Turkey Point Fuel 2-11
2-8. Operating History Inputs for Calvert Cliffs and Turkey Point Fuel 2-11

3-1. General Rules for Developing Standard Gadolinia Rod Position Maps for Boiling Water Reactor Fuels 3-2
3-2. GRCASMO3 Input (all dimensions in cm) 3-4
3-3. Isotopes Used For Comparison 3-8
3-4. Inputs for SAS2H Control Blade Homogenization Original Model 3-9
3-5. Inputs for SAS2H Control Blade Homogenization Modified Model 3-10
3-6. SAS2H 1-D (Path B) Zone Dimensions for Node YYYN4 3-12
3-7. Modified SAS2H 1-D Zone Dimensions for Node YYYN4 3-12
3-8. SAS2H Nodal Breakdown 3-15
3-9. Necessary Dimensions for SAS2H Cases – All Lattices 3-16

4-1. List of Isotopes Considered in Analysis 4-1
4-2. Δk_{inf} at BOL, MOL, and EOL for All Lattices 4-2
4-3. GRCASMO3 Results 4-38
4-4. Relative Fission Product Worths Based on GRCASMO3 Calculations 4-38
4-5. MCNP Results for 3.7wt% U^{235} Enriched, 5-year Cooled Cases 4-39
4-6. Comparison of MCNP and GRCASMO3 Results (%ΔP) 4-39
4-7. List of Isotopes Considered in Analysis 4-51
4-8. k_{inf} Results of Operating History Resolution Comparisons Using GRCASMO3 EOL Isotopic Concentrations 4-53
4-9. k_{inf} Results of Axial Format Comparisons Using GRCASMO3 EOL Isotopic Concentrations 4-54
4-10. k_{inf} Results of 1-D/2-D Comparisons Using GRCASMO3 and SAS2H EOL Isotopic Concentrations 4-55
4-11. k_{inf} Results of Total Code-to-Code Comparisons Using GRCASMO3 and SAS2H EOL Isotopic Concentrations 4-56
4-12. Bladed Nodes per Control Blade Insertion 4-57
4-13. Percentage Difference Between Measured and Calculated Isotopic Inventories 4-58
4-14. MCNP Calculated k_{inf} for Measured and Predicted Isotopic Inventories 4-59

A-1. Assumptions Used in the Analysis A-3
A-2. k-infinity Vs Burnup for Various BP Loading (Figures 01-04) A-19
A-3. k-infinity Vs Burnup for Various BP Loading (Figures 05-08) A-22

TABLES (Continued)

Page

A-4. k-infinity Vs Burnup for Various BP Loading (Figures 09-12) A-25
A-5. k-infinity Vs Burnup for Various BP Loading (Figures 13-16) A-28
A-6. k-infinity Vs Burnup for Various BP Loading (Figures 17-20) A-31
A-7. k-infinity Vs Burnup for Various BP Loading (Figures 21-24) A-34
A-8. k-infinity Vs Burnup for Various BP Loading (Figures 25-28) A-37
A-9. k-infinity Vs Burnup for Various BP Loading (Figures 29-32) A-40
A-10. k-infinity Vs Burnup for Various BP Loading (Figures 33-36) A-43
A-11. k-infinity Vs Burnup for Various BP Loading (Figures 37-40) A-46
A-12. k-infinity Vs Burnup for Various BP Loading (Figures 41-44) A-49
A-13. k-infinity Vs Burnup for Various BP Loading (Figures 45-48) A-52
A-14. k-infinity Vs Burnup for Various BP Loading (Figures 49-52) A-55
A-15. k-infinity Vs Burnup for Various BP Loading (Figures 53-56) A-58
A-16. Sample of Results (Number Density vs Burnup) A-61

ACRONYMS AND ABBREVIATIONS

BA	Burnable Absorber
BPR	Burnable Poison Rod
BPRA	Burnable Poison Rod Assembly
BOL	beginning of life
BSC	Bechtel SAIC Company
BWR	boiling water reactor
CC1	Calvert Cliffs Unit 1 Reactor
CE	Combustion Engineering
CRWMS	Civilian Radioactive Waste Management System
Cy	cycle
DFAC	Disadvantage Factor
DOE	U.S. Department of Energy
EFPD	Effective Full Power Days
EOL	end of life
FANP	Framatome Advanced Nuclear Power, Inc.
FCF	Framatome Cogema Fuels
GG1	Grand Gulf Unit 1 reactor
GUC	Gundremmingen Reactor
GWd/mtU	Gigawatt days per metric ton of Uranium
IBA	Integral Burnable Absorber
ID	inside diameter
IFBA	Integral Fuel Burnable Absorber
M&O	Management and Operating Contractor
MOL	middle of life
MWt	Megawatt (thermal)
NRC	U.S. Nuclear Regulatory Commission
OCRWM	Office of Civilian Radioactive Waste Management
OD	outside diameter
ppm	parts per million
RCA	Radiochemical Assay
RRX	Reaction Rate Method
QC2	Quad Cities Unit 2 reactor
SNF	spent nuclear fuel

ACRONYMS AND ABBREVIATIONS (Continued)

TP2	Turkey Point Unit 2 reactor
WABA	Wet Annular Burnable Absorber
wt%	weight percent
YMP	Yucca Mountain Site Characterization Project

1. INTRODUCTION

This report, *Summary Report of Code to Code Comparisons Performed for the Disposal Criticality Analysis Methodology*, contains a summary of the 1-Dimension and 2-Dimension lattice physics code to code comparisons used to support the validation of the disposal criticality analysis methodology.

1.1 BACKGROUND

The U.S. Department of Energy (DOE) Office of Civilian Radioactive Waste Management (OCRWM) is developing a methodology for criticality analysis to support disposal of commercial spent nuclear fuel in a geologic repository. A topical report on the Disposal Criticality Analysis Methodology was submitted to the U.S. Nuclear Regulatory Commission (NRC) for formal review in March 2001 (YMP 2000). This technical report is one of a series of reports that provides a summary of the results of the analyses that support the development of the disposal criticality analysis methodology.

1.2 OBJECTIVE

The objective of this report is to present a summary of the various code to code comparison results. Results from the code to code evaluations will support the development and validation of the criticality models used in the disposal criticality analysis methodology. These models and their validation have been discussed in the *Disposal Criticality Analysis Methodology Topical Report* (YMP 2000).

1.3 SCOPE

The scope of this *Summary Report* includes the code to code analytical results for the following types of calculations:

- Boiling Water Reactor (BWR) Standard Gadolinia Rod Patterns
- BWR Lattice Enrichment Smearing
- Pressurized Water Reactor (PWR) Fission Product Worth
- Burnable Poison Effects on Spent PWR Fuel
- BWR Control Blade Model
- PWR Radio-chemical Assay Code to Code Comparisons
- BWR Assembly Burnup Calculations

Additional types of code to code evaluations may be added in future revisions to this report.

1.4 QUALITY ASSURANCE

The development of this report has been subject to the U.S. Department of Energy OCRWM *Quality Assurance Requirements and Description* (QARD) (DOE 2000) controls. The information, provided in this report, will be used to develop the methodology for evaluation of the potential Monitored Geologic Repository engineered barrier system. A classification analysis (CRWMS M&O 1999a) has identified components of the engineered barrier system as items important to radiological safety and waste isolation.

No scientific and engineering software or computational software was used in the development of this report. Electronic management of data was accomplished in accordance with the controls specified in the *Technical Work Plan* (BSC 2001).

The work to be performed using this information to support the License Application will be performed in accordance with the then current versions of the QARD and NRC regulations. All information used for the License Application will be from acceptable sources and will be developed in accordance with the QARD requirements and NRC regulations.

1.5 COMPUTER SOFTWARE

This technical report provides a summary of calculations documented under the Framatome Advanced Nuclear Power, Inc. (FANP) documents system. The information regarding the use of software for the calculated results summarized in this technical report is documented in MO0109SPADRN04.003. No software is used directly in the generation of this technical report, but the software used in the supporting calculations is listed as follows:

The software specifications are as follows:

The MCNP code was used to calculate the eigenvalue for reactivity worth comparisons.
Program Name: MCNP
Version/Revision Number: Version 4B2LV (CRWMS M&O 1998)

The SAS2H code was used to model and deplete PWR and BWR fuel assemblies to predict their discharge isotopic inventories.
Program Name: SCALE4.4A, SAS2H Sequence (CRWMS M&O 2000)
Version/Revision Number: Version 4.4A
Program Name: SCALE4.3, SAS2H Sequence (CRWMS M&O 1997c)
Version/Revision Number: Version 4.3

The computer program CASMO-3 Version 4.8.3 was used in the supporting calculations MO0109SPADRN04.003, MO0204SPABCF04.012, and MO0204SPAIRB04.013 to determine the isotopic concentrations in the fuel assembly at specified burnup points. This version is referred to as GRCASMO3 and is licensed to FANP. All references to the calculated results presented herein are labeled either GRCASMO3 or CASMO. GRCASMO3 has received full certification in accordance with FANP procedures.

CASMO-3 Version 4.8.3 is an industry standard 2-D lattice physics depletion code. The purpose of utilizing CASMO is to compare and contrast the isotopic results from the 1-D SAS2H code to validate the use of SAS2H for generating depleted fuel assembly isotopic inventories.

2. DESIGN INPUTS

2.1 BWR ASSEMBLIES

Four different types of fuel assemblies are analyzed in Section 3.1 as documented in MO0109SPADRN04.003, Section 4.1. These were based on 6x6, 7x7, 8x8, and 9x9 lattices. The average U^{235} enrichment for the lattices ranged from 2.40 to 4.56 wt%.

For the 6x6 lattice the average enrichment was 2.40 wt% with no axial variation. Gadolinium was not present in any of the fuel rods. In addition, the lattice contained no water rods. The 6x6 lattice is based on the Gundremmingen Nuclear Power Plant (Barbero et al. 1979; Guardini and Guzzi 1983; Naito, Kurosawa, and Kaneko 1994).

For the 7x7 Cooper lattice the average U^{235} enrichment was 2.50 wt%. Again, there was no axial variation of the enrichment. An average of 3.4 wt% gadolinium in five rods was modeled. No water rods were present in the 7x7 lattice. The detailed lattice information is proprietary. The inputs used are documented in MO0109SPADRN04.003, Section 4.1.

For the 8x8 GG1 lattice, an average enrichment of 2.99 wt% with no axial variation was used. Five fuel rods contained gadolinium at an average of 3.0 wt%. In addition, two water rods were located in the center of the lattice. The detailed lattice information is proprietary. The inputs used are documented in MO0109SPADRN04.003, Section 4.1.

For the 9x9 GG1 lattice, the lattice contained five water rods. In addition, the average enrichment and the gadolinium content varied axially. Two axial locations were chosen for this analysis. Both had an average enrichment of 3.31 wt%. One had nine Gd rods at an average 3.5 wt% Gd, while the other had nine Gd rods at an average 7 wt% Gd. A third configuration was chosen such that it corresponded with the average of 3.5 wt% Gd configuration but did not contain any Gd. Finally, a third axial location was chosen for the 9x9 lattice. The average U^{235} enrichment at this location was 3.45 wt%. The detailed lattice information is proprietary. The inputs used are documented in MO0109SPADRN04.003, Section 4.1.

In Section 3.5.1, typical axial node information (45.72 cm) of a Grand Gulf Unit 1 BWR 9x9 assembly (MO0106SPASTA00.005) was used. This assembly region contains 8 gadolinia-bearing fuel rods, 5 water rods, and is selected from the middle of the assembly. Table 2-1 provides node design information for the lattice representation. Node YYYN4 contains two different size fuel pellets and clad dimensions. SAS2H inputs require modeling of assembly structures with only single dimension capability. Thus, smeared fuel pellet dimensions and weighted averages were calculated to represent the fuel rods in SAS2H. Table 2-2 provides the fuel rod clad material specifications for use in SAS2H. Table 2-3 provides typical operating history information as a function of effective full power days (EFPD) and control blade insertion times for the axial region of concern.

The depletion history for the YYYN4 axial region consists of 25 burnup intervals up to a total burnup of 43.872 GWd/mtU. Each burnup interval has changes in fuel temperature and in-channel moderator density (or void fraction).

Table 2-1. Assembly Axial Region YYYN4: Typical Specifications for SAS2H Case (assumed values)

Smeared fuel pellet OD[a] (cm)	0.9472
Clad OD (cm)	1.0848
Node axial height (cm)	45.72
Lattice	9 x 9
Water rods	5
Fuel density (g/cm^3)	10.16
Rod pitch (cm)	1.43
Control blade portion length (cm)	24.3687
Control blade portion half blade thickness (cm)	0.39624
Channel outer width (cm)	13.5509[b]
Channel inner width (cm)	13.2461
Smeared fuel density (g/cm^3)	9.739
# Fuel rods	76
# Gadolinia-bearing fuel rods	8

Source: MO0109SPADRN04.003, Section 4.3

NOTES: These are assumed typical values (not actual) for a 9x9, 8 gadolinia-bearing fuel rod BWR assembly to be used in development of the SAS2H path B model in Section 3.5.1 for this work only.
[a]OD = Outer Diameter
[b]13.5509 = The value is slightly different than that used in the GRCASMO3 model (13.8557). The effect of this will be insignificant for the purposes of the scoping analysis.

Table 2-2. SAS2H Fuel Rod Cladding Material Specifications

Material	wt%
Oxygen	0.12
Chromium	0.10
Iron	0.20
Tin	1.4
Zirconium	98.18

Source: CRWMS M&O 1999b, Section 5.11

Table 2-3. Assembly Node YYYN4 Depletion History

Statepoint	EFPD Steps	Cumulative Burnup (GWd/mtU)	Fuel Temperature (K)	Moderator Density (g/cm^3)	Control Blade Insertion
11	16.5	0.712	998.0	0.3916	—
12a	65.9	3.827	1057.8	0.4351	—
12	65.9	6.941	1057.8	0.4351	—
13	17	7.804	1113.4	0.4430	—
14	38.3	9.618	1058.1	0.4397	—
15a	68.4	12.638	1013.7	0.4142	—
15	68.4	15.658	1013.7	0.4142	—
16a	47.36	17.297	893.8	0.4319	INSERT
16	47.36	18.936	893.8	0.4319	—
17a	57.05	21.395	999.7	0.4292	—
17b	57.05	23.854	999.7	0.4292	INSERT
17c	57.05	26.312	999.7	0.4292	—
17	57.05	28.771	999.7	0.4292	—
18a	54.26	30.774	921.1	0.4374	—
18b	54.26	32.776	921.1	0.4374	INSERT
18c	54.26	34.779	921.1	0.4374	—
18	54.26	36.781	921.1	0.4374	—
19a	54.4	37.798	725.0	0.4424	—
19	54.4	38.815	725.0	0.4424	—
20a	68.15	40.003	713.2	0.4505	—
20	68.15	41.191	713.2	0.4505	—
21a	53.82	41.861	667.8	0.4640	—
21b	53.82	42.532	667.8	0.4640	—
21c	53.82	43.202	667.8	0.4640	—
21	53.82	43.872	667.8	0.4640	—

Source: MO0106SPASTA00.005, SAS2H Node 4, Fuel Type F, Assembly F05

Four fuel assemblies from two boiling water reactors were chosen for the analysis discussed in Section 3.5.2. Two were from Commonwealth Edison's Quad Cities Unit 2 and were 8x8 assemblies (CRWMS M&O 1999c). One had 9 gadolinia (Gd) rods and 4 water rods (Type C) while the other had 11 Gd rods and 1 large central water rod (Type F). The other two assemblies were from Entergy's Grand Gulf Unit 1 and were 9x9 assemblies with 10 Gd rods and 5 water rods (Type G) (MO0106SPASTA00.005).

Operating histories for each assembly were chosen such that one assembly from each reactor had no control blade insertions and the other assembly had significant control blade insertions. For

QC2 assemblies, the controlled history was taken from assembly C14 and the uncontrolled history was for assembly F09 (FCF 1999). For the GG1 assemblies, the chosen histories were from assembly F05 for the controlled history and F38 for the uncontrolled history (MO0106SPASTA00.005). All assemblies had average discharge burnups greater than 40 GWd/mtU. The input necessary for building the GRCASMO3 input cases for each lattice is found in MO0109SPADRN04.003, Table 4-16 and Figures 4-12 through 4-16.

The fuel densities for QC2 were calculated using the mass and volume of the fuel. For these assemblies, the mass and nodal lengths for the 10-node-axial format are given in Table 2-4.

Table 2-4. Fuel Density for QC2 Assemblies for SAS2H Cases

	QC2 Type C (Fuel Pellet Density = 10.045 g/cc)			QC2 Type F (Fuel Pellet Density = 10.088 g/cc)		
SAS2H Node	Mass (g U)	Node Length (cm)	# Fuel Rods	Mass (g U)	Node Length (cm)	# Fuel Rods
10	6122.1	15.24	51	5907.3	15.24	49
				7233.4	15.24	60
9	28810	60.96	60	21700	45.72	60
8	21607	45.72	60	21700	45.72	60
7	21607	45.72	60	21700	45.72	60
6	21607	45.72	60	21700	45.72	60
5	14405	30.48	60	14467	30.48	60
4	21607	45.72	60	21700	45.72	60
3	14405	30.48	60	14467	30.48	60
2	14405	30.48	60	14467	30.48	60
1	7202.5	15.24	60	7233.4	15.24	60

Source: FCF 1999, Tables 9-2 and 9-3

Table 2-5 lists the information needed to determine the fuel densities for the SAS2H case. Fuel pellet and inner clad radii used were for the average of all 76 fuel rods.

Table 2-5. Fuel Density for GG1 Assemblies for the SAS2H Cases

SAS2H Node	Mass (g U)	Axial Length (cm)	# Fuel Rods	Fuel Pellet Density (g/cm^3)
10	14013.6	30.48	76	9.74
9	7006.8	15.24	76	9.74
8	14013.6	30.48	76	9.74
7	28027.2	60.96	76	9.74
6	28027.2	60.96	76	9.74
5	21020.4	45.72	76	9.74
4	21020.4	45.72	76	9.74
3	14013.6	30.48	76	9.74
2	21020.4	45.72	76	9.74
1	7006.8	15.21	76	9.74

Source: MO0106SPASTA00.005, Table 12-3

2.1.1 BWR Control Blades

This information is used in Section 3.5.1. The BWR cruciform control blade is illustrated in Figure 2-1. Design specifications for this control blade are provided in Table 2-6.

Table 2-6. GRCASMO3 Case Control Blade Design Specifications

Parameter	Value[a]
Neutron Absorber Material	B_4C (natural boron)
Percent of B_4C Theoretical Density	70
Total Blade Span (in) tip to tip	9.804
Total Blade Support Span (in)	1.550
Active Absorber Length (in)	143.7 (min) 144.0 (typical)
Sheath Material	304 Stainless Steel
Sheath Thickness (in)	0.045
Blade Thickness (in)	0.328
Number of B_4C Rods per Blade	72
B_4C Cladding Material	304 Stainless Steel
B_4C Rod OD[b] (in)	0.220
B_4C Rod ID[c] (in)	0.166
B_4C Rod Wall Thickness (in)	0.027

Source: MO0106SPASTA00.005

NOTES: [a]This input is used for definition of GRCASMO3 control blade model only
[b]OD = Outer Diameter
[c]ID = Inner Diameter

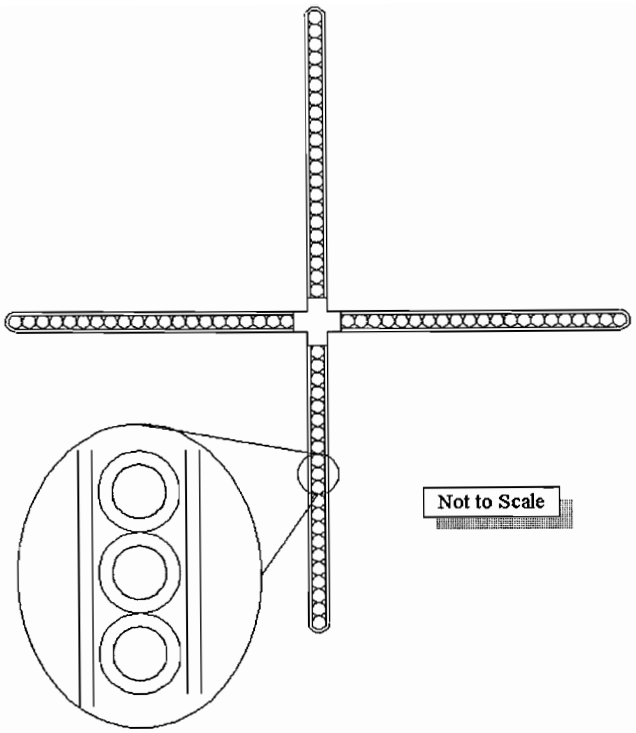

Source: CRWMS M&O 1999c

Figure 2-1. Typical BWR Control Blade

2.2 PWR ASSEMBLIES

Fuel assemblies for B&W designed reactors (MkB fuel) analyzed comprise a 15x15 array of fuel rods with 16 guide tubes and a central instrument tube (DOE 1992 , Section 2.8 and p. 2A-7). The guide tubes accommodate either control-rod fingers or burnable poison rods (BPRs) depending on the location of the assembly in the core and the specific fuel design.

Westinghouse-type fuel assemblies can include 14x14, 15x15, or 17x17 arrays of fuel rods, depending on the plant design (DOE 1992, Section 2.8 and p. 2A-26 through 2A-30). The 14x14 arrays contain 16 guide tubes and a central instrument tube. The 15x15 arrays contain 20 guide tubes and a central instrument tube. The 17x17 array contains 24 guide tubes and a central instrument tube. Like the MkB fuel, the guide tubes can accommodate either control-rod fingers or BPRs depending on the assembly location in the core and the specific fuel design.

Combustion Engineering (CE)-type fuel assemblies can include a 14x14 or a 16x16 array of fuel rods depending on plant design (DOE 1992, Section 2.8 and p. 2A-12 through 2A-14). Each of these fuel designs contains five large guide tubes; one centrally located with the other four symmetrically located in each quadrant of the lattice. Each guide-tube location occupies the space of four fuel rods, and is water filled when the control cluster is removed. (To date, BPRs have not been used in CE fuel.)

2.2.1 Integral Burnable Absorbers

PWR fuel uses several different types of integral burnable absorbers (IBAs) (DOE 1992, section 2.6.5). For example, in some IBAs, neutron absorbers such as gadolinia (Gd_2O_3) as shown in Figure 2-2, or erbia (Er_2O_3) as shown in Figure 2-3, are mixed directly with the uranium dioxide (UO_2) fuel in select rod locations within an assembly. The Westinghouse-designed Integral Fuel Boron Absorber (IFBA) rods contain uranium pellets with a thin coating of zirconium diboride (ZrB_2) as shown in Figure 2-4. Other integral absorbers, such as boron carbide (B_4C), are mixed in alumina-based (Al_2O_3) pellets and placed in rods that replace uranium fuel rods in some CE-designed fuel assemblies as shown in Figure 2-5.

Westinghouse and CE-type fuel assemblies have all used gadolinia in IBAs for some specific fuel designs. Presently, only Westinghouse-fabricated fuel assemblies use integral fuel burnable absorber (IFBA) fuel rods. The assemblies shown in Figures 2-2 through 2-5 provide hypothetical poison rod distributions.

Until recently, integral burnable absorber (IBA) rods were generally loaded symmetrically in a fuel assembly with similarly loaded assemblies symmetrically located within the core. More recently, aggressive core designs have been incorporating asymmetric IBA loadings to "fine-tune" fuel assembly local power peaking concerns. Fuel designs using gadolinia may incorporate as many as 20 Gd_2O_3 - UO_2 fuel rods in a single fuel assembly. CE fuel designs using erbia may incorporate approximately 90 Er_2O_3 - UO_2 fuel rods in a single fuel assembly. As many as one-half of the rods in some Westinghouse fuel assemblies may contain IFBA rods. Finally, some CE-designed fuel assemblies contain B_4C – Al_2O_3 rods that may replace approximately 20 uranium fuel rods. The fuel vendors usually consider the exact details of poison concentration, the number of poison rods, and rod locations to be proprietary information. For this reason, the concentrations have been omitted and only general numbers of poison rods have been described to give a relative idea of the possible variations in designs.

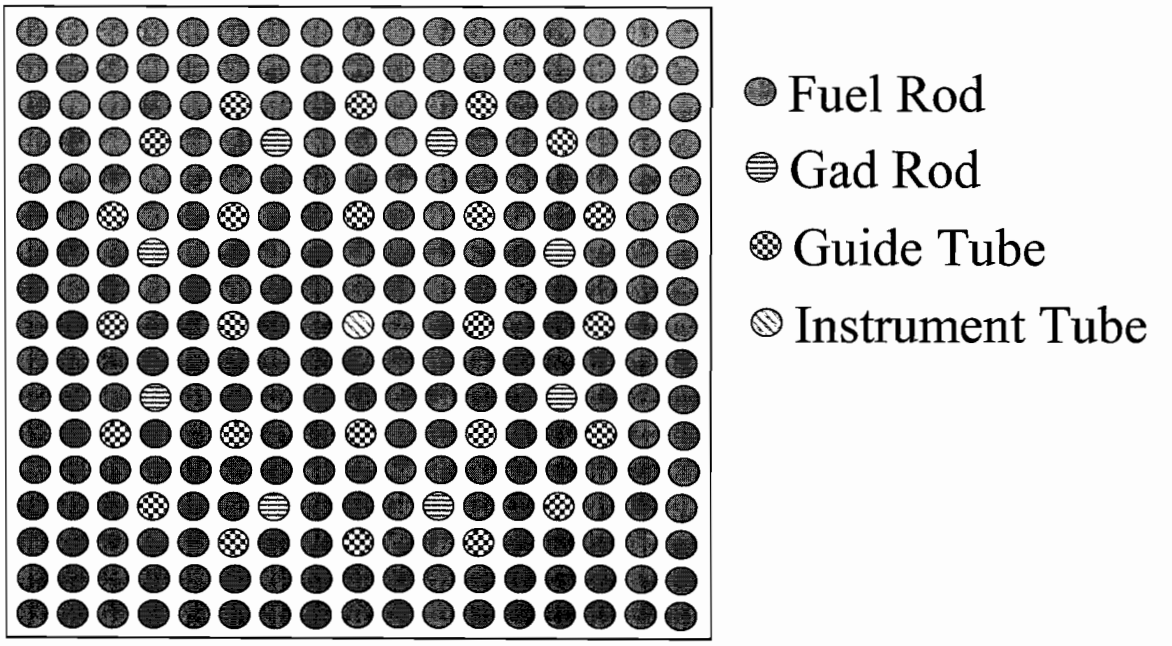

Figure 2-2. Hypothetical 17x17 PWR Lattice with 8 Gd Rods

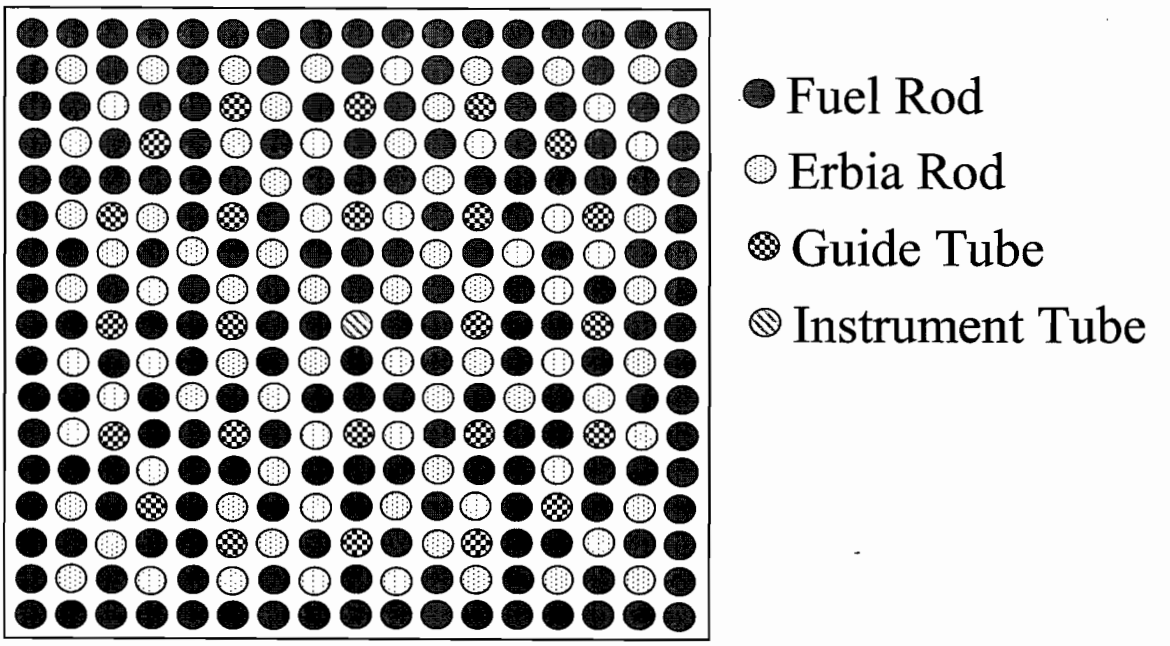

Figure 2-3. Hypothetical 17x17 PWR Lattice with 80 Erbia Rods

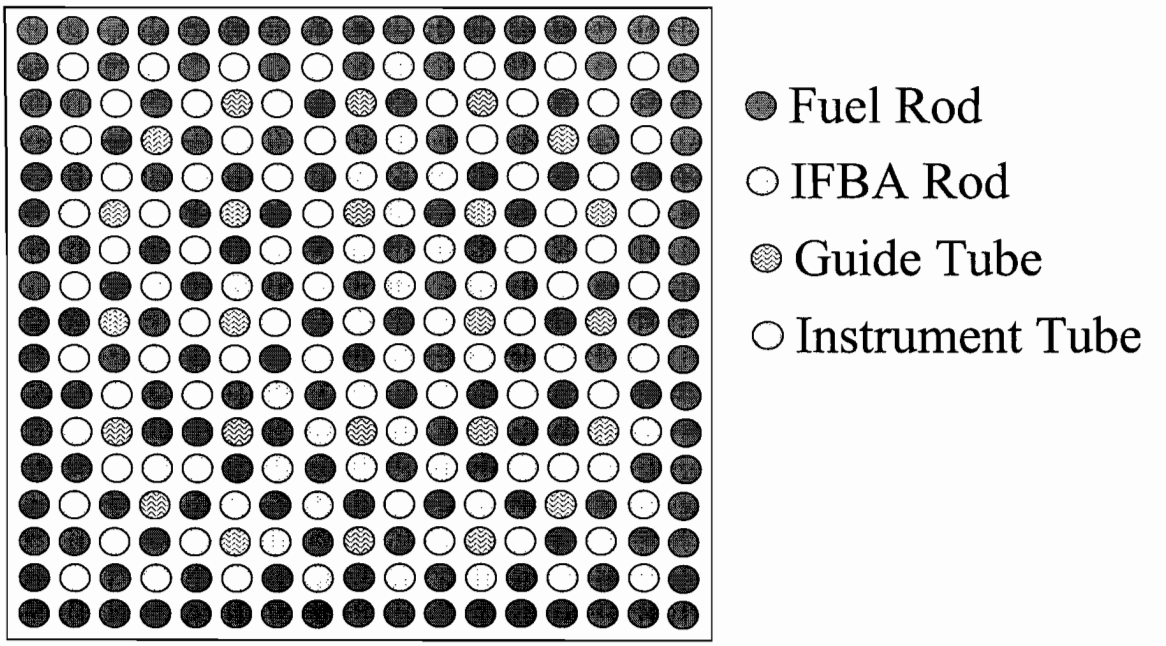

Figure 2-4. Hypothetical 17x17 PWR Lattice with 100 IFBA Rods

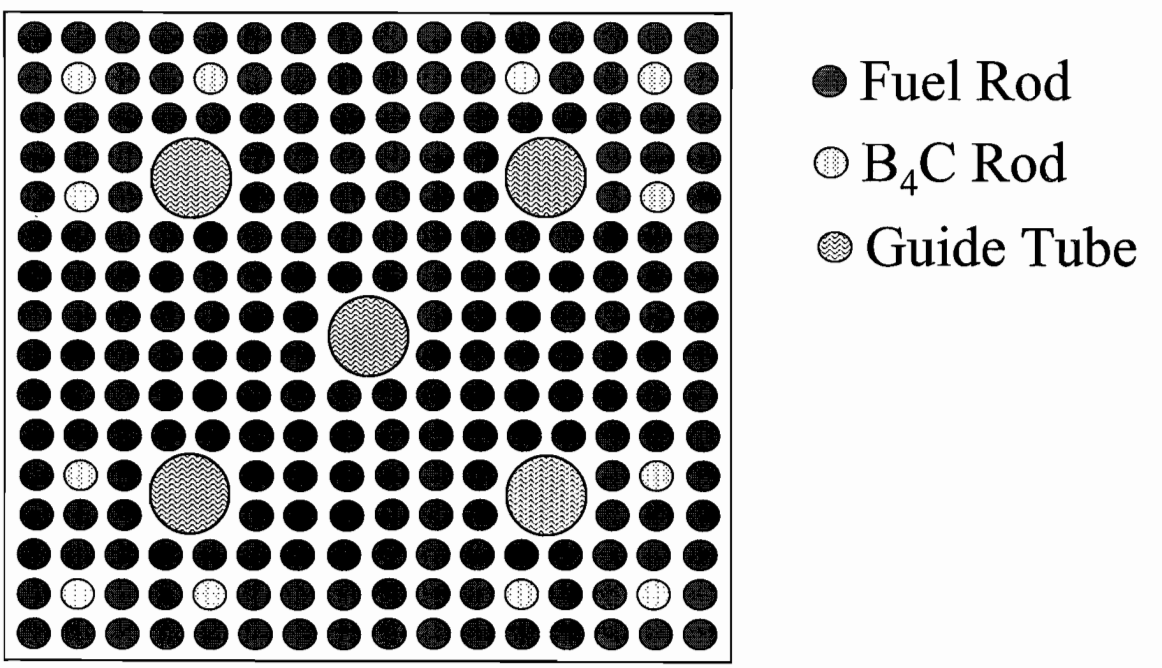

Figure 2-5. Hypothetical 16x16 PWR Lattice with12 B_4C-Alumina Rods

2.2.2 Burnable Poison Rods

Several general types of BPRs have been used in PWR fuel (DOE 1992, Sections 2.6.5 and 2.8). Framatome Cogema Fuels (FCF) uses BPRs, composed of B_4C – Al_2O_3 pellets contained in zircaloy tubing. The Westinghouse configuration for BPRs uses hollow Pyrex glass (B_2O_3 -

SiO_2) tubing sealed in stainless steel cladding. More recently, Westinghouse has used wet annular burnable absorbers (WABAs) that are similar to the Pyrex absorbers but use hollow B_4C – Al_2O_3 pellets clad in zircaloy with a central, flow-through, water region for enhanced neutron moderation.

In all cases, the BPR rodlets are attached to an assembly (burnable poison rod assembly [BPRA]) "spider" that can be mechanically attached to the fuel assembly upper tie plate, securing it in position during core operation. During a refueling outage, the spider can be removed from a fuel assembly using remote-handling tools before the assembly is returned to the core for another cycle of irradiation. FCF BPR clusters comprise between 4 and 24 rodlets. FCF also produces a 17x17 assembly with 24 rodlets. Westinghouse BPR clusters comprise between 4 and 20 rodlets for 14x14 and 15x15 arrays, or 24 rodlets for 17x17 arrays. It is uncommon for a BPRA to remain in a fuel assembly for more than one cycle of irradiation.

2.2.3 Control Rods

Several types of control rods have been used in PWR fuel (DOE 1992, Sections 2.6.5 and 2.8). However, the most common type is Ag-In-Cd clad in stainless steel tubes. The rods are clustered in a "spider" usually as groups of 4, 16, 20 or 24, depending on the fuel design to be used with. It is not common for a reactor while operating at power to have any control rods inserted to any significant amount. However, there may be a small number of rod clusters with a few inches of insertion (bite) in the top of the core, for axial offset control. These rods do not significantly affect the depletion of the fuel

2.2.4 PWR Chemical Assay Input

Assay sample CC1 was taken at 13.2 cm from the bottom of rod MKP109 in assembly D047 (14x14) located in Calvert Cliffs Unit 1 reactor core (Combustion Engineering). Specific assembly design and irradiation history information for Cycles 2 - 5 of Calvert Cliffs Unit 1, were obtained from the previous radiochemical assay (RCA) benchmark evaluations (CRWMS M&O 1997a). This information included, when available, fuel rod design, BPR design, control rod insertion history, boron letdown, average fuel temperatures, and axial burnup profiles. This information was used to develop a standard assembly depletion model in GRCASMO3. The assembly average discharge burnup for assembly D047 was 27.35 GWd/mtU with a cooling time of 1870 days.

Assay sample TP2 was taken at 167.0 cm from the bottom of rod G10 in assembly D01 (15x15) located in the Turkey Point Unit 3 reactor core (Westinghouse). Specific assembly design and irradiation history information was obtained from the previous RCA benchmark evaluations (CRWMS M&O 1997b). The assembly average discharge burnup was 30.51 GWd/mtU with a cooling time of 927 days. A standard depletion model for Cycles 2-4 for this assembly was developed in SAS2H using the required design and irradiation history information.

Supporting operating history and fuel design information used to develop the GRCASMO3 and MCNP input files for each sample were collected from the previously documented SAS2H calculations mentioned above. Table 2-7 provides fuel design specifications for both reactor fuel

types. Table 2-8 provides operating history information for both reactors. The SAS2H results were taken from CRWMS M&O 1997a and 1997b.

Table 2-7. Fuel Design Specifications for Calvert Cliffs and Turkey Point Fuel

	Calvert Cliffs	Turkey Point
Sample location (cm)	13.2 (from bottom)	167.0 (from bottom)
Sample enrichment (U^{235} wt%)	3.038	2.556
Sample burnup (GWd/mtU)	27.35	30.51
Cooling time (d)	1870	927
Lattice type	CE 14 x 14	W 15 x 15
#fuel rods	176	204
#guide tubes	5	21[a]
Assembly pitch (cm)	20.78	21.5
Fuel pellet density (g/cc)	10.018	10.235
Fuel rod pitch (cm)	1.4732	1.43
Fuel rod OD (cm)	1.1176	1.0719
Fuel rod Clad ID (cm)	0.9855	0.9484
Fuel pellet OD (cm)	0.9563	0.9296
Active fuel length (cm)	347.22	365.76
Guide tube OD (cm)	2.832	1.3868
Guide tube ID (cm)	2.628	1.3004
Cladding material	Zirc-4	Zirc-4

NOTE: [a] Includes 1 instrument tube

Table 2-8. Operating History Inputs for Calvert Cliffs and Turkey Point Fuel

	Calvert Cliffs	Turkey Point
Uptime (d)	Cy[a]2-306 Cy3-381.7 Cy4-466.0 Cy5-461.1	Cy2-314 Cy3-327 Cy4-312
Downtime (d)	Cy2-71.0 Cy3-81.3 Cy4-85.0 Cy5-1870	Cy2-58 Cy3-62 Cy4-927
Specific power (MW/mtU)	Cy2-17.24 Cy3-19.43 Cy4-17.04 Cy5-14.57	32.015
Average fuel temperature (K)	829 850 775 709	922
Cladding Temperature (K)	620	595
Moderator Temperature (K)	557	570
Moderator density (g/cc)	0.7575	0.731
Boron concentration (ppm)	Cy2-330.8 Cy3-469.4 Cy4-503.7 Cy5-492.1	450.0

NOTE: [a]Cy = Cycle

2.2.5 Assumptions

The comparisons summarized in this report are based on scoping calculations where fuel assembly input parameter values are varied, and results based on one-dimensional transport code calculations with point depletion and two-dimensional lattice physics code depletion calculations are made. Several assumptions are made relative to data used for code input for these analyses.

Assumed values are used in Table 2-1 for the assembly axial region designated as YYYN4. As previously noted in Section 2.1, the data presented in this table for the designated axial region is representing two different size fuel rods with an averaged dimension to accommodate limitations in the one-dimensional transport code (SAS2H) input modeling. The assumed values in this table are suitable for this work because they are representative values, and any conclusions drawn from these analyses would be based on the use of these data.

In Section 3.2 where BWR standard gadolinia rod patterns are addressed, two assumptions are made. First, the assumption is made that on a differential basis between gadolinia rod patterns, variations in k_{inf} have negligible void dependence. The calculations were performed at 40% void fraction. This assumption is suitable for this work because the primary effect is varying the gadolinia rod pattern, any void fraction effect would be a second order effect, and any conclusions drawn from these analyses would not change if multiple void fractions were used. Second, it is assumed that a single gadolinia rod enrichment of 3 wt% gadolinia is sufficient to demonstrate the effects of different gadolinia rod locations in the lattice. This assumption is suitable for this work because different gadolinia enrichments while affecting the burnup domain, will not affect the magnitude of the reactivity domain and will not alter any conclusions drawn from these analyses.

In Appendix A, Table A-1, assumed values are used for reactor, fuel assembly, fuel rod, and burnable absorber rod parameters. The assumed values are based on parameter values from the MO0204SPAIRB04.013 reference in Appendix A. These assumed values are suitable for these analyses because they represent parameter values from two pressurized water reactors with fuel cycles containing both removable and integral burnable absorbers, which is the subject of the results reported in Appendix A.

The assumed values for the parameters provided at the top of Tables A-2 through A-15 of Appendix A are suitable for these analyses because they represent parameter values from the two pressurized water reactors discussed in the preceding paragraph. The largest deviation of any parameter value from actual value is 2.25 %, which is totally appropriate for these analyses.

3. DESCRIPTION OF THE CALCULATIONS

The following sections summarize the calculations that comprise the "code-to-code" analyses as documented in MO0204SPABCF04.012 and MO0109SPADRN04.003. The initial sections define the reactivity effects of simplifications required for SAS2H and the final sections describe input refinements and cases for which results will be compared between SAS2H and GRCASMO3.

3.1 BWR LATTICE ENRICHMENT SMEARING

This section provides a summary of the process to assess the reactivity effect of homogenizing several BWR fuel lattice enrichments. Four different types of fuel assemblies are analyzed as documented in MO0109SPADRN04.003, Section 4.1. These were based on 6x6, 7x7, 8x8, and 9x9 lattices. For each type of lattice, different void conditions are looked at, namely 0%, 40%, and 80% void. The average U^{235} enrichment for the lattices ranged from 2.40 to 4.56 wt%. Input related to these assemblies is listed in Section 2.1.

Two GRCASMO3 inputs were set-up for each lattice configuration. The first input represented the fuel rods explicitly with respect to U^{235} enrichment and is referred to as the discrete model. The second, called the smeared model, defined all fuel rods as having the same lattice average U^{235} enrichment. The isotopic and k_{inf} results of the cases were compared to obtain the effect of enrichment smearing.

Four additional configurations were modeled for the 9x9 lattice from those described in Section 2.1. For each of the previous 9x9 configurations, all enrichments were scaled proportionally to raise the average enrichments of the lattices from 3.31 to 4.37 wt% and from 3.45 to 4.56 wt%. Doing this increased the range of the analysis.

3.2 BWR STANDARD GADOLINIA ROD PATTERNS

This section provides a summary of the process to assess the reactivity effect of going from the explicit pin model in GRCASMO3 to the pin-cell model in SAS2H based on generalized gadolinia rod patterns MO0109SPADRN04.003, Section 4.2. A number of BWR designs were surveyed resulting in the general rules identified in Table 3-1, which are intended to provide guidance in developing a standard set of gadolinia fuel rod position maps. The resultant maps are intended for representing fresh and irradiated commercial BWR assemblies in burnup and criticality calculations.

A select number of GRCASMO3 lattice calculations were performed to demonstrate the impact on lattice reactivity resulting from the use of a standard gadolinia rod pattern. Three lattices were chosen for this demonstration an 8x8NB-7Gd, 8x8NB-9Gd, and an 8x8NB-12Gd lattice. (The detailed lattice information is proprietary, MO0109SPADRN04.003, Section 4.2). This spans the range of 7 to 12 gadolinia rods in a lattice. Similar behavior should exist for the 9x9-5 lattice since its geometry is not significantly different.

Lattices containing 7, 9, and 12 gadolinia fuel rods were analyzed to compare k_{inf}s between standard and design gadolinia rod patterns. The lattice uranium enrichment distributions were

not altered. All calculations were performed at 40% void fraction. It is assumed that on a differential basis between gadolinia rod patterns, variations in k_{inf} have negligible void dependence.

Table 3-1. General Rules for Developing Standard Gadolinia Rod Position Maps for BWR Fuels

Follow diagonal symmetry from control blade corner.
Try to keep gadolinia rods 2 or 3 rows in from the outside row of the lattice.
Try to disperse the gadolinia rods evenly across the lattice (do not clump them).
Do not place gadolinia rods face adjacent to one another.
Gadolinia rods may be placed diagonally adjacent to one another.

It is assumed that a single gadolinia rod enrichment of 3 wt% gadolinia is sufficient to demonstrate the effects of different gadolinia rod locations in the lattice. Other gadolinia enrichments simply affect the burnup domain and not the magnitude of the reactivity domain.

The fuel temperature was assumed to be 900 K. This value is similar to those for other fuel types and therefore assumed to be reasonable for this application.

The power density was calculated by dividing the reference design power level by the heavy metal weight of the core. This serves as a reasonable value for this application.

3.3 PWR BURNABLE POISON EFFECTS

This section provides a summary of the process to assess the reactivity effect as a function of burnup for assemblies having burnable poisons compared to those without MO0109SPADRN04.003, Section 4.5. Two general types of burnable absorbers (BAs) are used with PWR fuel: IBAs and BPRs. IBAs are non-removable, neutron-absorbing materials used as components of a fuel assembly. BPRs, however, are rods that contain neutron-absorbing materials that can be inserted in PWR assembly guide tubes. Both types of BAs can be used to control core reactivity and local power peaking and optimize fuel utilization. In general, both types of BAs are designed to function during the first cycle of irradiation of a fresh, unirradiated fuel assembly. After one cycle of irradiation, the BPRs are typically removed from the fuel assembly allowing primary coolant to occupy the guide tube volume displaced by the BPRs. In the case of IBAs, the rods remain in the fuel assembly throughout its lifetime and usually account for a small reactivity penalty at end of life, due to incomplete consumption of the neutron-absorber material. Non-proprietary information is available in DOE 1992, Sections 2.6.5 and 2.8. The general information used is listed in Section 2.2.

PWR fuel assemblies containing typical loadings of gadolinia, erbia, boron carbide-alumina and IFBA rods have been analyzed to investigate their neutronic effects on PWR SNF. Each infinite-array lattice, poisoned and unpoisoned, was depleted with GRCASMO3 (3) under normal, hot-operating conditions. Three cycles of 15 GWd/mtU exposure each were used to represent the depletion history effects on the fuel. Restart calculations were then run at each burnup point removing the xenon, setting the soluble boron to 0 ppm B, and the fuel and moderator

temperatures to 300 K to simulate storage cask conditions. No radioactive decay periods were accounted for in the analyses, but should be in the future.

PWR fuel containing the maximum number of Pyrex and WABA BPRs have been analyzed to investigate their neutronic effects on PWR SNF. These arrays were depleted using the same method as that used for the IBA analyses. In addition, the BPRs were removed from the fuel after one and two cycles of depletion. After being removed, the BPRs were replaced with water and depleted to end-of-life conditions. To evaluate their effect on fuel assembly isotopic inventory, the BPRs were not included in the restart calculations.

3.4 PWR FISSION PRODUCT WORTH

This section provides a summary of the process to assess the reactivity worth of fission products in burnup credit for PWR assemblies (MO0204SPABCF04.012). The calculation uses GRCASMO3 and MCNP4B2. GRCASMO3 is used to deplete a single node of a hypothetical 17x17 PWR assembly and calculate the values of k_{inf} for the assembly at several depletion points. These values of k_{inf}, along with isotopic reaction rates calculated by GRCASMO3, are used to estimate the overall worth of the fission products relative to the entire burnup credit reactivity worth.

MCNP uses the isotopic composition of the fuel, from the GRCASMO3 output, to calculate k_{eff} for a variety of lattice conditions. Tally options in MCNP were used to generate reaction rates (absorption and production). These reaction rates, and the associated values of k_{eff}, were used to estimate the overall worth of the fission products relative to the entire burnup credit reactivity worth.

3.4.1 GRCASMO3 Depletion

Depletion calculations were performed on a single node of a 17x17 PWR assembly with enrichments of 2 wt%, 3.7 wt%, and 5 wt%. The fuel was depleted from 0 GWd/mtU to 50 GWd/mtU with reporting steps every 10 GWd/mtU. The calculations considered 5 year and 200 year cooling times. Inputs necessary for building the GRCASMO3 cases are presented in Table 3-2. The input represents a hypothetical fuel, and is used for the purposes of scoping calculations only. Figure 3-1 shows the lattice map for the 17x17 fuel assembly.

Through the use of the "FRR" card in GRCASMO3, the absorption ($\Sigma_a\Phi$), fission ($\Sigma_f\Phi$) and production ($\nu\Sigma_f\Phi$) reaction rates for identified isotopes can be obtained. These are available in two energy groups and the sum of the two groups. Each group, and the sum, is further broken down into finer groups. The last value in each group is the group total. A total is also available for the sum of the two groups. For the purposes of the reaction rate calculations (see Section 3.4.3), the totals of the sums for the absorption and production reaction rates are used.

Table 3-2. GRCASMO3 Input (all dimensions in cm)

Parameter	Dimension
Lattice Source	Hypothetical
Lattice Size	17x17
Fuel Rod	
Pellet Radius	0.410
Clad Inner Radius	0.418
Clad Outer Radius	0.475
Pellet Density (g/cc)	10.34
Guide Tubes	
Clad Inner Radius	0.552
Clad Outer Radius	0.593
Instrumentation Tube	
Inner Radius	0.561
Outer Radius	0.602
Rod Pitch	1.260
Assembly Pitch	21.504
Hot Depletion Coolant Temp (K)	584
Hot Depletion Fuel Temp (K)	950
Hot Depletion Boron (ppm)	700
Cold Reactivity Coolant Temp (K)	300
Cold Reactivity Fuel Temp (K)	300
Power Density (W/g)	38.1
Cold Reactivity Boron (ppm)	0
Burnup at EOL (GWd/mtU)	50

1	1	1	1	1	1	1	1	1	1	1	1	1	1	1	1	1
1	1	1	1	1	1	1	1	1	1	1	1	1	1	1	1	1
1	1	1	1	1	2	1	1	2	1	1	2	1	1	1	1	1
1	1	1	2	1	1	1	1	1	1	1	1	1	2	1	1	1
1	1	1	1	1	1	1	1	1	1	1	1	1	1	1	1	1
1	1	2	1	1	2	1	1	2	1	1	2	1	1	2	1	1
1	1	1	1	1	1	1	1	1	1	1	1	1	1	1	1	1
1	1	1	1	1	1	1	1	1	1	1	1	1	1	1	1	1
1	1	2	1	1	2	1	1	3	1	1	2	1	1	2	1	1
1	1	1	1	1	1	1	1	1	1	1	1	1	1	1	1	1
1	1	1	1	1	1	1	1	1	1	1	1	1	1	1	1	1
1	1	2	1	1	2	1	1	2	1	1	2	1	1	2	1	1
1	1	1	1	1	1	1	1	1	1	1	1	1	1	1	1	1
1	1	1	2	1	1	1	1	1	1	1	1	1	2	1	1	1
1	1	1	1	1	2	1	1	2	1	1	2	1	1	1	1	1
1	1	1	1	1	1	1	1	1	1	1	1	1	1	1	1	1
1	1	1	1	1	1	1	1	1	1	1	1	1	1	1	1	1

NOTE: 1 - Fuel Rod; 2 - Guide Tube; 3 - Instrumentation Tube

Figure 3-1. Lattice Map of Hypothetical 17x17 Assembly

3.4.2 MCNP Reactivity Calculations

Reactivity calculations were performed on a variety of lattices using the isotopics from the GRCASMO3 depletion calculations (MO0204SPABCF04.012, Section 4.2). The assembly lattices considered include: 21-PWR assembly waste package, infinite lattice with the same materials and geometry as the fuel lattice in the waste package, and an infinite lattice with the same materials and geometry as the GRCASMO3 calculations. Several variations on the composition of the basket structure used in the waste package were considered. These were used to estimate the impact of the boron in the absorber plates and the impact of the displacement of water by the thermal shunt.

For the purposes of these calculations, the waste package representation was simplified to include a single node for the fuel rod, instead of the multi-nodes typically used for the Yucca

Mountain Site Characterization Project (YMP). Due to changes in the YMP waste package design, this geometry may not exactly represent the current design being considered by the YMP but it is considered adequate for these scoping calculations.

The MCNP reactivity calculations were performed for 3.7 wt% U^{235} enriched fuel, burned over the same range as reported above. The MCNP calculations consider only the 5-year cooled fuel. The isotopic concentrations were obtained from the GRCASMO3 output. The values reported by GRCASMO3 are cell averaged. To obtain the pin average values, the concentrations were multiplied by the cell cross-sectional area and divided by the total cross-sectional area of all of the pins.

Figure 3-2 shows the lattice map for the 21-PWR assembly waste package. This is a simplified sketch and does not show the thermal shunts and other basket material. Each square in Figure 3-2 represents one 17x17 PWR assembly.

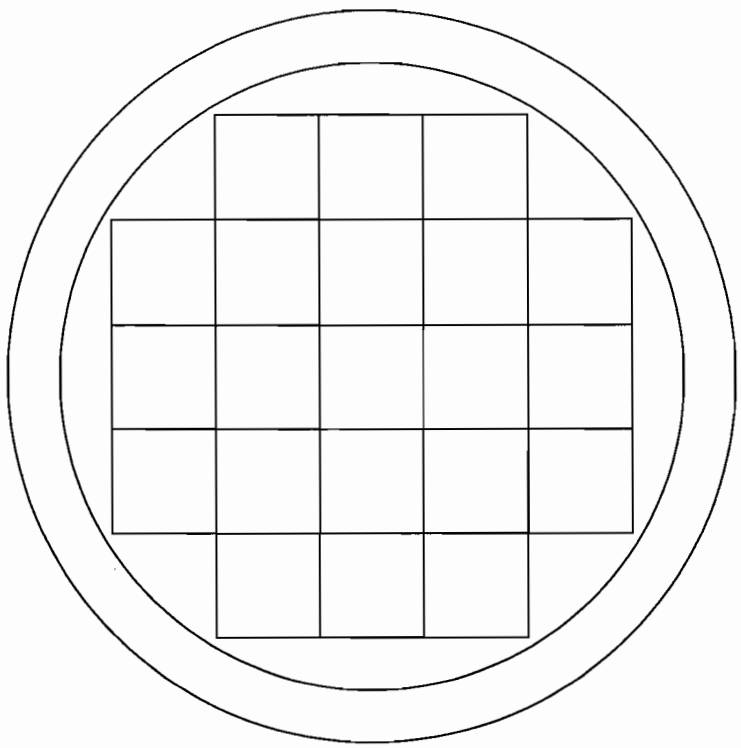

Figure 3-2. 21-PWR Assembly Waste Package

3.4.3 Reaction Rate Calculations

To calculate the worth of the fission products, while maintaining the neutron spectrum, the calculations use a simplified equation to estimate the change in k_{eff} (or k_{inf}) based on the reaction rates available in the code output. Equation 3-1 is the simplified expression for k_{eff} developed for use in this analysis and can be developed from the general principles on the multiplication factor discussed in Duderstadt and Hamilton (1976, Chapter 3).

$$k_{eff} = \frac{\nu \Sigma_f \Phi}{\Sigma_a \Phi + x} = \frac{Production}{Absorption\ in\ fuel + Other\ losses}$$

(Eq. 3-1)

where

ν is the average number of neutrons released per fission
Σ_f is the macroscopic neutron fission cross section
Σ_a is the macroscopic neutron absorption cross section
Φ is the neutron flux
x represents all neutron losses that occur outside of the fuel, and remains constant in the calculations for a given isotopic comparison set.

Equation 3-2 is the solution for calculating "x".

$$x = \frac{\sum_{all\ isotopes} \upsilon \Sigma_f \Phi}{k_{eff}} - \sum_{all\ isotopes} \Sigma_a \Phi$$

(Eq. 3-2)

Using this equation and the results of the MCNP, or GRCASMO3, calculations (reaction rates and k_{eff} or k_{inf}) "x" can be calculated. Isotopic reaction rates ($\nu\Sigma_f\Phi$ and $\Sigma_a\Phi$) are taken from the GRCASMO3 output files, and total reactions rates (Best-Estimate and Actinide Only) are generated in the MCNP output files using the type F4 MCNP tallies.

For the best-estimate case (i.e., systems containing all of the tracked isotopes) k_1 is calculated along with the reaction rates using the appropriate computer code. These values are fed into Equation 3-2 to solve for "x". The best-estimate "Absorption in fuel" value is then replaced with the "Actinide-only" absorption value in Equation 3-1 and using the calculated value for "x", a new k_{eff} (k_2) is calculated. k_2 represents the "actinide-only" k_{eff} in a system using the "best-estimate" neutron spectrum.

The "best-estimate" change in reactivity [$\Delta\rho$(BE)] and the "actinide-only" change in reactivity [$\Delta\rho$(AO)] are calculated with respect to the "fresh fuel" case (k_0). Equation 3-3 shows the base equation used (Duderstadt and Hamilton 1976, Chapter 5.V).

$$\Delta\rho(X) = \frac{k_X - k_0}{k_X\ k_0}$$

(Eq. 3-3)

where

k_x is the k_{eff} calculated from Equation 3-1 and
k_0 is the k_{eff} from MCNP or CASMO.

Considering that the fission product worth [$\Delta\rho$(FP)] is just $\Delta\rho$(BE) minus $\Delta\rho$(AO), it can then be calculated using Equation 3-4.

$$\Delta\rho = \frac{k_1 - k_2}{k_1 \, k_2} \qquad \text{(Eq. 3-4)}$$

where

k_1 is the "best-estimate" k_{inf} and
k_2 is the "actinide-only" k_{inf}.

3.5 CODE-TO-CODE COMPARISONS

3.5.1 BWR Control Blade Refinements in SAS2H

This section provides a summary of the refinements to the control blade representation in SAS2H based on comparisons to explicit representations in GRCASMO3 MO0109SPADRN04.003, Section 4.3. Comparisons of flux disadvantage factors (DFAC) and isotopic concentrations were performed using SAS2H and GRCASMO3. The input used in both codes was representative of a typical axial node (45.72 cm) for a Grand Gulf Unit 1 BWR 9x9 assembly (MO0106SPASTA00.005) as described in Section 2.1.

A list of isotopes used for comparison purposes is provided in Table 3-3. These actinides and fission products were selected based on the availability of results from each code. SAS2H independently depletes and decays approximately 200 isotopes, where GRCASMO3 is limited to approximately 25.

Table 3-3. Isotopes Used For Comparison

U^{235}	Pu^{239}	Pu^{241}	Am^{241}	Np^{237}
Eu^{153}	Gd^{155}	Ag^{109}	Nd^{143}	Rh^{103}
Sm^{151}	Sm^{149}	Sm^{152}	---	---

The thermal-hydraulic depletion history input used for the node cases in both SAS2H and GRCASMO3 inputs is listed in Table 2-3. Control blade insertion times were also represented identically in both codes.

Control blade input is listed in Section 2.1.1. For control blade modeling in SAS2H, materials were homogenized and specified for corresponding areal dimensions represented in the path B model. Table 3-4 provides volume fractions and homogenized input values necessary for development of the original bladed SAS2H 1-D model (CRWMS M&O 1999c). The spectrum was noted to be too hard in this case by comparing the SAS2H and CASMO fluxes, and the path B model was refined, as described in the following paragraphs, to provide a better physical representation of the control blades. Table 3-5 provides the homogenized input values for the modified SAS2H 1-D model. The control blade and pin lattice is modeled explicitly in GRCASMO3. Actual fuel pin types and U^{235} wt% enrichment are proprietary MO0109SPADRN04.003, Section 4.3. Control blade insertions were modeled as either fully

inserted in the axial region or completely removed. In SAS2H this is accomplished by a homogenized zone of bypass moderator and control blade material constituents.

The SAS2H 1-D input consists of a path A lattice representing typical fuel rods and a larger path B pin cell model describing characteristics of the assembly. For active fuel regions in BWR fuel, limitations of SAS2H require that water rod explicit representations in the path B model be omitted when gadolinia-bearing fuel rods are present in the region. Water rod moderator is implicitly accounted for in the bypass region of the BWR path B model. In the SAS2H path B model for the original model, the outer ring of the assembly cell model contains bypass water for non-bladed nodes and a homogenization of bypass water, stainless steel 304, and B_4C (total density = 1.6704 g/cc) for bladed nodes. During the depletion calculation when there is no control blade present, the mixture description is set for bypass water.

Table 3-4. Inputs for SAS2H Control Blade Homogenization Original Model

	SS304	Water	B_4C
Volume Fraction	0.1222	0.8289	0.0489
Density (g/cc)	7.94	0.7396	1.78 (70.6% theoretical)
Weight Fraction	0.5809	0.3670	0.0521
Homogenized Density	1.6704 (g/cc)		

Element	SS304 (wt%)	Water (wt%)	B_4C (wt%)	Homogenized
Carbon	0.080	—	21.739	1.1784
Nitrogen	0.100	—	—	0.0581
Silicon	0.750	—	—	0.4357
Phosphorus	0.045	—	—	0.0261
Sulfur	0.030	—	—	0.0174
Chromium	19.000	—	—	11.037
Manganese	2.000	—	—	1.1618
Iron	68.745	—	—	39.935
Nickel	9.250	—	—	5.3734
Hydrogen	—	11.190	—	4.1070
Oxygen	—	88.810	—	32.595
Boron-10	—	—	14.424	0.7510
Boron-11	—	—	63.837	3.3239

Source: CRWMS M&O 1999c, Tables 5-3 and 5-4.

Table 3-5. Inputs for SAS2H Control Blade Homogenization Modified Model

	SS304	Water	B_4C
Volume Fraction	0.4928	0.2973	0.2099
Density (g/cc)	7.94	0.7396	1.78 (70.6% theoretical)
Weight Fraction	0.8683	0.0488	0.0839
Homogenized Density	4.50658 (g/cm^3)		

Element	SS304 (wt%)	Water (wt%)	B_4C (wt%)	Homogenized
Carbon	0.080	—	21.739	1.8715
Nitrogen	0.100	—	—	0.0868
Silicon	0.750	—	—	0.6512
Phosphorus	0.045	—	—	0.0391
Sulfur	0.030	—	—	0.0261
Chromium	19.000	—	—	16.4980
Manganese	2.000	—	—	1.7366
Iron	68.745	—	—	59.6920
Nickel	9.250	—	—	8.0319
Hydrogen	—	11.190	—	0.5460
Oxygen	—	88.810	—	4.3331
Boron-10	—	—	14.424	1.1956
Boron-11	—	—	63.837	5.2916

NOTE: Values used to calculate these inputs are provided in Table 2-1.

Tables 3-6 and 3-7 provide radii of the original and modified path B models for the bladed axial region. In the original SAS2H path B model, the control blade material was homogenized with the bypass moderator in the outer zone (Zone 6). Radii for regions in the original SAS2H path B model are calculated using Equations 3-5 through 3-10 as derived in the calculations.

Gd/Water rod:

$$R_1 = R_{c,i} \qquad \text{(Eq. 3-5)}$$

where

$R_{c,i}$ is the inner radius of the Gd rod cladding (or water rod cladding if no Gd rod is present)

Gd/Water rod cladding:

$$R_2 = R_{c,o} \qquad \text{(Eq. 3-6)}$$

where

$R_{c,o}$ is the outer radius of the Gd rod cladding (or water rod cladding if no Gd rod is present)

Unit cell in-channel moderator:

$$R_3 = \sqrt{\frac{\#\,\text{waterrods} * \text{rodpitch}^2}{\pi}}$$

(Eq. 3-7)

Homogenized fuel:

$$R_4 = \sqrt{R_3^2 + \frac{\#\,\text{fuelrods} - \#\,\text{gdrods}}{\#\,\text{gdrods}} * \frac{\text{rodpitch}^2}{\pi}}$$

(Eq. 3-8)

Channel:

$$R_5 = \sqrt{R_4^2 + \frac{1}{\#\,\text{gdrods}} * \frac{\text{outwidth}^2 - \text{inwidth}^2}{\pi}}$$

(Eq. 3-9)

where

outwidth is the channel outer width and inwidth is the channel inner width

Homogenized bypass and control blade:

$$R_6 = \sqrt{\frac{1}{\#\,\text{gdrods}} * \frac{\text{assempitch}^2}{\pi}}$$

(Eq. 3-10)

For the modified SAS2H path B model, Equation 3-10 was replaced with Equations 3-11 and 3-12.

Bypass moderator:

$$R_6 = \sqrt{\frac{1}{\#\,\text{gdrods}} * \frac{\text{assempitch}^2 - (\text{hlfbldthk} * \text{bldlength})}{\pi}}$$

(Eq. 3-11)

where

assempitch is the assembly pitch,
hlfbldthk is the ½ control blade thickness
bldlength is the control blade length and
gdrods is the number of gadolinium rods

Homogenized control blade:

$$R_7 = \sqrt{\frac{1}{\#gdrods} * \frac{assempitch^2}{\pi}}$$

(Eq. 3-12)

Aside from the obvious shortcomings of this type of 1-D model representation for a heterogeneous BWR lattice, the neutron absorbing effect of the control blade is also over-emphasized. The B_4C normally contained in discrete pins in the wings of the control blades is now homogenized over a much larger volume and spread evenly around the entire assembly volume. The effective "cross-section" of absorber is much greater in this model. Errors of this type in the SAS2H representation contribute to a "hard" neutron spectrum in the case during control blade insertion times. For these reasons, the original SAS2H path B model was deemed to over-emphasize the control blade absorbing effect and create an incorrect representation of the bladed node. A graphical representation of the original path B model for SAS2H is depicted in Figure 3-3.

Table 3-6. SAS2H 1-D (Path B) Zone Dimensions for Node YYYN4

Region	Description	Radius (cm)	Areal Dimension (cm^2)
Zone 1	Gadolinia-bearing fuel rod (explicit)	0.4736	0.7047
Zone 2	Cladding	0.5424	0.2196
Zone 3	Unit cell in-channel moderator	0.8068	1.1207
Zone 4	Homogenized fuel zone	2.4867	17.3816
Zone 5	Channel	2.5512	1.0208
Zone 6	Bypass-homogenized control blade	3.03994	8.5848

Table 3-7. Modified SAS2H 1-D Zone Dimensions for Node YYYN4

Region	Description	Radius (cm)
Zone 1	Gadolinia-bearing fuel rod (explicit)	0.4736
Zone 2	Cladding	0.5424
Zone 3	Unit cell in-channel moderator	0.8068
Zone 4	Homogenized fuel zone	2.4867
Zone 5	Channel	2.5512
Zone 6	Bypass region	2.97608
Zone 7	Homogenized control blade	3.03994

In the modified SAS2H path B model depicted in Figure 3-4, an extra zone (Zone 7) was added. This new outer zone is the region representing the control blade homogenization. The zone between the outer control blade zone and the assembly channel zone represents the bypass moderator. This approach provides a better representation of the assembly-control blade geometry within the limitations of SAS2H. However, there is no current solution in SAS2H for the incorrect appearance of control blade material around the entire assembly when gadolinia-bearing fuel rods are required to be represented in the center zone of the path B model. The control blade "ring" in this modified SAS2H model is now much "thinner" allowing for

absorption self-shielding and more realistic neutron travel distances outside of the assembly channel. The calculation of the new Zone 6 radius amounts to subtracting out the volume of the smaller homogenized control blade from the bypass moderator region and adding it into Zone 7.

Additionally, thermal flux disadvantage factors (DFAC) were calculated for the bypass region of both the original and the modified SAS2H model as well as for the GRCASMO3 model of YYYN4. Comparisons of DFAC for the bypass region in the SAS2H and GRCASMO3 models provides additional means to evaluate the suitability of the SAS2H path B models for this type of BWR lattice. For this work, the definition of the bypass region thermal flux disadvantage factor is the flux in the bypass region multiplied by the bypass region volume divided by the same sum for the total volume.

Thermal flux ratios of bypass-to-total were chosen because the primary modification to the modeling approach in SAS2H concerned the definition of the bypass moderator region. A separate GRCASMO3 input file was generated to include input cards that would segment the assembly lattice structure into regions similar to those of the SAS2H 1-D model. From these regions the volume-weighted flux was obtained. In the SAS2H sequence, the output provides three broad group tallies of volume-weighted flux. In a likewise fashion, the volume-weighted thermal flux was obtained and used in the calculation of bypass DFAC.

Volume correction was required for the bypass region of the SAS2H original model because of limitations in SAS2H modeling for BWR assemblies. This correction was made to improve DFAC comparisons of the original SAS2H model bypass region to the GRCASMO3 model of that same region. The correction involved removing the water rod volume from the bypass region in the SAS2H model. This correction was not required for comparisons of the modified SAS2H model.

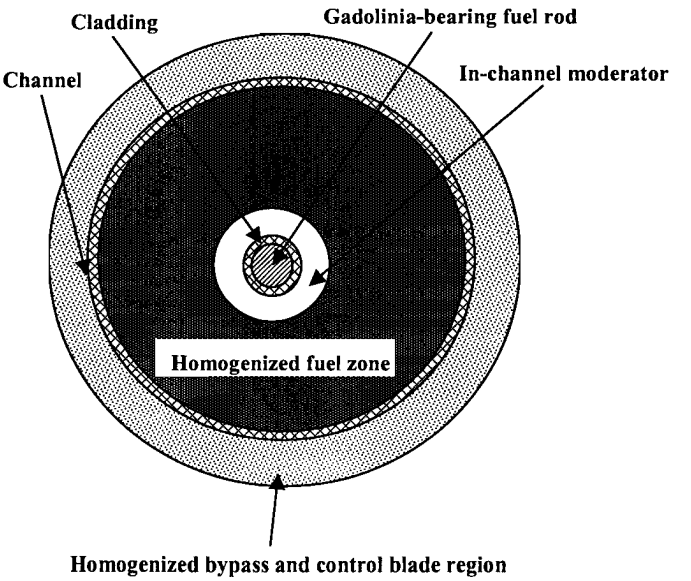

Figure 3-3. SAS2H 1-D Model for YYYNA

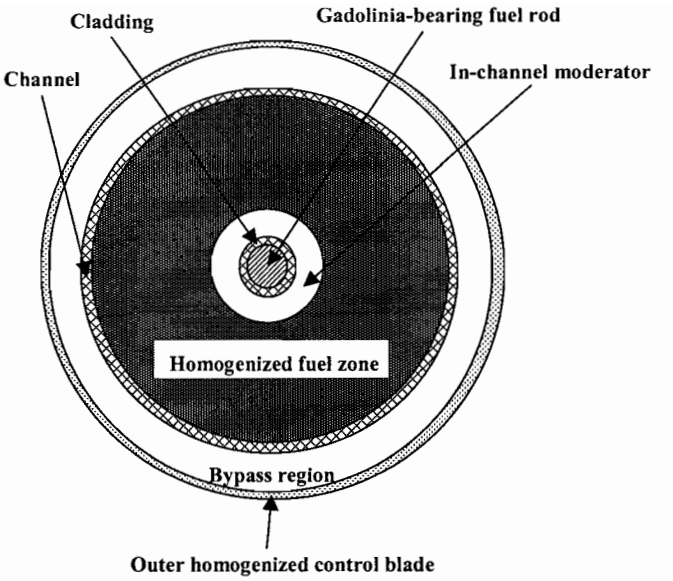

Figure 3-4. Modified SAS2H 1-D model for YYYN4

3.5.2 BWR Assembly Burnup Comparisons

This section provides a summary of the process to assess the reactivity worth of going from an explicit assembly representation (GRCASMO3) to a simplified representation (SAS2H) MO0109SPADRN04.003, Section 4.4. Four fuel assemblies from two BWRs were chosen for this analysis as discussed in Section 2.1. All four assemblies were evaluated using SAS2H with a 44-group cross section library and GRCASMO3 with a 40-group library. For SAS2H, the assemblies were represented using the modified "Path B" approach discussed in Section 3.5.1. Namely, a series of homogenized annular regions was formed with a Gd fuel rod located in the center. The control blade for the C14 and F05 operating histories was represented as the outer ring. A 10-node-axial format was used for the SAS2H representation to reduce the total number of calculations required. To do this, the 24 or 25-node information was volumetrically averaged to obtain the necessary input for 10 nodes. For the controlled histories, the control blade insertion times were approximated for the times the blade was inserted for less than the entire step. If the blade was inserted for at least half the depletion step, it was inserted for the whole step. Likewise, if the blade was inserted for less than half the depletion step, it was neglected for that whole step.

The assemblies were also modeled in GRCASMO3 for a 24 or 25-node-axial format using information from nuclear power-producing utilities (MO0109SPADRN04.003). The individual fuel rods were represented with their respective U^{235} and Gd enrichments. Two different operating history resolutions were used for GG1 assemblies. The first was a detailed operating history taken from core-follow information with the control blade insertion time accurately represented. The second was a coarser operating history in which the only depletion points entered corresponded to those used in the SAS2H calculations. Only this second type of operating history was used for the QC2 assemblies since no further detail was supplied by the utility. For all assemblies, the GRCASMO3 isotopic results were then averaged to correspond to the 10-node-axial format for comparison to the SAS2H results.

Finally, the SAS2H 10-node-axial format was also represented using GRCASMO3. For these cases, the input (e.g., fuel temperature, void history) were collapsed prior to running GRCASMO3. (The 24 (QC2) or 25 (GG1) nodes used in GRCASMO3 calculations were collapsed as shown in Table 3-8.).

For each of the above cases, the calculated end-of-life isotopic concentrations for 24 isotopes were used as the fuel specification in an MCNP infinite lattice model for each node of the 10-node-axial format. Comparison of the resulting k_{inf} values gives an indication of the change in reactivity due to the change in isotopics from the different cases.

The fuel densities for QC2 were calculated using the mass and volume of the fuel. For these assemblies, the mass and nodal lengths for the 10-node-axial format are given in Table 2-4. For the 24-node-axial format, the density of the corresponding 10-node-axial format was used. The density was calculated using the formula density = mass/(πr^2 * axial length * # fuel rods * 0.8815), where mass, axial length, and # fuel rods are given in Table 2-4, r is the fuel radius (0.5207 cm), and 0.8815 is the fraction of uranium in the fuel (UO_2).

Table 3-8. SAS2H Nodal Breakdown

SAS2H Node	Corresponding GRCASMO3 Nodes[a]		
	QC2-Type C	QC2-Type F	GG1-Type G
10 [b]	24	23-24	24-25
9	20-23	20-22	23
8	17-19	17-19	21-22
7	14-16	14-16	17-20
6	11-13	11-13	13-16
5	9-10	9-10	10-12
4	6-8	6-8	7-9
3	4-5	4-5	5-6
2	2-3	2-3	2-4
1	1	1	1

Source: MO0109SPADRN04.003

NOTES: [a] Each GRCASMO3 node represents 6 inches of fuel.
[b] Node 10 is top of assembly.

The control blade specifications used in the GRCASMO3 cases were derived from the information in Table 2-6. Figure 2-1 shows a typical control blade. The default absorber material in GRCASMO3 was used; however, the specification for the structural materials was calculated to homogenize the water and steel.

The information used in the SAS2H cases is given in Table 3-9. Equations 3-5 through 3-12 of Section 3.5.1 were used to calculate the SAS2H radii listed in Table 3-9.

Table 3-9. Necessary Dimensions for SAS2H Cases – All Lattices
(All dimensions given in cm)

Reactor	QC2	QC2	QC2	QC2	QC2	QC2	QC2	GG1	GG1	GG1
Lattice Type	C	C	C	F	F	F	F	G	G	G
SAS2H Node(s)	1	2-9	10	1	2-7,9	8	10	1,10	2-3,7-9	4-6
Avg Gd rod clad rad, inner	N/A	0.5321	N/A	N/A	0.5321	0.5321	N/A	N/A	0.4736	0.4736
Avg Gd rod clad rad, outer	N/A	0.6134	N/A	N/A	0.6134	0.6134	N/A	N/A	0.5504	0.5504
# Fuel rods	60	60	51	60	60	60	54.5	76	76	76
# Gd rods	0	9	0	0	9	11	0	0	10	9
# water/spacer rods	4	1	4	1	1	1	1	5	5	5
Avg water rod rad, inner	1.2281	N/A	1.2281	1.2281	N/A	N/A	1.2281	0.6215	N/A	N/A
Avg water rod rad, outer	1.3094	N/A	1.3094	1.3094	N/A	N/A	1.3094	0.6607	N/A	N/A
Pin Pitch	1.6256	1.6256	1.6256	1.6256	1.6256	1.6256	1.6256	1.4300	1.4300	1.4300
Channel width, inner	13.4061	13.4061	13.4061	13.4061	13.4061	13.4061	13.4061	13.2461	13.2461	13.2461
Channel width, outer	13.8125	13.8125	13.8125	13.8125	13.8125	13.8125	13.8125	13.8557	13.8557	13.8557
Assembly pitch	15.24	15.24	15.24	15.24	15.24	15.24	15.24	15.24	15.24	15.24
½ control blade thickness[a]	0.3962	0.3962	0.3962	0.3962	0.3962	0.3962	0.3962	0.3962	0.3962	0.3962
Control blade length	24.3688	24.3688	24.3688	24.3688	24.3688	24.3688	24.3688	24.3688	24.3688	24.3688
SAS2H Radii										
Gd/Water rod	1.2281	0.5321	1.2281	1.6002	0.5321	0.5321	1.6002	0.6215	0.4736	0.4736
Gd/Water rod cladding	1.3094	0.6134	1.3094	1.7018	0.6134	0.6134	1.7018	0.6607	0.5424	0.5424
In-channel moderator	1.8343	0.9171	1.8343	1.8343	0.9171	0.9171	1.8343	1.8041	0.8068	0.8068
Homogenized fuel	7.3372	2.3681	6.8017	7.3372	2.3681	2.1420	7.0148	7.2612	2.2242	2.3445
Channel	7.5733	2.4493	7.0558	7.5733	2.4493	2.2155	7.2615	7.6147	2.3394	2.4660
Bypass moderator	8.4176	2.8059	8.4176	8.4176	2.8059	2.5380	8.4176	8.4176	2.6619	2.8059
Control blade	8.5982	2.8661	8.5982	8.5982	2.8661	2.5925	8.5982	8.5982	2.7190	2.8661

Source: MO0109SPADRN04.003, Table 4-21

[a]Control blade information taken from Quad Cities 1 due to lack of non-proprietary data for use in SAS2H model. The blade length for the SAS2H model is defined as the length of the blade seen by the assembly (i.e., blade length at the top of the assembly + blade length at the side of the assembly). This is calculated using the following formula: 2*blade length – overlapping length (1/2 blade thickness).

The density found in the SAS2H input files for the fuel material is the density smeared to the clad inner radius. For the QC2 densities, 10.490 g/cm^3 for Type C and 10.535 g/cm^3 for Type F were used to calculate the smeared density. The formula used for this was $\rho_{cl} = \rho_{fp} * R_{fp}^2 / R_{cl}^2$, where ρ_{fp} and ρ_{cl} are the fuel densities based on the fuel pellet area and the clad area, respectively and R_{cl} and R_{fp} are the clad and fuel pellet inner radii, respectively.

For the GG1 fuel material densities, the same method as applied to the QC2 assemblies was used for GG1 for the SAS2H inputs. Table 2-5 lists the information needed to determine the fuel densities for the SAS2H case. Fuel pellet and inner clad radii used were for the average of all 76 fuel rods.

In both the GRCASMO3 and SAS2H cases, the values for the U^{234}, U^{236}, and U^{238} weight percents were calculated with the following formulas (CRWMS M&O 1999c, p. 14):

$$\text{wt\% } U^{234} = 0.007731 * (\text{wt\% } U^{235})^{1.0837}$$
$$\text{wt\% } U^{236} = 0.0046 * (\text{wt\% } U^{235})$$
$$\text{wt\% } U^{238} = 100 - [(\text{wt\% } U^{235}) + (\text{wt\% } U^{234}) + (\text{wt\% } U^{236})]$$

The weight percents given in the Gd material specifications were calculated using the formulas outlined in CRWMS M&O 1999c, pp. 15-16, for all assemblies in this analysis. All other material specifications other than coolant (e.g., clad, control blade) were also included in this reference. Coolant density for each reactor type is taken to be for saturated water at the given pressure (FCF 1999, MO0106SPASTA00.005).

The time length for each depletion step in SAS2H was determined using the EFPD of each state point (point at which burnup history information is available). If these steps were longer than 70 EFPD, they were broken into the number of intervals needed so that each interval was less than 70 EFPD. Temperatures and specific powers remained throughout the entire state point time step. For moderator density, the value of the density changed linearly in each interval of the state point time step and the value corresponding to the middle of the interval was used for that entire interval. For example, in Cycle 6 of QC2, one state point corresponded to 180.3 EFPD, which was broken down into three intervals of 60.1 EFPD each. The moderator density value listed in the previous state point, as 0.5630, was the beginning value for this state point while the value, 0.5720, listed for this state point was considered the final moderator density value. Linearly varying the moderator density from 0.5630 to 0.5720 and taking three equal steps leads to moderator density values of 0.5645, 0.5675, and 0.5705 for the intervals in that state point.

Power for the SAS2H cases was calculated using the formula given by Equation 3-13.

$$\text{power-s} = \text{delta_bu} * 10^3 * (1/\text{delta_efpd}) * \text{mass} \qquad \text{(Eq. 3-13)}$$

where

power-s = power used for SAS2H calculations (MW)
delta_bu = exposure increment (GWd/mtU)
delta_efpd = time step increment (days)
mass = mass of fuel (mtU).

The power density used in the GRCASMO3 cases was expressed in W/g and found using the formula given by Equation 3-14.

$$\text{power-g} = \text{delta_bu} * 10^9 * \text{mass} *(1/\text{delta_efpd}) / (\text{mass} * 10^6)$$
$$= \text{delta_bu} *10^3 *(1/\text{delta_efpd})$$

(Eq. 3-14)

where

power-g = power used for GRCAMSO3 calculations (W/g)
delta_bu = exposure increment (GWd/mtU)
delta_efpd = time step increment (days)
mass = mass of fuel (mtU)

GRCASMO3 and SAS2H were used to calculate the concentrations of certain isotopes in the fuel regions. The results were then used in MCNP to determine the k_{inf} of the node. GRCASMO3 calculated the isotopics in the form of atoms/barn-cm based on the lattice volume. The atom density values were re-normalized before use in MCNP to correspond to the fuel volume. For SAS2H, the isotopic concentrations were given in grams, which were converted to atom densities before use in MCNP.

3.5.3 PWR Radio-Chemical Assay Comparisons

This section provides a summary of the comparison of the results of using the SAS2H sequence available in the SCALE code package and GRCASMO3 to generate the isotopic inventories of spent nuclear fuel (SNF) (MO0109SPADRN04.003, Section 4.6). The calculations consider RCA information from PWR fuel samples taken from Calvert Cliffs (CRWMS M&O 1997a) Unit 1 and Turkey Point Unit 3 (CRWMS M&O 1997b). Pin cell models were developed using MCNP to provide examples of impact, in terms of Δk_{eff} resulting from differences in SAS2H predicted inventories, GRCASMO3 predicted inventories, and measured isotopic inventories. The inputs used are described in Section 2.2.4. Isotopic inventories predicted by GRCASMO3 and SAS2H were compared by calculating percentage differences for each isotope measured. Additionally, SNF material weight fractions were calculated for measured, SAS2H-calculated, and GRCASMO3-calculated isotopic inventories. These material specifications were placed in infinite pin-cell calculations using MCNP to quantify differences in k_{inf} resulting from changes in isotopic inventory. Frequently, large percentage differences in isotopic concentrations occur because of differences in very small numbers. Comparisons of effects of isotopic differences on k_{inf} in a reactivity model provides a more realistic understanding of the net reactivity impact resulting from small isotopic inventory differences.

4. RESULTS

4.1 LATTICE ENRICHMENT SMEARING RESULTS

This section summarizes the results from MO0109SPADRN04.003, Section 5.1. For each configuration and void condition, isotopic concentration and k_{inf} results using the discrete and smeared cases were compared. For each of the isotopics listed in Table 4-1, the relative difference between the smeared and discrete atom densities was calculated using the formula $(N_{i,smeared} - N_{i,discrete})/N_{i,discrete}$, where N_i is the atom density for the ith isotope. These are a subset of the principal isotopes (YMP 2000, p. 3-34) which are available in the GRCASMO3 library. The difference in k_{inf} was taken as $k_{inf,smeared} - k_{inf,discrete}$ For the 6x6 (GUC) and 7x7 (Cooper) lattices, end of life is considered to be 40 GWd/mtU. For the 8x8 and 9x9 (GG1) lattices, EOL is 55 GWd/mtU. Table 4-2 shows the differences in k_{inf} at beginning of life (BOL), middle of life (MOL), and end of life (EOL) for all voids. For all lattices, the differences in k_{inf} at BOL represent the maximum differences over all burnups.

Table 4-1. List of Isotopes Considered in Analysis

Rh^{103}	Sm^{149}	Eu^{155}	U^{238}	Pu^{241}
Ag^{109}	Sm^{150}	$Gd^{155\,(a)}$	Np^{237}	Pu^{242}
Nd^{143}	Sm^{151}	U^{234}	Pu^{238}	Am^{241}
Nd^{145}	Sm^{152}	U^{235}	Pu^{239}	Am^{242m}
Sm^{147}	Eu^{153}	U^{236}	Pu^{240}	Am^{243}

NOTE: [a] As a fission product.

Figures 4-1 through 4-11 show graphical representations of the relative differences in the isotopic concentrations at EOL. As evident by the graphs, the relative differences for all isotopes at EOL are within 4% with the exception of U^{235}. The EOL, MOL, and BOL differences for U^{235} are shown in Figures 4-12 through 4-14, respectively, for all lattice types. Figure 4-12 shows that the U^{235} is consistently under predicted by the smeared model at EOL, (i.e., for all lattices and all voids) the smeared model burns more U^{235} than the discrete model at EOL. This same trend is seen for the relative difference in U^{235} at MOL. However, the differences at MOL (Figure 4-13) are smaller than at EOL. The maximum difference at EOL is over –14% (for GG1-A) while the maximum difference at MOL is less than –3.1% (for Cooper). For BOL, the amount of U^{235} in the assembly should be the same between the discrete and smeared models. This is, in fact, seen in Figure 4-14 by the very small relative differences (between -0.10% and 0.10%).

Also using Figures 4-12 through 4-14, observations concerning void effect can be seen. Namely, as void increases, the relative difference of U^{235} becomes smaller at EOL. For the GG1-A lattice, the difference between 0% and 80% void values is greater than 6%. At MOL, all differences in the 0%, 40%, and 80 % void values are within 0.5%. For BOL, the 0%, 40%, and 80% void values are the same, as expected since all fuel is fresh.

Table 4-2. Δk_{inf} at BOL, MOL, and EOL for All Lattices

	U^{235} wt%[a]	gad wt%[a]	Δk_{inf}		
			BOL[b]	MOL	EOL
0 Void					
GUC 6x6	2.40	0	0.0049	0.0012	-0.0012
Cooper 7x7	2.50	3.4	0.0218	0.0058	-0.0045
GG1-A 8x8	2.99	3	0.0213	0.0080	-0.0034
GG1-M 9x9	3.45	0	0.0052	0.0033	-0.0015
GG1-M 9x9	3.31	0	0.0085	0.0048	-0.0021
GG1-M 9x9	3.31	3.5	0.0142	0.0050	-0.0022
GG1-M 9x9	3.31	7	0.0145	0.0050	-0.0022
GG1-M 9x9	4.56	0	0.0053	0.0050	-0.0009
GG1-M 9x9	4.37	0	0.0082	0.0071	-0.0025
GG1-M 9x9	4.37	3.5	0.0139	0.0070	-0.0024
GG1-M 9x9	4.37	7	0.0144	0.0067	-0.0024
40 Void					
GUC 6x6	2.40	0	0.0042	0.0010	-0.0010
Cooper 7x7	2.50	3.4	0.0216	0.0055	-0.0031
GG1-A 8x8	2.99	3	0.0208	0.0069	-0.0032
GG1-M 9x9	3.45	0	0.0047	0.0029	-0.0012
GG1-M 9x9	3.31	0	0.0076	0.0042	-0.0020
GG1-M 9x9	3.31	3.5	0.0142	0.0043	-0.0020
GG1-M 9x9	3.31	7	0.0146	0.0044	-0.0019
GG1-M 9x9	4.56	0	0.0047	0.0043	-0.0002
GG1-M 9x9	4.37	0	0.0073	0.0059	-0.0013
GG1-M 9x9	4.37	3.5	0.0140	0.0061	-0.0012
GG1-M 9x9	4.37	7	0.0145	0.0047	-0.0012
80 Void					
GUC 6x6	2.40	0	0.0032	0.0007	-0.0008
Cooper 7x7	2.50	3.4	0.0203	0.0041	-0.0018
GG1-A 8x8	2.99	3	0.0187	0.0054	-0.0018
GG1-M 9x9	3.45	0	0.0039	0.0021	-0.0007
GG1-M 9x9	3.31	0	0.0061	0.0029	-0.0011
GG1-M 9x9	3.31	3.5	0.0138	0.0038	-0.0010
GG1-M 9x9	3.31	7	0.0142	0.0042	-0.0010
GG1-M 9x9	4.56	0	0.0039	0.0031	0.0002
GG1-M 9x9	4.37	0	0.0058	0.0041	-0.0005
GG1-M 9x9	4.37	3.5	0.0136	0.0055	-0.0001
GG1-M 9x9	4.37	7	0.0141	0.0053	0.0000

NOTES: [a] Average enrichment

[b] Differences in k_{inf} at BOL are the maximum differences over all burnups.

Figure 4-1. Relative Difference (To Discrete) for Isotopic Concentrations at EOL, GUC 6x6 Fuel Assembly (2.40 wt% U^{235} avg. enr., no Gd)

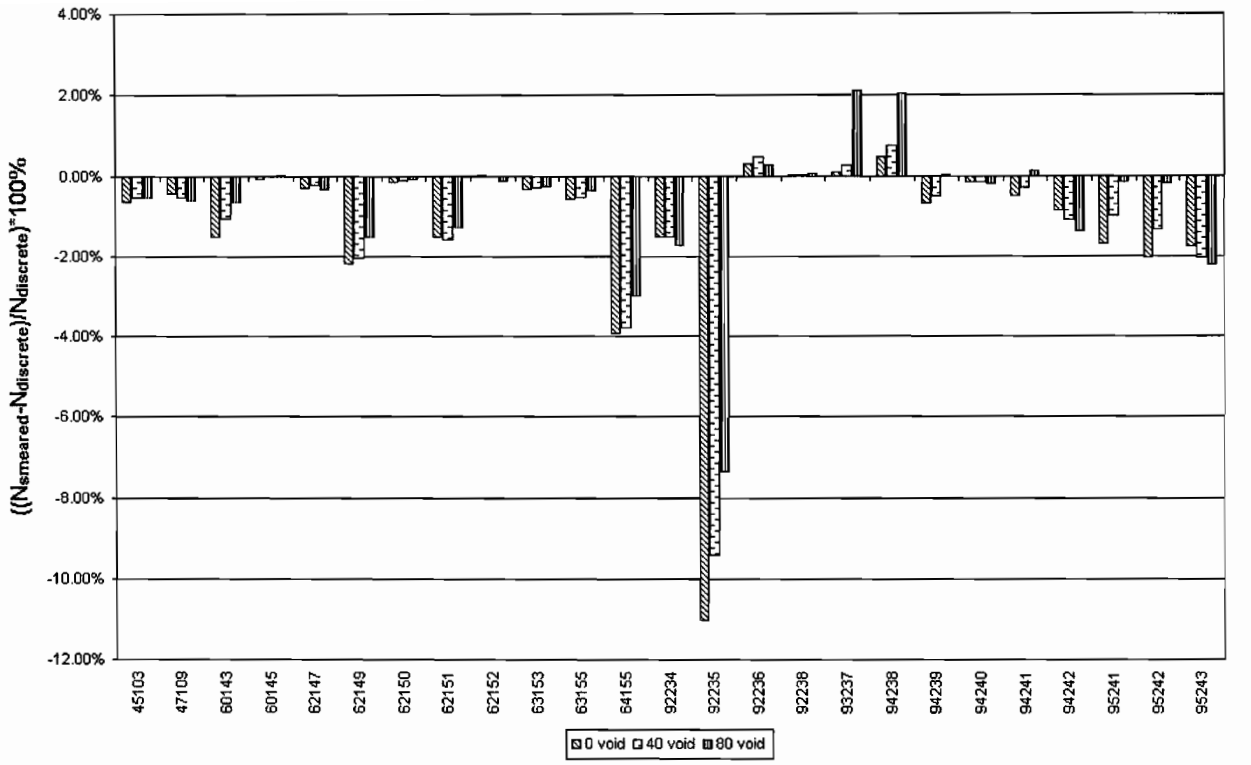

Figure 4-2. Relative difference (to discrete) for isotopic concentrations at EOL, Cooper 7x7 Fuel Assembly (2.50 wt% U^{235} avg. enr., 3.4 wt% Gd)

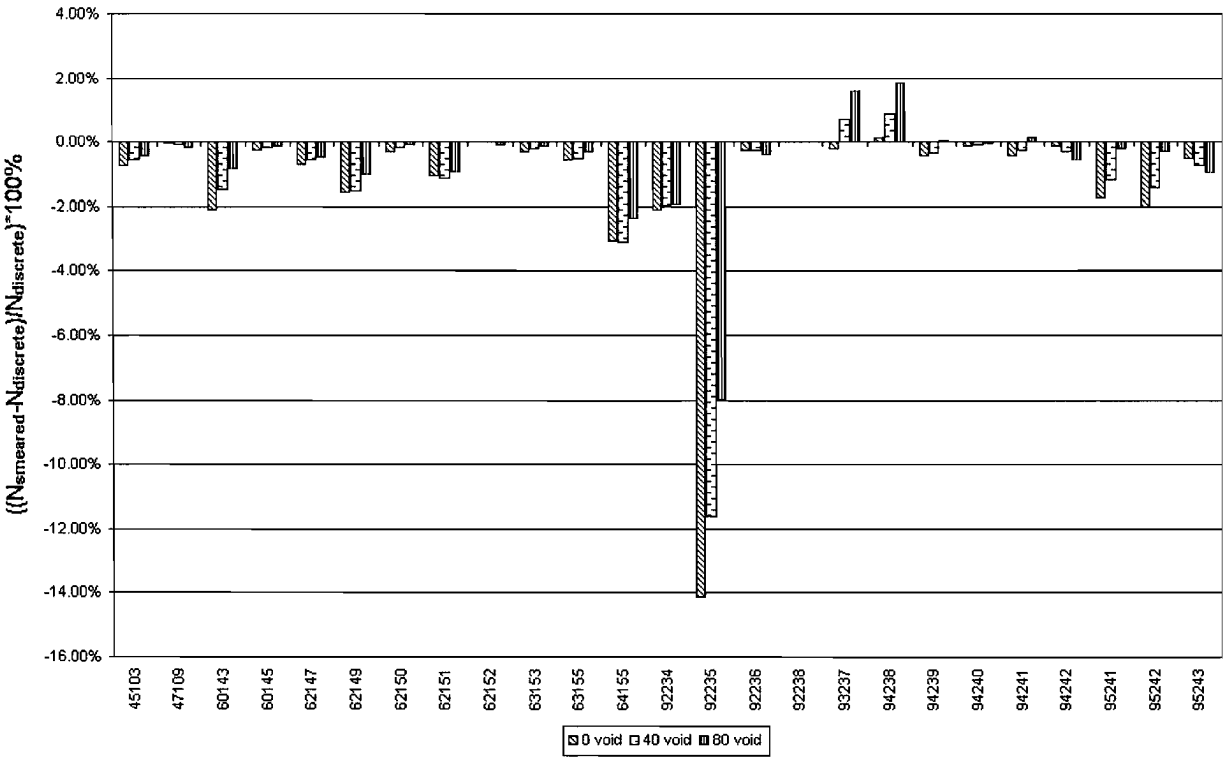

Figure 4-3. Relative difference (to discrete) for isotopic concentrations at EOL,GG1-A 8x8 Fuel Assembly (2.99 wt% U^{235} avg. enr., 3.0 wt% Gd)

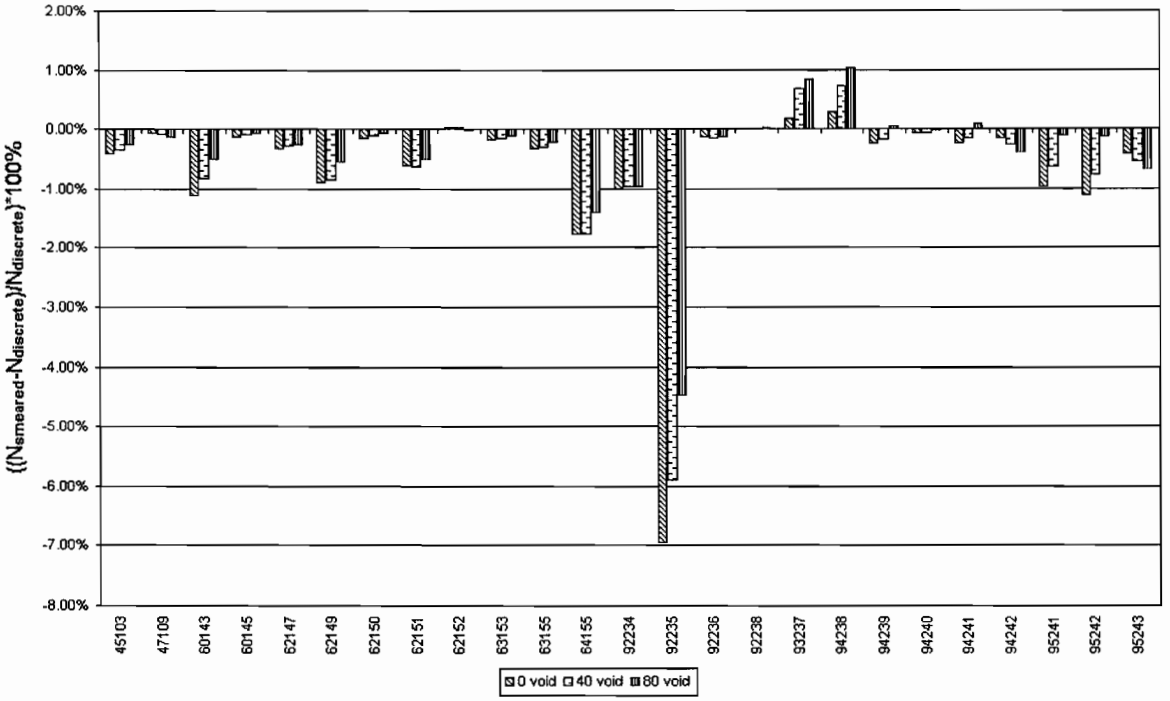

Figure 4-4. Relative difference (to discrete) for isotopic concentrations at EOL, GG1-M 9x9 Fuel Assembly (3.31 wt% U^{235} avg. enr., no Gd)

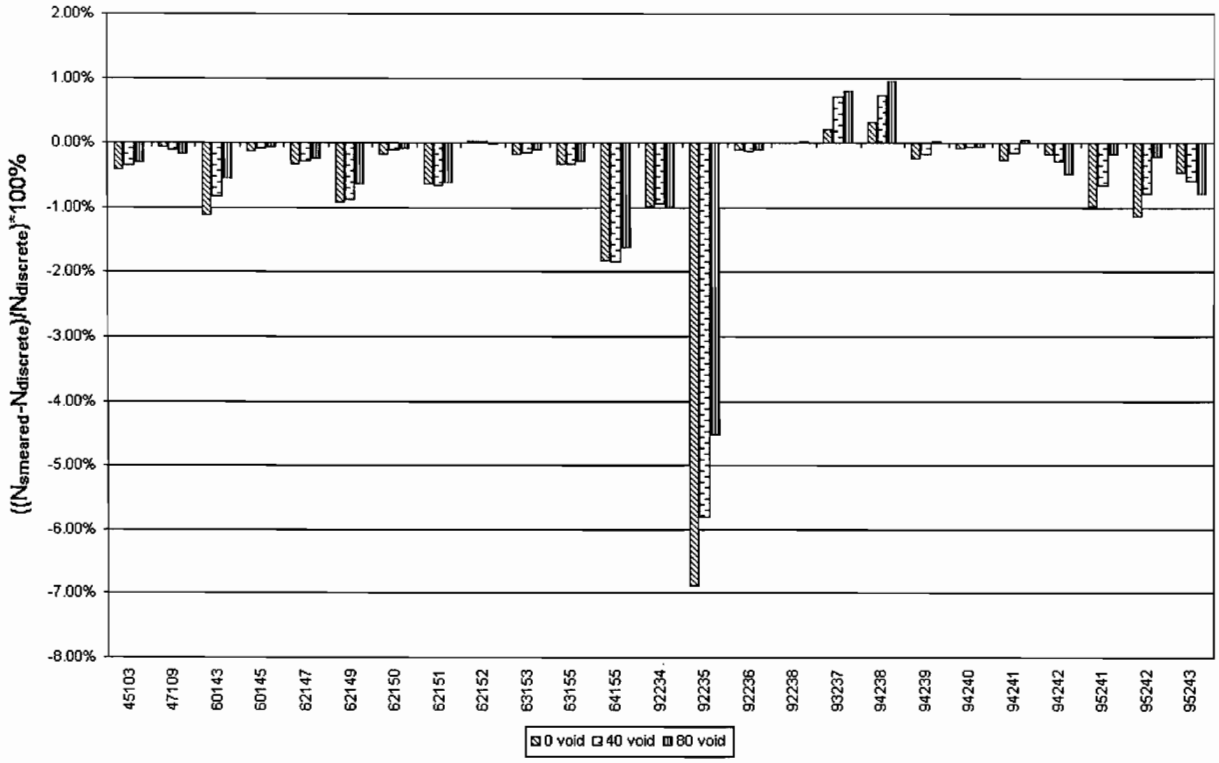

Figure 4-5. Relative difference (to discrete) for isotopic concentrations at EOL, GG1-M 9x9 Fuel Assembly (3.31 wt% U^{235} avg. enr., 3.5 wt% Gd)

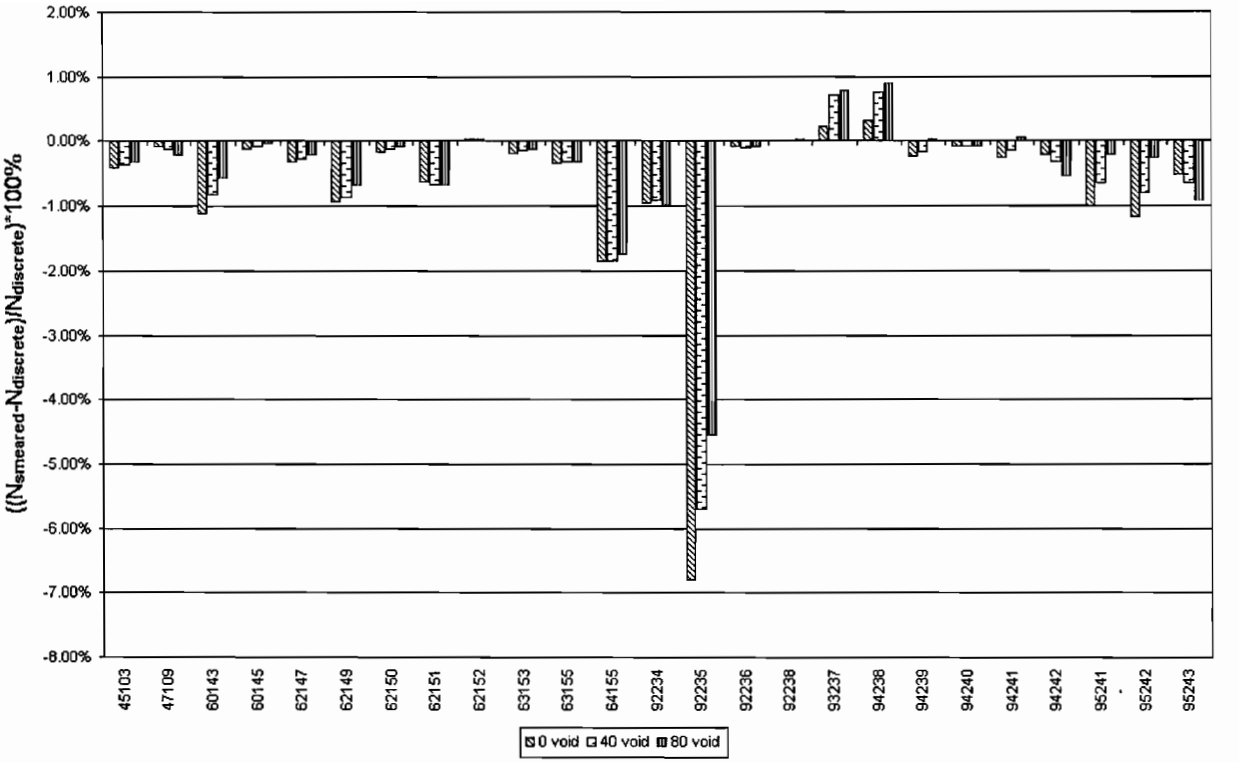

Figure 4-6. Relative difference (to discrete) for isotopic concentrations at EOL, GG1-M 9x9 Fuel Assembly (3.31 wt% U^{235} avg. enr., 7.0 wt% Gd)

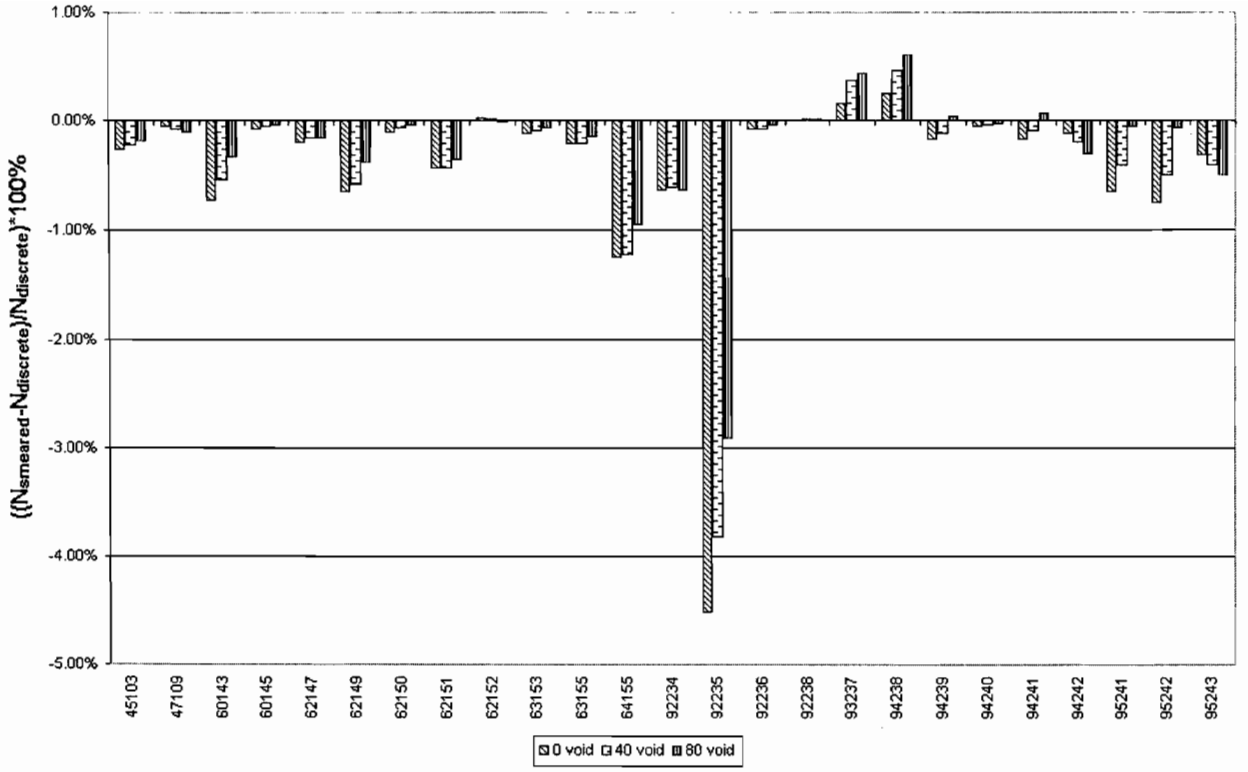

Figure 4-7. Relative difference (to discrete) for isotopic concentrations at EOL, GG1-M 9x9 Fuel Assembly (3.45 wt% U^{235} avg. enr., no Gd)

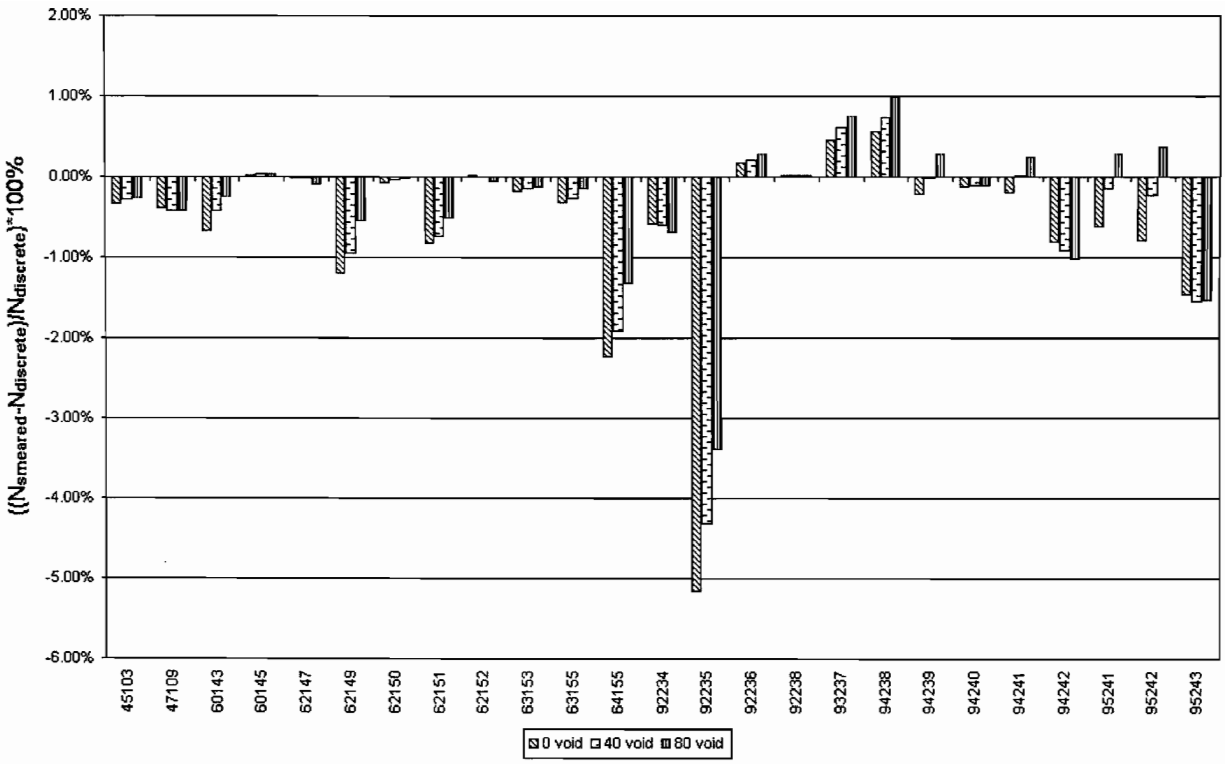

Figure 4-8. Relative difference (to discrete) for isotopic concentrations at EOL, GG1-M 9x9 Fuel Assembly (4.37 wt% U^{235} avg. enr., no Gd)

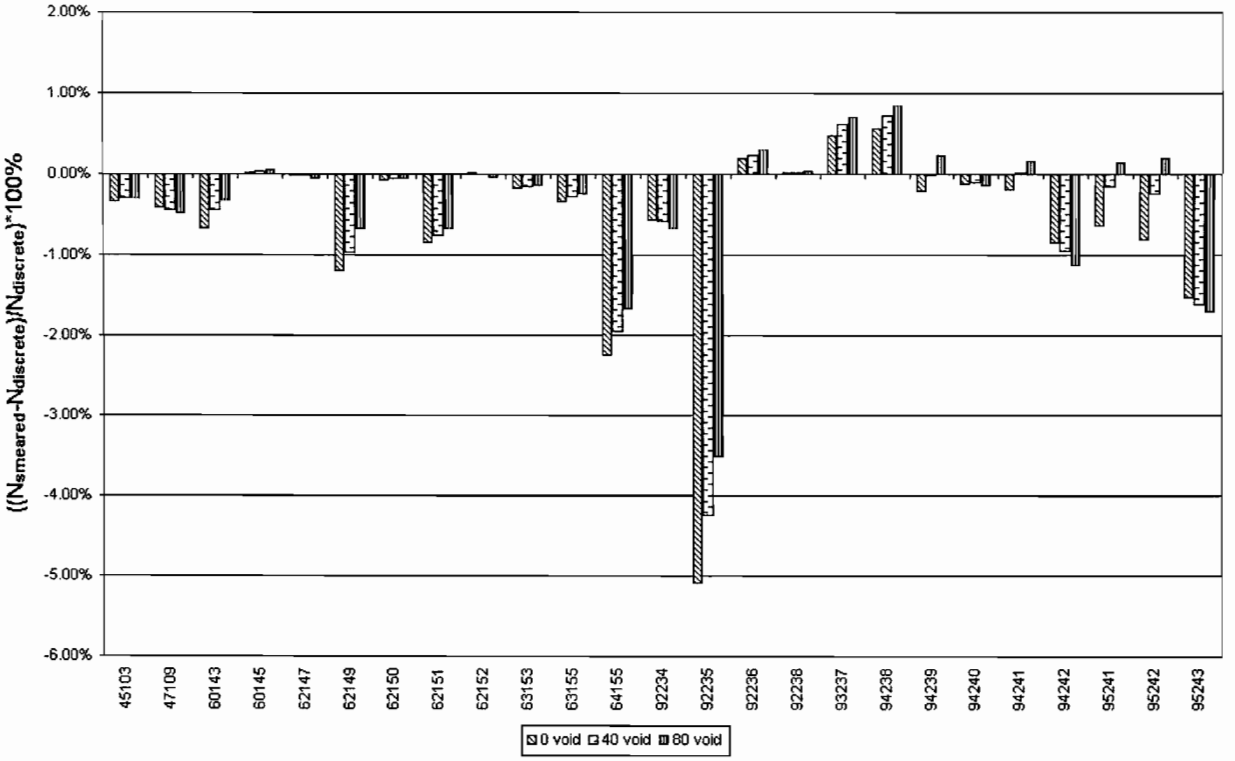

Figure 4-9. Relative difference (to discrete) for isotopic concentrations at EOL, GG1-M 9x9 Fuel Assembly (4.37 wt% U^{235} avg. enr., 3.5 wt% Gd)

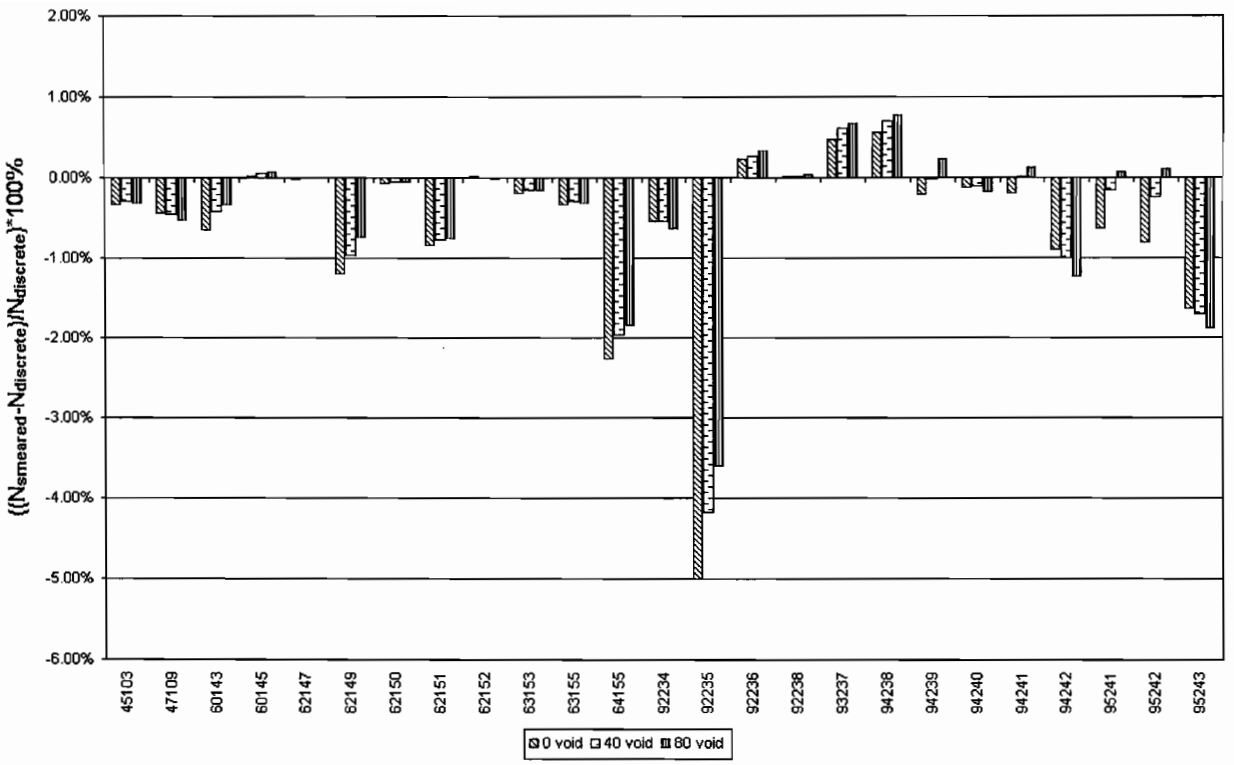

Figure 4-10. Relative difference (to discrete) for isotopic concentrations at EOL, GG1-M 9x9 Fuel Assembly (4.37 wt% U^{235} avg. enr., 7.0 wt% Gd)

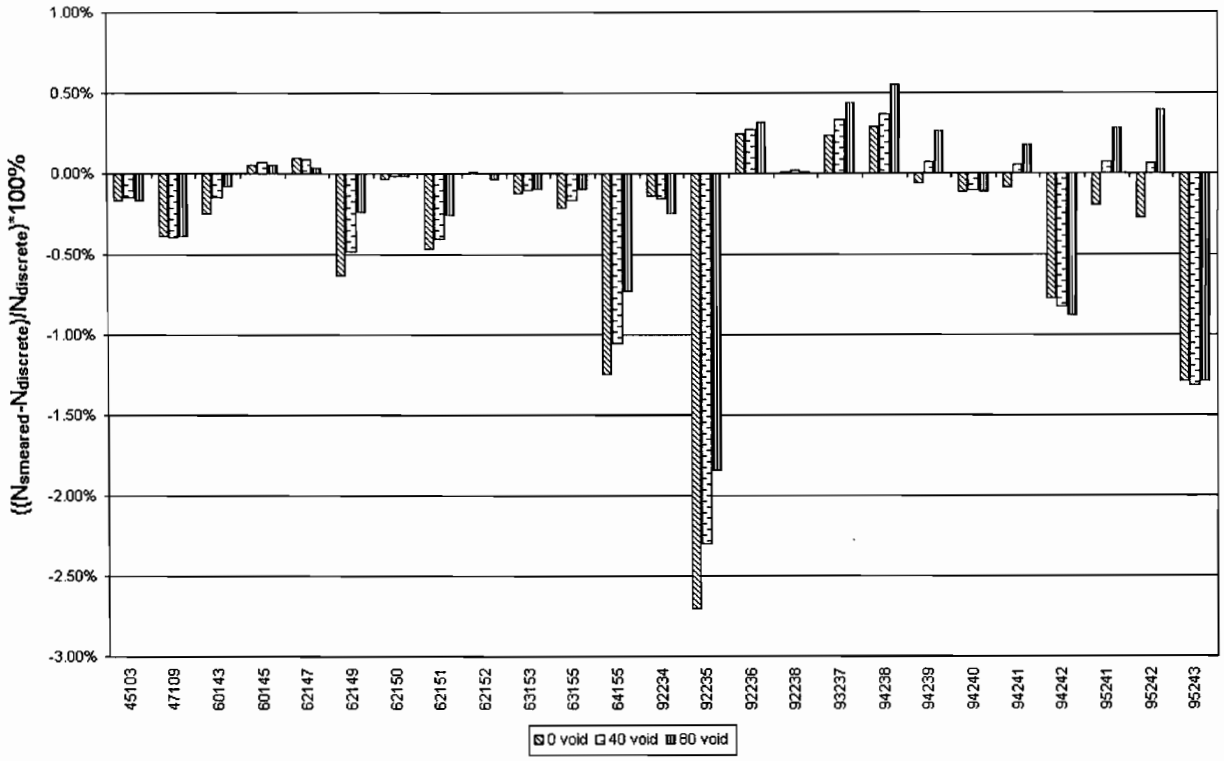

Figure 4-11. Relative difference (to discrete) for isotopic concentrations at EOL, GG1-M 9x9 Fuel Assembly (4.56 wt% U^{235} avg. enr., no Gd)

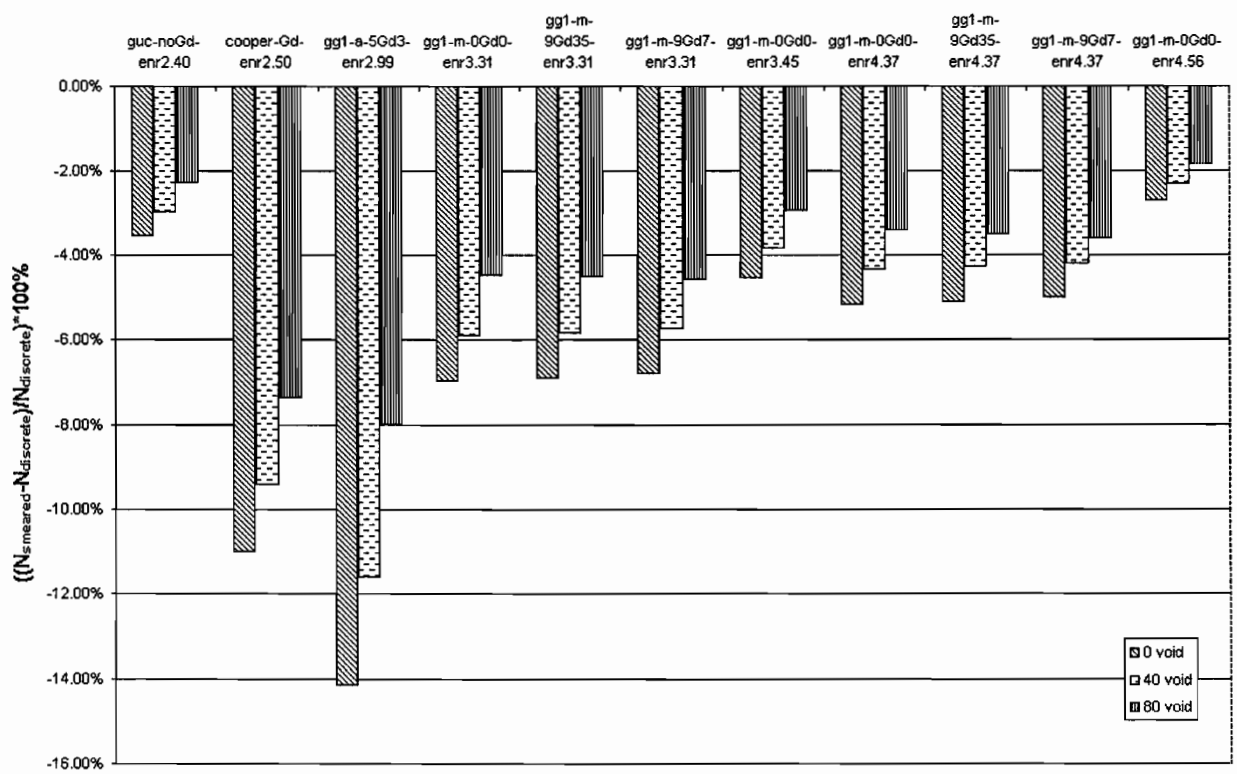

Figure 4-12. Relative difference (to discrete) for U^{235} at EOL

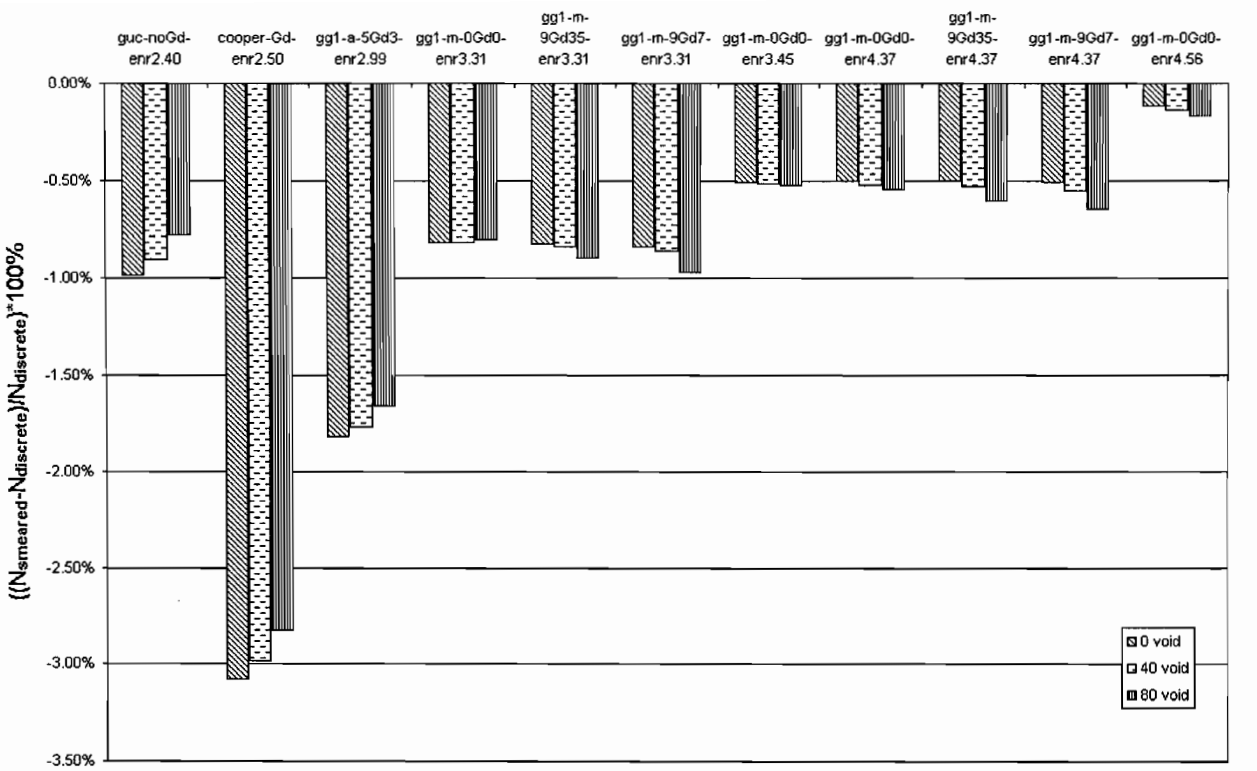

Figure 4-13. Relative difference (to discrete) for U^{235} at MOL (20 GWd/mtU)

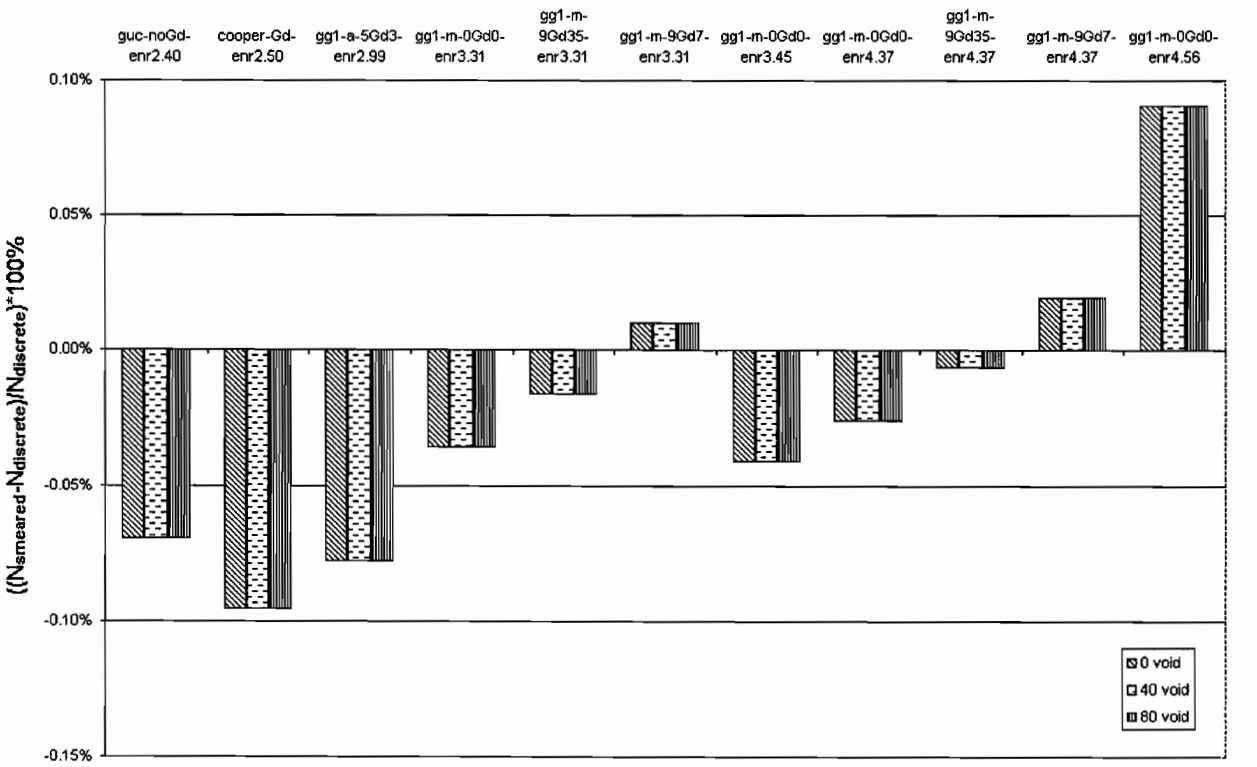

Figure 4-14. Relative difference (to discrete) for U^{235} at BOL (0 GWd/mtU)

The differences in k_{inf} between the smeared and discrete cases as a function of burnup are shown in Figures 4-15 through 4-21. Figures 4-22 and 4-23 show the difference in k_{inf} for all lattice types at BOL and EOL, respectively. Over all burnups and voids, the differences between the smeared and discrete k_{inf} values are between -0.004 and 0.022. At EOL, the smeared model under predicts U^{235} relative to the discrete model. In addition, k_{inf} at EOL is slightly under estimated by the smeared model for all lattice types and at all voids with two exceptions. For the GG1-M lattice, 4.37 wt% U^{235} average enrichment, 9 Gd rods at 7 wt%, 80% void fraction, the smeared model predicts the same k_{inf} as the discrete model, and for the GG1-M lattice, 4.56 wt% U^{235}average enrichment, no Gd, 80% void fraction, the smeared model over predicts k_{inf} by less than 0.0002 Δk_{inf} at EOL. For BOL, where the effects of averaging the enrichments are most pronounced, k_{inf} is over estimated for all lattice types and void conditions by as much as 0.0218 Δk_{inf}.

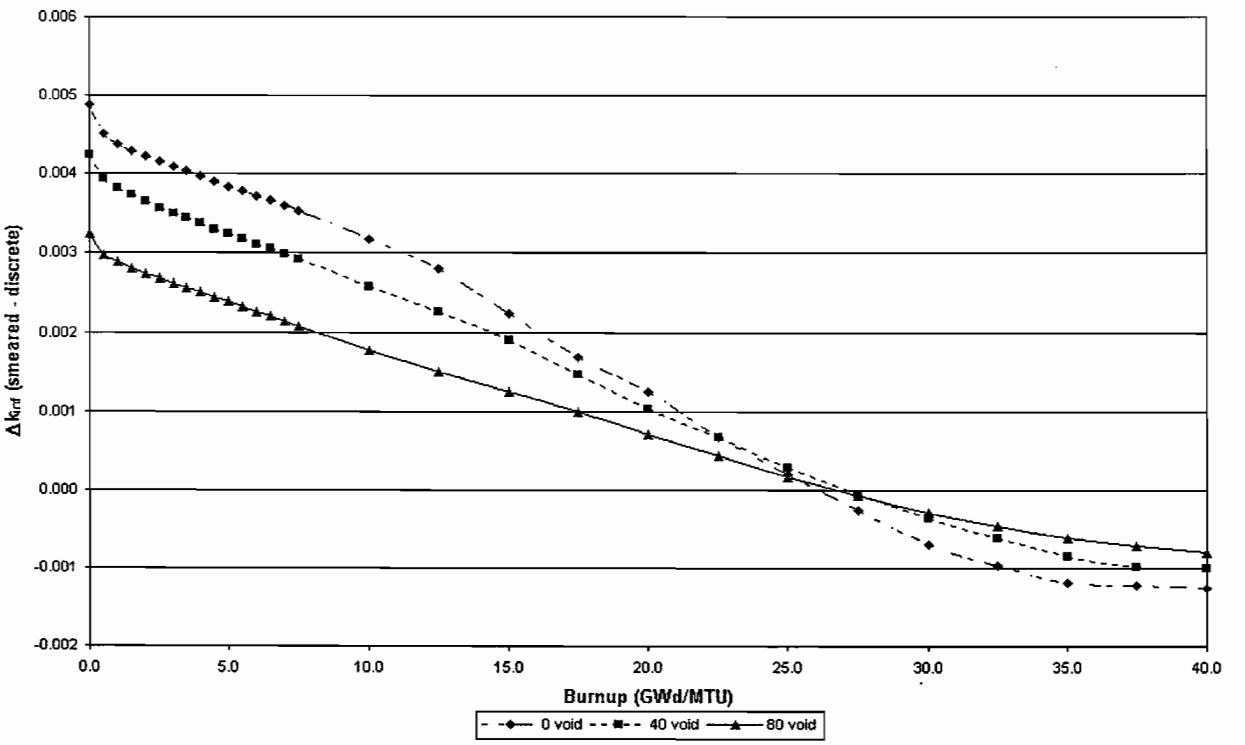

Figure 4-15. Δk_{inf} vs. BU for GUC 6x6 Fuel Assembly (2.40 wt% U^{235} avg. enr., no Gd)

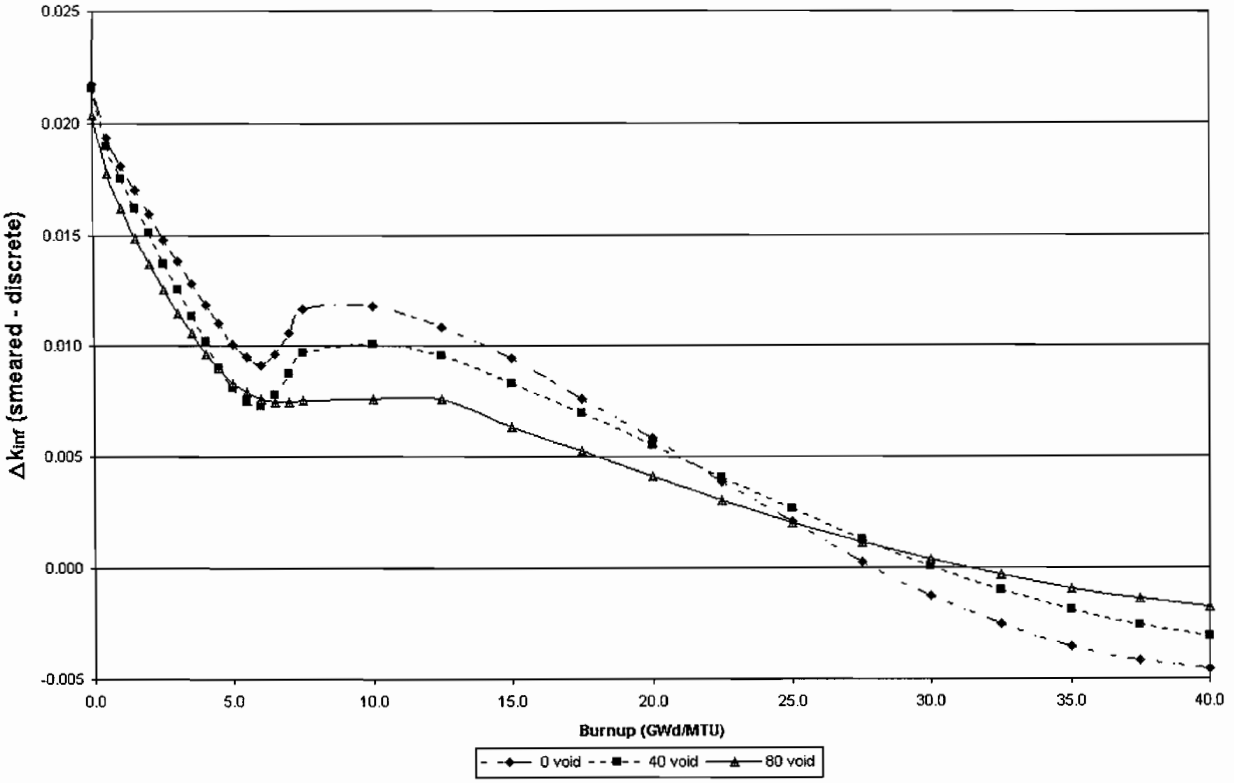

Figure 4-16. Δk_{inf} vs. BU for Cooper 7x7 Fuel Assembly (2.50 wt% U^{235} avg. enr., 3.4 wt% Gd)

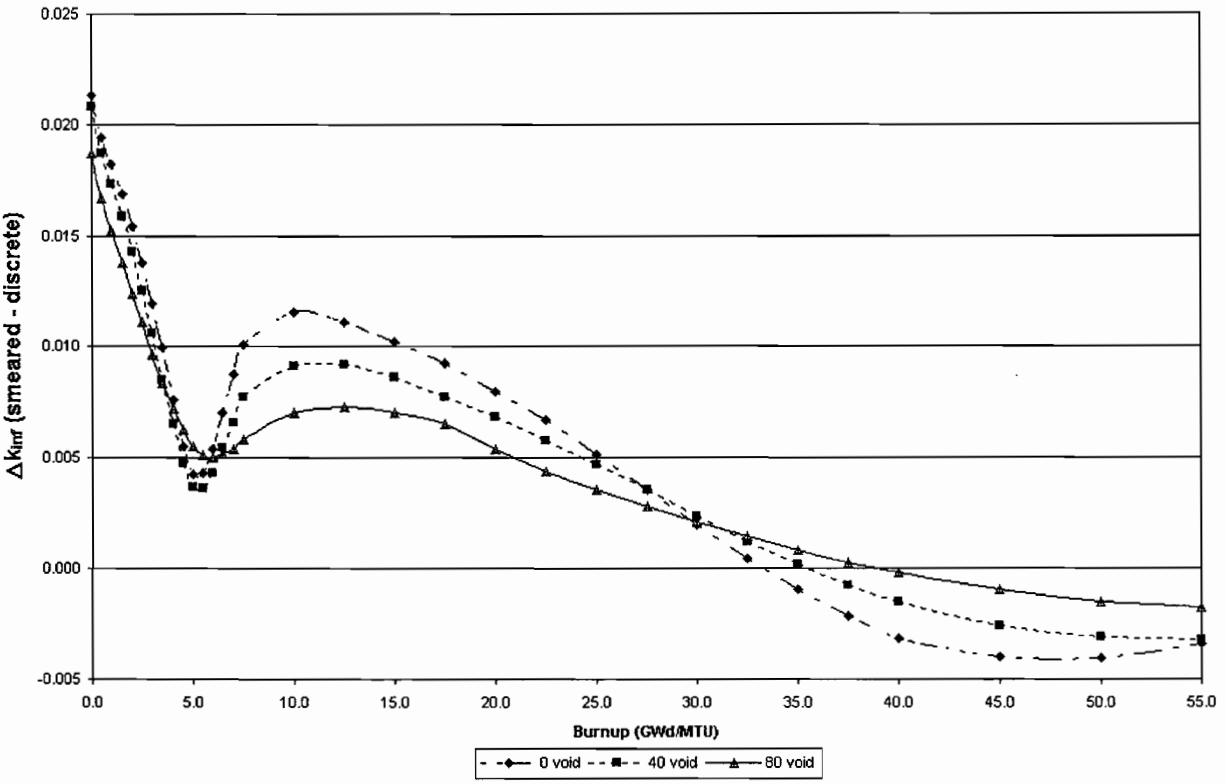

Figure 4-17. Δk_{inf} vs. BU for GG1-A 8x8 Fuel Assembly (2.99 wt% U^{235} avg. enr., 3.0 wt% Gd)

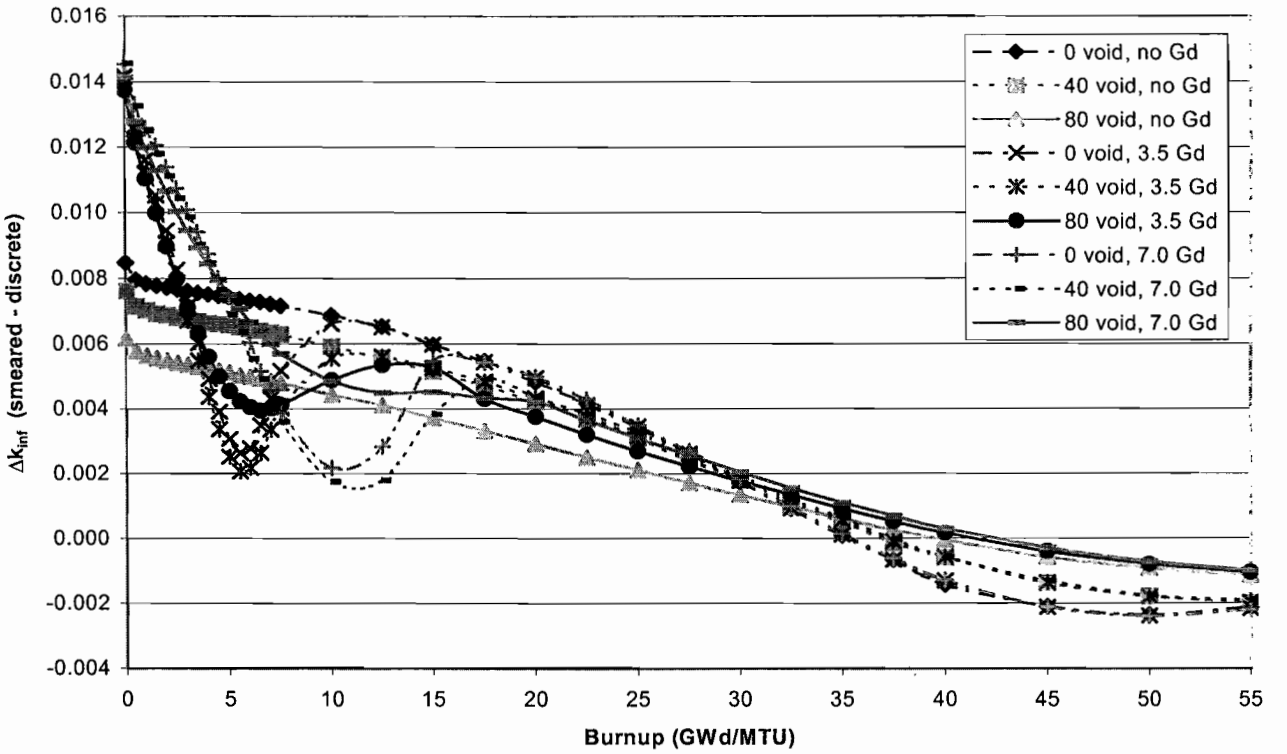

Figure 4-18. Δk_{inf} vs. BU for GG1-M 9x9 Fuel Assembly (3.31 wt% U^{235} avg. enr.)

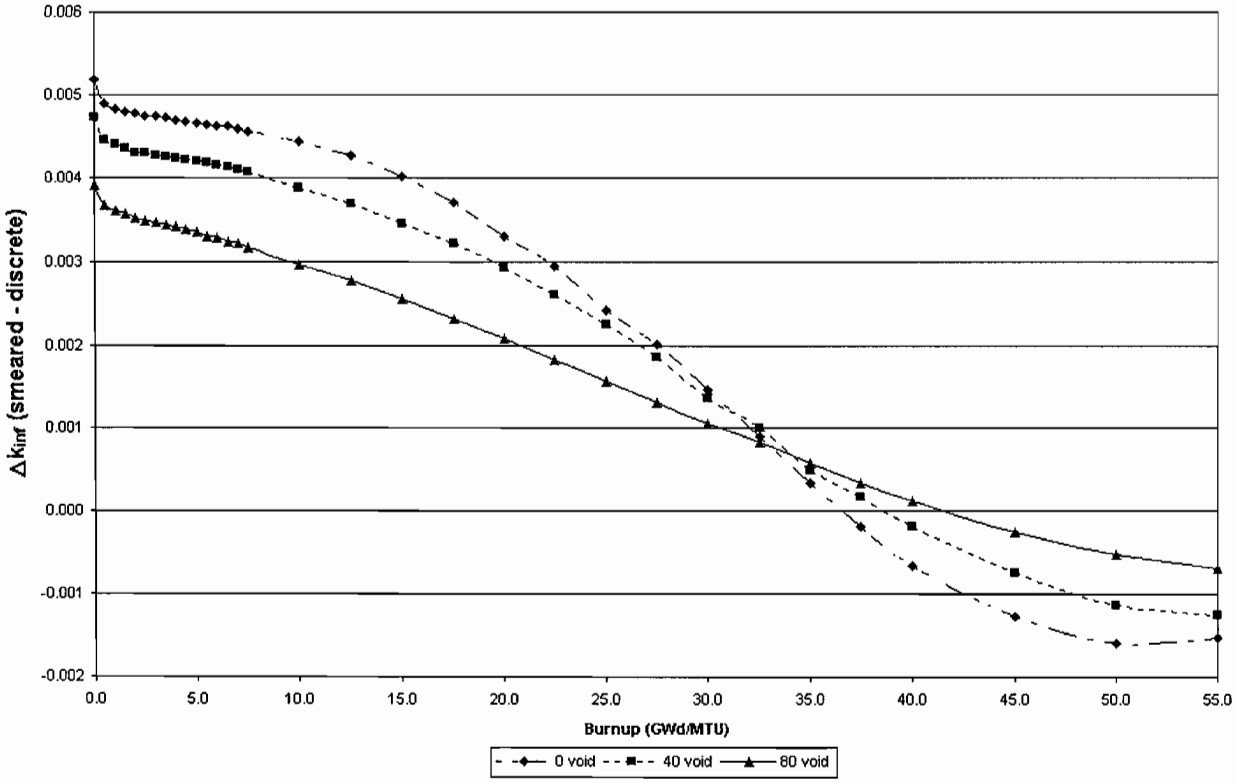

Figure 4-19. Δk_{inf} vs. BU for GG1-M 9x9 Fuel Assembly (3.45 wt% U^{235} avg. enr., no Gd)

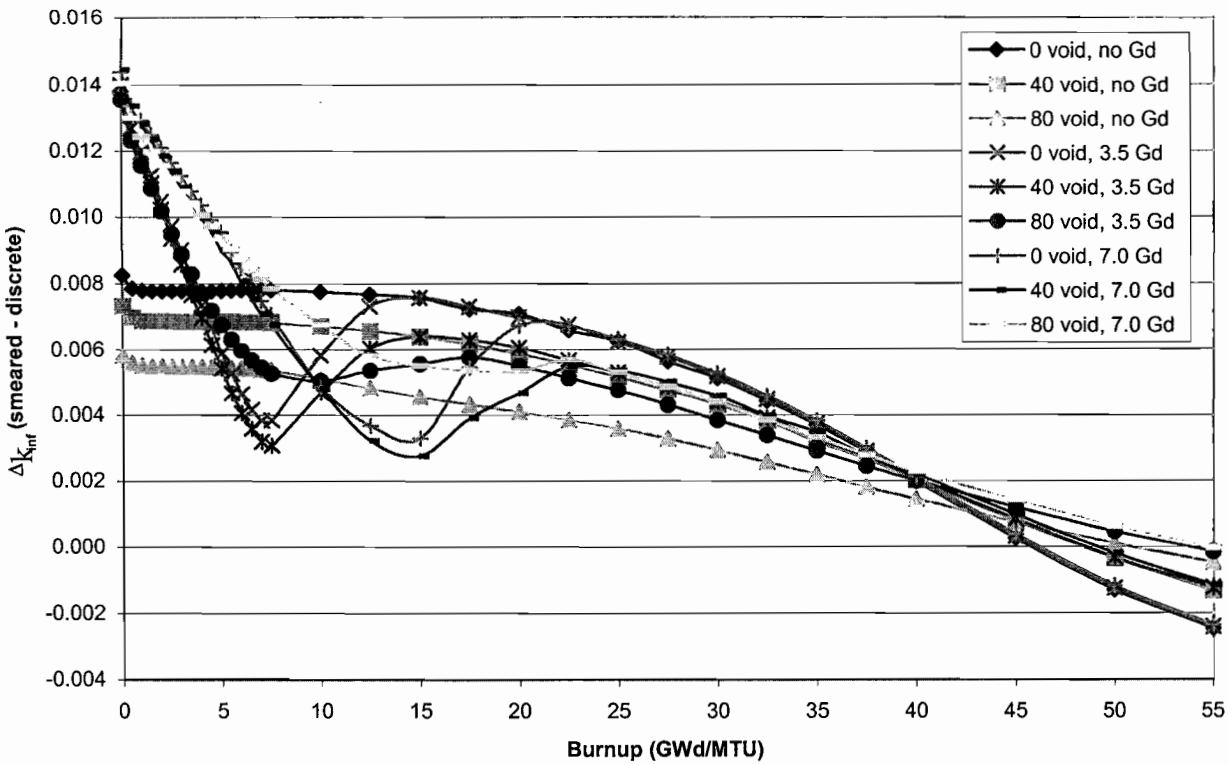

Figure 4-20. Δk_{inf} vs. BU for GG1-M 9x9 Fuel Assembly (4.37 wt% U^{235} avg. enr.)

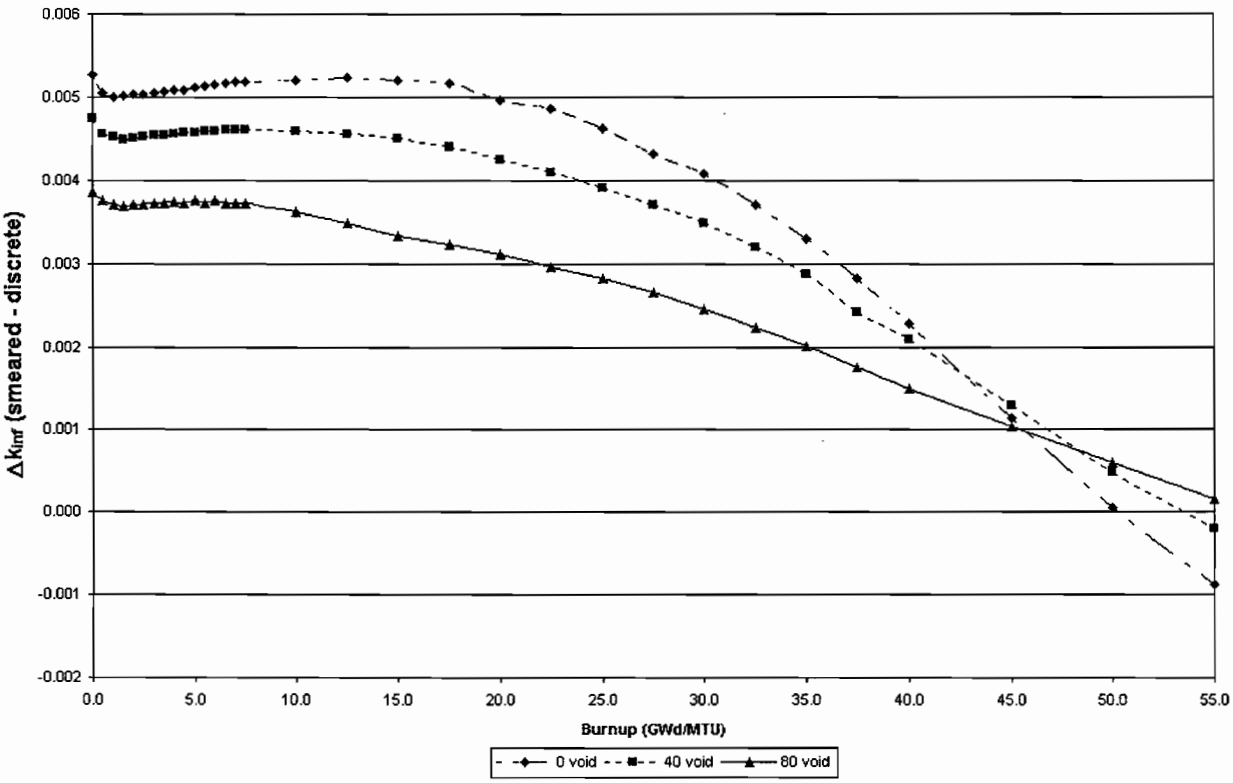

Figure 4-21. Δk_{inf} vs. BU for GG1-M 9x9 Fuel Assembly (4.56 wt% U^{235} avg. enr., no Gd)

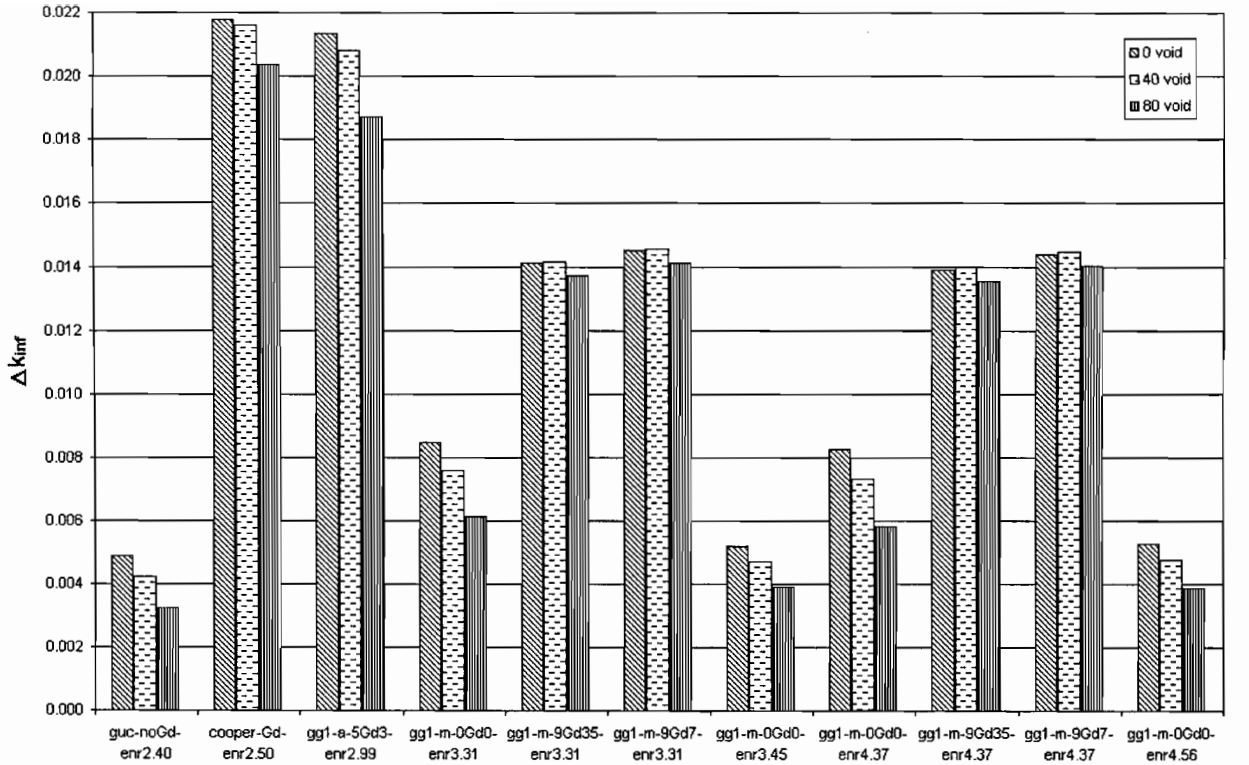

Figure 4-22. Difference between smeared and discrete k_{inf} values at BOL

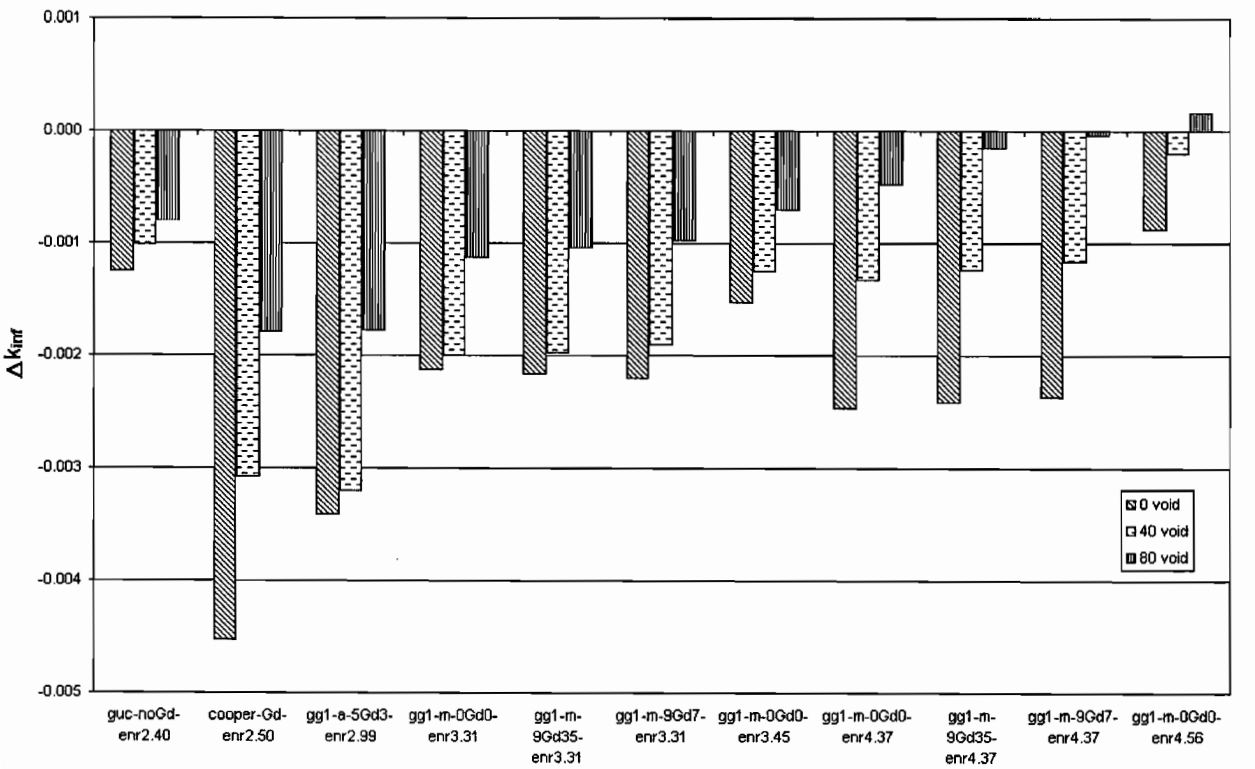

Figure 4-23. Difference between smeared and discrete k_{inf} values at EOL

4.2 BWR STANDARD GADOLINIA ROD PATTERN RESULTS

This section summarizes the results from MO0109SPADRN04.003, Section 5.2 on the comparison of lattice reactivity as a function of burnup for the "design" lattice to the "standard gadolinia position" lattice. Individual maps of standard gadolinia fuel rod locations based on the guidelines given in Table 3-1 is provided in Figures 4-24 through 4-32.

The GRCASMO3 k_{inf} results for 7, 9, and 12 Gd rod lattices were plotted to illustrate trends and effects. In the following figures case "DD" represents the design enrichment pattern with the design gadolinia rod pattern for the lattice. Case "DS" represents the design enrichment pattern with the "standard" gadolinia rod pattern for the lattice. Case "AS" represents the average enrichment pattern with the "standard" gadolinia rod pattern for the lattice. Case DD is used as the benchmark reactivity case. Case DS is compared to case DD to demonstrate the differences in reactivity which can be expected in using only the standardized gadolinia rod patterns while maintaining the design enrichment pattern in MCNP. Case AS is compared to case DD to demonstrate the differences in reactivity that can be expected in using these standardized gadolinia rod patterns in MCNP. The GRCASMO3 results for these cases are plotted in Figures 4-33, 4-34, and 4-35. Figures 4-36, 4-37, and 4-38 plot the differences in k_{inf} for the DD-DS and DD-AS cases, respectively.

Case AD in Figures 4-35 and 4-38 represents the average enrichment pattern with the design Gd rod pattern for the lattice. The comparison between Cases DD and AD show only the effect on reactivity of using an average enrichment value.

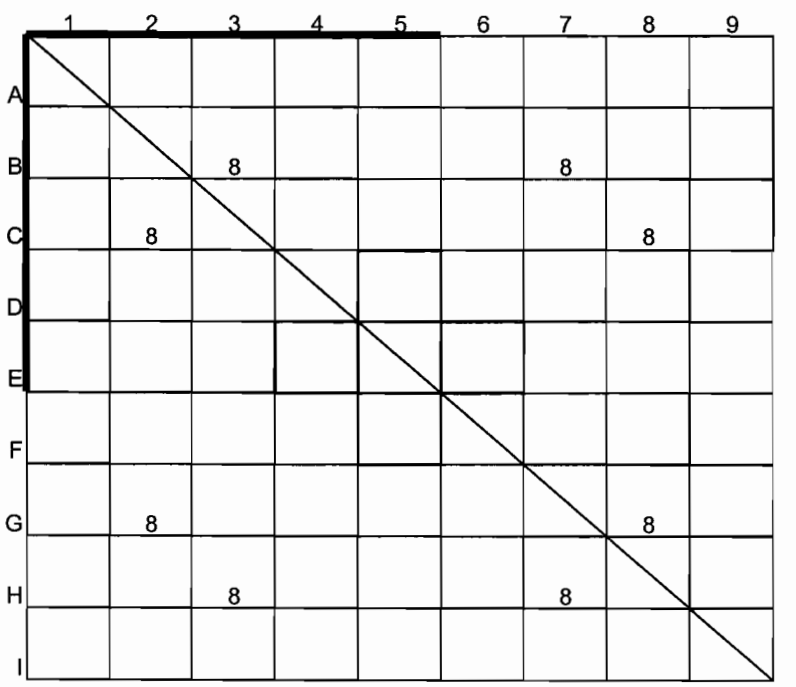

Figure 4-24. Standard Gadolinia Fuel Rod Lattice Map for 9x9-5 8Gd Fuel

	1	2	3	4	5	6	7	8	9
A									
B		9			9			9	
C									
D									
E		9						9	
F									
G								9	
H		9			9		9		
I									

Figure 4-25. Standard Gd fuel rod lattice map for 9x9-5 9 Gd fuel

	1	2	3	4	5	6	7	8	9
A									
B			10		10			10	
C		10							
D									
E		10						10	
F									
G								10	
H		10			10		10		
I									

Figure 4-26. Standard Gd fuel rod lattice map for 9x9-5 10 Gd fuel

	1	2	3	4	5	6	7	8
A								
B		7			7			
C							7	
D								
E		7						
F							7	
G			7			7		
H								

Figure 4-27. Standard Gadolinia Fuel Rod Lattice Map for 8x8-4 7Gd Fuel

	1	2	3	4	5	6	7	8
A								
B			8			8		
C		8					8	
D								
E								
F		8					8	
G			8			8		
H								

Figure 4-28. Standard Gadolinia Fuel Rod Lattice Map for 8x8-4 8Gd Fuel

	1	2	3	4	5	6	7	8
A								
B		9			9		9	
C								
D							9	
E		9						
F							9	
G		9		9		9		
H								

Figure 4-29. Standard Gadolinia Fuel Rod Lattice Map for 8x8-4 9Gd Fuel

	1	2	3	4	5	6	7	8
A								
B			10		10		10	
C		10						
D							10	
E		10						
F							10	
G		10		10		10		
H								

Figure 4-30. Standard Gadolinia Fuel Rod Lattice Map for 8x8-4 10Gd Fuel

	1	2	3	4	5	6	7	8
A								
B		11			11		11	
C								
D							11	
E		11				11		
F					11		11	
G		11		11		11		
H								

Figure 4-31. Standard Gadolinia Fuel Rod Lattice Map for 8x8-4 11Gd Fuel

	1	2	3	4	5	6	7	8
A								
B			12		12		12	
C		12						
D							12	
E		12				12		
F					12		12	
G		12		12		12		
H								

Figure 4-32. Standard Gadolinia Fuel Rod Lattice Map for 8x8-4 12Gd Fuel

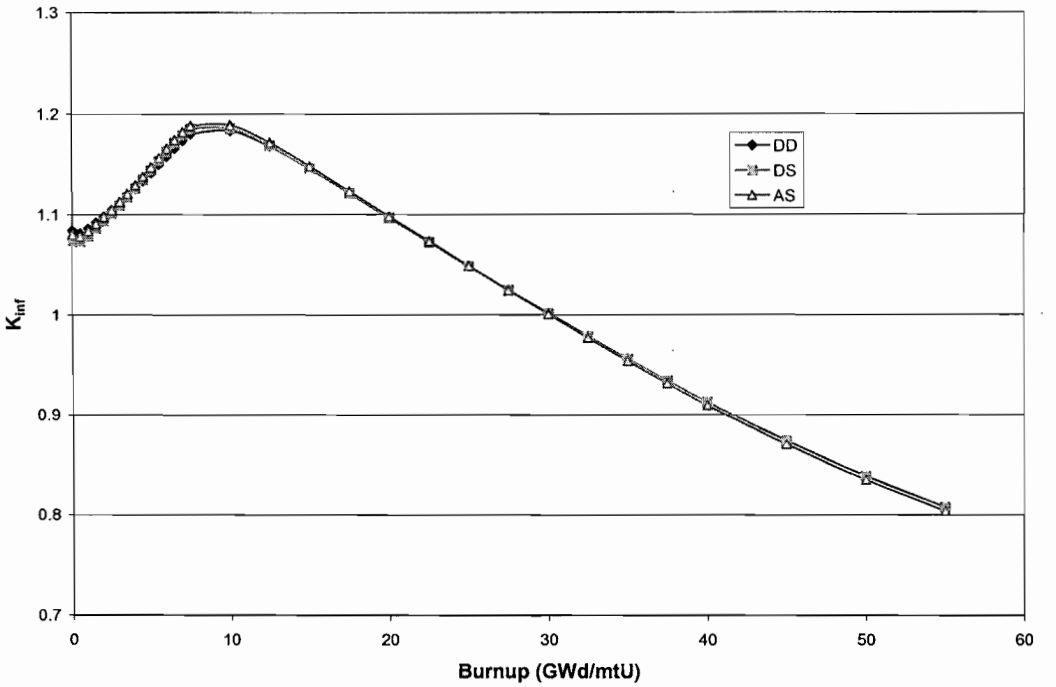

Figure 4-33. GRCASMO3 Δk_{inf} Results for 7 Gadolinia Rod Lattice

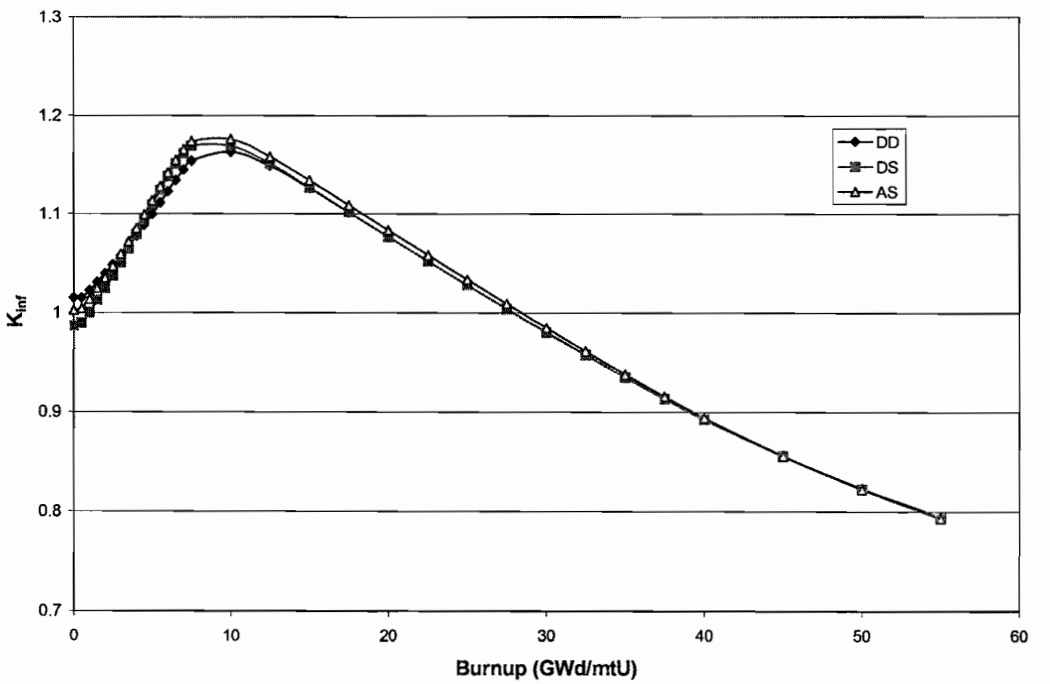

Figure 4-34. GRCASMO3 Δk_{inf} Results for 9 Gadolinia Rod Lattice

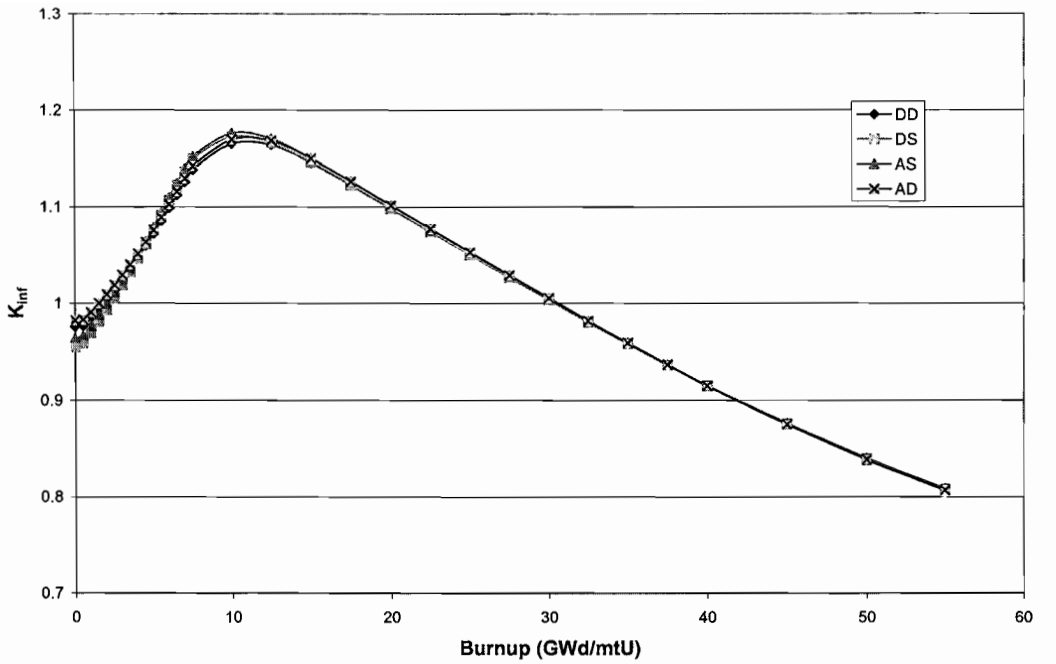

Figure 4-35. GRCASMO3 k_{inf} Results for 12 Gadolinia Rod Lattice

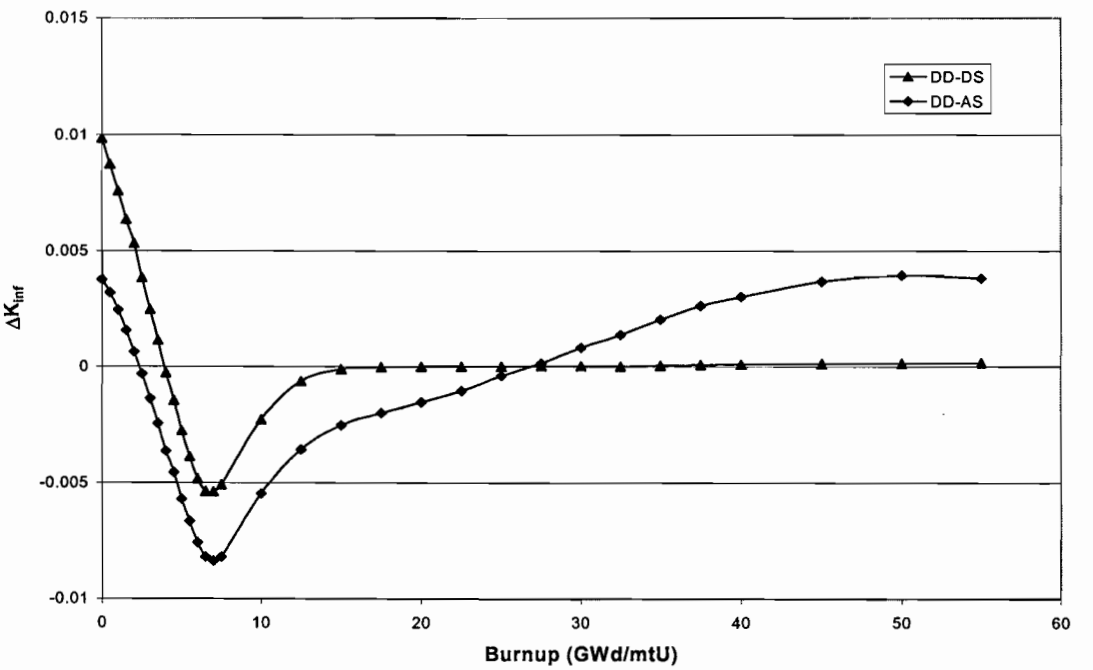

Figure 4-36. GRCASMO3 Δk_{inf} Results for 7 Gadolinia Rod Lattice

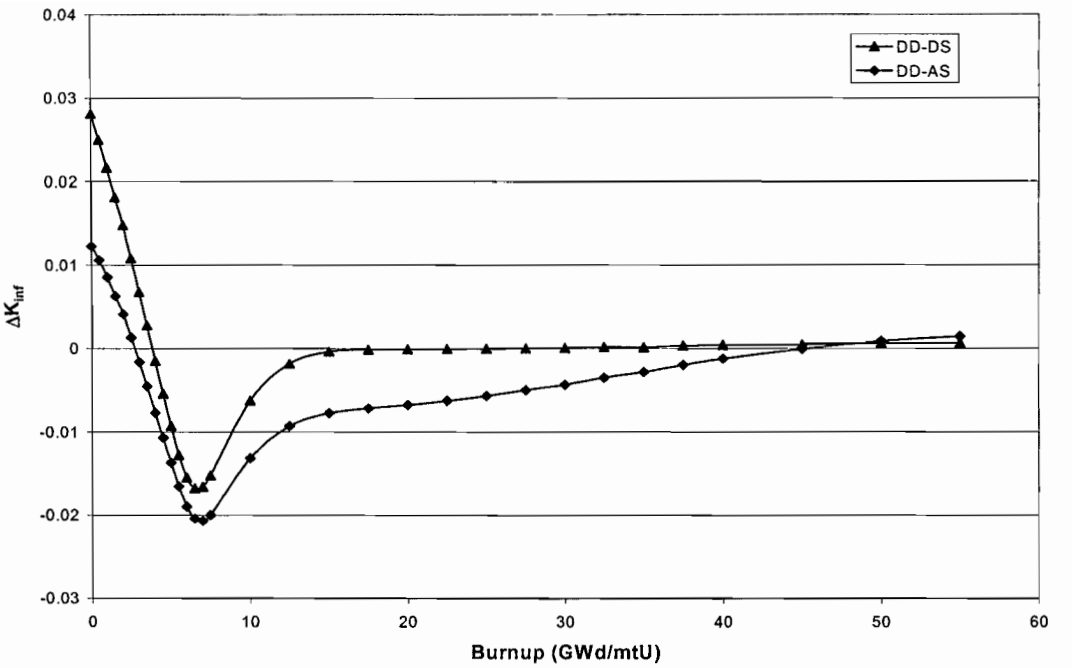

Figure 4-37. Delta GRCASMO3 k_{inf} Results for 9 Gadolinia Rod Lattice

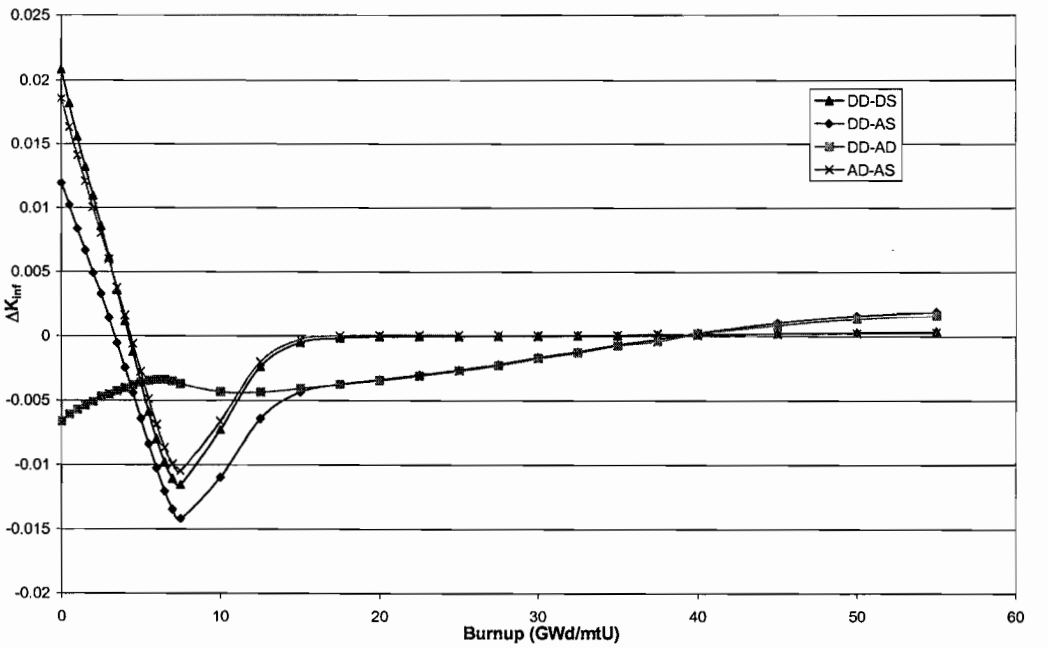

Figure 4-38. Delta GRCASMO3 k_{inf} Results for 12 Gadolinia Rod Lattice

4.3 PWR BURNABLE POISON EFFECTS RESULTS

This section provides a summary of information from MO0109SPADRN04.003, Section 5.5.

Plots of the results of the IBA (Figures 4-39 through 4-46) and BPR (Figures 4-47 through 4-50) analyses show the reactivity difference of "poisoned" and "unpoisoned" as a function of burnup for fuel with the same initial enrichment. In all cases analyzed, the results indicate that the reactivity effect from burnable absorbers on PWR SNF is generally small and well behaved (smoothly varying as a function of fuel burnup), and can be well characterized.

The k_{inf} for gadolinia-bearing fuel is always less than that for the non-gadolinia fuel. The difference, as shown in Figure 4-40, is less than 0.2 % Δk_{inf} near 45 GWd/mtU.

The k_{inf} for erbia-bearing fuel is also always less than that for the non-erbia fuel. The difference, as shown in Figure 4-42, is approximately 1 % Δk_{inf} near 45 GWd/mtU. The k_{inf} for IFBA-bearing fuel became greater than that for the non-IFBA fuel by less than 0.2 % Δk_{inf} near 35 GWd/mtU where it began to decrease with further burnup, as shown in Figure 4-44.

The case for B_4C-Al_2O_3 rods is different than the other IBA cases because the poison rods actually replace uranium fuel rods in the assembly. A 16x16 CE-design fuel assembly containing 12 B_4C-Al_2O_3 rods was analyzed using the same depletion method used for the other IBAs. The difference in k_{inf} varied, almost monotonically, over the complete depletion range of 0 to 45 GWd/mtU from approximately –0.14 Δk_{inf} to almost –0.002 Δk_{inf} as shown in Figure 4-46.

For Pyrex BPRs, the effect on k_{inf} shown in Figure 4-48 is approximately 2 % Δk_{inf} at the time of removal and diminishes slightly with further irradiation. For WABAs irradiated for one cycle, the effect on k_{inf} shown in Figure 4-50 is less than 1 % Δk_{inf} at the time of removal and diminishes slightly with further irradiation. Both Pyrex and WABA results, plotted in Figures 4-47 through 4-50, show similar neutronic behavior.

For Ag-In-Cd control rods, the effect on k_{inf} is shown in Figure 4-51. The effect on Δk_{inf} shown in Figure 4-52 is approximately 3 % Δk_{inf} after depletion to 15 GWd/mtU, the time of removal, and diminishes slightly with further irradiation. This case is not expected to occur in actual reactor operation but is included to illustrate the expected effects on reactivity from depleting with a control rod inserted for part of the fuel's in-core operating history.

For Figures 4-40, 4-42, and 4-44, the curves at the right are blow-ups of the left curves and correspond to the right y-axis. These curves were included to show the magnitude of the changes at higher burnups where the differences were smaller than at BOL.

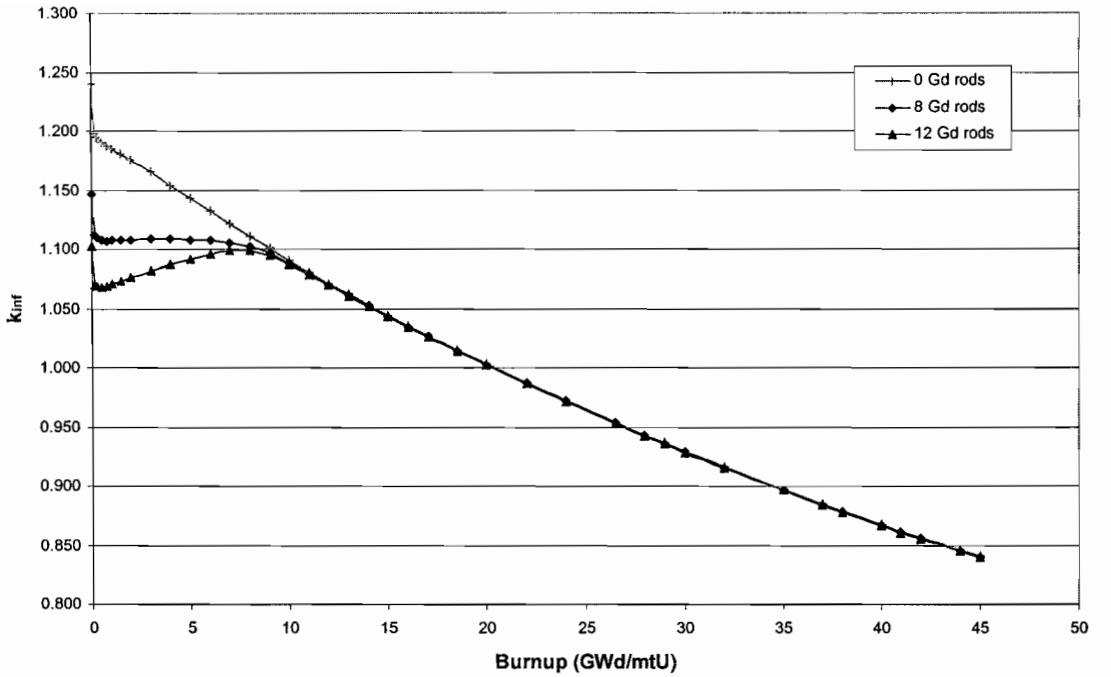

Figure 4-39. GRCASMO3 k_{inf} Results for Gadolinia Integral BA Rods

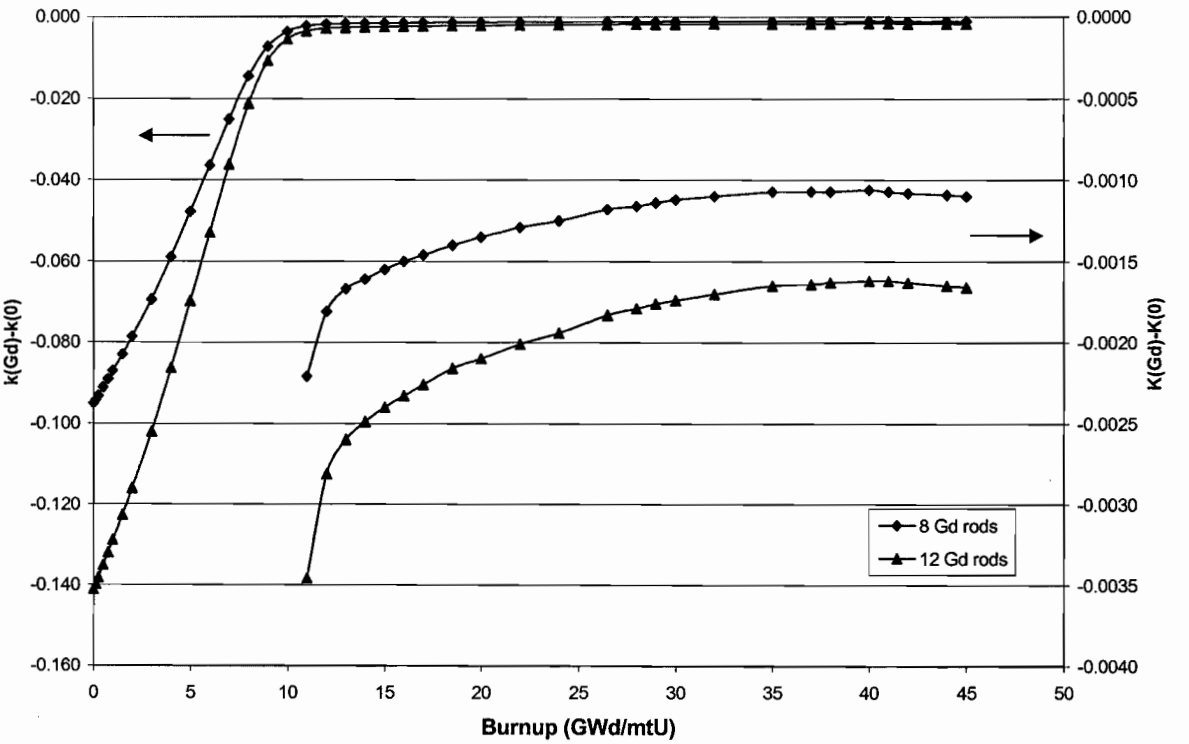

Figure 4-40 Δk_{inf} Results for Gadolinia Integral BA Rods at Cold Cask Conditions

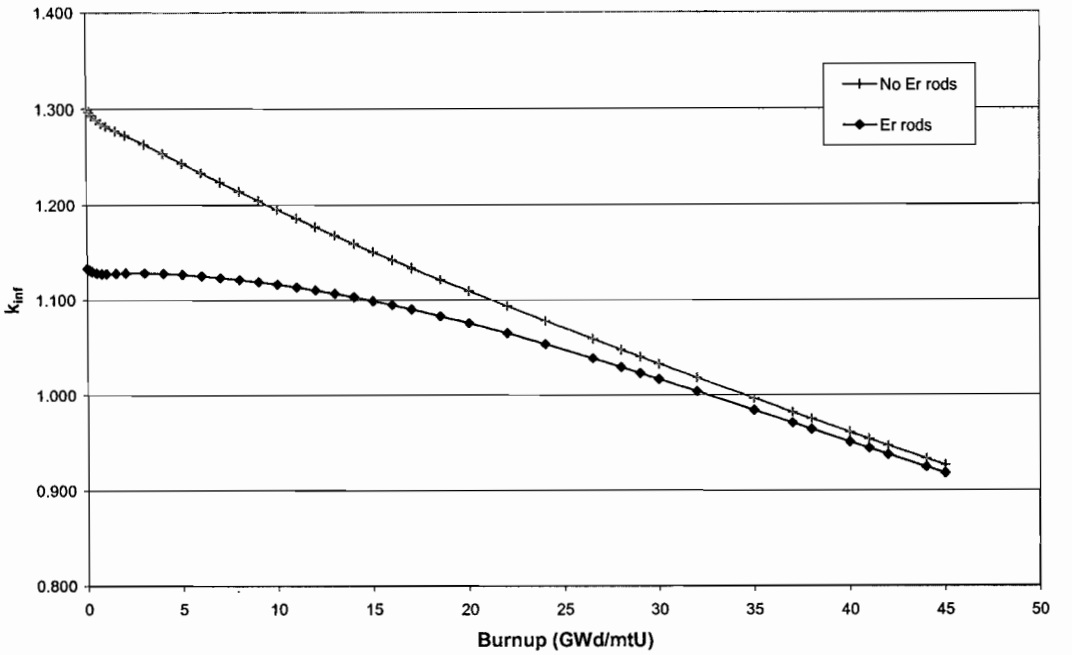

Figure 4-41. GRCASMO3 k_{inf} Results for Erbia Integral BA Rods

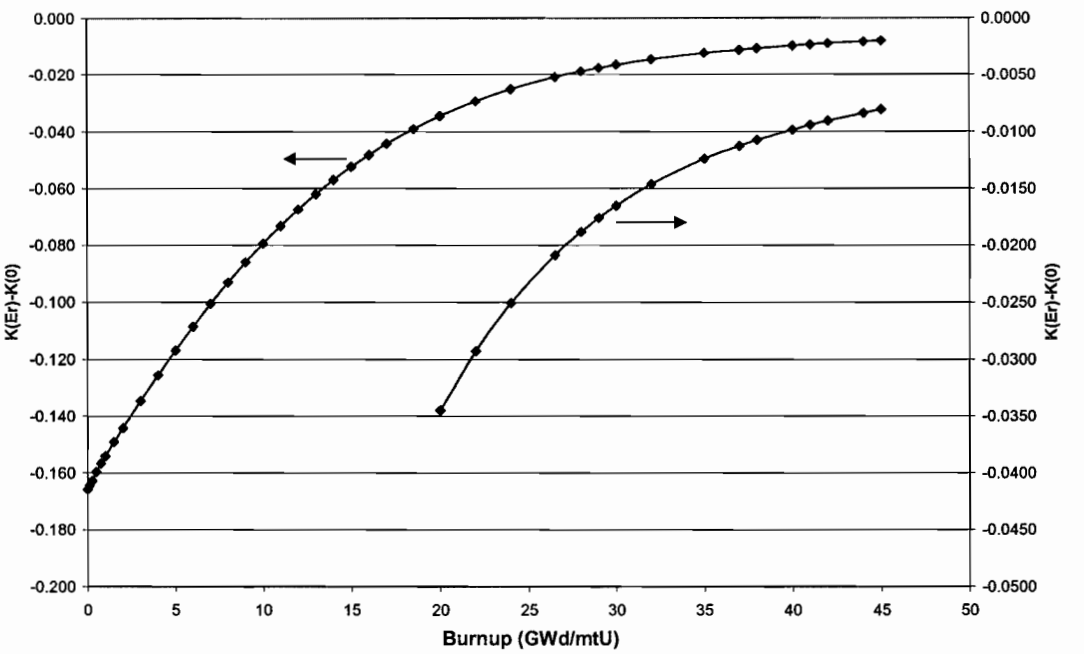

Figure 4-42. Δk_{inf} Results for Erbia Integral BA Rods at Cold Cask Conditions

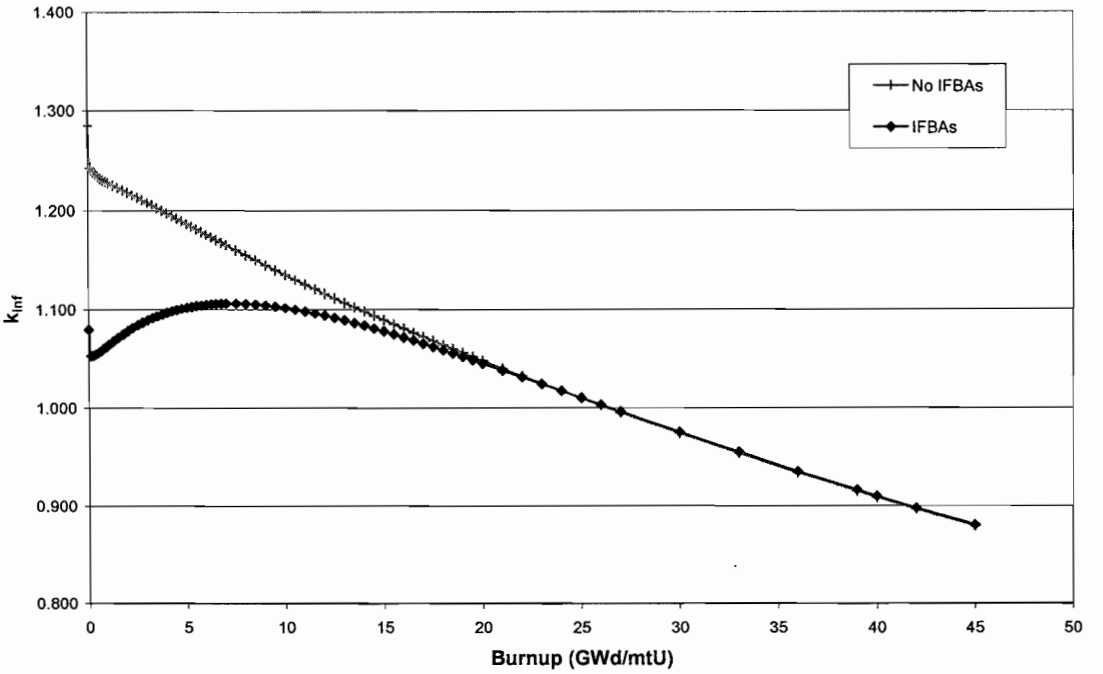

Figure 4-43. GRCASMO3 k_{inf} Results for IFBA Integral BA Rods

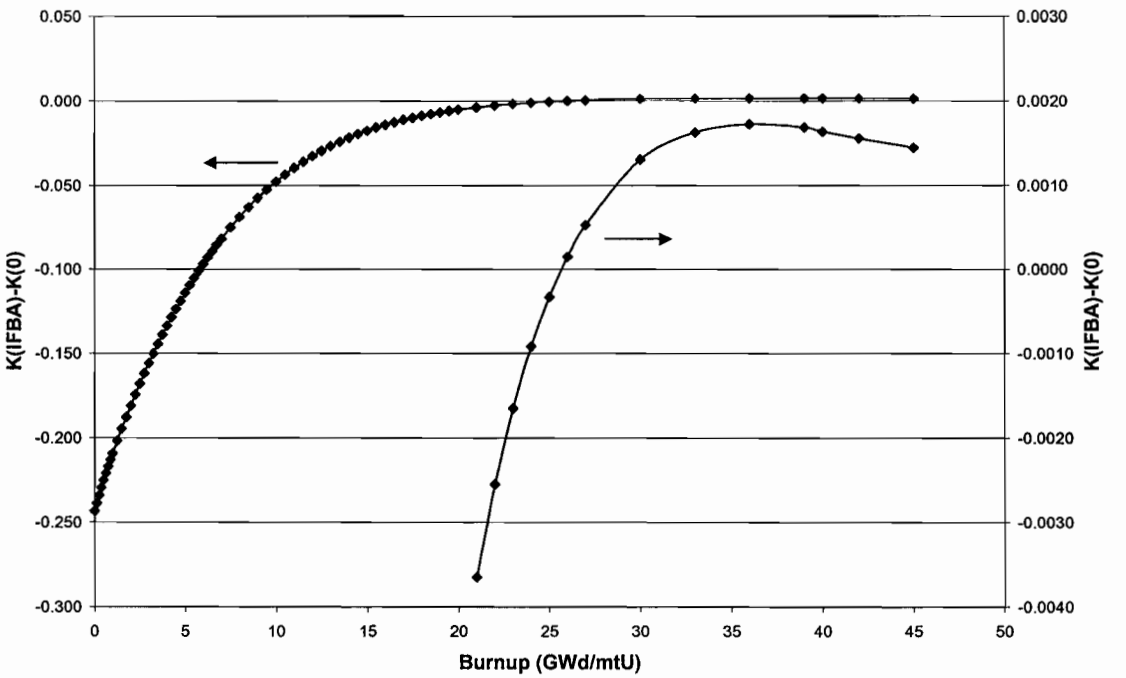

Figure 4-44. ΔK_{inf} Results for IFBA Integral BA Rods at Cold Cask Conditions

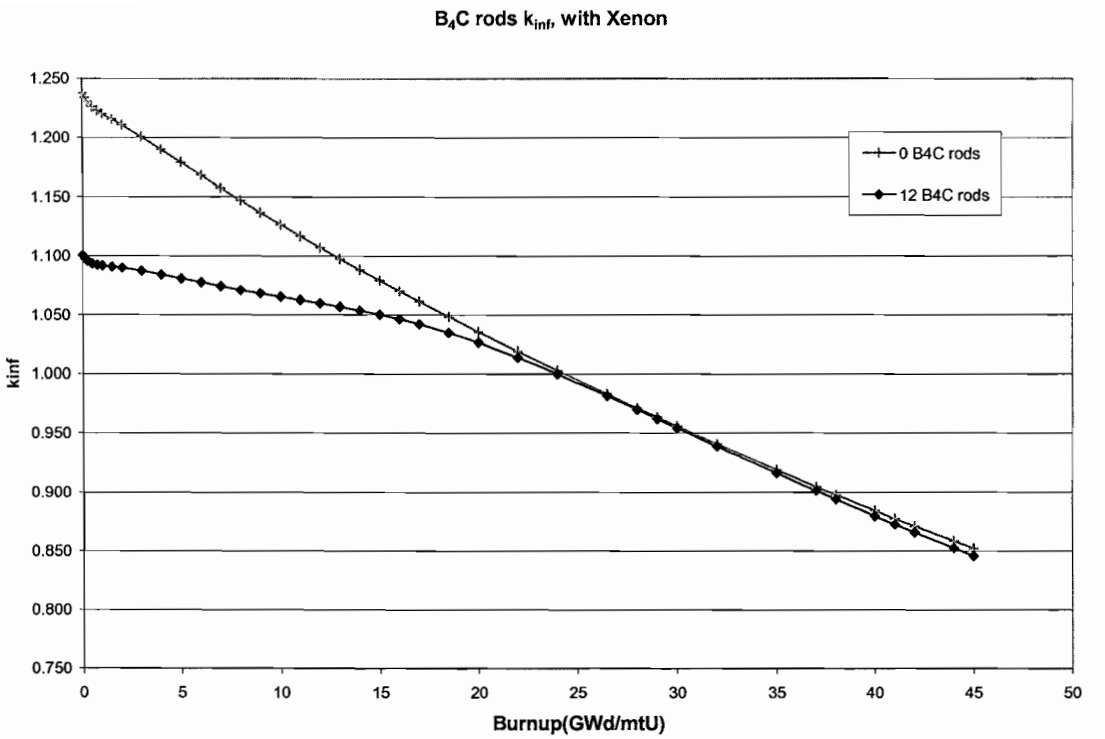

Figure 4-45. GRCASMO3 k_{inf} Results for B_4C Integral BA Rods

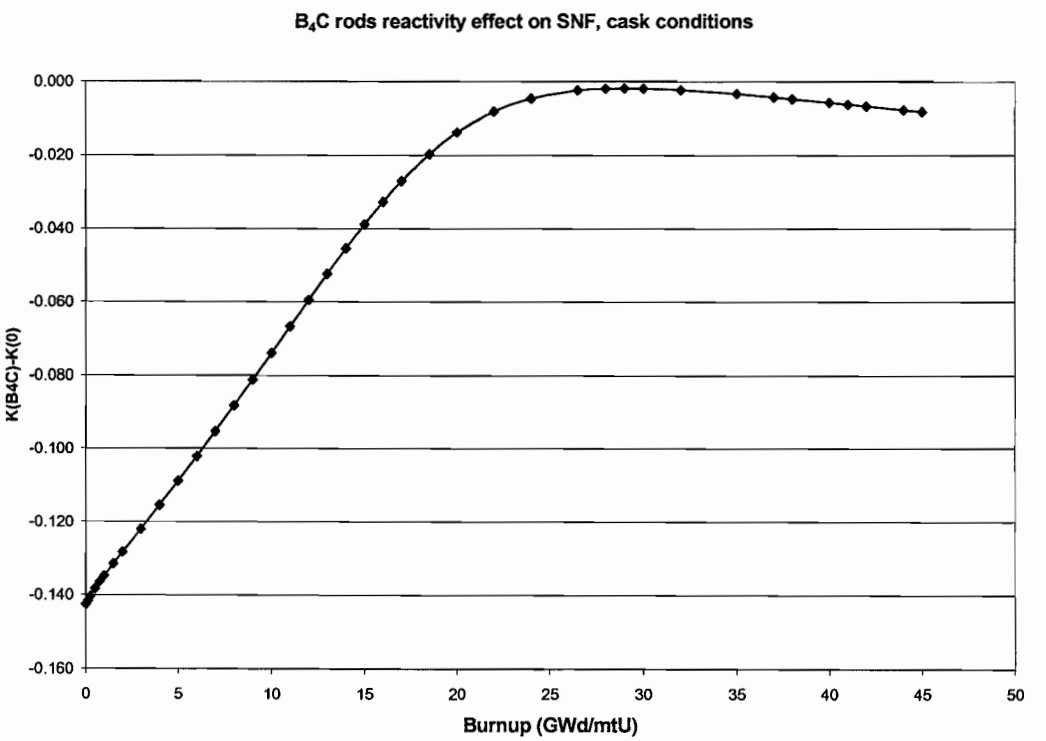

Figure 4-46. Δk_{inf} Results for B_4C Integral BA Rods at Cold Cask Conditions

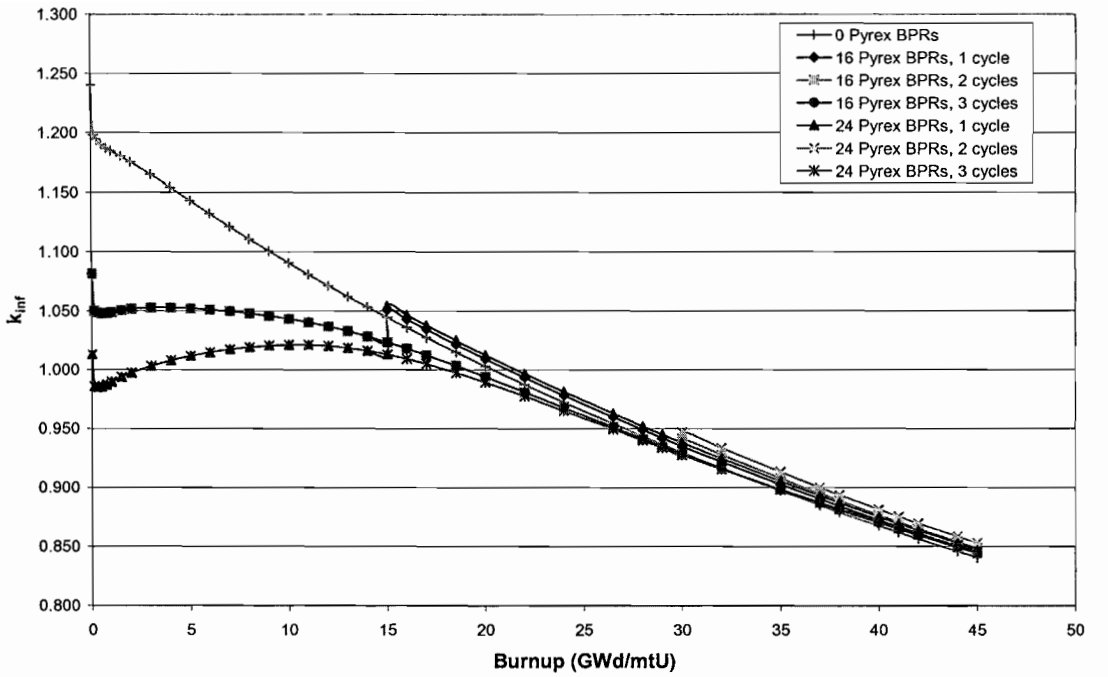

Figure 4-47. GRCASMO3 k_{inf} Results for Pyrex BPRs

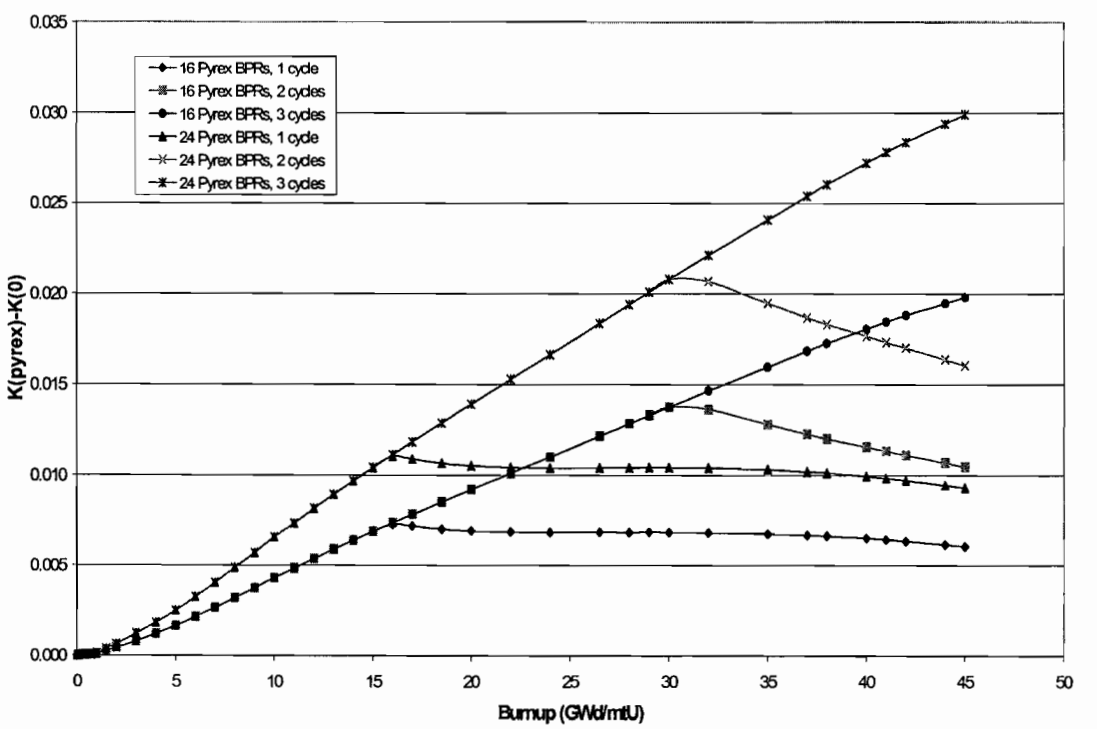

Figure 4-48. Δk_{inf} Results for Pyrex BPRs at Cold Cask Conditions

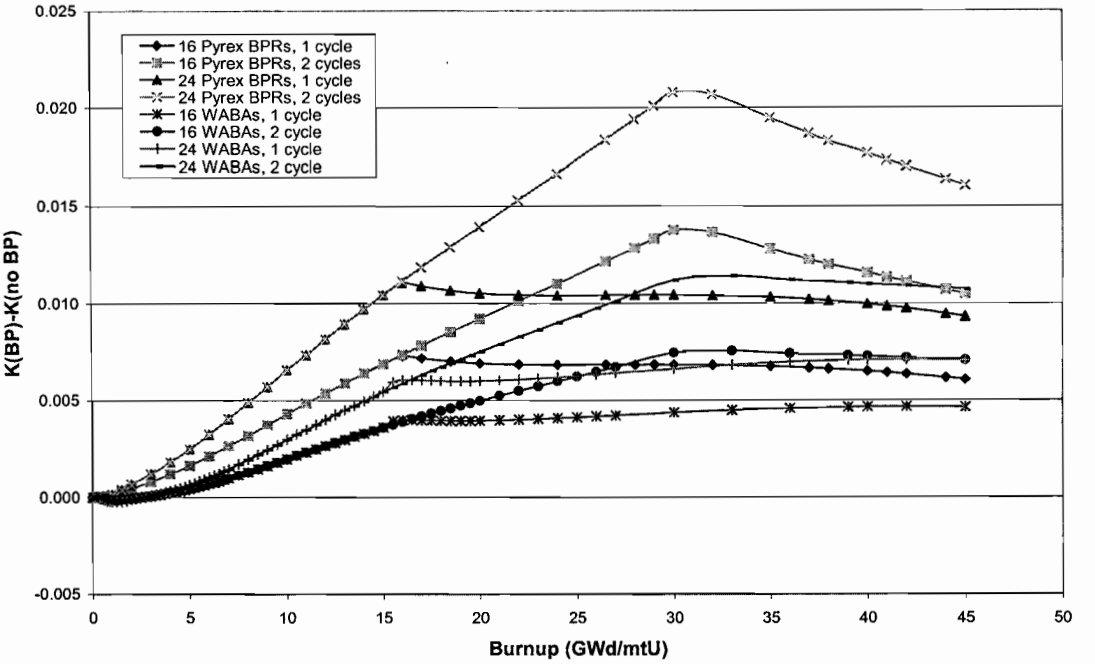

Figure 4-48a. Δk_{inf} Results for Pyrex and WABAs at Cold Cask Conditions

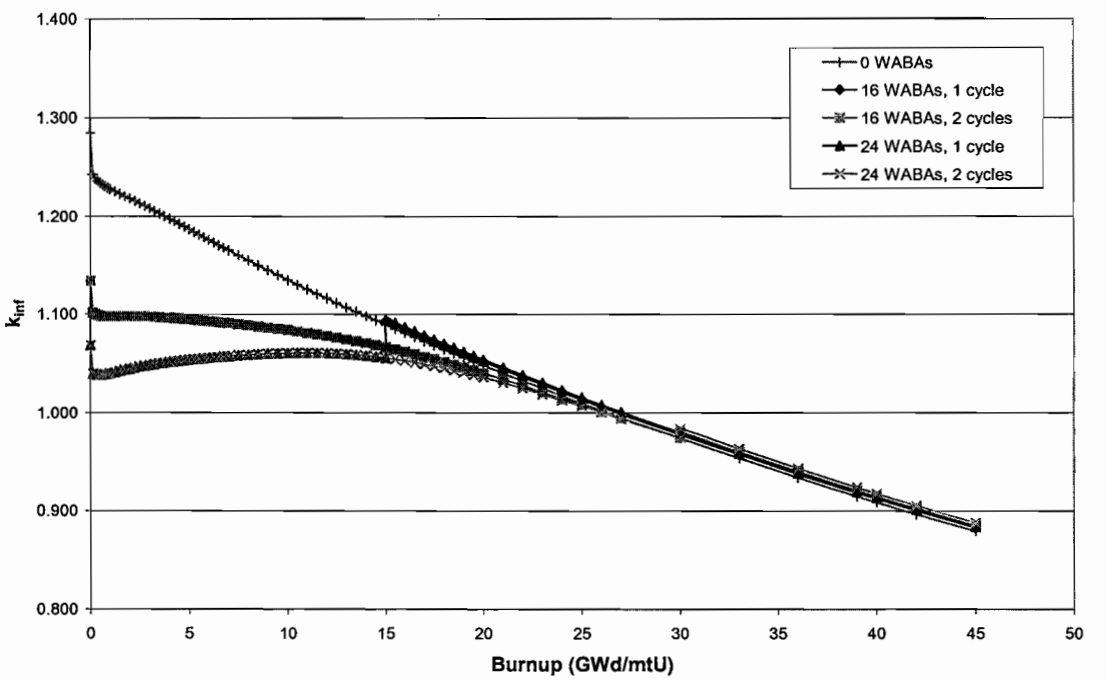

Figure 4-49. GRCASMO3 k_{inf} Results for WABAs

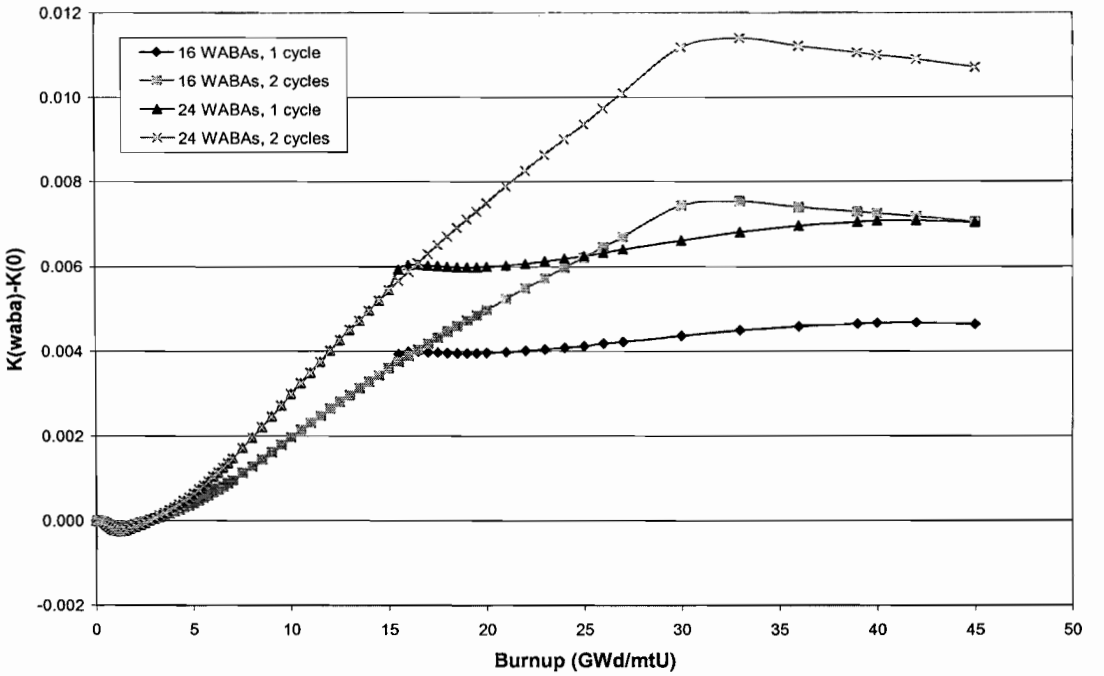

Figure 4-50. Δk_{inf} Results for WABAs at Cold Cask Conditions

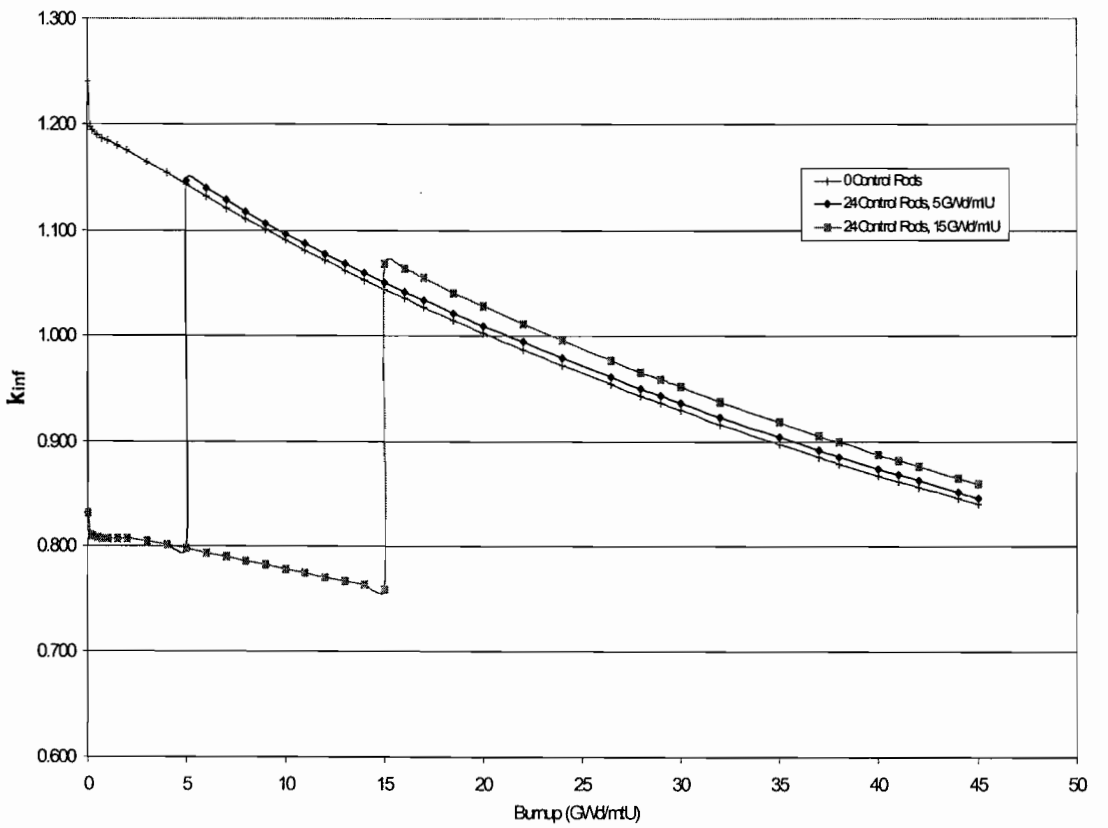

Figure 4-51. GRCASMO3 k_{inf} Results for a Lattice Controlled for Portions of its Depletion

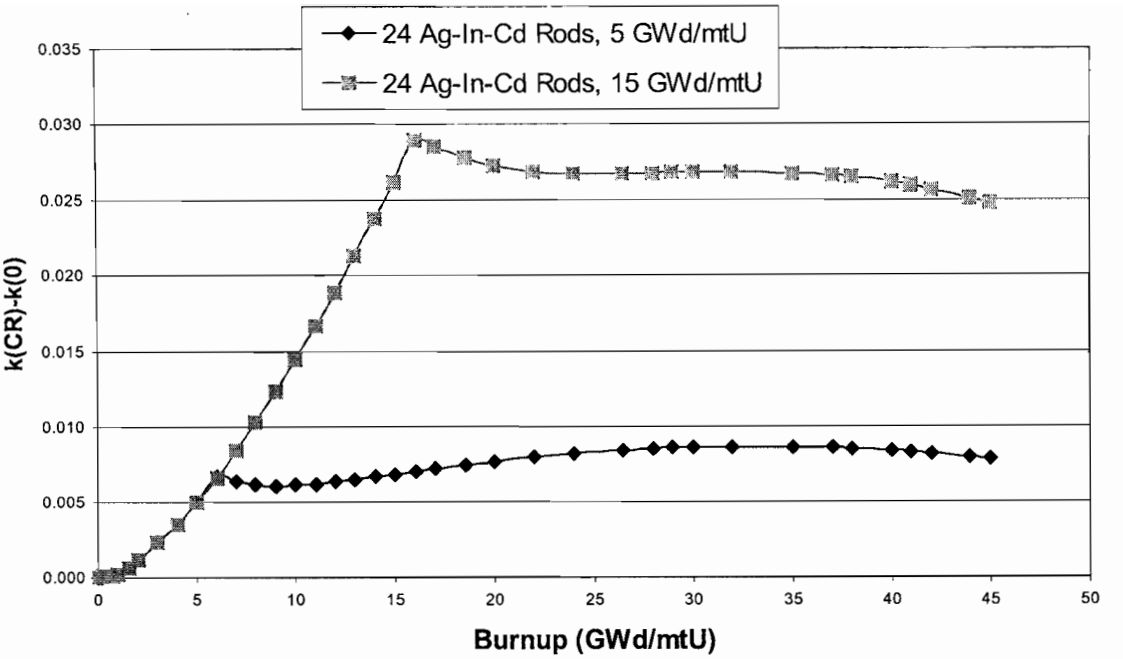

Figure 4-52. Δk_{inf} Results for a Lattice Controlled During Parts of its Depletion

4.4 PWR FISSION PRODUCT WORTH RESULTS

This section provides a summary of information from MO0204SPABCF04.012, Section 5. Table 4-3 shows the results of the GRCASMO3 k_{inf} calculations for storage cask conditions and the fission product worth calculations. The table also reports the calculated values for k_2, $\Delta\rho$(FP), $\Delta\rho$(BE), and %$\Delta\rho$(FP).

Table 4-4 demonstrates the effect that changes in neutron spectrum have on the calculation of the fraction fission product worth relative to the total burnup credit worth. The table considers only the 3.7 wt% enriched U^{235}, 5-year cooled cases. The first RRX column contains the results of the method described in Section 3.4.3. The next column (k_{inf}) shows the results of using a k_{inf} value calculated using GRCASMO3, without maintaining the best-estimate neutron spectrum. For these cases, k_2 was calculated for the system after the fission products were removed, and k_1 was the best-estimate case calculated by GRCASMO3 with all of the available isotopes considered. The last two columns (%Δk (FP)) show the results, for the same cases, in terms of %Δk [%$\Delta k = 100(k_1-k_0)/k_0$, where k_0 is for the fresh fuel case]. The reaction rate approach and the k_{inf} approach are both reported here also.

The results reported in Table 4-4 demonstrates that common errors can lead to significant deviations for fission product worth. Care must be taken to maintain the proper neutron spectrum. Also, it is important to work in terms of change in reactivity versus change in k_{inf}.

Table 4-3. GRCASMO3 Results

Enrichment (wt% ^{235}U)	Burnup (GWd/mtU)	K_{inf} (BE) [k_1]	K_{inf} (AO) [k_2]	Δρ(FP)	Δρ(BE)	%Δρ(FP)
5-yr Cooling						
2	0	1.27760	N/A	N/A	N/A	N/A
	10	1.13206	1.18520	-0.040	-0.101	39%
	50	0.79388	0.90589	-0.156	-0.477	33%
3.7	0	1.43825	N/A	N/A	N/A	N/A
	10	1.30916	1.35894	-0.028	-0.069	41%
	20	1.19995	1.27616	-0.050	-0.138	36%
	30	1.09743	1.19413	-0.074	-0.216	34%
	40	1.00074	1.11203	-0.100	-0.304	33%
	50	0.91536	1.03604	-0.127	-0.397	32%
5	0	1.49486	N/A	N/A	N/A	N/A
	10	1.38127	1.42850	-0.024	-0.055	44%
	50	1.02139	1.14473	-0.105	-0.310	34%
200-yr Cooling						
3.7	0	1.43825	N/A	N/A	N/A	N/A
	10	1.30414	1.34811	-0.025	-0.071	35%
	50	0.79482	0.88763	-0.132	-0.563	23%

Table 4-4. Relative Fission Product Worths Based on GRCASMO3 Calculations

		%Δρ(FP)		%Δk(FP)	
Enrichment (wt % U^{235})	Burnup GWd/mtU	RRX[a]	K_{inf}[b]	RRX[a]	K_{inf}[b]
3.7	10	*41%*	51%	39%	48%
	20	*36%*	46%	32%	42%
	30	*34%*	46%	28%	40%
	40	*33%*	47%	25%	38%
	50	*32%*	48%	23%	37%

Notes: [a] RRX - Indicates Reaction Rate Method for calculating k_2.
[b] k_{inf} - Indicates the use of an actinide-only k_{inf} without maintaining the actual neutron spectrum.

Table 4-5 displays the results of the MCNP calculations for the 3.7wt% U^{235} enriched fuel, with a cooling time of 5 years. Five different lattices were considered.

The first is an explicit representation of a 21-PWR assembly waste package. These calculations represent the depleted fuel in the geometry and spectrum expected in a fully flooded waste package. The second configuration considered is the same as the first, but with the boron in the borated stainless steel replaced with aluminum. These calculations were performed to get an estimate for the effect that the boron has on the worth of the fission products. The third configuration is similar, but replaces the borated stainless steel thermal shunts with water. This helps to quantify the magnitude of the effect that the displaced water has on the fission product worth.

The last two configurations are infinite lattices. One considers the internal lattice of the waste package but as an infinite lattice. This configuration maintains the assembly spacing and includes the borated stainless steel.

The last configuration is a representation of the GRCASMO3 k_{inf} calculations. This is an infinite lattice that maintains the geometry and assembly pitch that exists in the hypothetical reactor. The results of %Δρ estimations for these calculations are repeated in Table 4-6, along with the "explicit waste package" results, for comparison to the GRCASMO3 results. The lower %Δρ values for the MCNP calculations result primarily from the exclusion of the lumped fission products (GRCASMO3 isotopes 401 and 402) that are not available in the MCNP library.

Table 4-5. MCNP Results for 3.7wt% U^{235} Enriched, 5-yr Cooled Cases

Case	Burnup (GWd/mtU)	k_{eff} (BE) [k_1]	K_{eff} (AO) [k_2]	Δρ(BE)	Δρ(FP)	%Δρ(FP)
3.7 Explicit	0	1.09330	N/A	N/A	N/A	N/A
	10	1.00791	1.03389	-0.077	-0.025	32%
	20	0.93022	0.96855	-0.160	-0.043	27%
	30	0.86068	0.90890	-0.247	-0.062	25%
	40	0.79437	0.84914	-0.344	-0.081	24%
	50	0.74030	0.80018	-0.436	-0.101	23%
3.7 Boron Replaced	0	1.20063	N/A	N/A	N/A	N/A
	10	1.10606	1.13726	-0.071	-0.025	35%
	20	1.02336	1.06982	-0.144	-0.042	29%
	30	0.94519	1.00303	-0.225	-0.061	27%
	40	0.87563	0.94193	-0.309	-0.080	26%
	50	0.81307	0.88536	-0.397	-0.100	25%
3.7 BSS Replaced by Water	0	1.19881	N/A	N/A	N/A	N/A
	10	1.10252	1.13318	-0.073	-0.025	34%
	20	1.02180	1.06744	-0.145	-0.042	29%
	30	0.94682	1.00415	-0.222	-0.060	27%
	40	0.87454	0.93972	-0.309	-0.079	26%
	50	0.81387	0.88549	-0.395	-0.099	25%
3.7 Infinite WP Lattice	0	1.14107	N/A	N/A	N/A	N/A
	10	1.05226	1.08068	-0.074	-0.025	34%
	20	0.97165	1.01383	-0.153	-0.043	28%
	30	0.89887	0.95179	-0.236	-0.062	26%
	40	0.83221	0.89271	-0.325	-0.081	25%
	50	0.77483	0.84091	-0.414	-0.101	24%
3.7 Infinite Reactor Lattice	0	1.44371	N/A	N/A	N/A	N/A
	10	1.32022	1.36500	-0.065	-0.025	38%
	20	1.22244	1.28936	-0.125	-0.042	34%
	30	1.13263	1.21709	-0.190	-0.061	32%
	40	1.05059	1.14784	-0.259	-0.081	31%
	50	0.97903	1.08588	-0.329	-0.101	31%

Table 4-6. Comparison of MCNP and GRCASMO3 Results (%Δρ)

		MCNP		GRCASMO3
Enrichment (wt % U^{235})	Burnup GWd/mtU	Explicit WP	Infinite Reactor Lattice	Infinite Reactor Lattice
3.7	10	32%	38%	41%
	20	27%	34%	36%
	30	25%	32%	34%
	40	24%	31%	33%
	50	23%	31%	32%

Considering the results presented in Table 4-6, it is expected that the worth of the fission products in a 21-PWR waste package will be between one quarter to one third of the total burnup credit worth. However, this evaluation considered only unpoisoned fuel assemblies from PWRs. Consideration should be given to the effect of burnable poisons and control rods on the isotopic distributions (actinide build-up vs. fission product build-up). Also, consideration should be given to the effect that PWR operations have on the isotopic distributions.

4.5 CODE-TO-CODE COMPARISON RESULTS

4.5.1 SAS2H BWR Control Blade Case Refinements

This section provides a summary of information from MO0109SPADRN04.003, Section 5.3. Figures 4-53 through 4-65 provide plots of isotopic concentration comparisons between the SAS2H original case, SAS2H modified case, and GRCASMO3 case for node YYYN4. Isotopic concentration is plotted as a function of burnup until discharge. Figure 4-53 shows the comparison for Pu^{239}. It is apparent that inconsistencies exist between GRCASMO3 and SAS2H cases during time where control blades are inserted. Effects from an over-hardened spectrum show rapid buildup and subsequent depletion of Pu^{239} during and right after control blade insertion. These effects are the product of the sum total of approximations required in SAS2H for the representation of the heterogeneous BWR assembly lattice. This behavior is typical for all of the different isotopes. With the modified SAS2H case, this effect still exists but with smaller magnitude. The improvement in this predicted isotope concentration given the modified SAS2H case is most notable at discharge (~45 GWd/mtU) where the remaining Pu^{239} is in better agreement with GRCASMO3 results.

It is notable in Figure 4-64, that significant disagreement appears in the prediction of Gd^{155} concentrations between SAS2H and GRCASMO3. The Gd^{155} concentration is over-predicted in the GRCASMO3 case. The over-prediction of Gd^{155} by GRCASMO3 is caused by problems in the Eu^{155} cross section data, which is based on ENDF/B-IV data. This version of the Eu^{155} cross section results in the Eu^{155} not converting quickly enough, and a higher percentage being converted to Gd^{155}. Thus an over-prediction of Gd^{155} is expected with the version of GRCASMO3 used in this analysis. Later versions of the Eu^{155} cross section data (ENDF/B-V and ENDF/B-VI) address the problems but have not been included with GRCASMO3. Furthermore, since it is understood why Gd^{155} is over-predicted, the results for other isotopes in this study are valid.

Figure 4-66 provides a plot of bypass region thermal disadvantage factor for the original SAS2H case, the modified SAS2H case and for the GRCASMO3 case of node YYYN4. Bypass region DFAC is plotted as a function of burnup. Modifications to the SAS2H case appear to improve flux disadvantage factors (bypass region) when compared to GRCASMO3.

From analysis of isotopic concentration and flux disadvantage factor comparisons, it can be concluded that the development of the modified SAS2H 1-D control blade case is an improvement over the original modeling approach. Although there will always be significant differences in results between 1-D and 2-D model of BWR fuel lattices, discharge isotopic

concentrations predicted with the modified SAS2H case are expected to be closer to reality given the limitations of 1-D model.

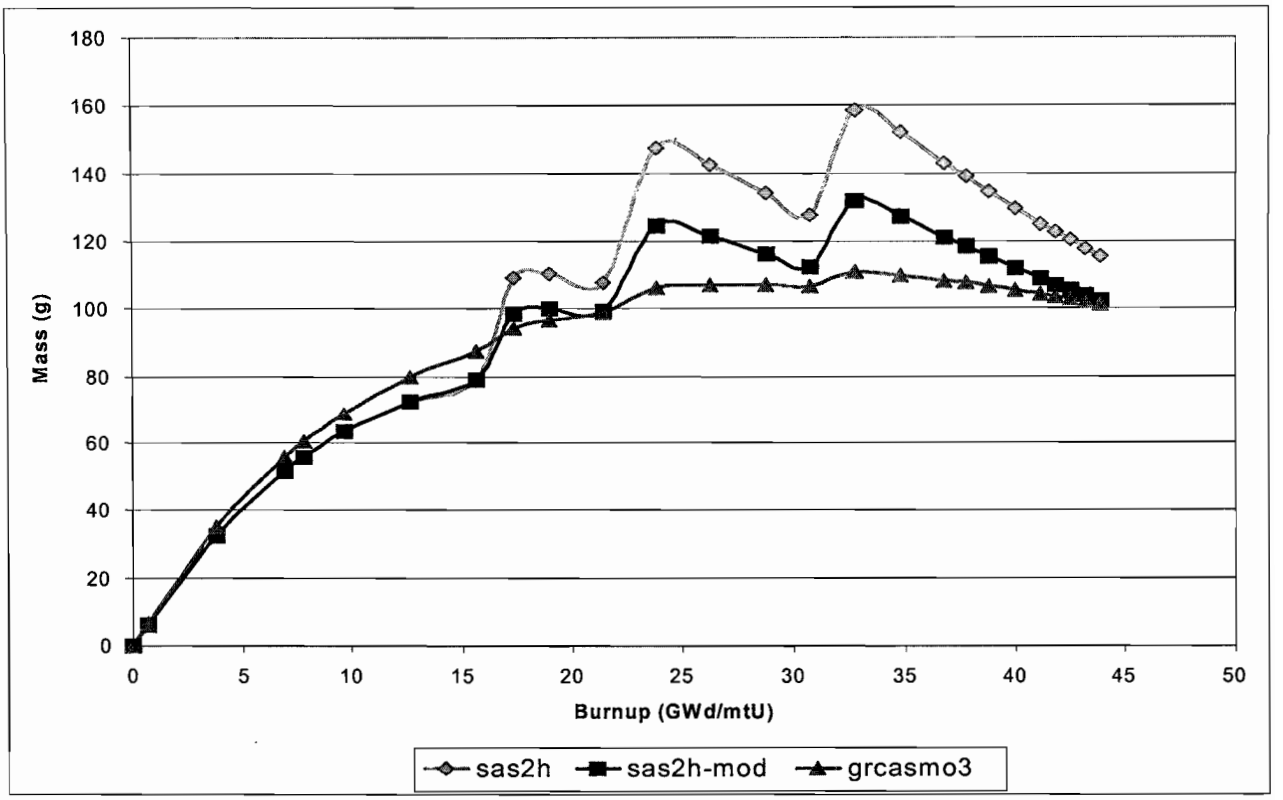

Figure 4-53. Comparisons of Isotopic Concentrations for Pu^{239}

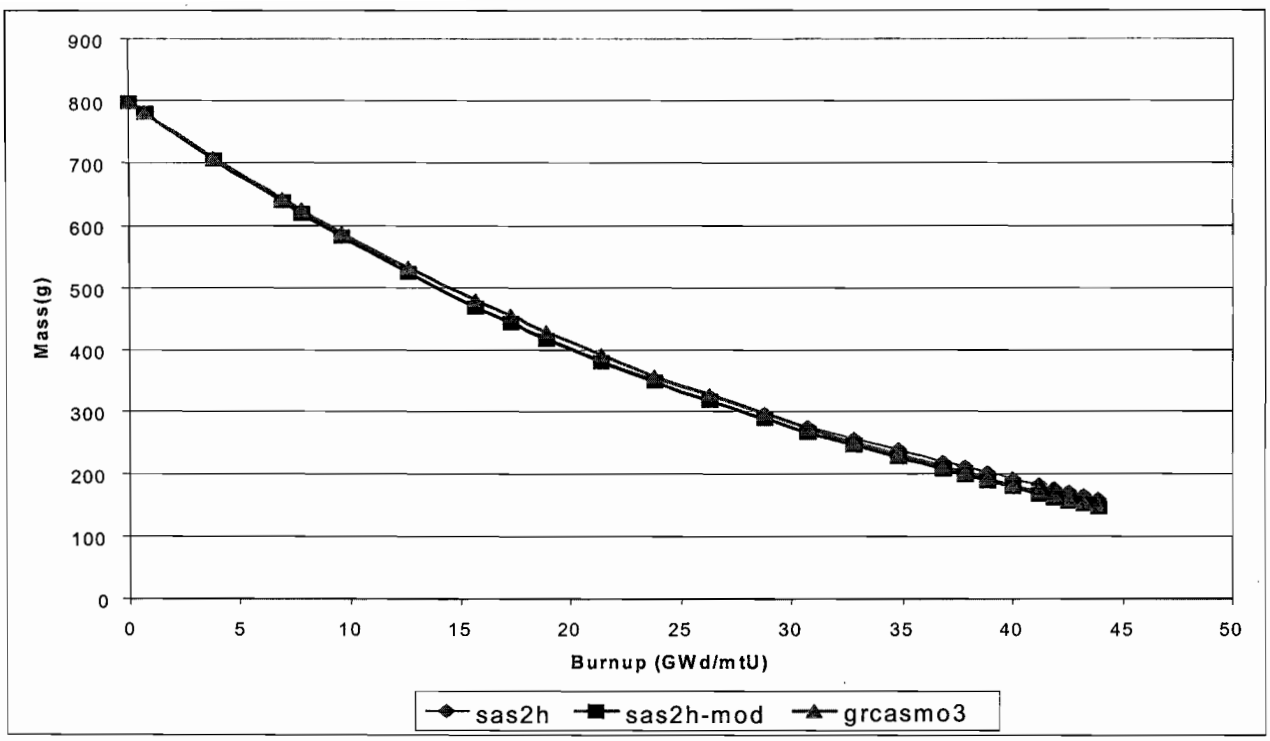

Figure 4-54. Comparisons of Isotopic Concentrations for U^{235}

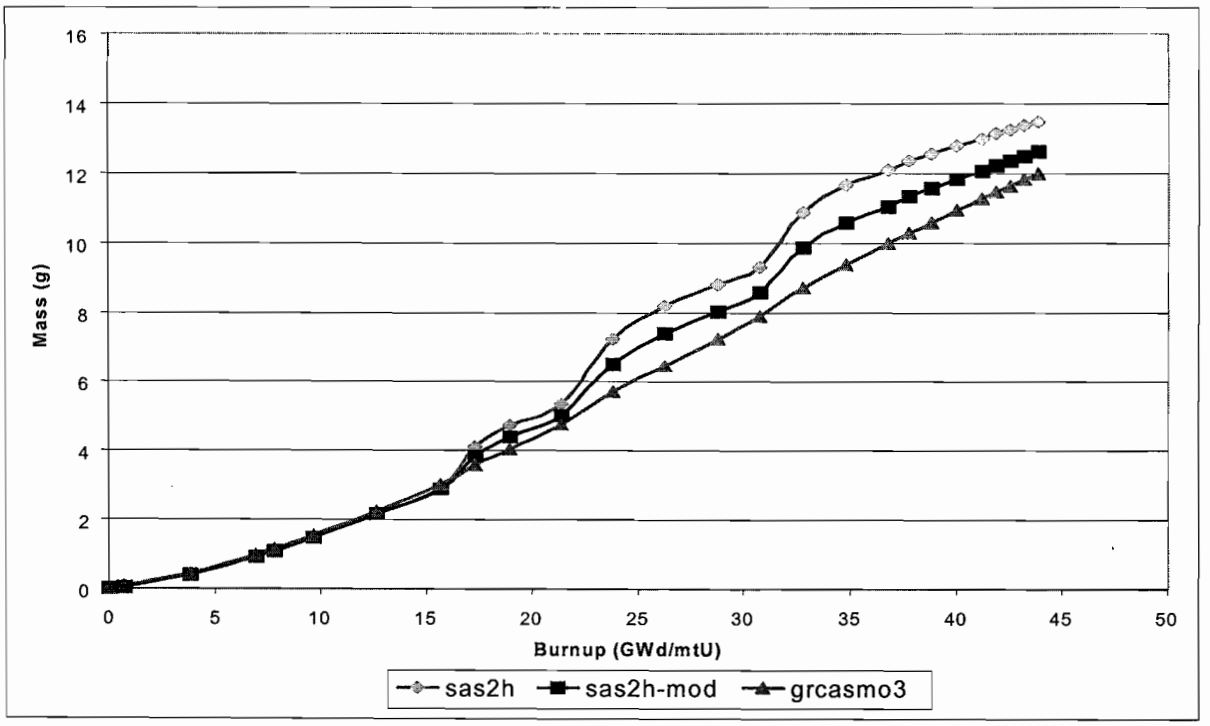

Figure 4-55. Comparisons of Isotopic Concentrations for Np^{237}

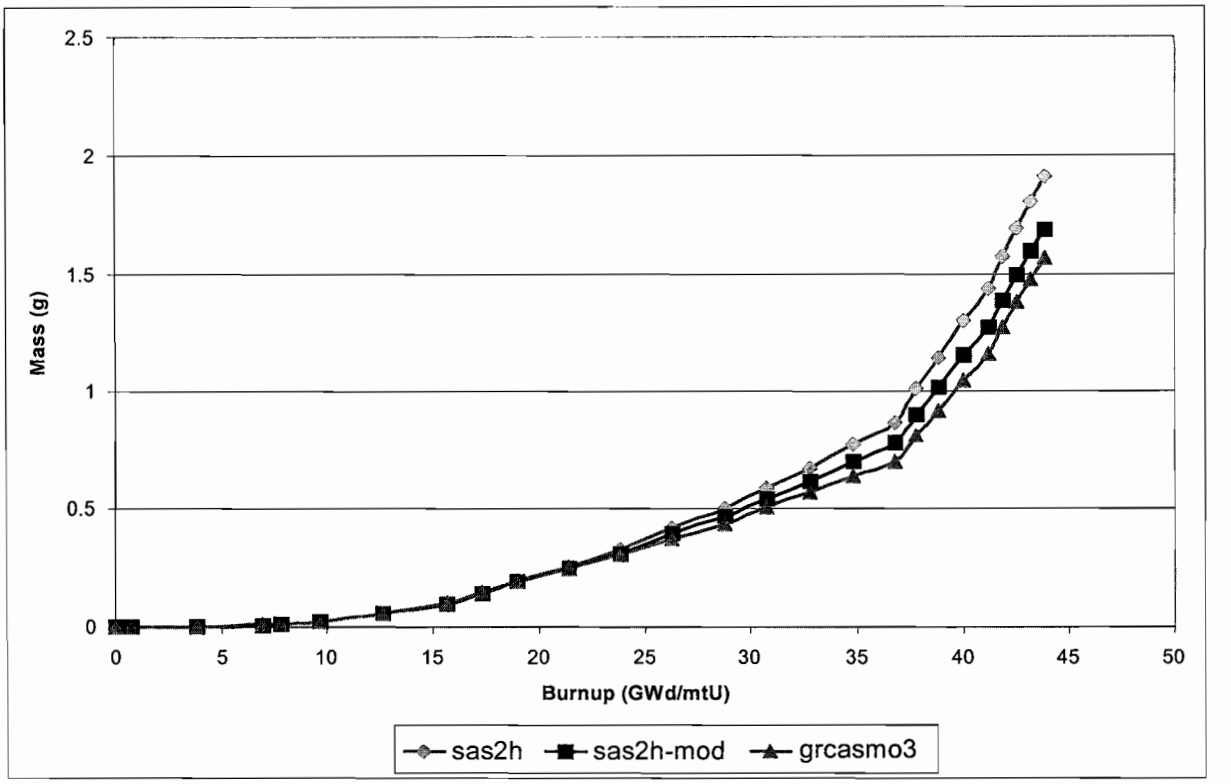

Figure 4-56. Comparisons of Isotopic Concentrations for Am^{241}

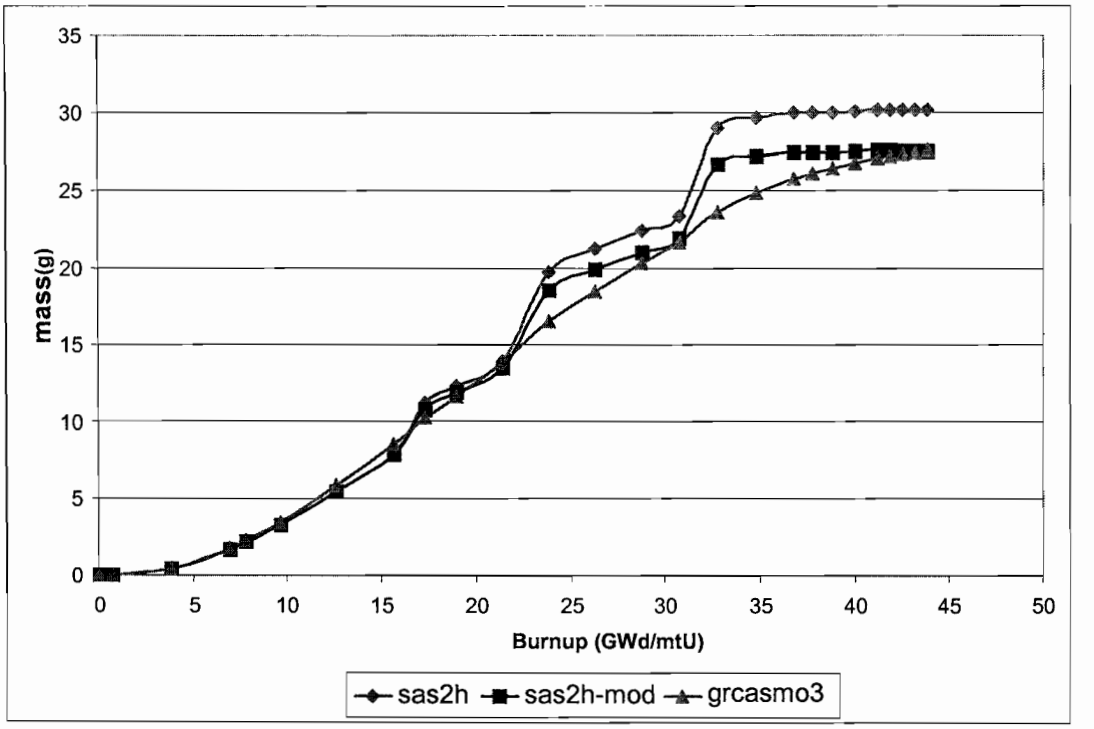

Figure 4-57. Comparisons of Isotopic Concentrations for Pu^{241}

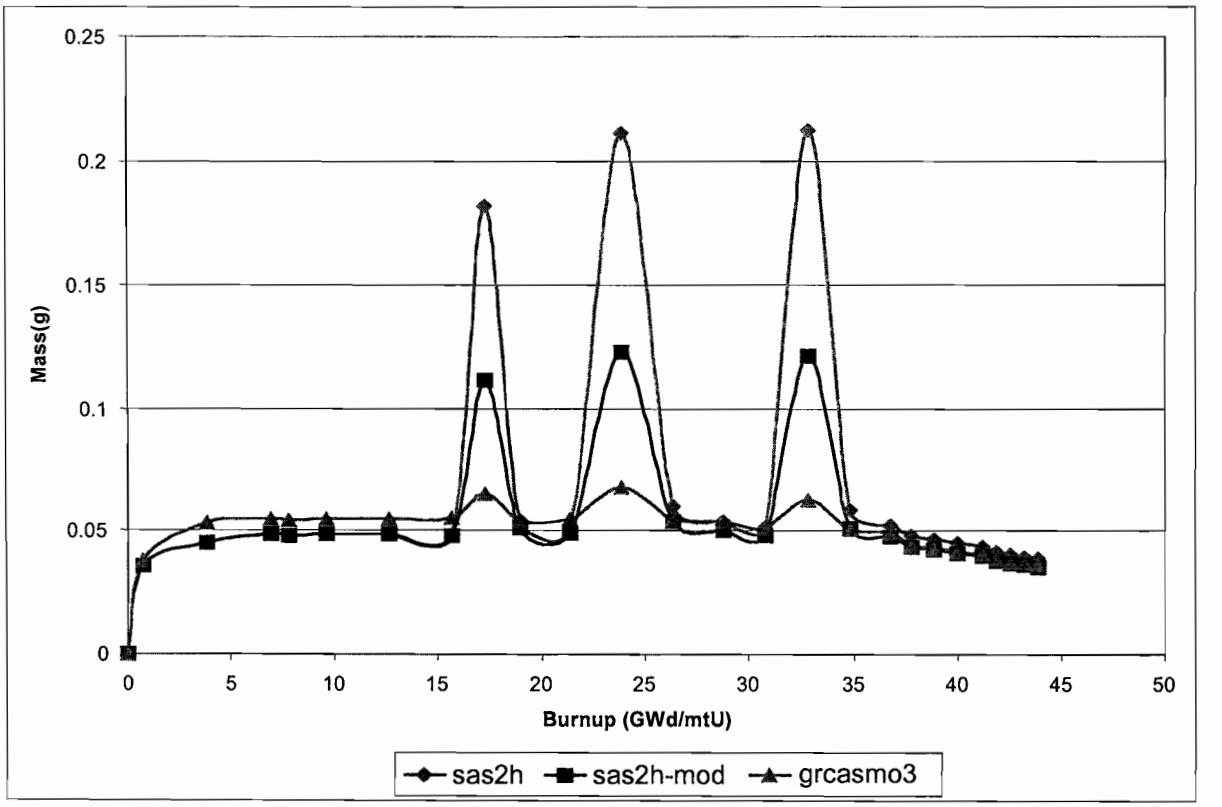

Figure 4-58. Comparisons of Isotopic Concentrations for Sm^{149}

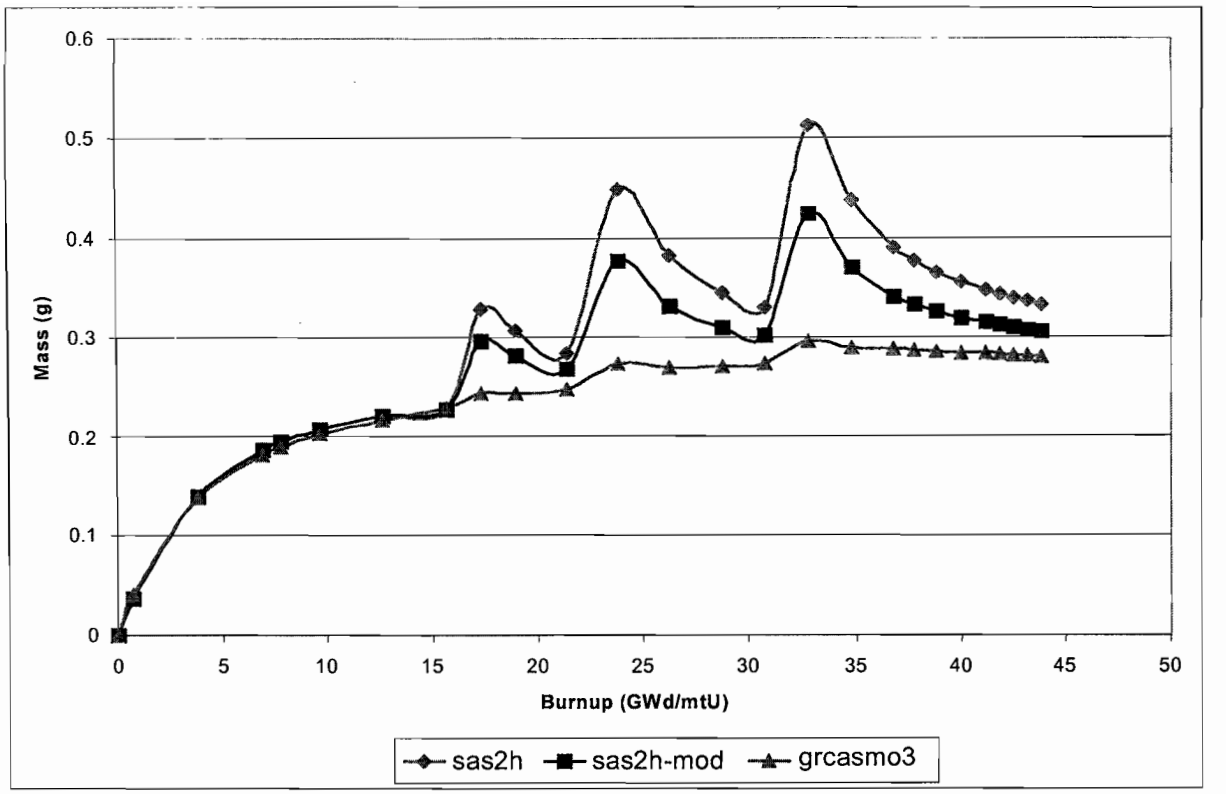

Figure 4-59. Comparisons of Isotopic Concentrations for Sm^{151}

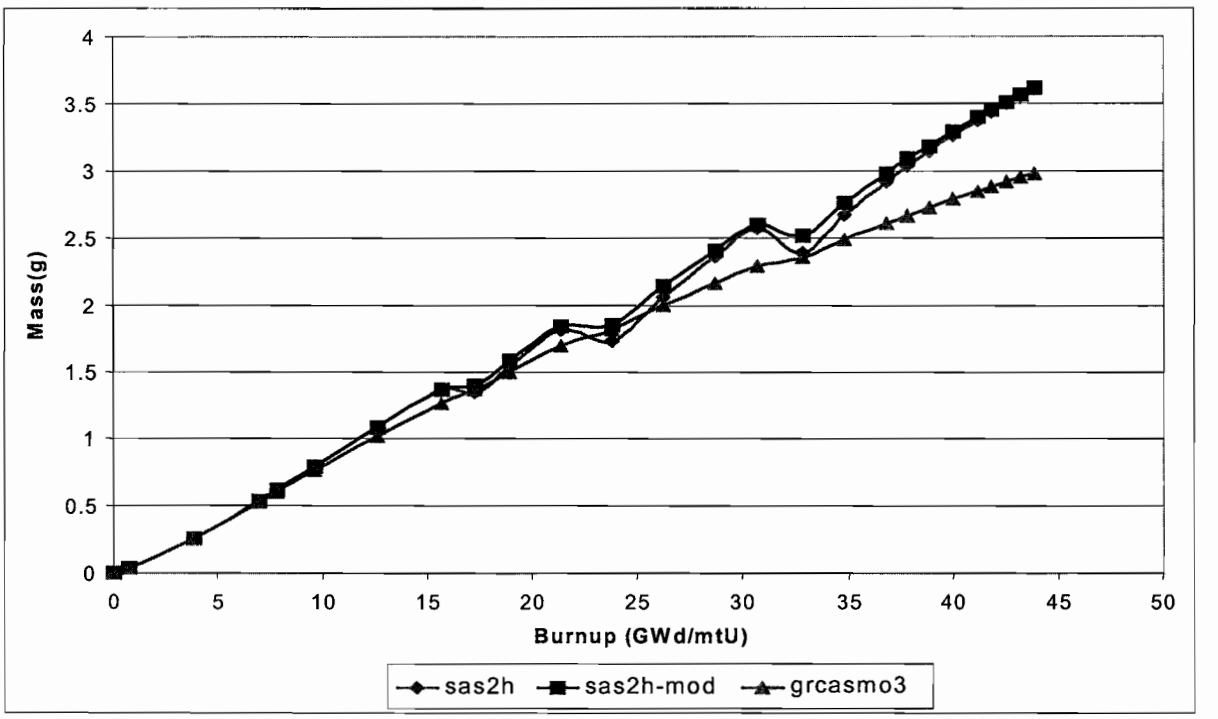

Figure 4-60. Comparisons of Isotopic Concentrations for Sm^{152}

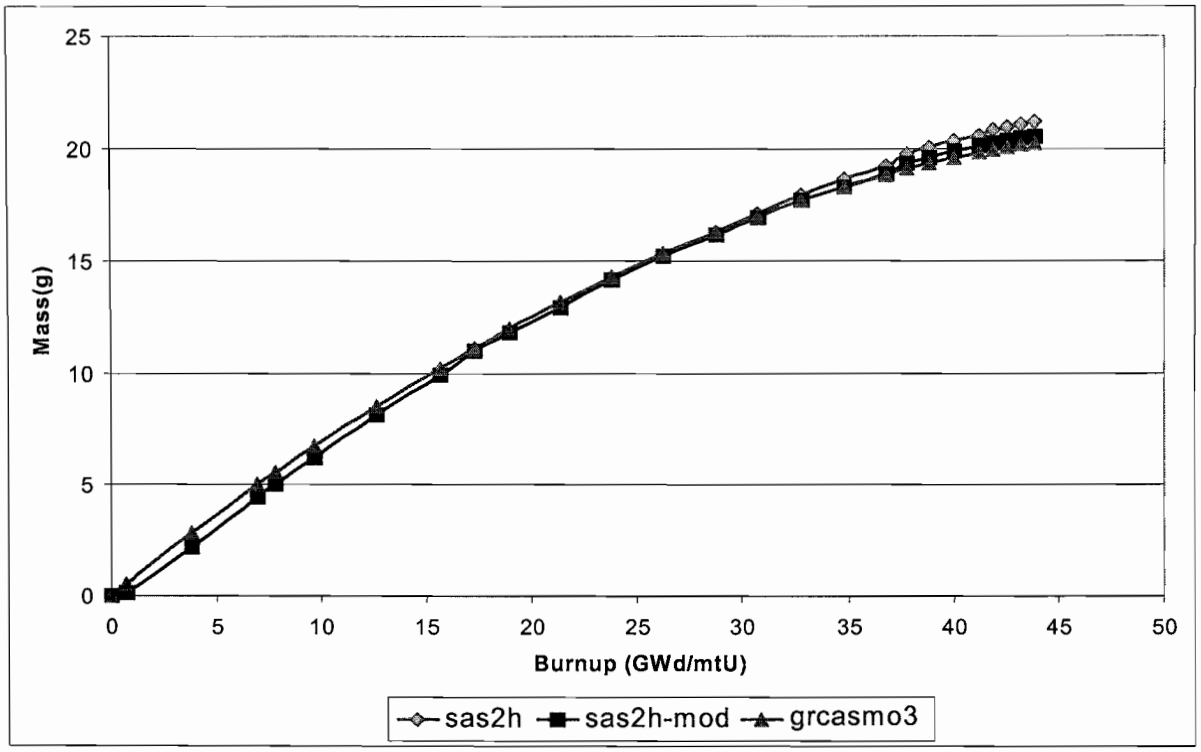

Figure 4-61. Comparisons of Isotopic Concentrations for Nd^{143}

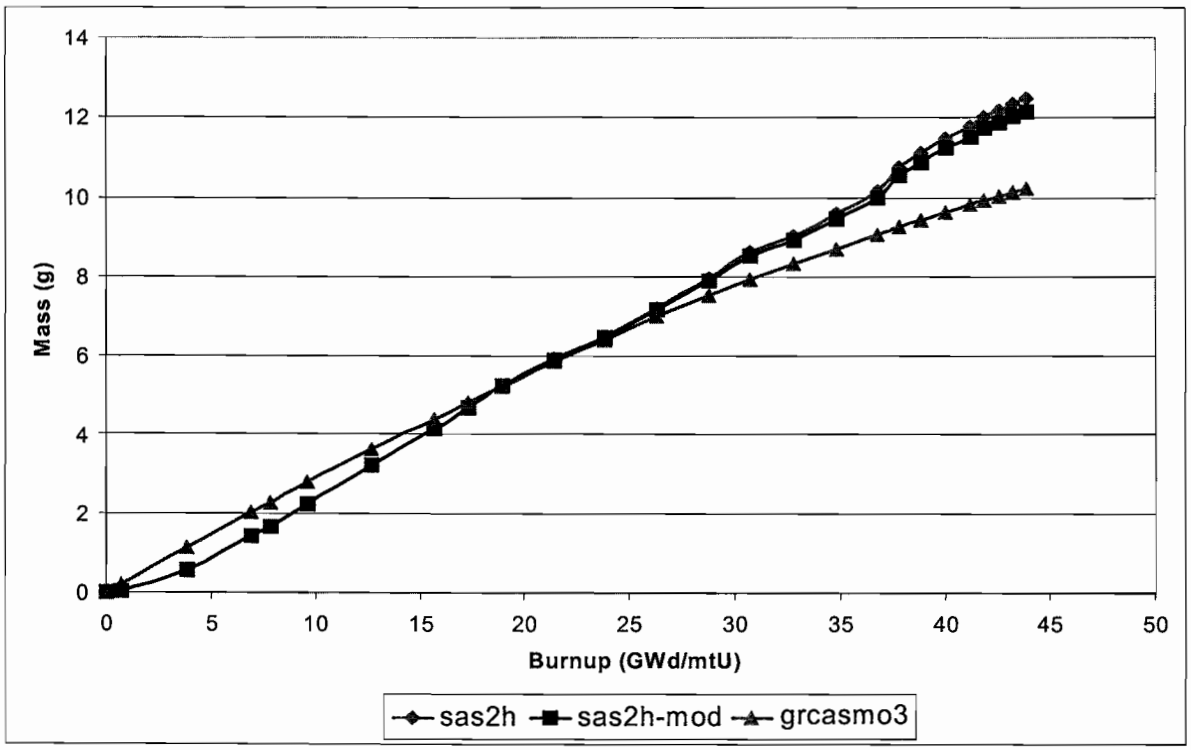

Figure 4-62. Comparisons of Isotopic Concentrations for Rh^{103}

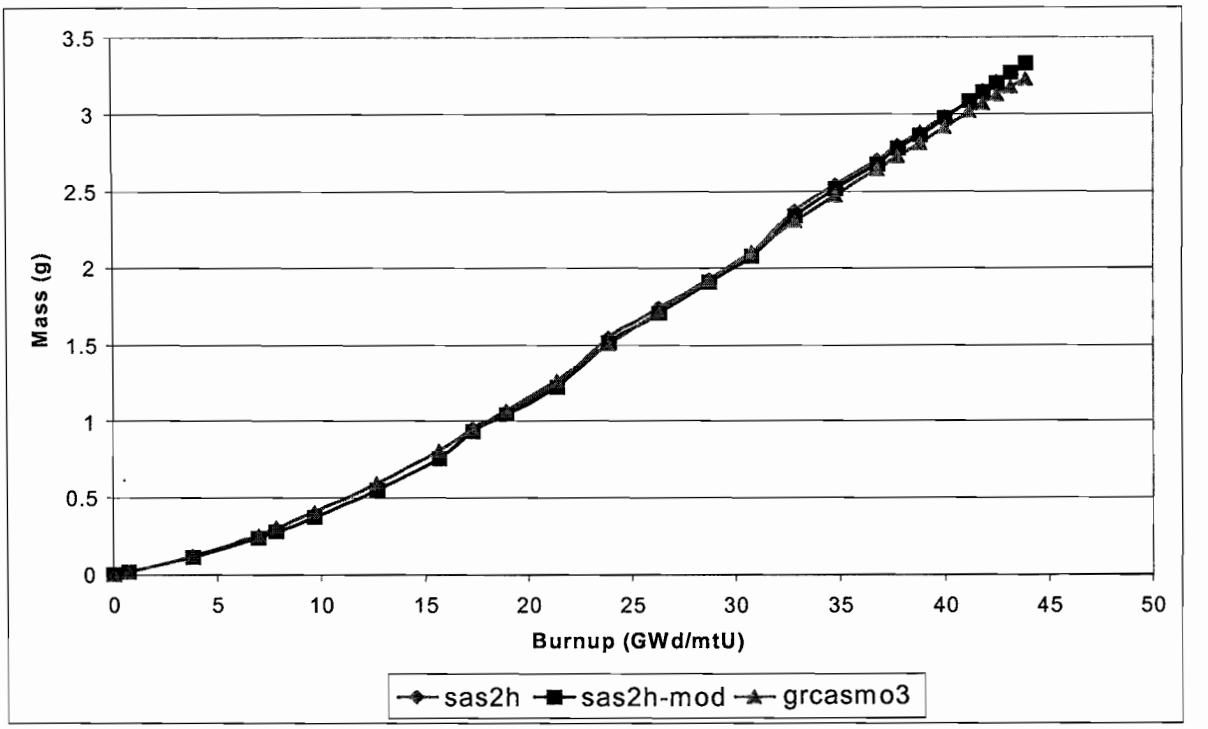

Figure 4-63. Comparisons of Isotopic Concentrations for Eu^{153}

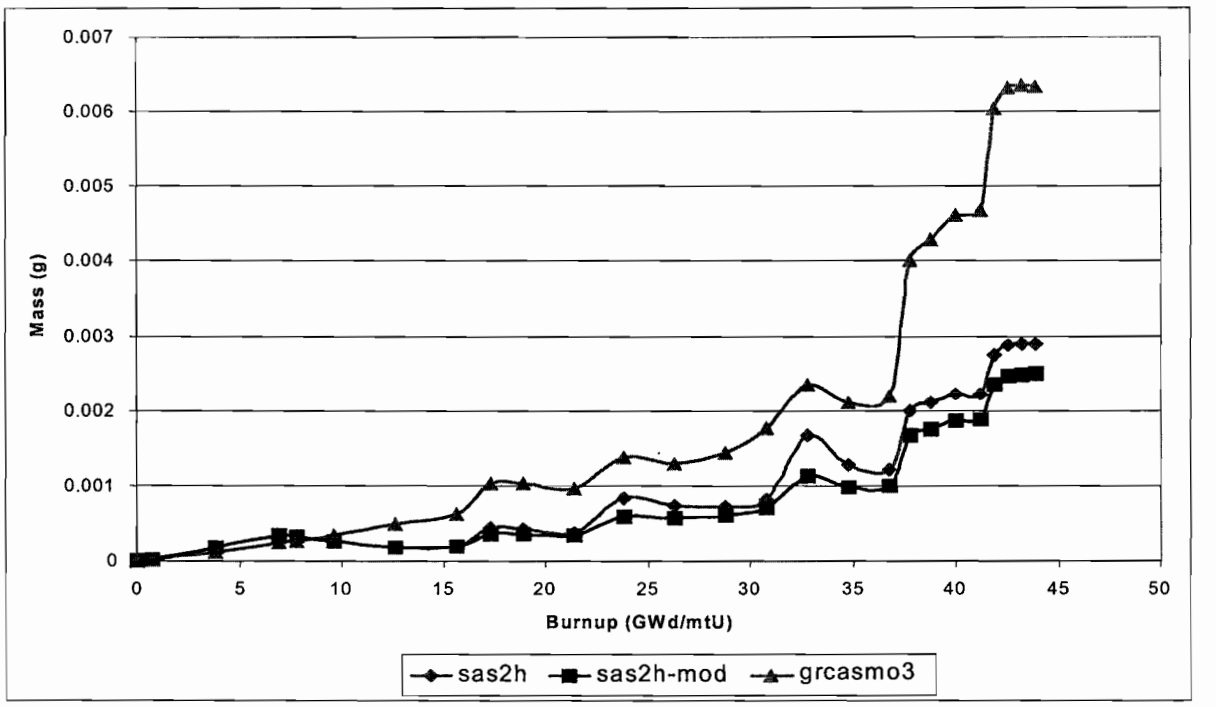

Figure 4-64. Comparisons of Isotopic Concentrations for Gd^{155}

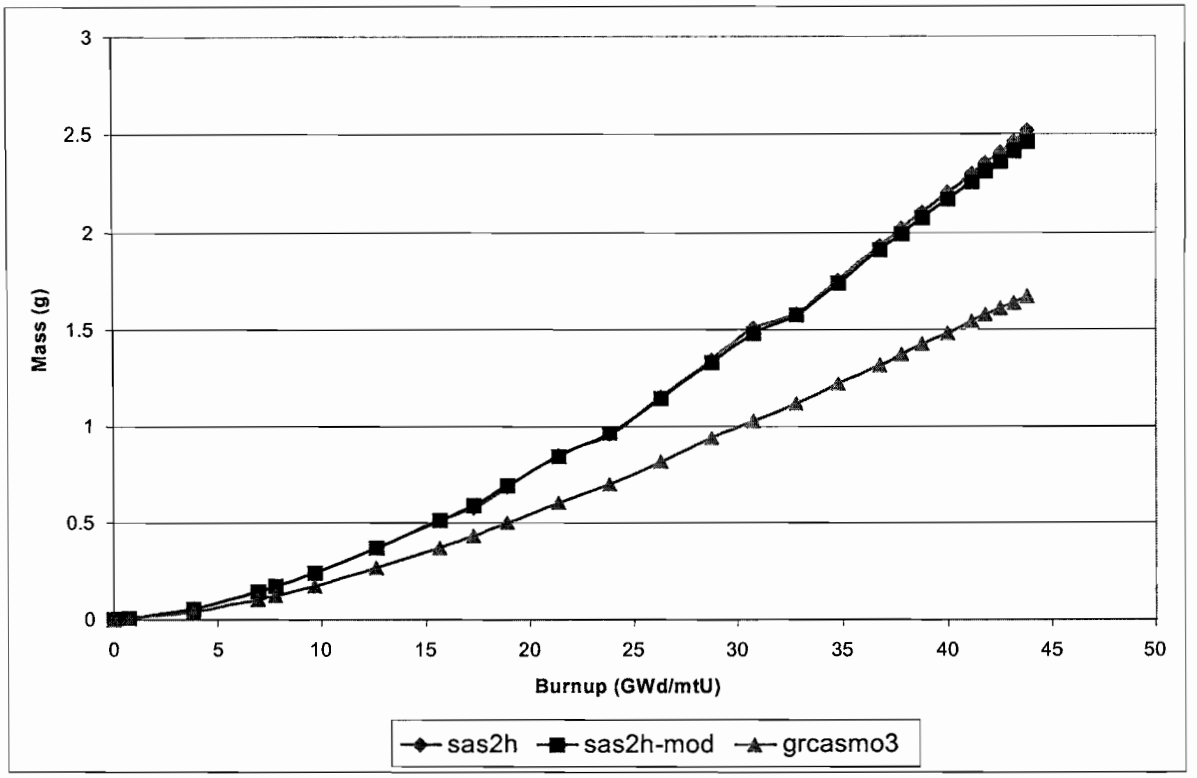

Figure 4-65. Comparisons of Isotopic Concentrations for Ag^{109}

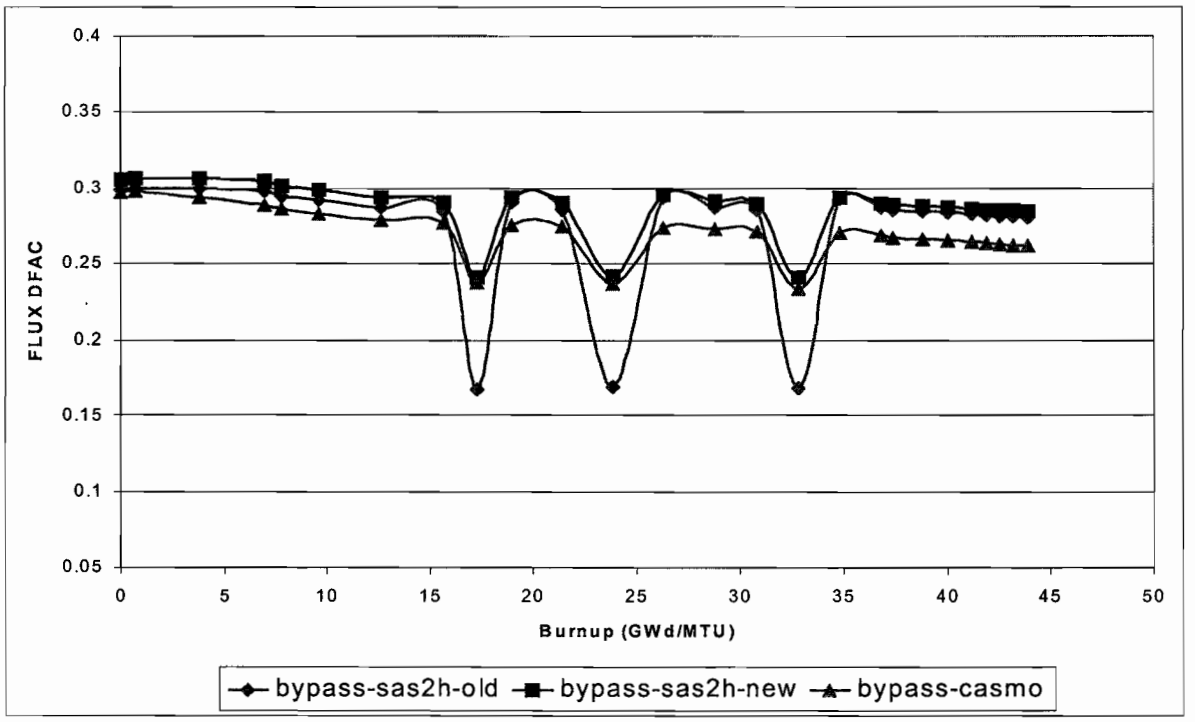

Figure 4-66. Comparisons of Flux Disadvantage Factor

4.5.2 BWR Assembly Burnup Results

This section provides a summary of information from MO0109SPADRN04.003, Section 5.4. Several different cases were developed for each of the four assemblies to determine the isotopic concentration at EOL. For the QC2 assemblies, two GRCASMO3 cases were developed: a 24-node case with coarse operating history, and a 10-node case with coarse operating history. For the GG1 assemblies, three GRCASMO3 cases were developed: a 25-node case with detailed operating history, a 25-node case with coarse operating history, and a 10-node case with coarse operating history. For both QC2 and GG1 assemblies, a 10-node case with coarse operating history was developed using SAS2H. For the 24 or 25-node cases, the EOL atom densities were collapsed to coincide with the 10-node-axial format. For all ten nodes of all cases and assemblies, the EOL atom densities for the isotopes listed in Table 4-7 were input into an MCNP infinite lattice case to determine the nodal k_{inf}. Due to the known over-prediction of Gd^{155} by GRCASMO3 as discussed in Section 4.5.1, the Gd^{155} isotope is not included in this analysis.

Table 4-7. List of Isotopes Considered in Analysis

Rh^{103}	Sm^{149}	Eu^{155}	Np^{237}	Pu^{242}
Ag^{109}	Sm^{150}	U^{234}	Pu^{238}	Am^{241}
Nd^{143}	Sm^{151}	U^{235}	Pu^{239}	Am^{242m}
Nd^{145}	Sm^{152}	U^{236}	Pu^{240}	Am^{243}
Sm^{147}	Eu^{153}	U^{238}	Pu^{241}	---

Comparisons were made to determine the effect on k_{inf} due to operating history resolution, axial spacing, 1-D/2-D approximations, and total code-to-code effects. The results for each of these are listed in Tables 4-8 through 4-11.

Table 4-8 shows that for the GG1 assemblies, the operating history resolution on a node-by-node basis has less than a 2% difference in k_{inf}. The largest difference for both assemblies is seen in the middle nodes (nodes 2-6) where the assembly is the highest burned. Also, it can be seen that the difference in k_{inf} is greater for the controlled history than for the uncontrolled history. This table shows that for all but two nodes, the difference between the coarse and detailed operating histories was positive. That is, the k_{inf} produced using isotopics from the coarse operating history was greater than the k_{inf} calculated using isotopics from the detailed operating history. This comparison was not done for the QC2 assemblies since detailed operating history was not available.

Table 4-9 shows the results of the axial format comparison using the 10-node and 24 or 25-node-axial formats. As can be seen, the largest percent difference was 0.5% Δk_{inf} for GG1, Type G, controlled, node 7 and -0.5% Δk_{inf} for GG1, Type G, uncontrolled, node 2. For the QC2 assemblies, the largest difference was –0.3% Δk_{inf} (nodes 2 and 9 of Type C), controlled.

The results of comparing the k_{inf} values using SAS2H and GRCASMO3 with the 10-node-axial format information are found in Table 4-10. For this comparison, the operating information was

the same for both codes. From the results, several observations can be noted. First, the difference is larger in magnitude in the middle nodes for the uncontrolled cases. Also, for the uncontrolled nodes, the k_{inf} value using the SAS2H isotopics was always less than the k_{inf} value using the GRCASMO3 isotopics for all enriched nodes. The largest difference for these assemblies was –4.6% Δk_{inf} for the QC2 uncontrolled assembly (nodes 7 and 8) and -4.5% Δk_{inf} for the GG1 uncontrolled assembly (node 6).

For the controlled assemblies, the k_{inf} value using the SAS2H isotopics was greater than the k_{inf} value using the GRCASMO3 isotopics for all controlled nodes except QC2, controlled, node 10 and GG1, controlled, nodes 6 and 7. For these nodes, the k_{inf} value using the GRCASMO3 isotopics was greater than when using the SAS2H isotopics. This is also true for the nodes in which a control blade had never been inserted. Table 4-12 lists the nodes that were bladed per insertion for controlled assemblies, where an insertion is considered control blade insertion per interval of each state point. As can be seen in Table 4-12, nodes 8-10 of the GG1 controlled assembly never saw any control blades. For the QC2, Type C, controlled assembly, the largest difference in magnitude was 9.0% Δk_{inf} for node 4. For the controlled nodes of the GG1, Type G assembly, the largest difference was 3.1% Δk_{inf} for node 2. Overall, the largest difference in magnitude for this assembly was found in node 8 (uncontrolled node) with a difference of –4.7% Δk_{inf}.

The results of comparing the k_{inf} values using SAS2H and the best estimate GRCASMO3 case are found in Table 4-11. For the QC2 assemblies, the best estimate case was the 24-node case with coarse operating history. For the GG1 assemblies, the best estimate case was the 25-node case with detailed operating history. For this analysis, the results are very similar to the 1-D/2-D comparison. For the uncontrolled nodes, the k_{inf} using the SAS2H isotopics was generally lower than the k_{inf} using the GRCASMO3 isotopics. The controlled nodes showed opposite behavior with the exceptions of node 10 of QC2, controlled, and node 7 of GG1, controlled. The largest differences in magnitude for these assemblies were 8.9% Δk_{inf} for the QC2 controlled assembly (node 4), –4.6% Δk_{inf} for the QC2 uncontrolled assembly (node 8), 3.6 and -4.3% Δk_{inf} for the GG1 controlled assembly (controlled node 3 and uncontrolled node 8, respectively), and -3.8% Δk_{inf} for the GG1 uncontrolled assembly (node 6).

Figure 4-67 shows a graphical representation of the relative differences by node in k_{inf} using SAS2H and GRCASMO3 best estimate case isotopics. Table 4-11 also shows the relative differences in the EOL atom density values for U^{235} and Pu^{239}. As can be seen, for uncontrolled nodes, SAS2H tends to over-deplete U^{235} and under-convert Pu^{239} relative to GRCASMO3. For the controlled nodes of the GG1, Type G assembly, the opposite is seen: SAS2H tends to under-deplete U^{235} and over-convert the Pu^{239} relative to GRCASMO3. This is due to the hardened spectrum in SAS2H caused by the control blade case encircling the entire assembly. For the controlled nodes of QC2, Type C assembly, the trend was mixed: while SAS2H tended to over-deplete the U^{235}, it also tended to over-convert the Pu^{239}.

The results from Tables 4-8 through 4-11 show that there is a significant difference in k_{inf} found using isotopics from SAS2H and GRCASMO3 with differences as large as 9% Δk_{inf} for nodes controlled late in life, and 4.6% Δk_{inf} for enriched nodes that were never controlled. Additional

analyses will be needed before appropriateness of the use of SAS2H for BWR spent fuel for disposal criticality can be determined.

Table 4-8. k_{inf} Results of Operating History Resolution Comparisons Using GRCASMO3 EOL Isotopic Concentrations

Node	EOL BU (10-node case)	Detailed op. history [a]		Coarse op. hist [a]		Δk_{inf} [b]	% Δk_{inf} [c]
		k_{inf}	σ	k_{inf}	σ		
GG1 – Type G (controlled)							
1	7.50	0.7089	0.0004	0.7110	0.0003	0.0021	0.3%
2	35.02	0.9456	0.0005	0.9474	0.0005	0.0018	0.2%
3	42.39	0.8887	0.0005	0.8955	0.0004	0.0068	0.8%
4	43.87	0.9055	0.0005	0.9201	0.0004	0.0146	1.6%
5	44.43	0.9340	0.0005	0.9508	0.0005	0.0168	1.8%
6	42.62	0.9709	0.0005	0.9863	0.0005	0.0154	1.6%
7	38.93	1.0129	0.0005	1.0221	0.0005	0.0092	0.9%
8	34.15	1.0430	0.0005	1.0482	0.0005	0.0053	0.5%
9	27.89	1.0783	0.0005	1.0822	0.0005	0.0038	0.4%
10	9.42	0.7698	0.0004	0.7782	0.0004	0.0084	1.1%
GG1 – Type G (uncontrolled)							
1	8.65	0.6964	0.0003	0.6959	0.0004	-0.0005	-0.1%
2	39.22	0.8953	0.0004	0.8937	0.0005	-0.0016	-0.2%
3	47.39	0.8240	0.0004	0.8292	0.0004	0.0053	0.6%
4	47.70	0.8567	0.0004	0.8674	0.0004	0.0107	1.2%
5	46.73	0.8997	0.0005	0.9102	0.0005	0.0105	1.2%
6	43.43	0.9499	0.0005	0.9590	0.0005	0.0090	1.0%
7	37.44	1.0081	0.0005	1.0133	0.0005	0.0051	0.5%
8	31.19	1.0537	0.0004	1.0567	0.0005	0.0029	0.3%
9	25.22	1.0892	0.0005	1.0918	0.0005	0.0026	0.2%
10	8.23	0.7680	0.0004	0.7703	0.0004	0.0022	0.3%

Notes: [a] Atom densities were collapsed into the 10-node-axial format before use in MCNP.

[b] $\Delta k_{inf} = k_{coarse} - k_{detailed}$. The MCNP related standard deviation on all Δk_{inf} values was less than 0.0008.

[c] $\% \Delta k_{inf} = 100\ \Delta k_{inf} / k_{detailed}$

Table 4-9. k_{inf} Results of Axial Format Comparisons Using GRCASMO3 EOL Isotopic Concentrations

Node	EOL BU (10-node case)	24- (QC2) / 25- (GG1) node cases [a]		10-node case		Δk_{inf} [b]	% Δk_{inf} [c]
		k_{inf}	σ	k_{inf}	σ		
QC2 – Type C (controlled)							
1	8.53	0.6945	0.0003	0.6945	0.0003	0.0000	0.0%
2	32.66	0.8778	0.0004	0.8752	0.0005	-0.0026	-0.3%
3	42.00	0.7847	0.0004	0.7851	0.0004	0.0004	0.1%
4	44.37	0.7950	0.0004	0.7945	0.0004	-0.0004	-0.1%
5	45.31	0.8200	0.0004	0.8193	0.0004	-0.0006	-0.1%
6	45.19	0.8460	0.0004	0.8454	0.0005	-0.0006	-0.1%
7	43.87	0.8774	0.0005	0.8773	0.0004	-0.0002	0.0%
8	40.63	0.9118	0.0004	0.9127	0.0005	0.0009	0.1%
9	29.16	0.9995	0.0005	0.9969	0.0004	-0.0027	-0.3%
10	7.85	0.6756	0.0004	0.6756	0.0004	0.0000	0.0%
QC2 – Type F (uncontrolled)							
1	7.45	0.6985	0.0003	0.6985	0.0003	0.0000	0.0%
2	28.76	0.9243	0.0005	0.9228	0.0005	-0.0015	-0.2%
3	37.22	0.8378	0.0004	0.8375	0.0004	-0.0004	0.0%
4	39.32	0.8465	0.0005	0.8459	0.0004	-0.0005	-0.1%
5	41.07	0.8773	0.0004	0.8773	0.0005	0.0000	0.0%
6	41.06	0.8994	0.0004	0.8990	0.0005	-0.0004	0.0%
7	40.13	0.9231	0.0004	0.9234	0.0005	0.0003	0.0%
8	36.71	0.9642	0.0005	0.9648	0.0005	0.0005	0.1%
9	27.64	1.0134	0.0005	1.0132	0.0005	-0.0002	0.0%
10	8.28	0.7327	0.0004	(d)	(d)	(d)	(d)
GG1 – Type G (controlled)							
1	7.50	0.7110	0.0003	0.7110	0.0003	0.0000	0.0%
2	35.02	0.9474	0.0005	0.9457	0.0005	-0.0017	-0.2%
3	42.39	0.8955	0.0004	0.8951	0.0005	-0.0004	0.0%
4	43.87	0.9201	0.0004	0.9178	0.0005	-0.0022	-0.2%
5	44.43	0.9508	0.0005	0.9506	0.0005	-0.0002	0.0%
6	42.62	0.9863	0.0005	0.9862	0.0005	-0.0001	0.0%
7	38.93	1.0221	0.0005	1.0267	0.0005	0.0047	0.5%
8	34.15	1.0482	0.0005	1.0476	0.0005	-0.0007	-0.1%
9	27.89	1.0822	0.0005	1.0822	0.0005	0.0000	0.0%
10	9.42	0.7782	0.0004	0.7778	0.0004	-0.0003	0.0%
GG1 – Type G (uncontrolled)							
1	8.65	0.6959	0.0004	0.6959	0.0004	0.0000	0.0%
2	39.22	0.8937	0.0005	0.8895	0.0004	-0.0042	-0.5%
3	47.39	0.8292	0.0004	0.8288	0.0004	-0.0004	0.0%
4	47.70	0.8674	0.0004	0.8674	0.0004	0.0000	0.0%
5	46.73	0.9102	0.0005	0.9104	0.0005	0.0003	0.0%
6	43.43	0.9590	0.0005	0.9565	0.0005	-0.0025	-0.3%
7	37.44	1.0133	0.0005	1.0135	0.0005	0.0003	0.0%
8	31.19	1.0567	0.0005	1.0569	0.0005	0.0002	0.0%
9	25.22	1.0918	0.0005	1.0918	0.0005	0.0000	0.0%
10	8.23	0.7703	0.0004	0.7714	0.0004	0.0011	0.1%

NOTES: [a] Atom densities were collapsed into the 10-node-axial format before use in MCNP.

[b] $\Delta k_{inf} = k_{10\text{-node}} - k_{2X\text{-node}}$. The MCNP related standard deviation on all Δk_{inf} values was less than 0.0008.

[c] % $\Delta k_{inf} = 100\ \Delta k_{inf} / k_{2X\text{-node}}$.

[d] The 10-node-axial format case could not be completed for this node since two different pin layouts (GRCASMO3 nodes 23 and 24) were combined to form one SAS2H node (node 10).

Table 4-10. k_{inf} Results of 1-D/2-D Comparisons Using GRCASMO3 and SAS2H EOL Isotopic Concentrations

Node	EOL BU (10-node case)	GRCASMO3 (10-node-axial format)		SAS2H			
		k_{inf}	σ	k_{inf}	σ	Δk_{inf} [a]	% Δk_{inf} [b]
QC2 – Type C (controlled)							
1	8.53	0.6945	0.0003	0.7162	0.0003	0.0217	3.1%
2	32.66	0.8752	0.0005	0.9068	0.0005	0.0316	3.6%
3	42.00	0.7851	0.0004	0.8460	0.0004	0.0609	7.8%
4	44.37	0.7945	0.0004	0.8660	0.0004	0.0715	9.0%
5	45.31	0.8193	0.0004	0.8901	0.0005	0.0707	8.6%
6	45.19	0.8454	0.0005	0.9102	0.0005	0.0648	7.7%
7	43.87	0.8773	0.0004	0.9289	0.0005	0.0517	5.9%
8	40.63	0.9127	0.0005	0.9463	0.0005	0.0336	3.7%
9	29.16	0.9969	0.0004	1.0028	0.0005	0.0060	0.6%
10	7.85	0.6756	0.0004	0.6592	0.0003	-0.0164	-2.4%
QC2 – Type F (uncontrolled)							
1	7.45	0.6985	0.0003	0.7046	0.0004	0.0060	0.9%
2	28.76	0.9228	0.0005	0.9065	0.0004	-0.0163	-1.8%
3	37.22	0.8375	0.0004	0.8164	0.0005	-0.0211	-2.5%
4	39.32	0.8459	0.0004	0.8182	0.0004	-0.0278	-3.3%
5	41.07	0.8773	0.0005	0.8434	0.0004	-0.0339	-3.9%
6	41.06	0.8990	0.0005	0.8595	0.0005	-0.0395	-4.4%
7	40.13	0.9234	0.0005	0.8814	0.0005	-0.0420	-4.6%
8	36.71	0.9648	0.0005	0.9201	0.0005	-0.0447	-4.6%
9	27.64	1.0132	0.0005	0.9822	0.0005	-0.0310	-3.1%
10	8.28	(c)	(c)	0.6950	0.0004	(c)	(c)
GG1 – Type G (controlled)							
1	7.50	0.7110	0.0003	0.7266	0.0004	0.0156	2.2%
2	35.02	0.9457	0.0005	0.9753	0.0004	0.0296	3.1%
3	42.39	0.8951	0.0005	0.9209	0.0004	0.0258	2.9%
4	43.87	0.9178	0.0005	0.9308	0.0005	0.0130	1.4%
5	44.43	0.9506	0.0005	0.9537	0.0005	0.0032	0.3%
6	42.62	0.9862	0.0005	0.9801	0.0005	-0.0061	-0.6%
7	38.93	1.0267	0.0005	1.0115	0.0005	-0.0153	-1.5%
8	34.15	1.0476	0.0005	0.9980	0.0005	-0.0495	-4.7%
9	27.89	1.0822	0.0005	1.0491	0.0005	-0.0330	-3.1%
10	9.42	0.7778	0.0004	0.7593	0.0004	-0.0185	-2.4%
GG1 – Type G (uncontrolled)							
1	8.65	0.6959	0.0004	0.6990	0.0003	0.0031	0.4%
2	39.22	0.8895	0.0004	0.8754	0.0005	-0.0141	-1.6%
3	47.39	0.8288	0.0004	0.8088	0.0004	-0.0200	-2.4%
4	47.70	0.8674	0.0004	0.8368	0.0004	-0.0306	-3.5%
5	46.73	0.9104	0.0005	0.8714	0.0005	-0.0391	-4.3%
6	43.43	0.9565	0.0005	0.9138	0.0004	-0.0427	-4.5%
7	37.44	1.0135	0.0005	0.9718	0.0005	-0.0417	-4.1%
8	31.19	1.0569	0.0005	1.0203	0.0005	-0.0366	-3.5%
9	25.22	1.0918	0.0005	1.0676	0.0005	-0.0242	-2.2%
10	8.23	0.7714	0.0004	0.7600	0.0004	-0.0113	-1.5%

NOTES: [a] $\Delta k_{inf} = k_{SAS2H} - k_{GRCASMO3}$. The MCNP related standard deviation on all Δk_{inf} values was less than 0.0008.

[b] % $\Delta k_{inf} = 100\ \Delta k_{inf} / k_{GRCASMO3}$.

[c] The 10-node-axial format case could not be completed for this node since two different pin layouts (GRCASMO3 nodes 23 and 24) were combined to form one SAS2H node (node 10).

Table 4-11. k_{inf} Results of Total Code-to-Code Comparisons Using GRCASMO3 and SAS2H EOL Isotopic Concentrations

Node	EOL BU (10 node case)	% diff U^{235} [a]	% diff Pu^{239} [a]	GRCASMO3 [b]		SAS2H		Δk_{inf} [c]	% Δk_{inf} [d]
				k_{inf}	σ	k_{inf}	σ		
QC2 – Type C (controlled)									
1	8.53	3.55%	8.39%	0.6945	0.0003	0.7162	0.0003	0.0217	3.1%
2	32.66	-4.52%	25.31%	0.8778	0.0004	0.9068	0.0005	0.0290	3.3%
3	42.00	-0.69%	34.26%	0.7847	0.0004	0.8460	0.0004	0.0614	7.8%
4	44.37	-0.08%	39.19%	0.7950	0.0004	0.8660	0.0004	0.0710	8.9%
5	45.31	-1.11%	39.76%	0.8200	0.0004	0.8901	0.0005	0.0701	8.5%
6	45.19	-2.67%	37.78%	0.8460	0.0004	0.9102	0.0005	0.0643	7.6%
7	43.87	-4.68%	32.66%	0.8774	0.0005	0.9289	0.0005	0.0515	5.9%
8	40.63	-6.39%	26.12%	0.9118	0.0004	0.9463	0.0005	0.0345	3.8%
9	29.16	-7.90%	14.27%	0.9995	0.0005	1.0028	0.0005	0.0033	0.3%
10	7.85	-3.19%	-3.71%	0.6756	0.0004	0.6592	0.0003	-0.0164	-2.4%
QC2 – Type F (uncontrolled)									
1	7.45	1.66%	2.97%	0.6985	0.0003	0.7046	0.0004	0.0060	0.9%
2	28.76	-8.12%	0.83%	0.9243	0.0005	0.9065	0.0004	-0.0178	-1.9%
3	37.22	-11.15%	0.41%	0.8378	0.0004	0.8164	0.0005	-0.0215	-2.6%
4	39.32	-13.44%	-1.63%	0.8465	0.0005	0.8182	0.0004	-0.0283	-3.3%
5	41.07	-14.13%	-4.12%	0.8773	0.0004	0.8434	0.0004	-0.0340	-3.9%
6	41.06	-15.59%	-6.24%	0.8994	0.0004	0.8595	0.0005	-0.0399	-4.4%
7	40.13	-15.60%	-8.39%	0.9231	0.0004	0.8814	0.0005	-0.0417	-4.5%
8	36.71	-14.33%	-10.16%	0.9642	0.0005	0.9201	0.0005	-0.0442	-4.6%
9	27.64	-9.31%	-8.24%	1.0134	0.0005	0.9822	0.0005	-0.0312	-3.1%
10	8.28	-7.94%	-9.91%	0.7327	0.0004	0.6950	0.0004	-0.0377	-5.1%
GG1 – Type G (controlled)									
1	7.50	5.27%	5.11%	0.7089	0.0004	0.7266	0.0004	0.0177	2.5%
2	35.02	8.43%	16.95%	0.9456	0.0005	0.9753	0.0004	0.0298	3.1%
3	42.39	10.58%	17.14%	0.8887	0.0005	0.9209	0.0004	0.0322	3.6%
4	43.87	5.93%	15.81%	0.9055	0.0005	0.9308	0.0005	0.0253	2.8%
5	44.43	4.02%	15.02%	0.9340	0.0005	0.9537	0.0005	0.0197	2.1%
6	42.62	1.18%	9.91%	0.9709	0.0005	0.9801	0.0005	0.0092	0.9%
7	38.93	0.00%	4.83%	1.0129	0.0005	1.0115	0.0005	-0.0014	-0.1%
8	34.15	-11.29%	-16.63%	1.0430	0.0005	0.9980	0.0005	-0.0449	-4.3%
9	27.89	-7.02%	-14.66%	1.0783	0.0005	1.0491	0.0005	-0.0292	-2.7%
10	9.42	-4.41%	-1.76%	0.7698	0.0004	0.7593	0.0004	-0.0104	-1.4%
GG1 – Type G (uncontrolled)									
1	8.65	0.28%	-0.03%	0.6964	0.0003	0.6990	0.0003	0.0026	0.4%
2	39.22	-9.42%	-0.75%	0.8953	0.0004	0.8754	0.0005	-0.0199	-2.2%
3	47.39	-8.92%	-0.45%	0.8240	0.0004	0.8088	0.0004	-0.0151	-1.8%
4	47.70	-10.48%	-1.61%	0.8567	0.0004	0.8368	0.0004	-0.0199	-2.3%
5	46.73	-12.63%	-4.81%	0.8997	0.0005	0.8714	0.0005	-0.0283	-3.1%
6	43.43	-12.69%	-9.03%	0.9499	0.0005	0.9138	0.0004	-0.0361	-3.8%
7	37.44	-10.45%	-12.58%	1.0081	0.0005	0.9718	0.0005	-0.0363	-3.6%
8	31.19	-8.53%	-14.14%	1.0537	0.0004	1.0203	0.0005	-0.0334	-3.2%
9	25.22	-5.57%	-12.24%	1.0892	0.0005	1.0676	0.0005	-0.0216	-2.0%
10	8.23	-3.61%	-1.20%	0.7680	0.0004	0.7600	0.0004	-0.0080	-1.0%

NOTES: [a] The difference in U^{235} atom densities was defined as $(U^{235}_{SAS} - U^{235}_{GRCASMO3}) / U^{235}_{GRCASMO3}$. Similarly, for the Pu^{239} atom densities. The differences are given here for ease of discussion although isotopic values were not the primary comparison in this study.

[b] For the values listed for the GG1 assemblies, the 25-node case with detailed operating history was used. For the QC2 assemblies, the 24-node case with coarse operating history was used. These are the best estimate cases for each reactor type. Atom densities were collapsed into the 10-node-axial format before use in MCNP.

[c] $\Delta k_{inf} = k_{SAS2H} - k_{GRCASMO3}$. The MCNP related standard deviation on all Δk_{inf} values was less than 0.0008.

[d] % $\Delta k_{inf} = 100\ \Delta k_{inf} / k_{GRCASMO3}$.

Table 4-12. Bladed Nodes per Control Blade Insertion.

Insertion #	QC2 – Type C 10-node (24-node)	GG1 – Type G 10-node (25-node)
1	1-9 (1-21)	1-2 (1-3)
2	1-8 (1-19)	1-3 (1-7)
3	1-10 (1-24)	1-7 (1-18)
4	1-10 (1-24)	1-7 (1-18)
5	1-10 (1-24)	1-7 (1-19)
6	1-10 (1-24)	

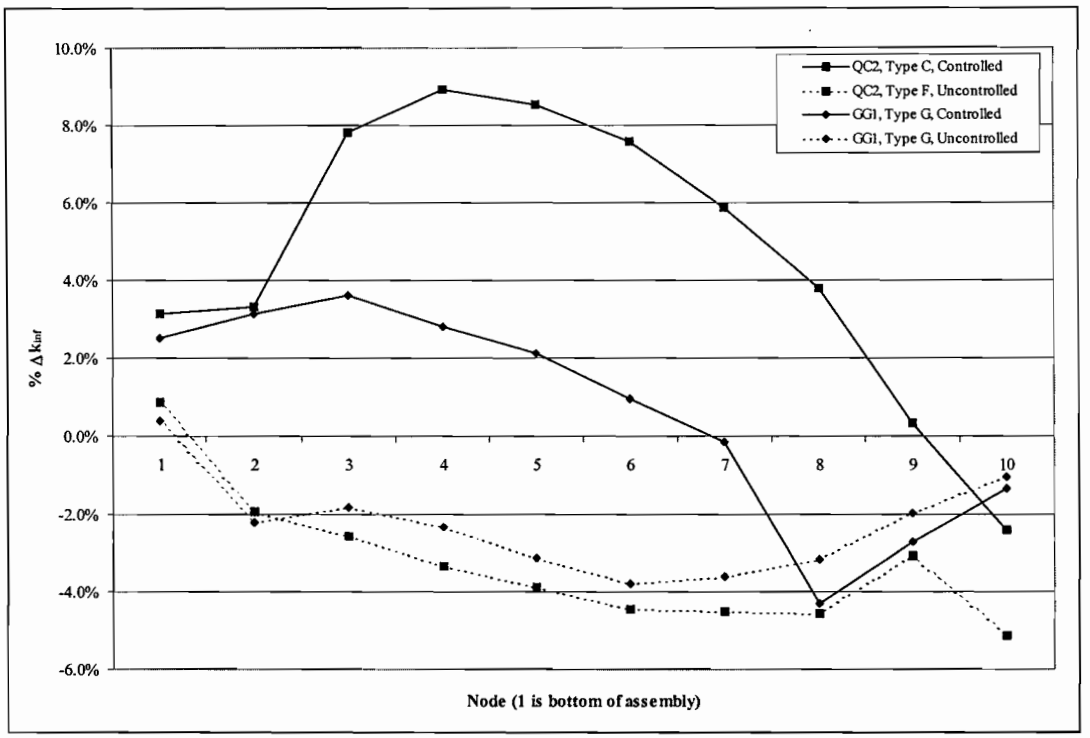

NOTE: % Δk_{inf} = 100* (k_{SAS2H} – $k_{GRCASMO3}$)/$k_{GRCASMO3}$

Figure 4-67. Total Code-to-Code Differences in k_{inf} Using SAS2H and GRCASMO3 EOL Isotopics

4.5.3 PWR Radio-Chemical Assay Comparison Results

This section provides a summary of information from MO0109SPADRN04.003, Section 5.4. Table 4-13 shows percentage difference results for the CC1 and TP2 PWR RCA benchmark comparisons using SAS2H and GRCASMO3. The SAS2H results were taken from CRWMS M&O 1997a and 1997b, which used the SCALE4.3 code package. Results in Table 4-13 are presented in percentage difference between measured and calculated isotopic concentrations [(calculated/measured-1)*100]. Code-to-code comparisons between SAS2H and GRCASMO3 agree well for U^{235} in both samples. GRCASMO3 shows a smaller difference between calculated and measured values for Pu^{239}. Predicted fission product concentrations for Sm^{149} differ more than 30% for both code cases. For Sm^{152}, GRCASMO3 predicts a concentration closer to the measured value. Figures 4-68 and 4-69 are graphical presentations of isotope percentage differences.

Table 4-14 summarizes results from the MCNP pin-cell k_{inf} calculations. The largest difference in k_{inf} (~1.4%) occurs between that calculated for the Calvert Cliffs measured isotopics and the Calvert Cliffs GRCASMO3 predicted isotopics. This may be the result of the cumulative effect of under-predication (compared to SAS2H) of absorber materials in the discharged fuel for the GRCASMO3 depletion. The compelling conclusion of these k_{inf} results is that seemingly large percentage differences in isotope species typically result in less than 1.5% change in k_{inf}.

Table 4-13. Percentage Difference Between Measured and Calculated Isotopic Inventories

Isotope	CC1-SAS2H (CRWMS M&O 1997a)	CC1- GRCASMO3	TP2-SAS2H (CRWMS M&O 1997b)	TP2- GRCASMO3
U^{234}	-0.6	-12.6	2.2	-10.0
U^{235}	-1.7	-4.3	-1.2	-1.2
U^{236}	2.9	-0.8	2.6	-0.4
U^{238}	-0.7	-0.6	-0.2	-0.02
Np^{237}	3.7	-0.8	(a)	(a)
Pu^{238}	-5.4	-12.2	-2.2	-1.1
Pu^{239}	-13.9	-4.3	4.3	-1.7
Pu^{240}	4.7	-2.1	1.6	-0.4
Pu^{241}	-2.2	-5.1	-0.8	-0.4
Pu^{242}	16.6	-9.0	2.3	-4.8
Am^{241}	-5.3	-9.9	(a)	(a)
Nd^{143}	1.8	0.3	(a)	(a)
Nd^{145}	-0.2	-2.7	(a)	(a)
Sm^{149}	-35.5	-33.4	(a)	(a)
Sm^{150}	0.0	-5.5	(a)	(a)
Sm^{152}	14.9	0.6	(a)	(a)
Eu^{153}	0.8	-0.2	(a)	(a)

NOTE: [(a)] Measurement not made for this isotope.

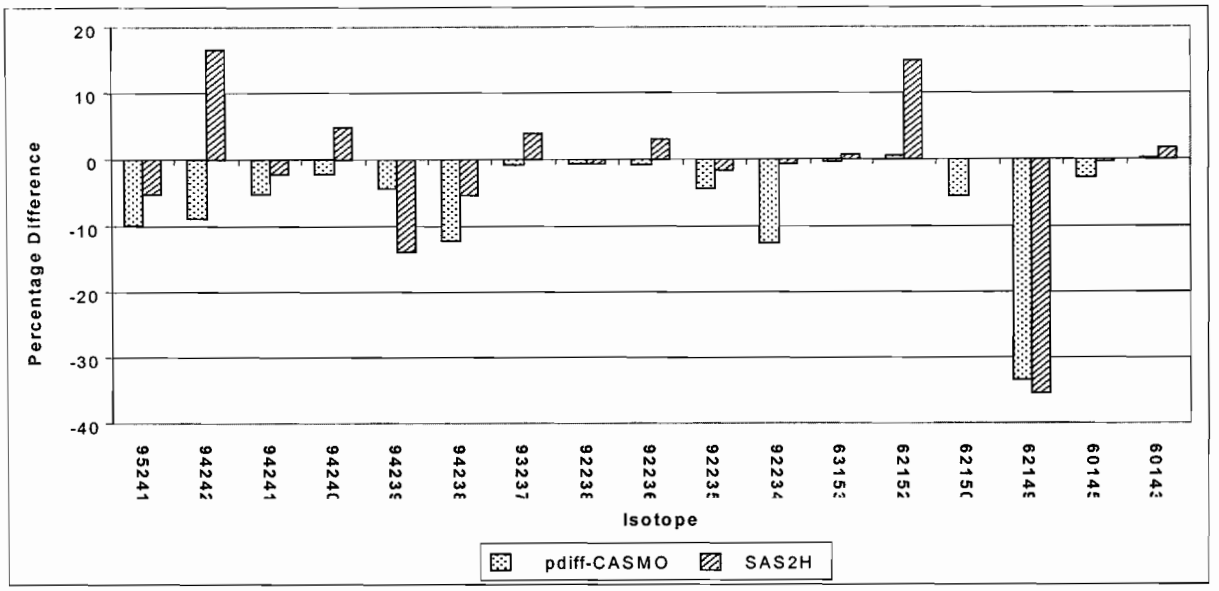

Figure 4-68. Isotope Percentage Differences ((calc/meas-1)*100) for Calvert Cliffs Sample

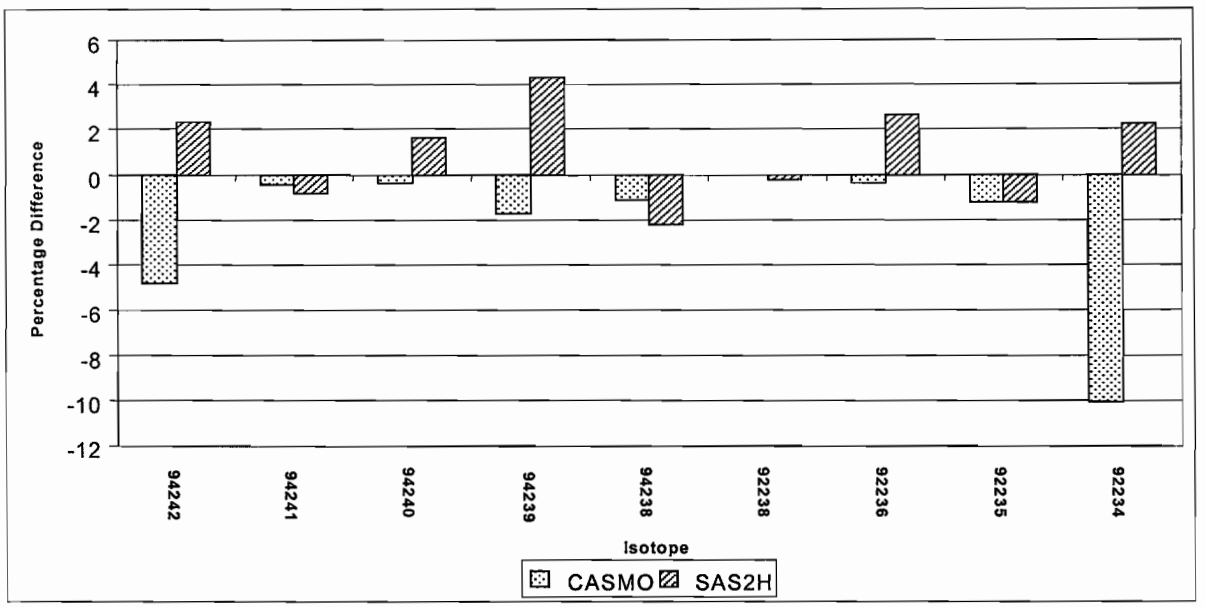

Figure 4-69. Isotope Percentage Differences ((calc/meas-1)*100) for Turkey Point Sample

Table 4-14. MCNP Calculated k_{inf} for Measured and Predicted Isotopic Inventories

	k_{inf}	Error	Difference in k_{inf} (meas – calc isotopics)
Calvert Cliffs - measured	1.05628	0.00104	0
Calvert Cliffs – SAS2H	1.04204	0.00114	+0.01424
Calvert Cliffs - GRCASMO3	1.05718	0.00116	-0.00090
Turkey Point - measured	1.09378	0.00110	0
Turkey Point – SAS2H	1.09524	0.00114	-0.00146
Turkey Point - GRCASMO3	1.08924	0.00110	+0.00454

INTENTIONALLY LEFT BLANK

5. SUMMARY & CONCLUSIONS

In the BWR assembly enrichment smearing analysis, the relative differences in the isotopic concentrations at EOL are within 4% with the exception of U^{235}. The U^{235} is consistently under predicted by the smeared case at MOL and EOL, with a maximum EOL under-prediction of over 14%. It was also observed that as the moderator void fraction increases, the relative difference in U^{235} concentration becomes smaller at EOL. Although the isotopic concentrations might vary, the more important consideration is the effect on k_{inf}. Over all burnups and voids, the differences between the smeared and discrete k_{inf} values are between -0.004 and 0.022. In addition, k_{inf} at EOL is slightly under estimated by the smeared case for all lattice types and at all voids with two exceptions. For the GG1-M lattice, 4.37 average enrichment, 9 Gd rods at 7 wt%, 80% void, the smeared case predicts the same k_{inf} as the discrete case, and for the GG1-M lattice, 4.56 average enrichment, no Gd, 80% void, the smeared case over predicts k_{inf} by less than 0.0002 Δk_{inf} at EOL. For BOL, k_{inf} is over estimated for all lattice types and void conditions by as much as 0.0218 Δk_{inf} for the smeared model. For BOL and MOL, results of using the enrichment smearing approximation is conservative (higher k_{inf} with smeared results). However, for EOL, k_{inf} is under-predicted slightly and not conservative. Therefore, when using a smeared enrichment approximation (as needed when using SAS2H), the under-prediction at EOL should be accommodated with a small bias.

Using the general rules for placement of gadolinia rods in hypothetical BWR assemblies, reasonably representative configurations can be generated, based on comparison of the k_{inf} values between actual designs and hypothetical designs. The Δk_{inf} from burnups greater than 15 GWd/mtU out to EOL is essentially zero. At BOL the Δk_{inf} is ~2.8%, but decreases rapidly with burnup. From 4.5 to 25 GWd/mtU, the general gadolinia rod arrangement results in an over-prediction of k_{inf}. When the general rod pattern is coupled with enrichment smearing, the under-prediction of k_{inf} is reduced to 1% at BOL and the range that k_{inf} is over-predicted falls between 3.5 and 37.5 GWd/mtU.

For PWR assemblies with burnable absorbers, the results indicate that the reactivity effect from burnable absorbers is generally small and well behaved. The k_{inf} for gadolinia-bearing fuel is always less than that for non-gadolinia fuel, with the difference being less that 0.2% Δk_{inf} at 45 GWd/mtU. The k_{inf} for erbia-bearing fuel is also always less than that for the non-erbia fuel, with the difference being approximately 1% Δk_{inf} at 45 GWd/mtU. The k_{inf} for IFBA-bearing fuel becomes greater than that for the non-IFBA fuel near 35 GWd/mtU, but only by 0.2%, and then it decreases with burnup. For the IBA cases, where the poison rods replace uranium fuel rods, the k_{inf} is obviously always less than the non-IBA cases, but the difference decreases from $-0.14\ \Delta k_{inf}$ to $-0.002\Delta k_{inf}$ between 0 and 45 GWd/mtU, respectively. For both Pyrex BPRs and WABAs, k_{inf} is higher at time of removal by up to 2%, but diminishes with further burnup. Although not expected in actual reactor operation, the case with Ag-In-Cd control rods was investigated and found to result in approximately a 3% Δk_{inf} at time of removal (15 GWd/mtU) and diminishes slightly with further irradiation. Burning with control rods would, therefore, result in the most conservative k_{inf} results for PWR assemblies.

This analysis has given an overview of the effects of in-reactor irradiation on the isotopic inventory of PWR fuels containing different types of burnable absorbers. The work presented

illustrates typical magnitudes of the reactivity effects from depleting PWR fuel with the various types of burnable absorbers used to date. It is believed, from a phenomenological basis, that specific BA fuel designs will behave similarly. Because there appears to be a negative reactivity impact on SNF that used gadolinia or erbia, it may be conservative to ignore those neutron absorbers when performing depletion calculations for burnup credit applications. This approach would of course need to be validated as a part of a criticality methodology seeking approval from a licensing authority. In addition, since the neutronic behavior of other types of BAs and control rods can be predicted, their effects can be accounted for in the development of a criticality methodology involving them.

Five different lattices were considered in evaluating the fission product worth in a 3.7 wt% U^{235} enriched PWR assembly, with a cooling time of 5 years. These are as follows:

1. explicit 21-PWR assembly waste package
2. same as above with boron in borated stainless steel replaced by aluminum
3. same as above with borated stainless steel replaced by water
4. infinite lattice with same lattice as 1
5. infinite lattice based on hypothetical reactor lattice

Based on review of the results from the MCNP calculations for these various lattices at 10 to 50 GWd/mtU burnup, the worth of fission products in a 21-PWR waste package is estimated to be one-quarter to one-third of the total burnup credit worth. This evaluation considers only unpoisoned PWR fuel assemblies, so future work should consider absorber effects.

The code-to-code comparisons were focused on demonstrating the ability of SAS2H to adequately represent BWR and PWR assemblies by comparing the GRCASMO3 and SAS2H results.

Initially, the BWR control blade case in SAS2H was refined by comparing results to GRCASMO3 results and adjusting the 1-D SAS2H representation to better match the 2-D representation in GRCASMO3. This case was then applied in burnup calculations for four assemblies. Two GRCASMO3 cases were developed for comparison. For uncontrolled nodes, SAS2H tends to over-deplete U^{235} and under-convert Pu^{239} relative to GRCASMO3. For controlled nodes of the GG1, type G assembly, the opposite is seen. For the controlled nodes of the QC2, Type C assembly, SAS2H tended to over-deplete the U^{235} and over convert the Pu^{239}. Differences between SAS2H and GRCASMO were as large as 9% Δk_{inf} for nodes controlled late in life and 4.6% Δk_{inf} for enriched nodes that were never controlled. Additional analyses will be needed before the bias and uncertainty associated with the use of SAS2H for BWR spent fuel for disposal criticality can be determined.

For PWR assemblies, SAS2H results from previous calculations were compared to RCA benchmark results, along with GRCASMO3 results generated for this report. Results for a Calvert Cliffs sample and one from Turkey Point were used. The U^{235} concentration agreed well between SAS2H and GRCASMO3 and the RCA information for TP2, but the SAS2H concentration was significantly more under-predicted for CC1. For Pu^{239} the difference between calculated and measured concentrations was a factor of 3 higher for SAS2H results compared to

those for GRCASMO3 for CC1 with both codes under-predicting concentration. For TP2, SAS2H over-predicted the Pu^{239} concentration, while GRCASMO3 under-predicted it. The calculated concentration for Sm149 differs by more than -30% from the radiochemical assay information for both codes. For the concentration of Sm152, GRCASMO3 predicts a value close to measurement but SAS2H over-predicts the value by 15%. The cumulative impact on k_{inf} is relatively small, with the maximum difference being only 1.5% between SAS2H and measured for CC1. For TP2, SAS2H isotopics, though slightly under-predicting k_{inf}, resulted in a closer match in k_{inf} than GRCASMO3. Overall, SAS2H-calculated isotopics appear to result in k_{inf} values that match measurement nearly as well as GRCASMO.

These results demonstrate the ability of SAS2H to adequately predict the isotopic inventory of spent commercial nuclear fuel based on the assumptions and approximations inherent to a 1-Dimension lattice physics code methodology.

INTENTIONALLY LEFT BLANK

6. REFERENCES

Barbero, P.; Bidoglio, G.; Bresesti, M.; Caldiroli, A.; Daniele, F.; De Meester, R.; Dierckx, R.; Ernstberger, R.; Facchetti, S.; Frigo, A.; Guardini, S.; Ghezzi, E.; Guzzi, G.; Ullah, H.; Lezzoli, L.; Koch, L.; Konrad, W.; Mammarella, L.; Mannone, F.; Marell, A.; Schurekmper, A.; Trincherini, P.R.; and Tsuruta, H. 1979. *Post-Irradiation Analysis of the Gundremmingen BWR Spent Fuel.* EUR 6301 EN. Luxembourg, Luxembourg: Commission of the European Communities. TIC: 249145.

BSC (Bechtel SAIC Company) 2001. *Technical Work Plan for: Waste Package Design Description for LA.* TWP-EBS-MD-000004 REV 02. Las Vegas, Nevada: Bechtel SAIC Company. ACC: MOL.20011106.0177.

CRWMS M&O (Civilian Radioactive Waste Management System Management and Operating Contractor) 2000. *Software Code: SCALE.* V4.4A. HP. 10129-4.4A-00.

CRWMS M&O 1999a. *Classification of the MGR Uncanistered Spend Nuclear Fuel Disposal Container System*, ANL-UDC-SE-000001 REV 00. Las Vegas, Nevada: CRWMS M&O. ACC: MOL.19990928.0216.

CRWMS M&O 1999b. *Waste Package Materials Properties.* BBA000000-01717-0210-00017 REV 00. Las Vegas, Nevada: CRWMS M&O. ACC: MOL.19990407.0172.

CRWMS M&O 1999c. *CRC Depletion Calculations for Quad Cities Unit 2.* B00000000-01717-0210-00009 REV. 01. Las Vegas, Nevada: CRWMS M&O. ACC: MOL.19990929.0121.

CRWMS M&O 1998 . *Software Code: MCNP.* 4B2LV. HP. 30033 V4B2LV.

CRWMS M&O 1997a. *SAS2H Analysis of Radiochemical Assay Samples from Calvert Cliffs PWR Reactor.* B00000000-01717-0200-00138 REV 00. Las Vegas, Nevada: CRWMS M&O. ACC: MOL.19971210.0578.

CRWMS M&O 1997b. *SAS2H Analysis of Radiochemical Assay Samples from Turkey Point PWR Reactor.* B00000000-01717-0200-00141 REV 00. Las Vegas, Nevada: CRWMS M&O. ACC: MOL.19971229.0350.

CRWMS M&O 1997c. *Software Code: SCALE.* V4.3. HP. 30011 V4.3.

DOE (U.S. Department of Energy) 2002. *Quality Assurance Requirements and Description.* DOE/RW-0333P, Rev. 11. Washington, D.C.: U.S. Department of Energy, Office of Civilian Radioactive Waste Management. ACC: MOL.20020506.0915.

DOE 1992. *Characteristics of Potential Repository Wastes.* DOE/RW-0184-R1. Volume 1. Washington, D.C.: U.S. Department of Energy, Office of Civilian Radioactive Waste Management. ACC: HQO.19920827.0001.

Duderstadt, J.J. and Hamilton L.J. 1976. *Nuclear Reactor Analysis.* New York, New York: John Wiley & Sons. TIC: 245454.

FCF (Framatome Cogema Fuels) 1999. *Quad Cities 2 State Points and Depletion Cycles 9 to 14 (HLW).* Proprietary 32-1267366-01. Lynchburg, Virginia: Framatome Cogema Fuels. ACC: MOL.19990628.0239.

Guardini, S. and Guzzi, G. 1983. *Benchmark, Reference Data on Post Irradiation Analysis of Light Water Reactor Fuel Samples.* EUR 7879 EN. Luxembourg, Luxembourg: Commission of the European Communities. TIC: 250397.

Naito, Y.; Kurosawa, M.; and Kaneko, T. 1994. *Data Book of the Isotopic Composition of Spent Fuel in Light Water Reactors.* JAERI-M-94-034. [Tokyo, Japan]: Japan Atomic Energy Research Institute. TIC: 250378.

YMP (Yucca Mountain Site Characterization Project) 2000. *Disposal Criticality Analysis Methodology Topical Report.* YMP/TR-004Q REV. 01. Yucca Mountain Site Characterization Office. Las Vegas, Nevada: YMP. ACC: MOL.20001214.0001.

6.1 SOURCE DATA, LISTED BY DATA TRACKING NUMBER

MO0109SPADRN04.003. Code-To-Code Comparisons for the Disposal Criticality Methodology. Submittal date: 09/13/2001.

MO0106SPASTA00.005. GG1 Statepoints & DEPL CY2-8. Submittal date: 06/21/2001.

MO0204SPABCF04.012. Burnup Credit Fission Product Worth Scoping Calculations. Submittal date: 04/19/2002.

Appendix A INTEGRAL & REMOVABLE BURNABLE ABSORBER STUDY

INTENTIONALLY LEFT BLANK

APPENDIX A
RESULTS FROM INTEGRAL AND REMOVABLE BURNABLE ABSORBER STUDY

Appendix A provides the results from a fuel assembly burnup study (MO0204SPAIRB04.013) considering different amounts of integral burnable absorber (Gd_2O_3 – UO_2) and removable burnable absorber (B_4C – Al_2O_3). Only fuel assemblies that contain uranium fuel with Gadolinia are considered. The results are provided as a function of burnup based on two cycles of operation in which the removable burnable absorber is removed after the first cycle.

The selected fuel assembly for the model is a B&W Fuel Company fuel assembly with a "15x15" fuel pin array. Table A-1 provides the assumptions used in the analysis.

Table A-1. Assumptions Used in the Analysis

Description	Assumption[a]
Reactor Power	2568 MWt (cases 1-32 & 41-56) 2544 MWt (cases 33-40)
Number Fuel Assemblies	177 FA
Fuel Assembly	B&W 15x15 array 208 Fuel Pins, 16 Guide Tubes 1 Instrument Tube
Fuel Assembly Type	Mark-B9
Assembly Pitch	21.81098 cm
Pin Pitch	1.44272 cm
Irradiation Period	First Cycle with BP rods = 27.391GWd/mtU Second Cycle no BP rods = 24.757 GWd/mtU
Pressure/Fuel Temp/Coolant Temp Soluble Boron Concentration	1.517×10^7 Pa / 921.89 K / 577.44 K 700 ppmB
Assembly Loading	463.45 Kg U
Fuel Pellet OR Fuel Clad IR Fuel Clad OR	0.46990 cm 0.47897 cm 0.54610 cm
Fuel Pellet Density for Standard Fuel Gd_2O_3-UO_2 Fuel (2.00 wt% Gd_2O_3) Gd_2O_3-UO_2 Fuel (3.01 wt% Gd_2O_3) Gd_2O_3-UO_2 Fuel (6.08 wt% Gd_2O_3) Gd_2O_3-UO_2 Fuel (8.17 wt% Gd_2O_3)	 10.2036 g/cm^3 10.1308 g/cm^3 10.0950 g/cm^3 9.9895 g/cm^3 9.9207 g/cm^3
Stainless Steel Rod OR	0.5461 cm
Fuel Active Height	357.111 cm
Instrument Tube IR Instrument Tube OR	0.56007 cm 0.62611 cm
Guide Tube IR Guide Tube OR	0.63246 cm 0.67310 cm
Burnable Poison Pellet OR Burnable Poison Clad IR Burnable Poison Clad OR	0.4318 cm 0.4572 cm 0.5461 cm

[a]Reference: MO0204SPAIRB04.013

Additional information on the Mark-B9 fuel assembly used for this study are presented in Section 2.3 of Punatar, M.K. 2001 and Section 2.4 of Wimmer, L.B. 2001. The fuel assembly burnup calculations were performed with the two-dimensional CASMO-3 lattice physics code (MO0204SPAIRB04.013). The results from these analyses may be used in future code-to-code evaluations.

A cross-sectional view of the 15 x 15 pin array is indicated in Figures A-1 through A-56 (for cases 1 through 56) depicting the different burnable absorber loadings. A description of the layout is provided below each figure. For cases 25 through 32 (Figures A-25 through A-32), ten of the standard fuel rods (i.e., rods that did not contain Gd_2O_3) were replaced with stainless steel rods.

Tables A-2 through A-15 summarize the results for k-infinity vs. burnup for the selected burnable poison loadings. A description of the assumptions for each case is provided at the top of each table. These results are provided in graph form in Figures A-57 through A-70.

Table A-16 provides isotopic concentration values versus burnup for selected fission products and actinides. The data in this table are from case 4 (see cross-sectional view of assembly in Figure A-4).

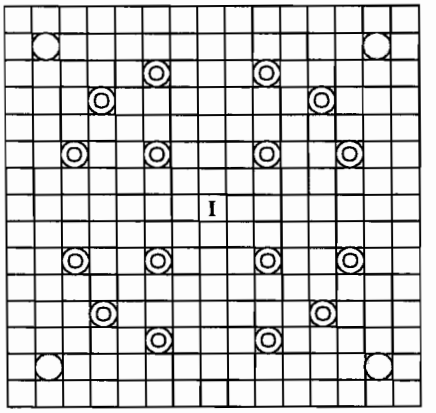

Figure A-1. 4 Gd Rods with 2.00 wt% Gd_2O_3 and 4.19 wt% ^{235}U, No B_4C - Al_2O_3 rods

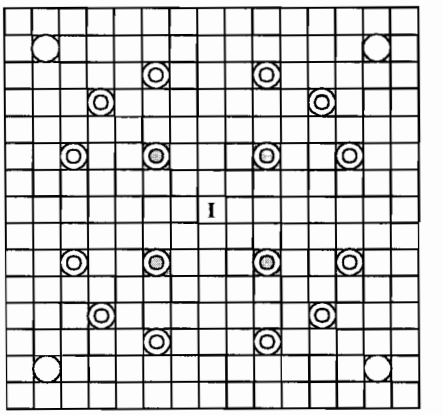

Figure A-2. 4 Gd Rods with 2.00 wt% Gd_2O_3 and 4.19 wt% ^{235}U, 4 B_4C - Al_2O_3 rods with 2.10 wt% B_4C

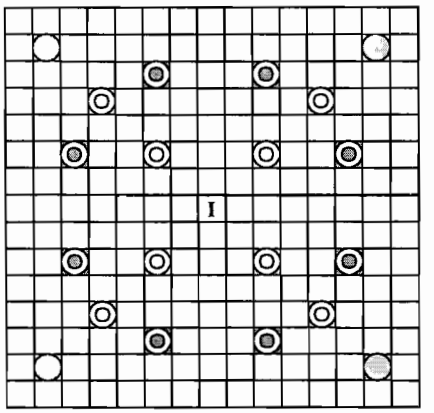

Figure A-3. 4 Gd Rods with 2.00 wt% Gd_2O_3 and 4.19 wt% ^{235}U, 8 B_4C - Al_2O_3 rods with 2.10 wt% B_4C

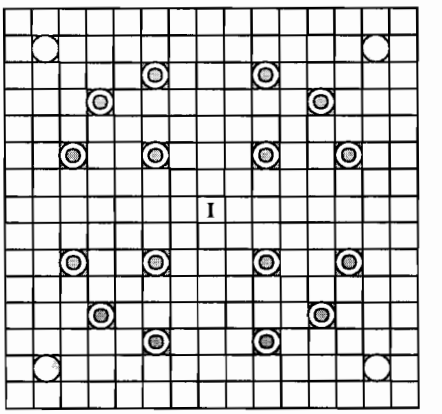

Figure A-4. 4 Gd Rods with 2.00 wt% Gd_2O_3 and 4.19 wt% ^{235}U, 16 B_4C - Al_2O_3 rods with 2.10 wt% B_4C

- Gd_2O_3 - UO_2 rod
- Guide tube
- B_4C - Al_2O_3 rod
- UO_2 rod 4.65 wt% ^{235}U
- I Instrument tube

Figures A-1 to A-4. Gd (2.00 wt%), U235 (4.19 wt%), B_4C (2.10 wt%)

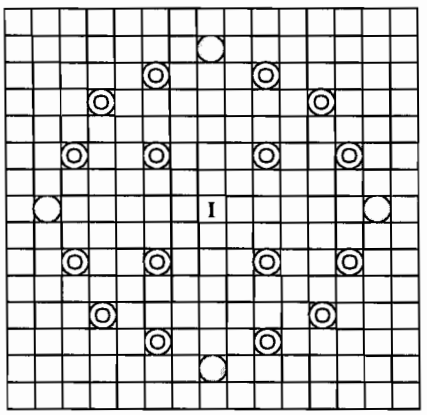

Figure A-5. 4 Gd Rods with 2.00 wt% Gd_2O_3 and 4.19 wt% ^{235}U, No B_4C - Al_2O_3 rods

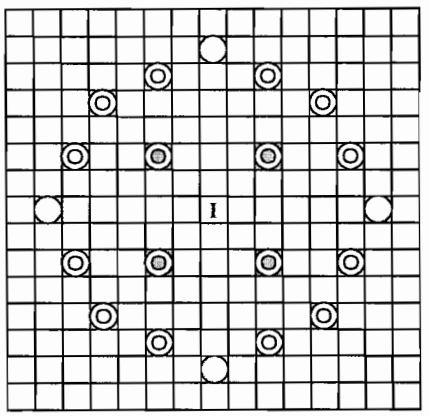

Figure A-6. 4 Gd Rods with 2.00 wt% Gd_2O_3 and 4.19 wt% ^{235}U, 4 B_4C - Al_2O_3 rods with 2.10 wt% B_4C

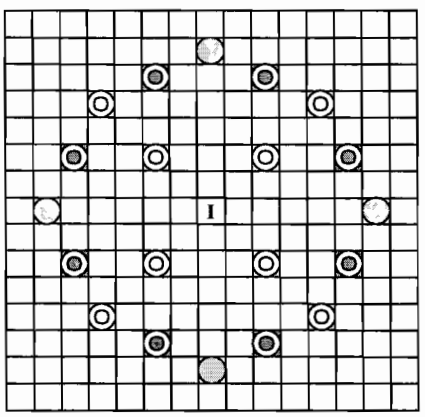

Figure A-7. 4 Gd Rods with 2.00 wt% Gd_2O_3 and 4.19 wt% ^{235}U, 8 B_4C - Al_2O_3 rods with 2.10 wt% B_4C

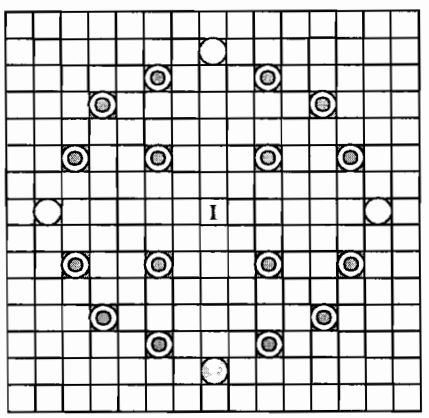

Figure A-8. 4 Gd Rods with 2.00 wt% Gd_2O_3 and 4.19 wt% ^{235}U, 16 B_4C - Al_2O_3 rods with 2.10 wt% B_4C

- Gd_2O_3 - UO_2 rod
- Guide tube
- B_4C - Al_2O_3 rod
- UO_2 rod 4.65 wt% ^{235}U
- I Instrument tube

Figures A-5 to A-8. Gd (2.00 wt%), U235 (4.19 wt%), B_4C (2.10 wt%)

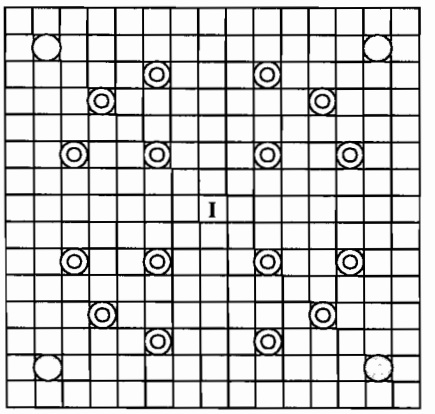

Figure A-9. 4 Gd Rods with 2.00 wt% Gd_2O_3 and 3.60 wt% ^{235}U, No B_4C - Al_2O_3 rods

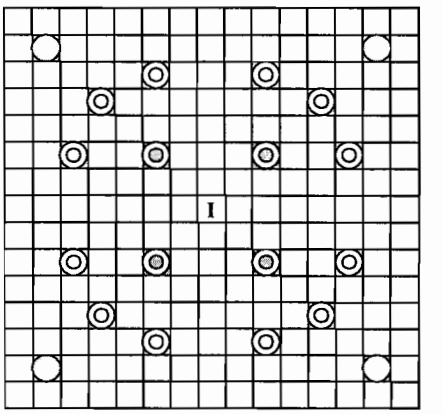

Figure A-10. 4 Gd Rods with 2.00 wt% Gd_2O_3 and 3.60 wt% ^{235}U, 4 B_4C - Al_2O_3 rods with 3.50 wt% B_4C

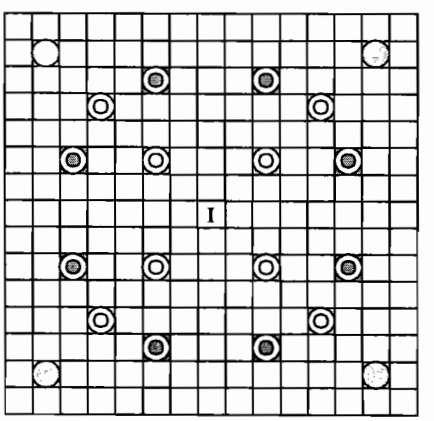

Figure A-11. 4 Gd Rods with 2.00 wt% Gd_2O_3 and 3.60 wt% ^{235}U, 8 B_4C - Al_2O_3 rods with 3.50 wt% B_4C

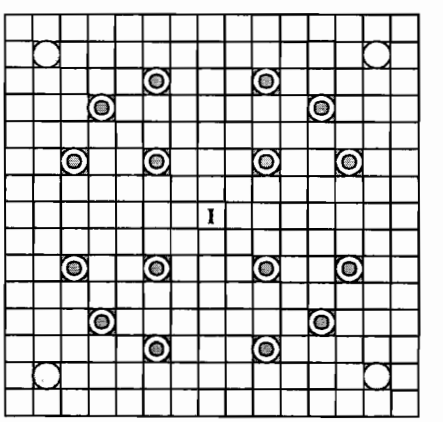

Figure A-12. 4 Gd Rods with 2.00 wt% Gd_2O_3 and 3.60 wt% ^{235}U, 16 B_4C - Al_2O_3 rods with 3.50 wt% B_4C

- Gd_2O_3 - UO_2 rod
- Guide tube
- B_4C - Al_2O_3 rod
- UO_2 rod 4.50 wt% ^{235}U
- I Instrument tube

Figures A-9 to A-12. Gd (2.00 wt%), U235 (3.60 wt%), B_4C (3.50 wt%)

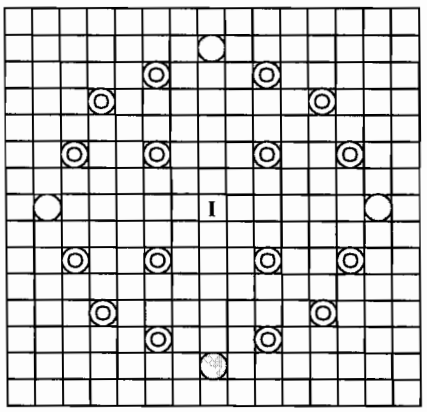

Figure A-13. 4 Gd Rods with 2 wt% Gd_2O_3 and 3.6 wt% ^{235}U, No B_4C - Al_2O_3 rods

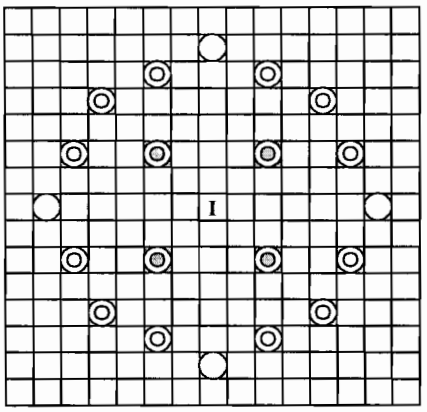

Figure A-14. 4 Gd Rods with 2 wt% Gd_2O_3 and 3.6 wt% ^{235}U, 4 B_4C - Al_2O_3 rods with 3.5 wt% B_4C

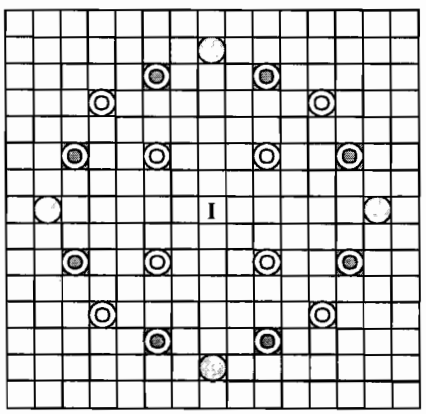

Figure A-15. 4 Gd Rods with 2.00 wt% Gd_2O_3 and 3.60 wt% ^{235}U, 8 B_4C - Al_2O_3 rods with 3.50 wt% B_4C

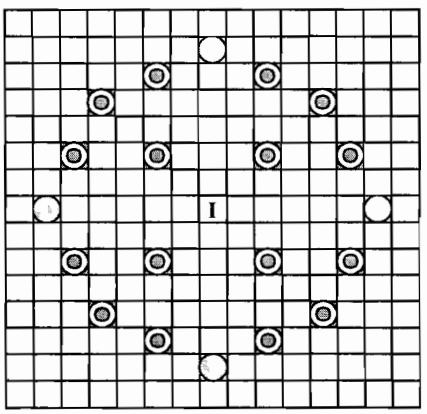

Figure A-16. 4 Gd Rods with 2.00 wt% Gd_2O_3 and 3.60 wt% ^{235}U, 16 B_4C - Al_2O_3 rods with 3.50 wt% B_4C

- Gd_2O_3 - UO_2 rod
- Guide tube
- B_4C - Al_2O_3 rod
- UO_2 rod 4.50 wt% ^{235}U
- I Instrument tube

Figures A-13 to A-16. Gd (2.00 wt%), U235 (3.60 wt%), B_4C (3.50 wt%)

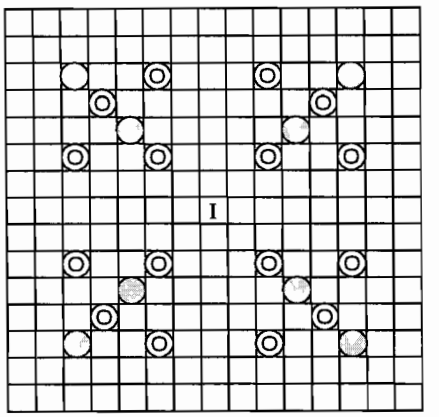

Figure A-17. 8 Gd Rods with 2.00 wt% Gd_2O_3 and 3.60 wt% ^{235}U, No B_4C - Al_2O_3 rods

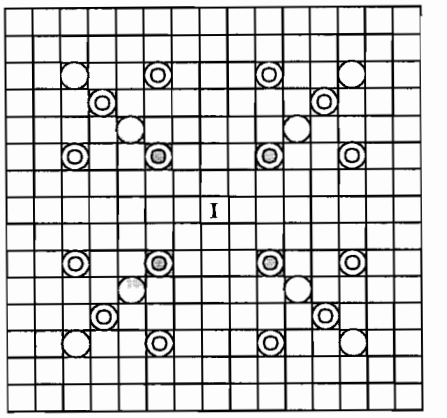

Figure A-18. 8 Gd Rods with 2.00 wt% Gd_2O_3 and 3.60 wt% ^{235}U, 4 B_4C - Al_2O_3 rods with 0.0 wt% B_4C

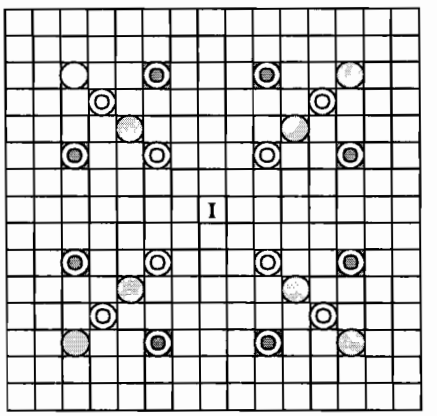

Figure A-19. 8 Gd Rods with 2.00 wt% Gd_2O_3 and 3.60 wt% ^{235}U, 8 B_4C - Al_2O_3 rods with 0.0 wt% B_4C

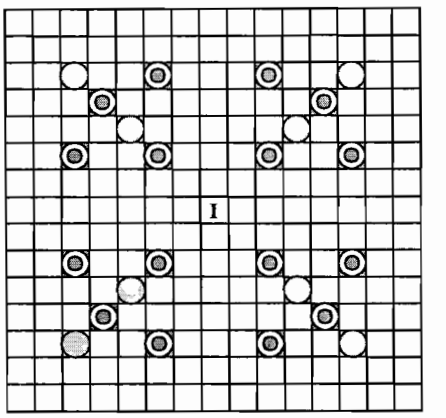

Figure A-20. 8 Gd Rods with 2.00 wt% Gd_2O_3 and 3.60 wt% ^{235}U, 16 B_4C - Al_2O_3 rods with 0.0 wt% B_4C

- Gd_2O_3 - UO_2 rod
- Guide tube
- B_4C - Al_2O_3 rod
- UO_2 rod 4.50 wt% ^{235}U
- I Instrument tube

Figures A-17 to A-20. Gd (2.00 wt%), U235 (3.60 wt%), B_4C (0.0 wt%)

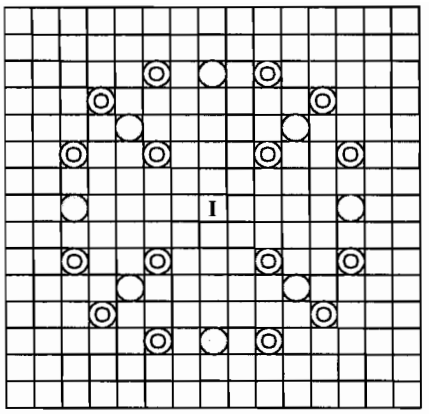

Figure A-21. 8 Gd Rods with 2.00 wt% Gd_2O_3 and 3.60 wt% ^{235}U, No B_4C - Al_2O_3 rods

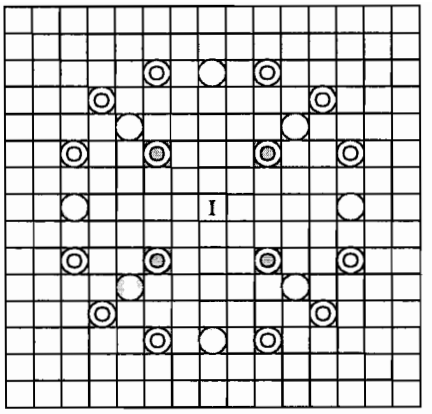

Figure A-22. 8 Gd Rods with 2.00 wt% Gd_2O_3 and 3.60 wt% ^{235}U, 4 B_4C - Al_2O_3 rods with 0.0 wt% B_4C

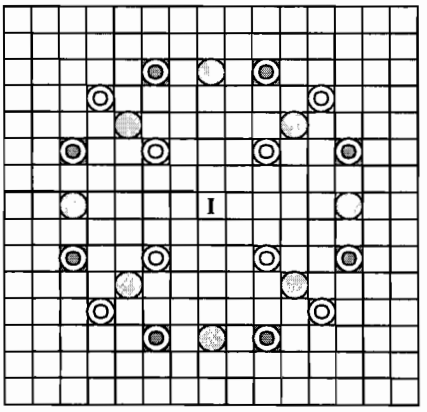

Figure A-23. 8 Gd Rods with 2.00 wt% Gd_2O_3 and 3.60 wt% ^{235}U, 8 B_4C - Al_2O_3 rods with 0.0 wt% B_4C

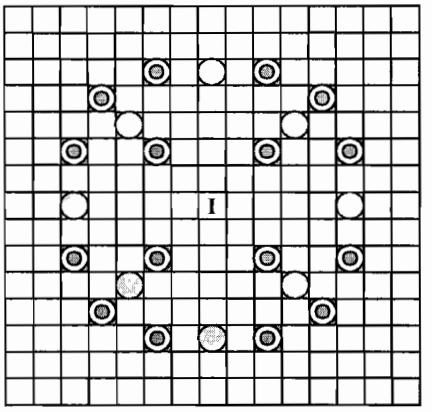

Figure A-24. 8 Gd Rods with 2.00 wt% Gd_2O_3 and 3.60 wt% ^{235}U, 16 B_4C - Al_2O_3 rods with 0.0 wt% B_4C

- Gd_2O_3 - UO_2 rod
- Guide tube
- B_4C - Al_2O_3 rod
- UO_2 rod 4.50 wt% ^{235}U
- I Instrument tube

Figures A-21 to A-24. Gd (2.00 wt%), U235 (3.60 wt%), B_4C (0.0 wt%)

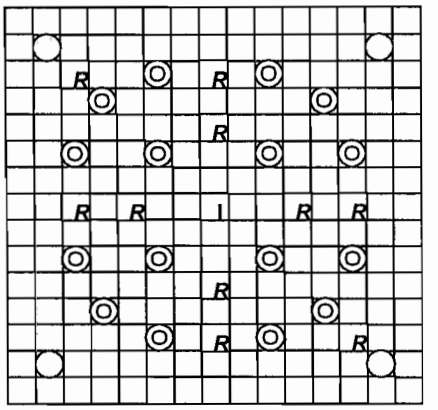

Figure A-25. 4 Gd Rods with 2.00 wt% Gd_2O_3 and 4.19 wt% ^{235}U, No B_4C - Al_2O_3 rods

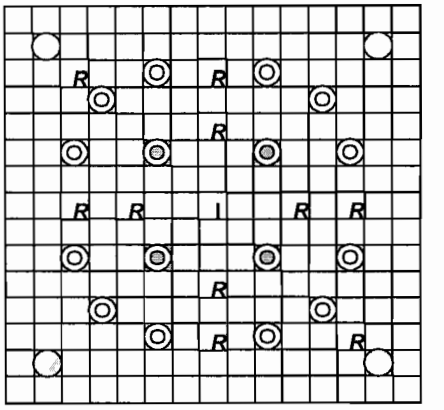

Figure A-26. 4 Gd Rods with 2.00 wt% Gd_2O_3 and 4.19 wt% ^{235}U, 4 B_4C - Al_2O_3 rods with 2.10 wt% B_4C

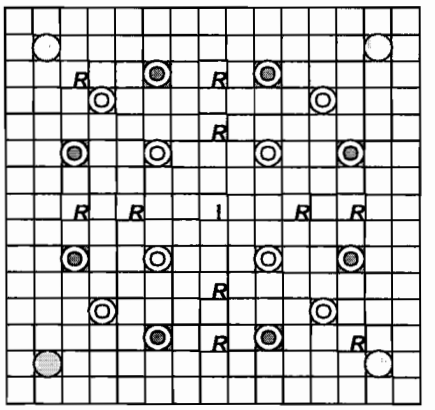

Figure A-27. 4 Gd Rods with 2.00 wt% Gd_2O_3 and 4.19 wt% ^{235}U, 8 B_4C - Al_2O_3 rods with 2.10 wt% B_4C

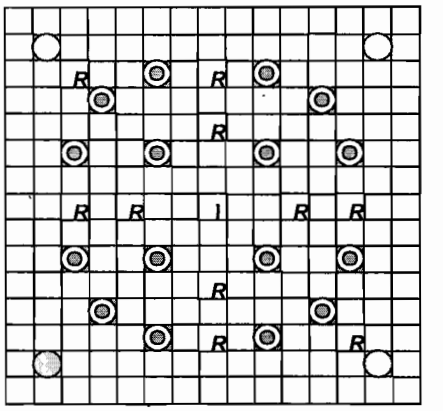

Figure A-28. 4 Gd Rods with 2.00 wt% Gd_2O_3 and 4.19 wt% ^{235}U, 16 B_4C - Al_2O_3 rods with 2.10 wt% B_4C

- Gd_2O_3 - UO_2 rod
- Guide tube
- B_4C - Al_2O_3 rod
- UO_2 rod 4.65 wt% ^{235}U
- Instrument tube
- R — Stainless steel rod inserted for two cycles

Figures A-25 to A-28. Gd (2.00 wt%), U235 (4.19 wt%), B_4C (2.10 wt%)

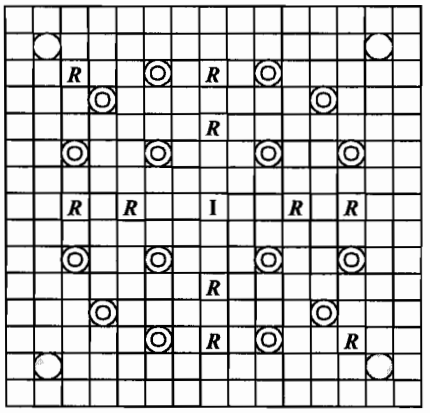

Figure A-29. 4 Gd Rods with 2.00 wt% Gd_2O_3 and 4.19 wt% ^{235}U, No B_4C - Al_2O_3 rods

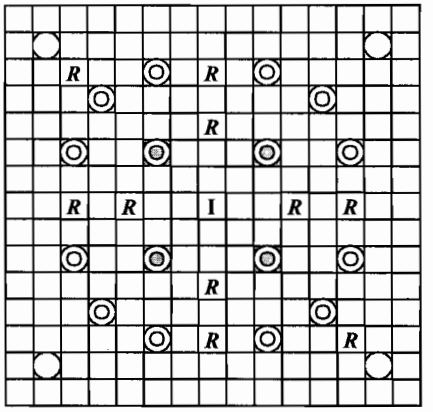

Figure A-30. 4 Gd Rods with 2.00 wt% Gd_2O_3 and 4.19 wt% ^{235}U, 4 B_4C - Al_2O_3 rods with 2.10 wt% B_4C

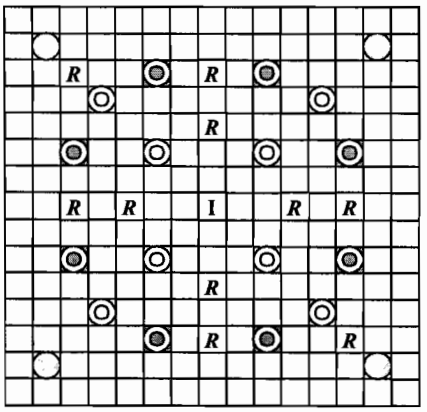

Figure A-31. 4 Gd Rods with 2.00 wt% Gd_2O_3 and 4.19 wt% ^{235}U, 8 B_4C - Al_2O_3 rods with 2.10 wt% B_4C

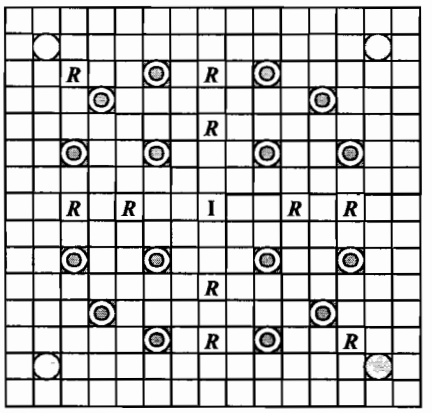

Figure A-32. 4 Gd Rods with 2.00 wt% Gd_2O_3 and 4.19 wt% ^{235}U, 16 B_4C - Al_2O_3 rods with 2.10 wt% B_4C

- Gd_2O_3 - UO_2 rod
- Guide tube
- B_4C - Al_2O_3 rod
- UO_2 rod 4.65 wt% ^{235}U
- I — Instrument tube
- R — Stainless steel rod inserted for second of two cycles

Figures A-29 to A-32. Gd (2.00 wt%), U235 (4.19 wt%), B_4C (2.10 wt%)

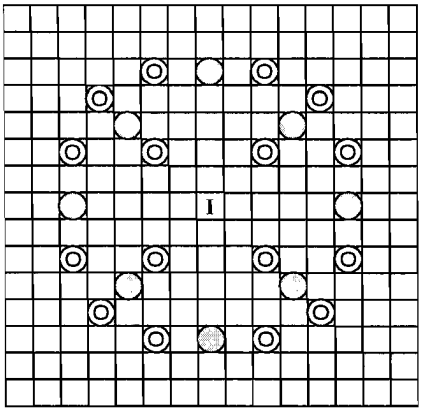

Figure A-37. 8 Gd Rods with 6.08 wt% Gd_2O_3 and 3.40 wt% ^{235}U, No B_4C - Al_2O_3 rods

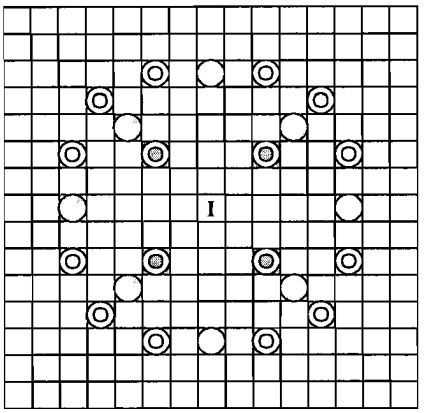

Figure A-38. 8 Gd Rods with 6.08 wt% Gd_2O_3 and 3.40 wt% ^{235}U, 4 B_4C - Al_2O_3 rods with 2.60 wt% B_4C

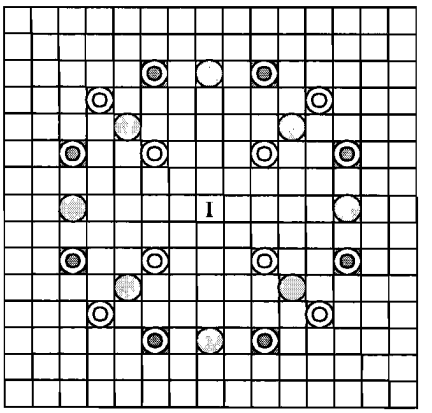

Figure A-39. 8 Gd Rods with 6.08 wt% Gd_2O_3 and 3.40 wt% ^{235}U, 8 B_4C - Al_2O_3 rods with 2.60 wt% B_4C

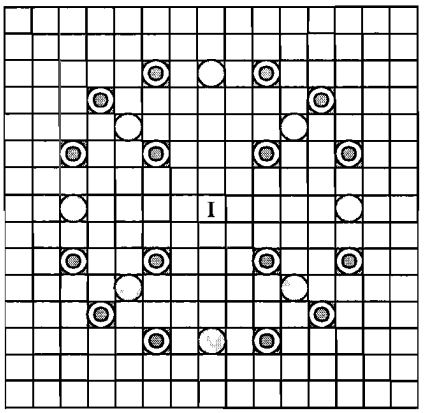

Figure A-40. 8 Gd Rods with 6.08 wt% Gd_2O_3 and 3.40 wt% ^{235}U, 16 B_4C - Al_2O_3 rods with 2.60 wt% B_4C

- Gd_2O_3 - UO_2 rod
- Guide tube
- B_4C - Al_2O_3 rod
- UO_2 rod 4.96 wt% ^{235}U
- I Instrument tube

Figures A-37 to A-40. Gd (6.08 wt%), U235 (3.40 wt%), B_4C (2.60 wt%)

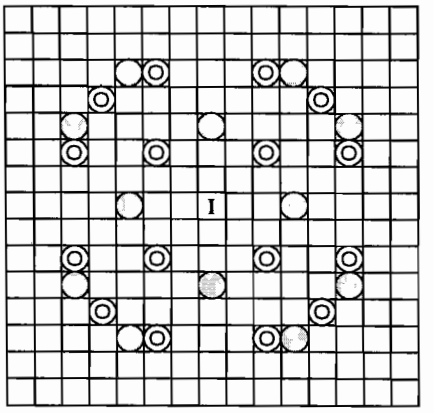

Figure A-41. 12 Gd Rods with 3.01 wt% Gd_2O_3 and 3.99 wt% ^{235}U, No B_4C - Al_2O_3 rods

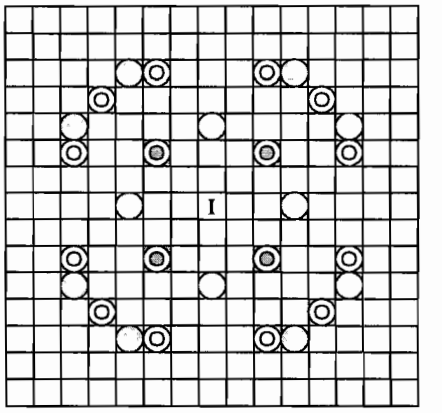

Figure A-42. 12 Gd Rods with 3.01wt% Gd_2O_3 and 3.99 wt% ^{235}U, 4 B_4C - Al_2O_3 rods with 2.10 wt% B_4C

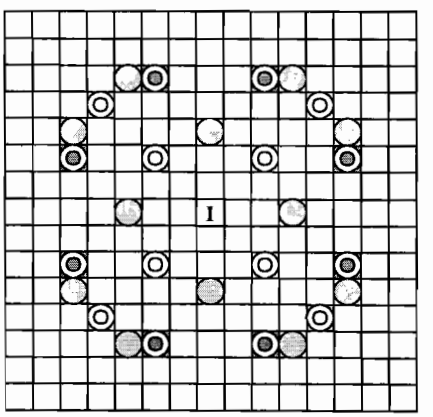

Figure A-43. 12 Gd Rods with 3.01 wt% Gd_2O_3 and 3.99 wt% ^{235}U, 8 B_4C - Al_2O_3 rods with 2.10 wt% B_4C

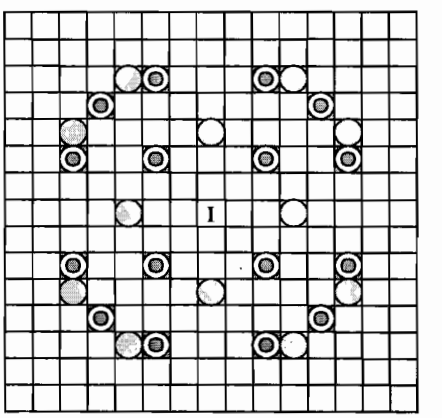

Figure A-44. 12 Gd Rods with 3.01 wt% Gd_2O_3 and 3.99 wt% ^{235}U, 16 B_4C - Al_2O_3 rods with 2.10 wt% B_4C

- Gd_2O_3 - UO_2 rod
- Guide tube
- B_4C - Al_2O_3 rod
- UO_2 rod 4.79 wt% ^{235}U
- I Instrument tube

Figures A-41 to A-44. Gd (3.01 wt%), U235 (3.99 wt%), B_4C (2.10 wt%)

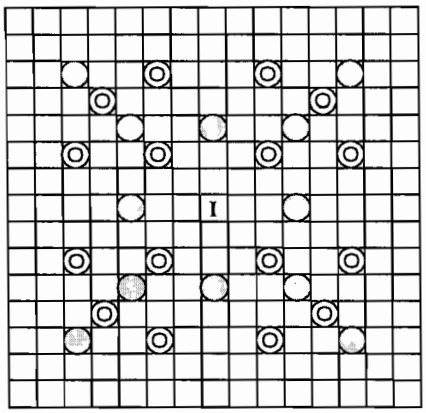

Figure A-45. 12 Gd Rods with 3.01 wt% Gd_2O_3 and 3.99 wt% ^{235}U, No B_4C - Al_2O_3 rods

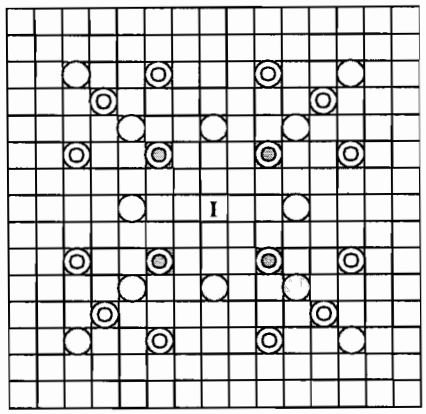

Figure A-46. 12 Gd Rods with 3.01 wt% Gd_2O_3 and 3.99 wt% ^{235}U, 4 B_4C - Al_2O_3 rods with 2.10 wt% B_4C

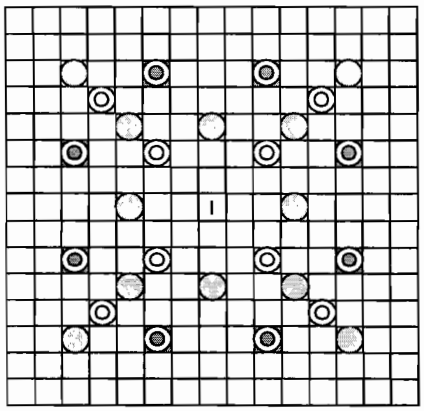

Figure A-47. 12 Gd Rods with 3.01 wt% Gd_2O_3 and 3.99 wt% ^{235}U, 8 B_4C - Al_2O_3 rods with 2.10 wt% B_4C

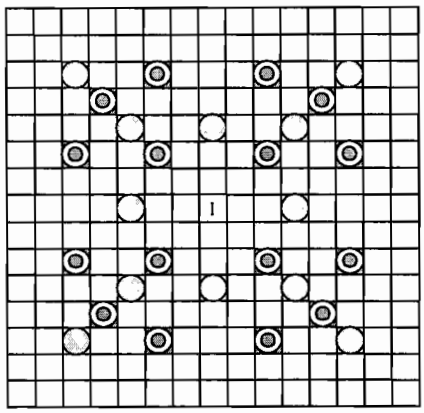

Figure A-48. 12 Gd Rods with 3.01 wt% Gd_2O_3 and 3.99 wt% ^{235}U, 16 B_4C - Al_2O_3 rods with 2.10 wt% B_4C

- Gd_2O_3 - UO_2 rod
- Guide tube
- B_4C - Al_2O_3 rod
- UO_2 rod 4.79 wt% ^{235}U
- I Instrument tube

Figures A-45 to A-48. Gd (3.01 wt%), U235 (3.99 wt%), B_4C (2.10 wt%)

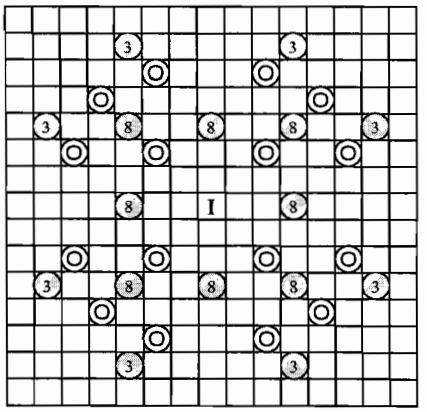

Figure A-49. 8 Gd Rods with 3.01 wt% Gd_2O_3 and 3.99 wt% ^{235}U, 8 Gd Rods with 8.17 wt% Gd_2O_3 and 2.87 wt% ^{235}U, No B_4C - Al_2O_3 rods

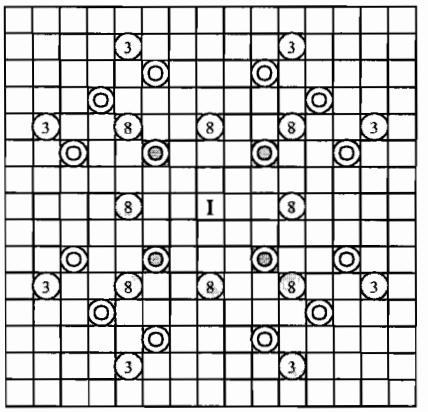

Figure A-50. 8 Gd Rods with 3.01 wt% Gd_2O_3 and 3.99 wt% ^{235}U, 8 Gd Rods with 8.17 wt% Gd_2O_3 and 2.87 wt% ^{235}U, 4 B_4C - Al_2O_3 rods with 2.10 wt% B_4C

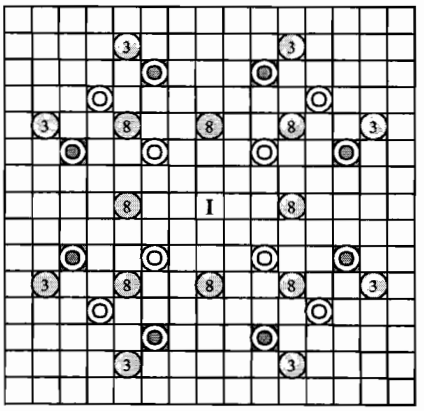

Figure A-51. 8 Gd Rods with 3.01 wt% Gd_2O_3 and 3.99 wt% ^{235}U, 8 Gd Rods with 8.17 wt% Gd_2O_3 and 2.87 wt% ^{235}U, 8 B_4C - Al_2O_3 rods with 2.10 wt% B_4C

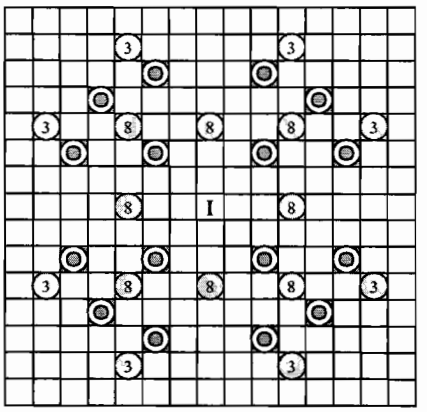

Figure A-52. 8 Gd Rods with 3.01 wt% Gd_2O_3 and 3.99 wt% ^{235}U, 8 Gd Rods with 8.17 wt% Gd_2O_3 and 2.87 wt% ^{235}U, 16 B_4C - Al_2O_3 rods with 2.10 wt% B_4C

- Gd_2O_3 - UO_2 rod
- Guide tube
- B_4C - Al_2O_3 rod
- UO_2 rod 4.79 wt% ^{235}U
- Instrument tube

Figures A-49 to A-52. Gd (3.01/8.17 wt%), U235 (3.99/2.87 wt%), B_4C (2.10 wt%)

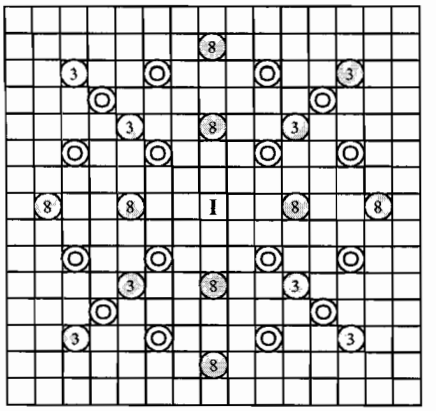

Figure A-53. 8 Gd Rods with 3.01 wt% Gd_2O_3 and 3.99 wt% ^{235}U, 8 Gd Rods with 8.17 wt% Gd_2O_3 and 2.87 wt% ^{235}U, No B_4C - Al_2O_3 rods

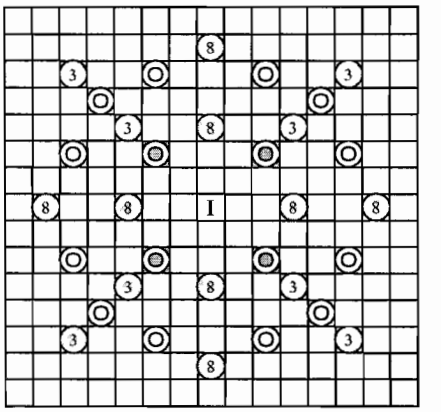

Figure A-54. 8 Gd Rods with 3.01 wt% Gd_2O_3 and 3.99 wt% ^{235}U, 8 Gd Rods with 8.17 wt% Gd_2O_3 and 2.87 wt% ^{235}U, 4 B_4C - Al_2O_3 rods with 2.10 wt% B_4C

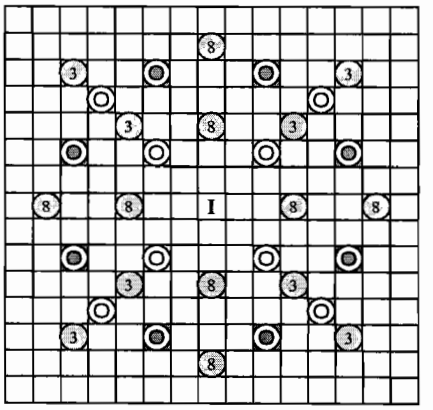

Figure A-55. 8 Gd Rods with 3.01 wt% Gd_2O_3 and 3.99 wt% ^{235}U, 8 Gd Rods with 8.17 wt% Gd_2O_3 and 2.87 wt% ^{235}U, 8 B_4C - Al_2O_3 rods with 2.10 wt% B_4C

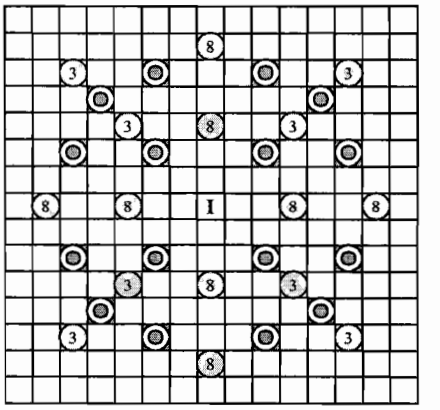

Figure A-56. 8 Gd Rods with 3.01 wt% Gd_2O_3 and 3.99 wt% ^{235}U, 8 Gd Rods with 8.17 wt% Gd_2O_3 and 2.87 wt% ^{235}U, 16 B_4C - Al_2O_3 rods with 2.10 wt% B_4C

- Gd_2O_3 - UO_2 rod
- Guide tube
- B_4C - Al_2O_3 rod
- UO_2 rod 4.79 wt% ^{235}U
- Instrument tube

Figures A-53 to A-56. Gd (3.01/8.17 wt%), U235 (3.99/2.87 wt%), B_4C (2.10 wt%)

Table A-2. k-infinity Vs Burnup for Various BP Loading (Figures 01-04)

Std UO_2 = 4.65 wt % ^{235}U, Gd_2O_3-UO_2 = 2.0 wt % - 4.19 wt % ^{235}U, B_4C= 2.1 wt %, 4 Gd rods

Burnup	k-infinity Vs Burnup			
GWd/mtU	0 BP rods	4 BP rods	8 BP rods	16 BP rods
0.000	1.30538	1.26847	1.23205	1.16481
0.125	1.26855	1.23379	1.19948	1.13597
0.250	1.26572	1.23140	1.19749	1.13469
0.375	1.26353	1.22959	1.19604	1.13389
0.500	1.26177	1.22817	1.19496	1.13341
0.625	1.26029	1.22701	1.19412	1.13315
0.750	1.25910	1.22614	1.19355	1.13312
0.875	1.25810	1.22543	1.19314	1.13323
1.000	1.25721	1.22484	1.19283	1.13343
1.250	1.25572	1.22390	1.19243	1.13399
1.500	1.25432	1.22307	1.19214	1.13469
1.750	1.25300	1.22232	1.19192	1.13543
2.000	1.25171	1.22158	1.19172	1.13618
2.250	1.25042	1.22084	1.19150	1.13691
2.500	1.24912	1.22008	1.19126	1.13762
2.750	1.24781	1.21932	1.19102	1.13831
3.000	1.24650	1.21854	1.19076	1.13897
3.250	1.24517	1.21775	1.19048	1.13961
3.500	1.24384	1.21695	1.19018	1.14022
3.750	1.24249	1.21613	1.18986	1.14080
4.000	1.24114	1.21529	1.18952	1.14135
4.250	1.23977	1.21444	1.18916	1.14187
4.500	1.23840	1.21357	1.18877	1.14236
4.750	1.23701	1.21268	1.18837	1.14280
5.000	1.23561	1.21177	1.18792	1.14320
5.250	1.23418	1.21081	1.18743	1.14352
5.500	1.23271	1.20980	1.18688	1.14378
5.750	1.23121	1.20875	1.18627	1.14395
6.000	1.22966	1.20762	1.18559	1.14405
6.250	1.22805	1.20643	1.18483	1.14406
6.500	1.22638	1.20518	1.18401	1.14398
6.750	1.22466	1.20385	1.18310	1.14382
7.000	1.22287	1.20246	1.18213	1.14360
7.500	1.21908	1.19943	1.17995	1.14290
8.000	1.21515	1.19627	1.17762	1.14203
8.500	1.21106	1.19294	1.17510	1.14097

Table A-2. k-infinity Vs Burnup for Various BP Loading (Figures 01-04), Cont.

Burnup	k-infinity Vs Burnup			
GWd/mtU	0 BP rods	4 BP rods	8 BP rods	16 BP rods
9.000	1.20684	1.18947	1.17244	1.13973
9.500	1.20253	1.18589	1.16965	1.13835
10.000	1.19814	1.18222	1.16678	1.13688
10.500	1.19372	1.17852	1.16384	1.13532
11.000	1.18927	1.17480	1.16086	1.13370
11.500	1.18483	1.17107	1.15785	1.13202
12.000	1.18039	1.16733	1.15481	1.13028
12.500	1.17599	1.16361	1.15176	1.12849
13.000	1.17161	1.15987	1.14871	1.12664
13.500	1.16726	1.15616	1.14563	1.12475
14.000	1.16295	1.15248	1.14254	1.12280
14.500	1.15868	1.14879	1.13945	1.12082
15.000	1.15444	1.14513	1.13633	1.11875
15.500	1.15024	1.14147	1.13321	1.11663
16.000	1.14606	1.13781	1.13007	1.11445
16.500	1.14192	1.13417	1.12690	1.11219
17.000	1.13781	1.13054	1.12372	1.10989
17.500	1.13372	1.12691	1.12052	1.10752
18.000	1.12967	1.12328	1.11729	1.10509
18.500	1.12564	1.11966	1.11405	1.10259
19.000	1.12164	1.11603	1.11080	1.10004
19.500	1.11767	1.11242	1.10752	1.09743
20.000	1.11372	1.10882	1.10423	1.09477
21.000	1.10585	1.10158	1.09758	1.08925
22.000	1.09811	1.09440	1.09089	1.08356
23.000	1.09045	1.08722	1.08415	1.07770
24.000	1.08287	1.08006	1.07736	1.07170
25.000	1.07537	1.07291	1.07055	1.06556
26.000	1.06790	1.06577	1.06369	1.05929
27.391	1.05761	1.05585	1.05412	1.05043
27.392	1.05757	1.05910	1.06054	1.06365
30.000	1.03872	1.04037	1.04195	1.04536
33.000	1.01746	1.01905	1.02058	1.02386
36.000	0.99657	0.99814	0.99963	1.00286
39.000	0.97609	0.97765	0.97913	0.98232
42.000	0.95601	0.95756	0.95904	0.96224
45.000	0.93636	0.93791	0.93939	0.94258
50.000	0.90533	0.90686	0.90834	0.91150
52.148	0.89183	0.89335	0.89482	0.89798

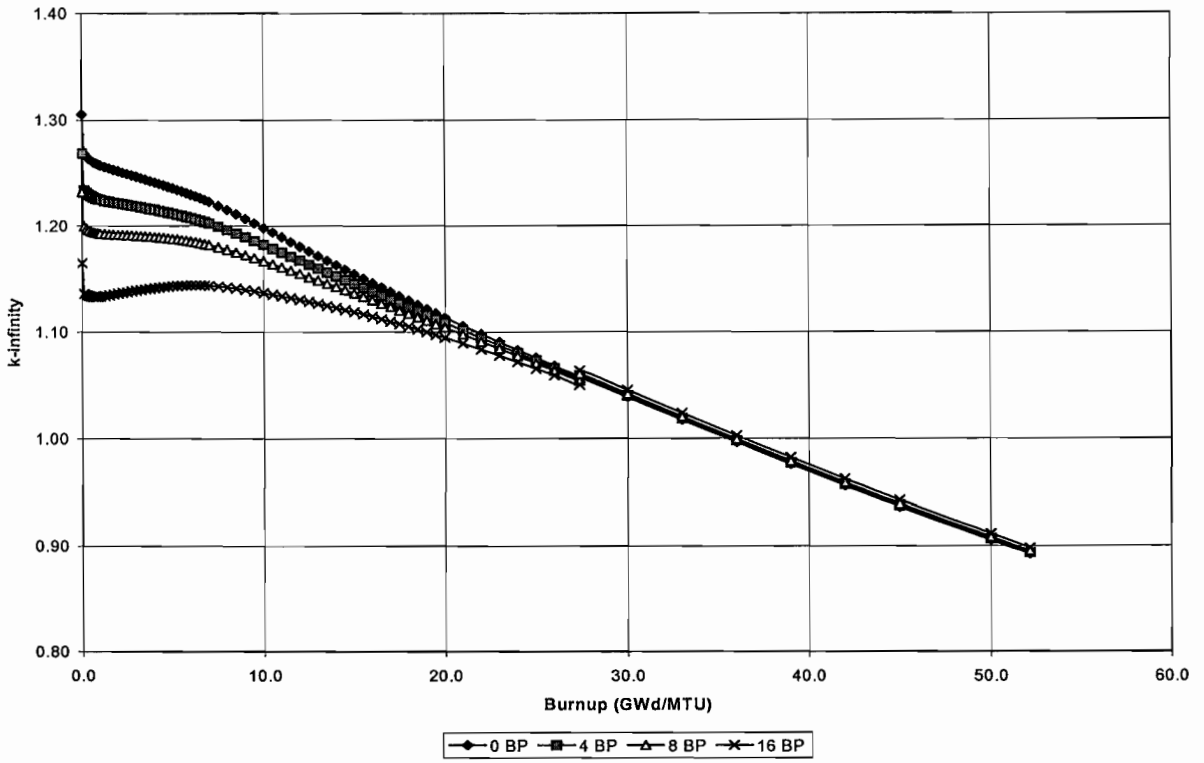

Figure A-57. k-infinity Vs Burnup for Various BP Loading (Figures 01-04)

Table A-3. k-infinity Vs Burnup for Various BP Loading (Figures 05-08)

Std UO_2 = 4.65 wt % ^{235}U, Gd_2O_3-UO_2 = 2.0 wt % - 4.19 wt % ^{235}U, B_4C= 2.1 wt %, 4 Gd rods

Burnup	k-infinity Vs Burnup			
GWd/mtU	0 BP rods	4 BP rods	8 BP rods	16 BP rods
0.000	1.30434	1.26819	1.23530	1.16786
0.125	1.26760	1.23354	1.20241	1.13874
0.250	1.26480	1.23116	1.20032	1.13737
0.375	1.26265	1.22936	1.19878	1.13647
0.500	1.26091	1.22795	1.19760	1.13591
0.625	1.25946	1.22681	1.19669	1.13556
0.750	1.25832	1.22595	1.19603	1.13545
0.875	1.25734	1.22526	1.19553	1.13547
1.000	1.25649	1.22468	1.19513	1.13558
1.250	1.25506	1.22377	1.19455	1.13597
1.500	1.25373	1.22296	1.19409	1.13649
1.750	1.25249	1.22223	1.19369	1.13705
2.000	1.25127	1.22152	1.19329	1.13762
2.250	1.25005	1.22080	1.19290	1.13817
2.500	1.24882	1.22007	1.19248	1.13869
2.750	1.24759	1.21934	1.19205	1.13920
3.000	1.24634	1.21859	1.19161	1.13969
3.250	1.24509	1.21782	1.19115	1.14015
3.500	1.24382	1.21705	1.19067	1.14059
3.750	1.24254	1.21625	1.19018	1.14100
4.000	1.24125	1.21543	1.18967	1.14140
4.250	1.23994	1.21460	1.18914	1.14176
4.500	1.23862	1.21375	1.18861	1.14210
4.750	1.23729	1.21288	1.18805	1.14242
5.000	1.23593	1.21197	1.18747	1.14270
5.250	1.23453	1.21102	1.18687	1.14293
5.500	1.23309	1.21001	1.18623	1.14312
5.750	1.23160	1.20895	1.18555	1.14325
6.000	1.23005	1.20782	1.18484	1.14332
6.250	1.22844	1.20661	1.18406	1.14332
6.500	1.22676	1.20534	1.18323	1.14325
6.750	1.22501	1.20400	1.18233	1.14310
7.000	1.22320	1.20260	1.18136	1.14289
7.500	1.21937	1.19954	1.17923	1.14224
8.000	1.21540	1.19635	1.17696	1.14144
8.500	1.21126	1.19299	1.17451	1.14044

Table A-3. k-infinity Vs Burnup for Various BP Loading (Figures 05-08), Cont.

Burnup	k-infinity Vs Burnup			
GWd/mtU	0 BP rods	4 BP rods	8 BP rods	16 BP rods
9.000	1.20700	1.18950	1.17192	1.13928
9.500	1.20264	1.18589	1.16921	1.13797
10.000	1.19822	1.18222	1.16640	1.13655
10.500	1.19378	1.17851	1.16351	1.13502
11.000	1.18932	1.17477	1.16058	1.13343
11.500	1.18487	1.17103	1.15760	1.13178
12.000	1.18042	1.16729	1.15458	1.13006
12.500	1.17600	1.16357	1.15156	1.12829
13.000	1.17162	1.15984	1.14852	1.12646
13.500	1.16727	1.15613	1.14546	1.12457
14.000	1.16296	1.15244	1.14238	1.12263
14.500	1.15869	1.14876	1.13930	1.12066
15.000	1.15445	1.14510	1.13618	1.11858
15.500	1.15024	1.14143	1.13307	1.11649
16.000	1.14606	1.13779	1.12994	1.11432
16.500	1.14193	1.13414	1.12678	1.11207
17.000	1.13781	1.13051	1.12361	1.10977
17.500	1.13373	1.12688	1.12041	1.10741
18.000	1.12967	1.12326	1.11719	1.10498
18.500	1.12564	1.11964	1.11396	1.10250
19.000	1.12164	1.11601	1.11071	1.09995
19.500	1.11767	1.11240	1.10745	1.09735
20.000	1.11372	1.10880	1.10416	1.09469
21.000	1.10586	1.10157	1.09752	1.08919
22.000	1.09811	1.09439	1.09084	1.08351
23.000	1.09046	1.08721	1.08411	1.07766
24.000	1.08288	1.08005	1.07733	1.07166
25.000	1.07537	1.07290	1.07052	1.06553
26.000	1.06791	1.06576	1.06367	1.05927
27.391	1.05761	1.05585	1.05410	1.05041
27.392	1.05758	1.05910	1.06055	1.06366
30.000	1.03872	1.04038	1.04196	1.04536
33.000	1.01746	1.01906	1.02058	1.02387
36.000	0.99657	0.99814	0.99964	1.00286
39.000	0.97609	0.97765	0.97913	0.98233
42.000	0.95601	0.95756	0.95905	0.96225
45.000	0.93636	0.93791	0.93939	0.94259
50.000	0.90533	0.90686	0.90834	0.91151
52.148	0.89183	0.89335	0.89483	0.89798

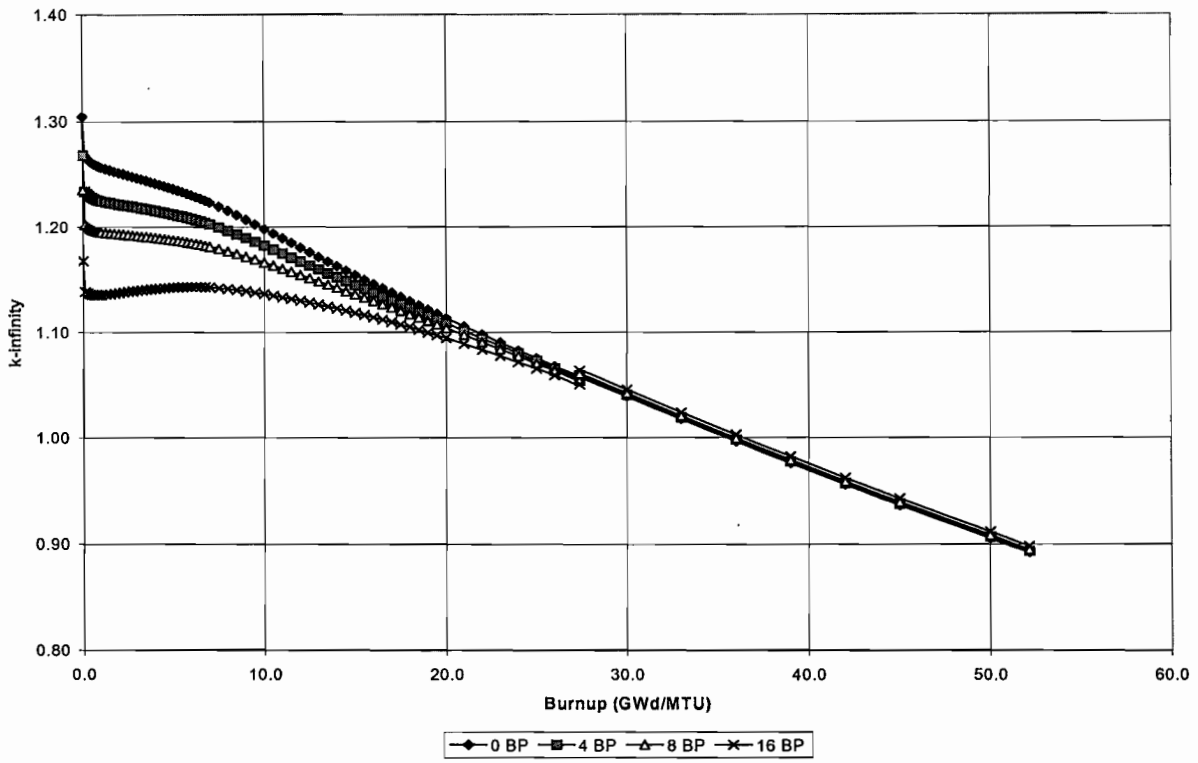

Figure A-58. k-infinity Vs Burnup for Various BP Loading (Figures 05-08)

Table A-4. k-infinity Vs Burnup for Various BP Loading (Figures 09-12)

Std UO_2 = 4.50 wt % ^{235}U, Gd_2O_3-UO_2 = 2.0 wt % - 3.60 wt % ^{235}U, B_4C= 3.5 wt %, 4 Gd rods

Burnup	k-infinity Vs Burnup			
GWd/mtU	0 BP rods	4 BP rods	8 BP rods	16 BP rods
0.000	1.29746	1.25062	1.20438	1.1212
0.125	1.26044	1.21620	1.17248	1.0936
0.250	1.25760	1.21381	1.17051	1.0924
0.375	1.25541	1.21201	1.16909	1.0915
0.500	1.25366	1.21062	1.16805	1.0912
0.625	1.25221	1.20950	1.16725	1.0909
0.750	1.25107	1.20866	1.16671	1.0909
0.875	1.25009	1.20799	1.16633	1.0911
1.000	1.24924	1.20743	1.16605	1.0912
1.250	1.24779	1.20654	1.16567	1.0918
1.500	1.24645	1.20575	1.16542	1.0925
1.750	1.24516	1.20503	1.16522	1.0932
2.000	1.24391	1.20433	1.16505	1.0940
2.250	1.24265	1.20362	1.16486	1.0947
2.500	1.24139	1.20291	1.16467	1.0954
2.750	1.24012	1.20220	1.16446	1.0962
3.000	1.23885	1.20147	1.16425	1.0968
3.250	1.23757	1.20074	1.16402	1.0975
3.500	1.23629	1.20000	1.16378	1.0982
3.750	1.23499	1.19924	1.16353	1.0988
4.000	1.23369	1.19847	1.16326	1.0994
4.250	1.23237	1.19769	1.16296	1.1000
4.500	1.23106	1.19688	1.16265	1.1005
4.750	1.22972	1.19605	1.16230	1.1010
5.000	1.22836	1.19518	1.16191	1.1014
5.250	1.22697	1.19426	1.16144	1.1017
5.500	1.22552	1.19326	1.16092	1.1020
5.750	1.22402	1.19220	1.16031	1.1021
6.000	1.22245	1.19105	1.15961	1.1022
6.250	1.22082	1.18983	1.15884	1.1021
6.500	1.21911	1.18853	1.15799	1.1021
6.750	1.21734	1.18716	1.15707	1.1019
7.000	1.21550	1.18572	1.15609	1.1017
7.500	1.21160	1.18261	1.15387	1.1010
8.000	1.20754	1.17935	1.15152	1.1001
8.500	1.20330	1.17593	1.14901	1.0992

Table A-4. k-infinity Vs Burnup for Various BP Loading (Figures 09-12), Cont.

Burnup	k-infinity Vs Burnup			
GWd/mtU	0 BP rods	4 BP rods	8 BP rods	16 BP rods
9.000	1.19895	1.17239	1.14639	1.0981
9.500	1.19450	1.16877	1.14370	1.0970
10.000	1.19000	1.16511	1.14097	1.0959
10.500	1.18548	1.16143	1.13823	1.0947
11.000	1.18095	1.15776	1.13549	1.0936
11.500	1.17642	1.15411	1.13275	1.0924
12.000	1.17192	1.15048	1.13003	1.0913
12.500	1.16746	1.14687	1.12733	1.0902
13.000	1.16303	1.14330	1.12466	1.0890
13.500	1.15864	1.13977	1.12199	1.0879
14.000	1.15429	1.13625	1.11935	1.0868
14.500	1.14998	1.13277	1.11672	1.0857
15.000	1.14570	1.12931	1.11409	1.0845
15.500	1.14145	1.12586	1.11146	1.0833
16.000	1.13724	1.12244	1.10884	1.0821
16.500	1.13306	1.11903	1.10620	1.0809
17.000	1.12891	1.11565	1.10356	1.0796
17.500	1.12479	1.11227	1.10091	1.0783
18.000	1.12070	1.10890	1.09824	1.0769
18.500	1.11664	1.10554	1.09556	1.0755
19.000	1.11261	1.10219	1.09286	1.0740
19.500	1.10860	1.09883	1.09013	1.0724
20.000	1.10462	1.09548	1.08738	1.0708
21.000	1.09669	1.08874	1.08175	1.0672
22.000	1.08889	1.08205	1.07605	1.0635
23.000	1.08118	1.07532	1.07022	1.0594
24.000	1.07354	1.06857	1.06425	1.0550
25.000	1.06597	1.06179	1.05817	1.0503
26.000	1.05846	1.05498	1.05195	1.0453
27.391	1.04810	1.04543	1.04312	1.0379
27.392	1.04806	1.05015	1.05213	1.0563
30.000	1.02909	1.03130	1.03340	1.0379
33.000	1.00770	1.00983	1.01186	1.0162
36.000	0.98672	0.98881	0.99079	0.9951
39.000	0.96617	0.96824	0.97021	0.9744
42.000	0.94606	0.94811	0.95007	0.9543
45.000	0.92645	0.92848	0.93044	0.9346
50.000	0.89565	0.89764	0.89957	0.9037
52.148	0.88224	0.88422	0.88614	0.8902

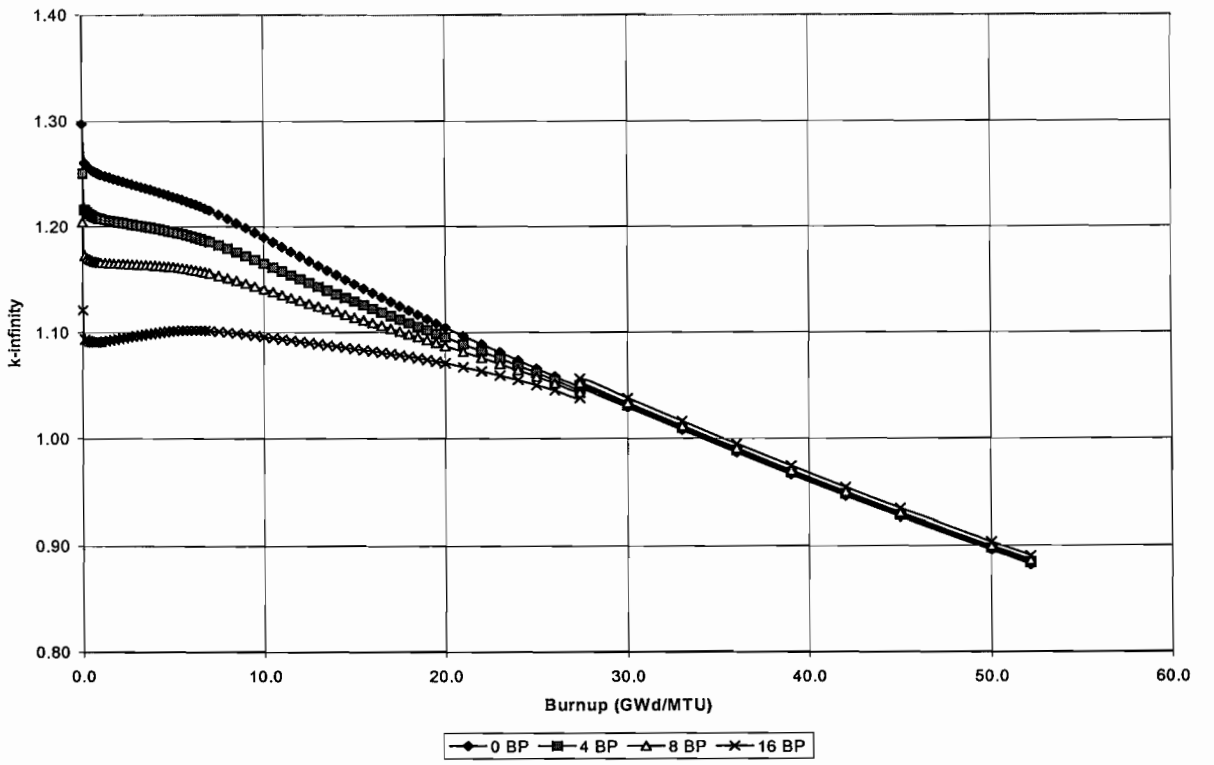

Figure A-59. k-infinity Vs Burnup for Various BP Loading (Figures 09-12)

Table A-5. k-infinity Vs Burnup for Various BP Loading (Figures 13-16)

Std UO_2 = 4.50 wt % ^{235}U, Gd_2O_3-UO_2 = 2.0 wt % - 3.60 wt % ^{235}U, B_4C= 3.5 wt %, 4 Gd rods

Burnup	k-infinity Vs Burnup			
GWd/mtU	0 BP rods	4 BP rods	8 BP rods	16 BP rods
0.000	1.29637	1.25005	1.20860	1.12518
0.125	1.25946	1.21567	1.17630	1.09724
0.250	1.25664	1.21328	1.17422	1.09589
0.375	1.25449	1.21152	1.17268	1.09494
0.500	1.25278	1.21016	1.17153	1.09445
0.625	1.25136	1.20907	1.17062	1.09412
0.750	1.25025	1.20827	1.16998	1.09392
0.875	1.24931	1.20763	1.16949	1.09401
1.000	1.24849	1.20710	1.16910	1.09412
1.250	1.24712	1.20629	1.16850	1.09444
1.500	1.24584	1.20557	1.16802	1.09490
1.750	1.24464	1.20492	1.16759	1.09540
2.000	1.24346	1.20430	1.16717	1.09590
2.250	1.24228	1.20368	1.16675	1.09639
2.500	1.24109	1.20306	1.16630	1.09687
2.750	1.23991	1.20244	1.16585	1.09733
3.000	1.23872	1.20180	1.16539	1.09777
3.250	1.23751	1.20116	1.16492	1.09819
3.500	1.23630	1.20050	1.16443	1.09860
3.750	1.23508	1.19984	1.16393	1.09900
4.000	1.23385	1.19915	1.16342	1.09938
4.250	1.23259	1.19845	1.16290	1.09973
4.500	1.23133	1.19771	1.16237	1.10007
4.750	1.23005	1.19694	1.16183	1.10038
5.000	1.22872	1.19611	1.16126	1.10065
5.250	1.22736	1.19520	1.16066	1.10089
5.500	1.22593	1.19422	1.16003	1.10106
5.750	1.22443	1.19314	1.15935	1.10118
6.000	1.22285	1.19197	1.15863	1.10123
6.250	1.22120	1.19072	1.15785	1.10122
6.500	1.21948	1.18939	1.15700	1.10114
6.750	1.21768	1.18798	1.15610	1.10100
7.000	1.21582	1.18651	1.15514	1.10080
7.500	1.21187	1.18332	1.15301	1.10019
8.000	1.20775	1.17998	1.15076	1.09948
8.500	1.20347	1.17649	1.14837	1.09862

Table A-5. k-infinity Vs Burnup for Various BP Loading (Figures 13-16), Cont.

Burnup	k-infinity Vs Burnup			
GWd/mtU	0 BP rods	4 BP rods	8 BP rods	16 BP rods
9.000	1.19907	1.17289	1.14585	1.09765
9.500	1.19459	1.16922	1.14325	1.09661
10.000	1.19005	1.16552	1.14060	1.09552
10.500	1.18551	1.16182	1.13791	1.09441
11.000	1.18097	1.15813	1.13520	1.09329
11.500	1.17643	1.15446	1.13250	1.09218
12.000	1.17193	1.15082	1.12980	1.09106
12.500	1.16746	1.14721	1.12712	1.08994
13.000	1.16303	1.14363	1.12446	1.08883
13.500	1.15864	1.14008	1.12180	1.08771
14.000	1.15429	1.13656	1.11916	1.08659
14.500	1.14998	1.13307	1.11653	1.08546
15.000	1.14570	1.12960	1.11391	1.08432
15.500	1.14145	1.12615	1.11129	1.08315
16.000	1.13723	1.12272	1.10867	1.08195
16.500	1.13305	1.11931	1.10605	1.08071
17.000	1.12890	1.11591	1.10341	1.07944
17.500	1.12478	1.11253	1.10077	1.07812
18.000	1.12069	1.10915	1.09811	1.07675
18.500	1.11663	1.10578	1.09543	1.07532
19.000	1.11260	1.10242	1.09274	1.07384
19.500	1.10859	1.09905	1.09002	1.07228
20.000	1.10461	1.09570	1.08727	1.07066
21.000	1.09669	1.08894	1.08166	1.06713
22.000	1.08889	1.08222	1.07597	1.06337
23.000	1.08117	1.07548	1.07015	1.05930
24.000	1.07353	1.06871	1.06420	1.05491
25.000	1.06597	1.06191	1.05813	1.05024
26.000	1.05846	1.05507	1.05192	1.04526
27.391	1.04809	1.04550	1.04310	1.03790
27.392	1.04805	1.04957	1.05214	1.05636
30.000	1.02908	1.03066	1.03341	1.03792
33.000	1.00770	1.00920	1.01187	1.01622
36.000	0.98672	0.98815	0.99080	0.99506
39.000	0.96616	0.96756	0.97021	0.97443
42.000	0.94605	0.94740	0.95007	0.95428
45.000	0.92644	0.92775	0.93043	0.93462
50.000	0.89564	0.89690	0.89956	0.90368
52.148	0.88224	0.88344	0.88614	0.89022

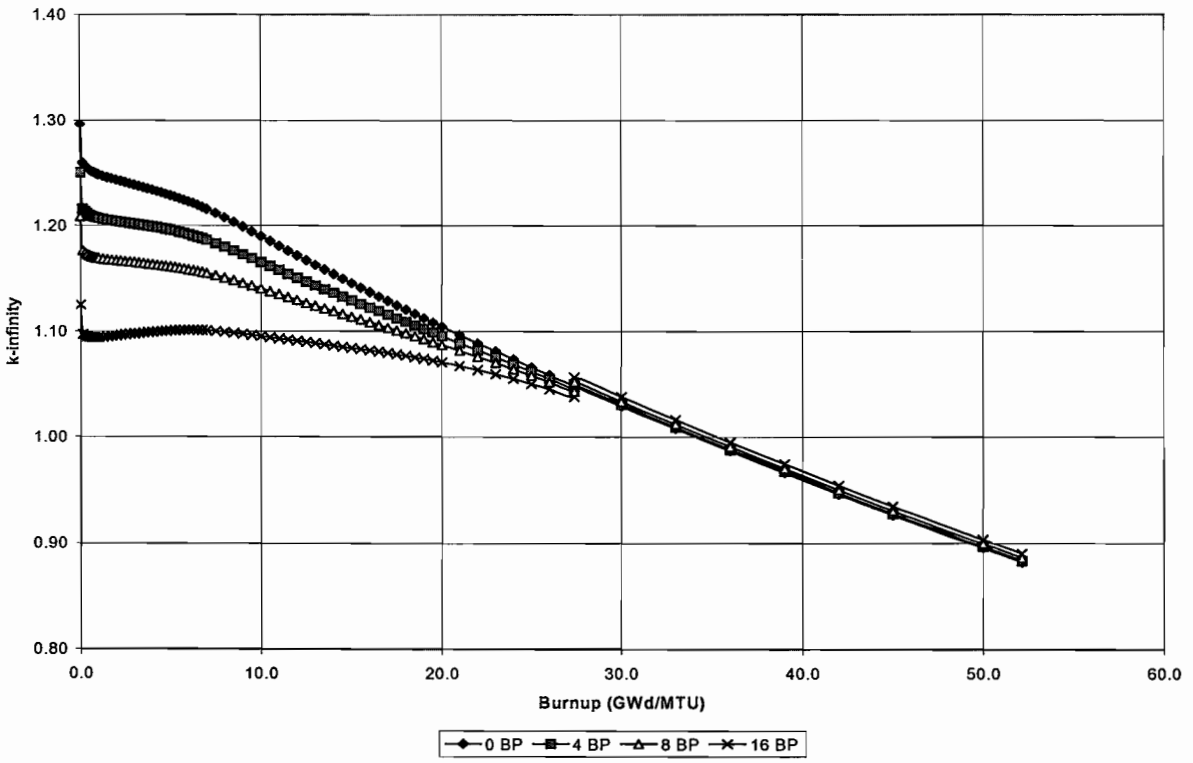

Figure A-60. k-infinity Vs Burnup for Various BP Loading (Figures 13-16)

Table A-6. k-infinity Vs Burnup for Various BP Loading (Figures 17-20)

Std UO_2 = 4.50 wt % ^{235}U, Gd_2O_3-UO_2 = 2.0 wt % - 3.60 wt % ^{235}U, B_4C= 0.0 wt %, 8 Gd rods

Burnup	k-infinity Vs Burnup			
GWd/mtU	0 BP rods	4 BP rods	8 BP rods	16 BP rods
0.000	1.25459	1.25303	1.25053	1.24821
0.125	1.22053	1.21902	1.21664	1.21442
0.250	1.21840	1.21691	1.21457	1.21232
0.375	1.21694	1.21546	1.21313	1.21086
0.500	1.21591	1.21442	1.21211	1.20981
0.625	1.21510	1.21361	1.21132	1.20897
0.750	1.21467	1.21316	1.21089	1.20850
0.875	1.21441	1.21289	1.21064	1.20819
1.000	1.21427	1.21274	1.21051	1.20801
1.250	1.21432	1.21277	1.21057	1.20795
1.500	1.21445	1.21288	1.21071	1.20796
1.750	1.21469	1.21308	1.21095	1.20807
2.000	1.21497	1.21335	1.21125	1.20823
2.250	1.21528	1.21362	1.21156	1.20838
2.500	1.21563	1.21394	1.21191	1.20859
2.750	1.21600	1.21426	1.21227	1.20878
3.000	1.21637	1.21459	1.21264	1.20898
3.250	1.21675	1.21493	1.21302	1.20919
3.500	1.21714	1.21528	1.21339	1.20939
3.750	1.21751	1.21561	1.21375	1.20958
4.000	1.21785	1.21591	1.21408	1.20973
4.250	1.21816	1.21618	1.21437	1.20986
4.500	1.21841	1.21639	1.21460	1.20995
4.750	1.21856	1.21651	1.21474	1.20996
5.000	1.21860	1.21652	1.21475	1.20987
5.250	1.21845	1.21636	1.21458	1.20963
5.500	1.21812	1.21602	1.21423	1.20926
5.750	1.21759	1.21549	1.21368	1.20869
6.000	1.21687	1.21476	1.21293	1.20794
6.250	1.21596	1.21385	1.21201	1.20703
6.500	1.21488	1.21277	1.21091	1.20596
6.750	1.21364	1.21154	1.20964	1.20473
7.000	1.21225	1.21015	1.20824	1.20336
7.500	1.20898	1.20690	1.20494	1.20016
8.000	1.20535	1.20329	1.20129	1.19660
8.500	1.20137	1.19933	1.19729	1.19271

Table A-6. k-infinity Vs Burnup for Various BP Loading (Figures 17-20), Cont.

Burnup	k-infinity Vs Burnup			
GWd/mtU	0 BP rods	4 BP rods	8 BP rods	16 BP rods
9.000	1.19716	1.19513	1.19306	1.18856
9.500	1.19279	1.19076	1.18869	1.18425
10.000	1.18833	1.18631	1.18423	1.17984
10.500	1.18382	1.18181	1.17972	1.17537
11.000	1.17930	1.17729	1.17522	1.17088
11.500	1.17477	1.17278	1.17071	1.16641
12.000	1.17028	1.16830	1.16622	1.16196
12.500	1.16582	1.16385	1.16177	1.15754
13.000	1.16139	1.15943	1.15737	1.15315
13.500	1.15700	1.15506	1.15300	1.14881
14.000	1.15266	1.15073	1.14868	1.14451
14.500	1.14835	1.14643	1.14439	1.14025
15.000	1.14407	1.14216	1.14014	1.13603
15.500	1.13982	1.13793	1.13593	1.13185
16.000	1.13561	1.13374	1.13175	1.12771
16.500	1.13144	1.12957	1.12760	1.12359
17.000	1.12729	1.12545	1.12349	1.11951
17.500	1.12318	1.12135	1.11942	1.11547
18.000	1.11909	1.11729	1.11536	1.11147
18.500	1.11503	1.11325	1.11135	1.10750
19.000	1.11100	1.10924	1.10736	1.10356
19.500	1.10699	1.10525	1.10340	1.09964
20.000	1.10301	1.10129	1.09946	1.09575
21.000	1.09509	1.09342	1.09165	1.08805
22.000	1.08729	1.08569	1.08396	1.08046
23.000	1.07958	1.07803	1.07635	1.07296
24.000	1.07194	1.07045	1.06883	1.06555
25.000	1.06438	1.06294	1.06138	1.05823
26.000	1.05687	1.05549	1.05399	1.05097
27.391	1.04651	1.04522	1.04381	1.04097
27.392	1.04647	1.04751	1.04852	1.05067
30.000	1.02751	1.02865	1.02977	1.03216
33.000	1.00613	1.00720	1.00825	1.01049
36.000	0.98515	0.98618	0.98718	0.98934
39.000	0.96461	0.96562	0.96659	0.96869
42.000	0.94451	0.94549	0.94645	0.94851
45.000	0.92491	0.92588	0.92683	0.92886
50.000	0.89415	0.89509	0.89602	0.89800
52.148	0.88077	0.88170	0.88261	0.88457

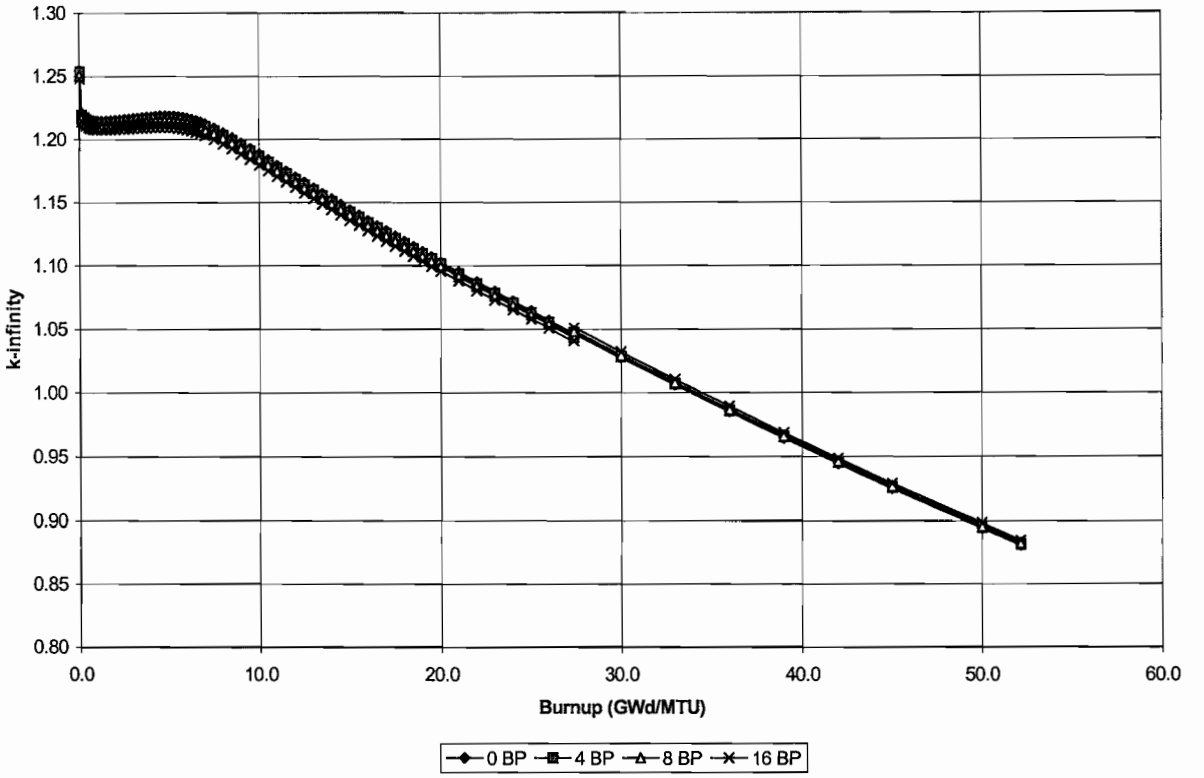

Figure A-61. k-infinity Vs Burnup for Various BP Loading (Figures 17-20)

Table A-7. k-infinity Vs Burnup for Various BP Loading (Figures 21-24)

Std UO_2 = 4.50 wt % ^{235}U, Gd_2O_3-UO_2 = 2.0 wt % - 3.60 wt % ^{235}U, B_4C= 0.0 wt %, 8 Gd rods

Burnup	k-infinity Vs Burnup			
GWd/mtU	0 BP rods	4 BP rods	8 BP rods	16 BP rods
0.000	1.25496	1.25360	1.25166	1.24850
0.125	1.22091	1.21958	1.21773	1.21471
0.250	1.21876	1.21746	1.21563	1.21261
0.375	1.21729	1.21599	1.21416	1.21114
0.500	1.21625	1.21494	1.21312	1.21009
0.625	1.21543	1.21411	1.21229	1.20924
0.750	1.21499	1.21365	1.21183	1.20876
0.875	1.21472	1.21336	1.21155	1.20844
1.000	1.21457	1.21320	1.21138	1.20825
1.250	1.21460	1.21319	1.21138	1.20818
1.500	1.21470	1.21325	1.21143	1.20817
1.750	1.21490	1.21341	1.21160	1.20826
2.000	1.21517	1.21363	1.21181	1.20839
2.250	1.21544	1.21386	1.21203	1.20853
2.500	1.21576	1.21413	1.21229	1.20870
2.750	1.21609	1.21440	1.21256	1.20887
3.000	1.21643	1.21468	1.21283	1.20905
3.250	1.21678	1.21498	1.21312	1.20923
3.500	1.21713	1.21527	1.21339	1.20940
3.750	1.21747	1.21556	1.21366	1.20956
4.000	1.21778	1.21580	1.21390	1.20969
4.250	1.21806	1.21603	1.21410	1.20980
4.500	1.21828	1.21620	1.21426	1.20986
4.750	1.21841	1.21629	1.21432	1.20985
5.000	1.21842	1.21627	1.21428	1.20974
5.250	1.21827	1.21609	1.21408	1.20950
5.500	1.21794	1.21576	1.21372	1.20911
5.750	1.21741	1.21522	1.21317	1.20854
6.000	1.21669	1.21450	1.21244	1.20780
6.250	1.21579	1.21361	1.21153	1.20689
6.500	1.21472	1.21254	1.21046	1.20582
6.750	1.21349	1.21132	1.20922	1.20460
7.000	1.21211	1.20995	1.20785	1.20324
7.500	1.20887	1.20674	1.20462	1.20006
8.000	1.20526	1.20316	1.20104	1.19652
8.500	1.20131	1.19924	1.19712	1.19265

Table A-7. k-infinity Vs Burnup for Various BP Loading (Figures 21-24), Cont.

Burnup	k-infinity Vs Burnup			
GWd/mtU	0 BP rods	4 BP rods	8 BP rods	16 BP rods
9.000	1.19712	1.19507	1.19296	1.18852
9.500	1.19277	1.19073	1.18862	1.18422
10.000	1.18833	1.18629	1.18419	1.17982
10.500	1.18382	1.18180	1.17970	1.17536
11.000	1.17930	1.17728	1.17521	1.17088
11.500	1.17478	1.17278	1.17072	1.16642
12.000	1.17029	1.16831	1.16624	1.16197
12.500	1.16583	1.16386	1.16180	1.15754
13.000	1.16140	1.15945	1.15740	1.15316
13.500	1.15702	1.15508	1.15303	1.14882
14.000	1.15267	1.15074	1.14871	1.14452
14.500	1.14836	1.14644	1.14442	1.14026
15.000	1.14409	1.14218	1.14018	1.13605
15.500	1.13984	1.13795	1.13596	1.13186
16.000	1.13563	1.13375	1.13178	1.12772
16.500	1.13145	1.12959	1.12763	1.12360
17.000	1.12730	1.12546	1.12352	1.11953
17.500	1.12319	1.12137	1.11945	1.11548
18.000	1.11910	1.11730	1.11539	1.11148
18.500	1.11505	1.11327	1.11137	1.10751
19.000	1.11101	1.10926	1.10739	1.10357
19.500	1.10701	1.10526	1.10343	1.09965
20.000	1.10302	1.10130	1.09949	1.09576
21.000	1.09510	1.09344	1.09169	1.08806
22.000	1.08730	1.08570	1.08399	1.08047
23.000	1.07959	1.07804	1.07638	1.07297
24.000	1.07195	1.07046	1.06885	1.06556
25.000	1.06439	1.06295	1.06140	1.05824
26.000	1.05688	1.05551	1.05402	1.05098
27.391	1.04652	1.04523	1.04384	1.04098
27.392	1.04648	1.04752	1.04853	1.05068
30.000	1.02752	1.02866	1.02978	1.03217
33.000	1.00614	1.00721	1.00826	1.01050
36.000	0.98516	0.98619	0.98719	0.98934
39.000	0.96462	0.96562	0.96660	0.96870
42.000	0.94451	0.94550	0.94646	0.94852
45.000	0.92491	0.92588	0.92683	0.92886
50.000	0.89416	0.89510	0.89602	0.89800
52.148	0.88077	0.88170	0.88262	0.88457

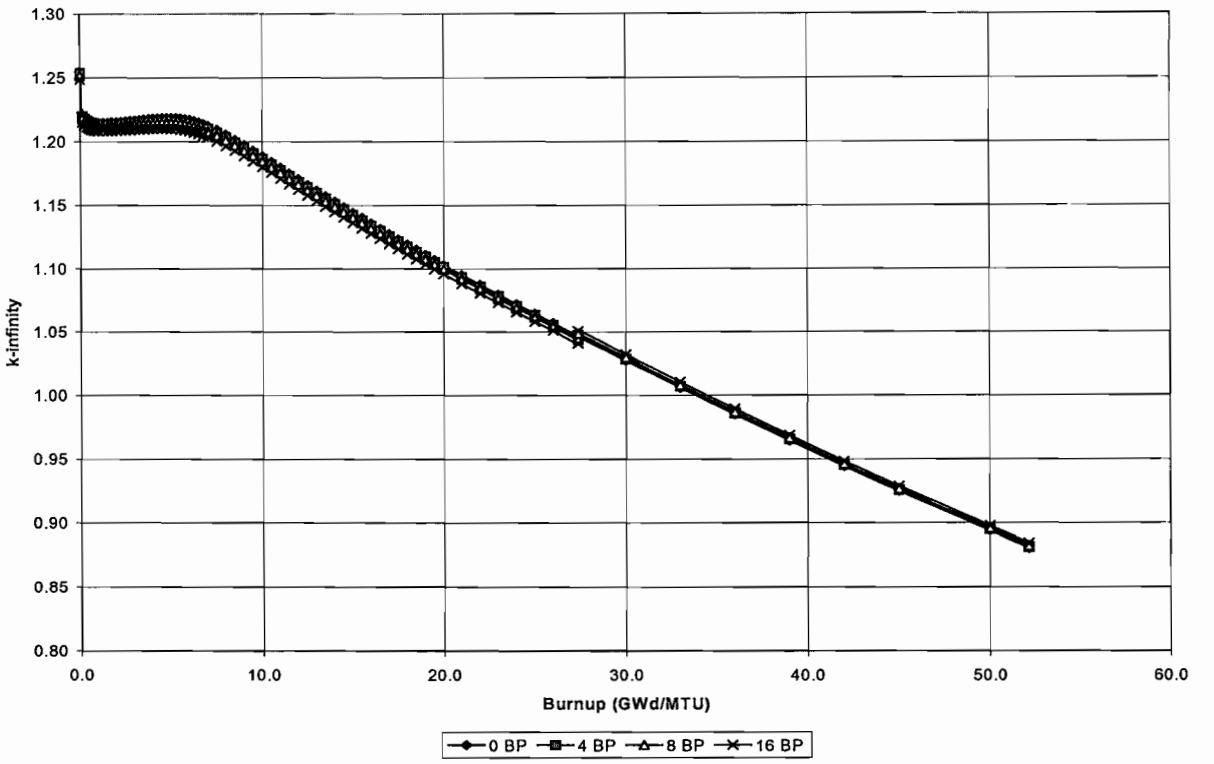

Figure A-62. k-infinity Vs Burnup for Various BP Loading (Figures 21-24)

Table A-8. k-infinity Vs Burnup for Various BP Loading (Figures 25-28)

Assembly contains 10 SS fuel rods
Std UO_2 = 4.65 wt % ^{235}U, Gd_2O_3-UO_2 = 2.0 wt % - 4.19 wt % ^{235}U, B_4C= 2.1 wt %, 4 Gd rods

Burnup	k-infinity Vs Burnup			
GWd/mtU	0 BP rods	4 BP rods	8 BP rods	16 BP rods
0.000	1.27856	1.24196	1.20540	1.13849
0.125	1.24312	1.20862	1.17415	1.11089
0.250	1.24044	1.20636	1.17230	1.10974
0.375	1.23838	1.20466	1.17096	1.10904
0.500	1.23672	1.20335	1.16999	1.10867
0.625	1.23535	1.20230	1.16926	1.10851
0.750	1.23426	1.20152	1.16878	1.10857
0.875	1.23335	1.20090	1.16845	1.10877
1.000	1.23255	1.20040	1.16823	1.10905
1.250	1.23120	1.19961	1.16798	1.10976
1.500	1.22995	1.19892	1.16784	1.11060
1.750	1.22878	1.19831	1.16776	1.11148
2.000	1.22762	1.19771	1.16769	1.11237
2.250	1.22647	1.19710	1.16762	1.11323
2.500	1.22530	1.19648	1.16752	1.11409
2.750	1.22413	1.19586	1.16741	1.11491
3.000	1.22295	1.19521	1.16729	1.11572
3.250	1.22176	1.19456	1.16715	1.11649
3.500	1.22056	1.19389	1.16698	1.11724
3.750	1.21935	1.19320	1.16680	1.11796
4.000	1.21812	1.19250	1.16660	1.11865
4.250	1.21689	1.19178	1.16637	1.11931
4.500	1.21564	1.19104	1.16612	1.11994
4.750	1.21438	1.19029	1.16585	1.12052
5.000	1.21310	1.18950	1.16553	1.12105
5.250	1.21180	1.18867	1.16517	1.12151
5.500	1.21045	1.18779	1.16475	1.12190
5.750	1.20907	1.18685	1.16427	1.12220
6.000	1.20764	1.18585	1.16371	1.12242
6.250	1.20615	1.18478	1.16307	1.12255
6.500	1.20459	1.18364	1.16237	1.12259
6.750	1.20298	1.18242	1.16157	1.12255
7.000	1.20129	1.18114	1.16071	1.12244
7.500	1.19770	1.17832	1.15874	1.12195
8.000	1.19396	1.17535	1.15661	1.12129
8.500	1.19004	1.17220	1.15428	1.12042

Table A-8. k-infinity Vs Burnup for Various BP Loading (Figures 25-28), Cont.

Burnup	k-infinity Vs Burnup			
GWd/mtU	0 BP rods	4 BP rods	8 BP rods	16 BP rods
9.000	1.18598	1.16890	1.15179	1.11937
9.500	1.18182	1.16547	1.14916	1.11818
10.000	1.17758	1.16196	1.14644	1.11687
10.500	1.17328	1.15839	1.14365	1.11547
11.000	1.16896	1.15480	1.14081	1.11401
11.500	1.16463	1.15119	1.13793	1.11247
12.000	1.16030	1.14757	1.13503	1.11088
12.500	1.15599	1.14394	1.13209	1.10922
13.000	1.15171	1.14032	1.12914	1.10751
13.500	1.14745	1.13671	1.12617	1.10574
14.000	1.14321	1.13311	1.12319	1.10391
14.500	1.13901	1.12952	1.12019	1.10204
15.000	1.13485	1.12592	1.11717	1.10007
15.500	1.13071	1.12234	1.11412	1.09805
16.000	1.12660	1.11876	1.11105	1.09596
16.500	1.12251	1.11518	1.10797	1.09380
17.000	1.11845	1.11161	1.10485	1.09158
17.500	1.11441	1.10803	1.10171	1.08929
18.000	1.11040	1.10445	1.09855	1.08693
18.500	1.10641	1.10088	1.09536	1.08450
19.000	1.10245	1.09731	1.09215	1.08201
19.500	1.09851	1.09373	1.08892	1.07945
20.000	1.09459	1.09015	1.08567	1.07684
21.000	1.08677	1.08298	1.07909	1.07141
22.000	1.07907	1.07583	1.07245	1.06579
23.000	1.07144	1.06869	1.06575	1.05999
24.000	1.06388	1.06155	1.05899	1.05402
25.000	1.05637	1.05441	1.05219	1.04791
26.000	1.04890	1.04727	1.04534	1.04165
27.391	1.03859	1.03733	1.03574	1.03277
27.392	1.03856	1.04032	1.04186	1.04534
30.000	1.01963	1.02149	1.02315	1.02687
33.000	0.99821	1.00000	1.00160	1.00518
36.000	0.97712	0.97888	0.98043	0.98394
39.000	0.95640	0.95812	0.95966	0.96312
42.000	0.93603	0.93774	0.93927	0.94272
45.000	0.91606	0.91776	0.91929	0.92272
50.000	0.88455	0.88620	0.88772	0.89109
52.148	0.87076	0.87239	0.87391	0.87726

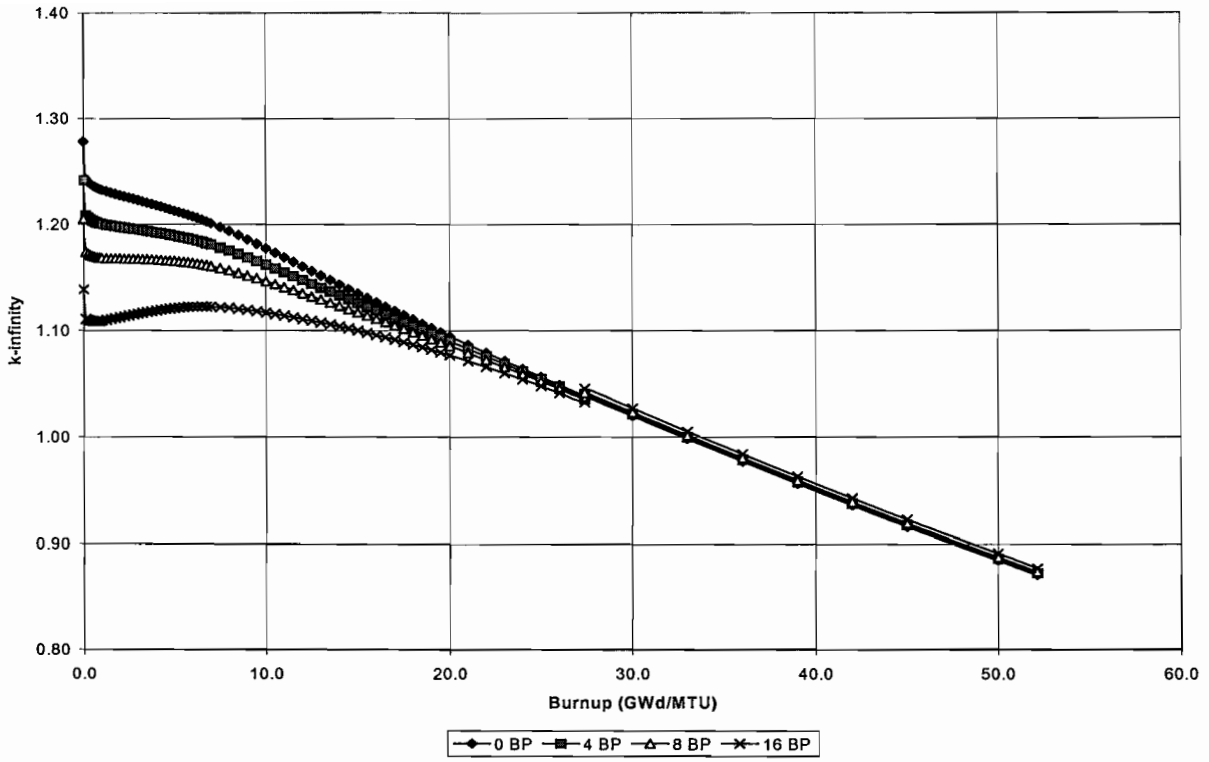

Figure A-63. k-infinity Vs Burnup for Various BP Loading (Figures 25-28)

Table A-9. k-infinity Vs Burnup for Various BP Loading (Figures 29-32)

Assembly contains 10 SS fuel rods
Std UO_2 = 4.65 wt % ^{235}U, Gd_2O_3-UO_2 = 2.0 wt % - 4.19 wt % ^{235}U, B_4C= 2.1 wt %, 4 Gd rods

Burnup	k-infinity Vs Burnup			
GWd/mtU	0 BP rods	4 BP rods	8 BP rods	16 BP rods
0.000	1.30538	1.26847	1.23205	1.16481
0.125	1.26855	1.23379	1.19948	1.13597
0.250	1.26572	1.23140	1.19749	1.13469
0.375	1.26353	1.22959	1.19604	1.13389
0.500	1.26177	1.22817	1.19496	1.13341
0.625	1.26029	1.22701	1.19412	1.13315
0.750	1.25910	1.22614	1.19355	1.13312
0.875	1.25810	1.22543	1.19314	1.13323
1.000	1.25721	1.22484	1.19283	1.13343
1.250	1.25572	1.22390	1.19243	1.13399
1.500	1.25432	1.22307	1.19214	1.13469
1.750	1.25300	1.22232	1.19192	1.13543
2.000	1.25171	1.22158	1.19172	1.13618
2.250	1.25042	1.22084	1.19150	1.13691
2.500	1.24912	1.22008	1.19126	1.13762
2.750	1.24781	1.21932	1.19102	1.13831
3.000	1.24650	1.21854	1.19076	1.13897
3.250	1.24517	1.21775	1.19048	1.13961
3.500	1.24384	1.21695	1.19018	1.14022
3.750	1.24249	1.21613	1.18986	1.14080
4.000	1.24114	1.21529	1.18952	1.14135
4.250	1.23977	1.21444	1.18916	1.14187
4.500	1.23840	1.21357	1.18877	1.14236
4.750	1.23701	1.21268	1.18837	1.14280
5.000	1.23561	1.21177	1.18792	1.14320
5.250	1.23418	1.21081	1.18743	1.14352
5.500	1.23271	1.20980	1.18688	1.14378
5.750	1.23121	1.20875	1.18627	1.14395
6.000	1.22966	1.20762	1.18559	1.14405
6.250	1.22805	1.20643	1.18483	1.14406
6.500	1.22638	1.20518	1.18401	1.14398
6.750	1.22466	1.20385	1.18310	1.14382
7.000	1.22287	1.20246	1.18213	1.14360
7.500	1.21908	1.19943	1.17995	1.14290
8.000	1.21515	1.19627	1.17762	1.14203
8.500	1.21106	1.19294	1.17510	1.14097

Table A-9. k-infinity Vs Burnup for Various BP Loading (Figures 29-32), Cont.

Burnup	k-infinity Vs Burnup			
GWd/mtU	0 BP rods	4 BP rods	8 BP rods	16 BP rods
9.000	1.20684	1.18947	1.17244	1.13973
9.500	1.20253	1.18589	1.16965	1.13835
10.000	1.19814	1.18222	1.16678	1.13688
10.500	1.19372	1.17852	1.16384	1.13532
11.000	1.18927	1.17480	1.16086	1.13370
11.500	1.18483	1.17107	1.15785	1.13202
12.000	1.18039	1.16733	1.15481	1.13028
12.500	1.17599	1.16361	1.15176	1.12849
13.000	1.17161	1.15987	1.14871	1.12664
13.500	1.16726	1.15616	1.14563	1.12475
14.000	1.16295	1.15248	1.14254	1.12280
14.500	1.15868	1.14879	1.13945	1.12082
15.000	1.15444	1.14513	1.13633	1.11875
15.500	1.15024	1.14147	1.13321	1.11663
16.000	1.14606	1.13781	1.13007	1.11445
16.500	1.14192	1.13417	1.12690	1.11219
17.000	1.13781	1.13054	1.12372	1.10989
17.500	1.13372	1.12691	1.12052	1.10752
18.000	1.12967	1.12328	1.11729	1.10509
18.500	1.12564	1.11966	1.11405	1.10259
19.000	1.12164	1.11603	1.11080	1.10004
19.500	1.11767	1.11242	1.10752	1.09743
20.000	1.11372	1.10882	1.10423	1.09477
21.000	1.10585	1.10158	1.09758	1.08925
22.000	1.09811	1.09440	1.09089	1.08356
23.000	1.09045	1.08722	1.08415	1.07770
24.000	1.08287	1.08006	1.07736	1.07170
25.000	1.07537	1.07291	1.07055	1.06556
26.000	1.06790	1.06577	1.06369	1.05929
27.391	1.05761	1.05585	1.05412	1.05043
27.392	1.04020	1.04194	1.04355	1.04706
30.000	1.02148	1.02333	1.02507	1.02885
33.000	0.99996	1.00174	1.00341	1.00706
36.000	0.97881	0.98055	0.98218	0.98575
39.000	0.95804	0.95975	0.96137	0.96489
42.000	0.93765	0.93936	0.94097	0.94448
45.000	0.91768	0.91936	0.92098	0.92446
50.000	0.88614	0.88778	0.88938	0.89281
52.148	0.87234	0.87397	0.87557	0.87897

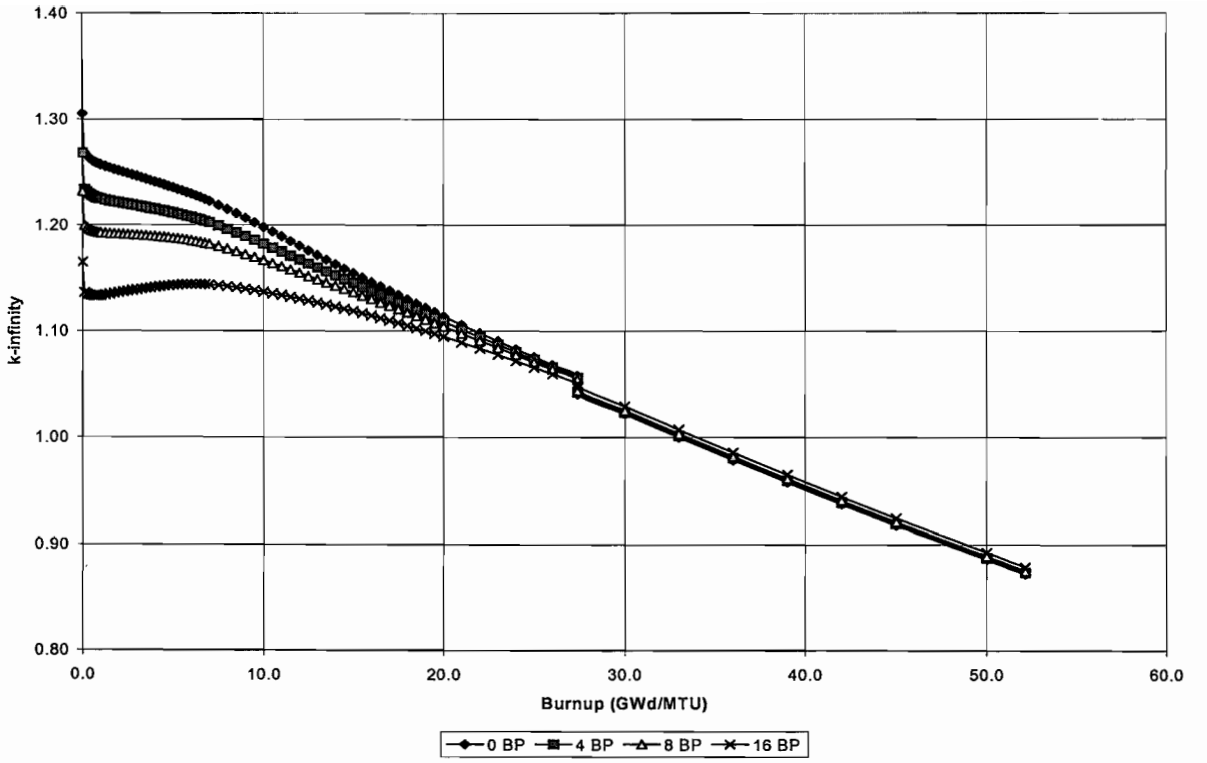

Figure A-64. k-infinity Vs Burnup for Various BP Loading (Figures 29-32)

Table A-10. k-infinity Vs Burnup for Various BP Loading (Figures 33-36)

Std UO_2 = 4.96 wt % ^{235}U, Gd_2O_3-UO_2 = 6.08 wt % - 3.40 wt % ^{235}U, B_4C= 2.6 wt %, 8 Gd rods

Burnup	k-infinity Vs Burnup			
GWd/mtU	0 BP rods	4 BP rods	8 BP rods	16 BP rods
0.000	1.26351	1.22918	1.18719	1.12062
0.125	1.22983	1.19729	1.15768	1.09450
0.250	1.22726	1.19501	1.15583	1.09327
0.375	1.22524	1.19326	1.15447	1.09244
0.500	1.22358	1.19185	1.15343	1.09191
0.625	1.22221	1.19071	1.15262	1.09158
0.750	1.22105	1.18977	1.15202	1.09142
0.875	1.22006	1.18898	1.15155	1.09138
1.000	1.21918	1.18829	1.15117	1.09140
1.250	1.21761	1.18709	1.15055	1.09155
1.500	1.21618	1.18604	1.15009	1.09186
1.750	1.21482	1.18505	1.14969	1.09223
2.000	1.21347	1.18406	1.14928	1.09259
2.250	1.21214	1.18308	1.14888	1.09294
2.500	1.21077	1.18207	1.14846	1.09327
2.750	1.20928	1.18106	1.14791	1.09348
3.000	1.20790	1.17993	1.14746	1.09377
3.250	1.20650	1.17888	1.14699	1.09404
3.500	1.20510	1.17783	1.14650	1.09428
3.750	1.20367	1.17675	1.14599	1.09451
4.000	1.20224	1.17567	1.14547	1.09472
4.250	1.20080	1.17459	1.14496	1.09493
4.500	1.19937	1.17351	1.14443	1.09513
4.750	1.19794	1.17243	1.14390	1.09532
5.000	1.19652	1.17134	1.14344	1.09557
5.250	1.19516	1.17032	1.14291	1.09576
5.500	1.19374	1.16925	1.14239	1.09593
5.750	1.19233	1.16819	1.14184	1.09612
6.000	1.19092	1.16712	1.14132	1.09632
6.250	1.18953	1.16607	1.14084	1.09653
6.500	1.18818	1.16505	1.14036	1.09676
6.750	1.18684	1.16405	1.13990	1.09699
7.000	1.18552	1.16306	1.13945	1.09723
7.500	1.18290	1.16110	1.13852	1.09766
8.000	1.18030	1.15918	1.13759	1.09814
8.500	1.17778	1.15730	1.13679	1.09868

Table A-10. k-infinity Vs Burnup for Various BP Loading (Figures 33-36), Cont.

Burnup	k-infinity Vs Burnup			
GWd/mtU	0 BP rods	4 BP rods	8 BP rods	16 BP rods
9.000	1.17535	1.15553	1.13601	1.09922
9.500	1.17297	1.15378	1.13526	1.09978
10.000	1.17064	1.15208	1.13452	1.10036
10.500	1.16835	1.15042	1.13385	1.10096
11.000	1.16616	1.14883	1.13322	1.10159
11.500	1.16403	1.14731	1.13263	1.10223
12.000	1.16195	1.14584	1.13203	1.10285
12.500	1.15989	1.14438	1.13141	1.10343
13.000	1.15787	1.14293	1.13081	1.10399
13.500	1.15587	1.14152	1.13019	1.10451
14.000	1.15390	1.14012	1.12954	1.10497
14.500	1.15193	1.13870	1.12887	1.10538
15.000	1.15000	1.13729	1.12815	1.10572
15.500	1.14803	1.13587	1.12734	1.10593
16.000	1.14600	1.13439	1.12639	1.10598
16.500	1.14386	1.13281	1.12528	1.10584
17.000	1.14158	1.13110	1.12401	1.10552
17.500	1.13918	1.12924	1.12244	1.10492
18.000	1.13656	1.12717	1.12073	1.10407
18.500	1.13380	1.12492	1.11868	1.10304
19.000	1.13085	1.12251	1.11657	1.10164
19.500	1.12773	1.11991	1.11415	1.10018
20.000	1.12443	1.11717	1.11162	1.09840
21.000	1.11739	1.11106	1.10596	1.09429
22.000	1.11016	1.10463	1.10002	1.08973
23.000	1.10282	1.09797	1.09386	1.08478
24.000	1.09543	1.09120	1.08759	1.07956
25.000	1.08805	1.08438	1.08119	1.07412
26.000	1.08074	1.07754	1.07474	1.06852
27.391	1.07065	1.06803	1.06567	1.06050
27.392	1.07062	1.07213	1.07351	1.07657
30.000	1.05206	1.05372	1.05526	1.05864
33.000	1.03109	1.03269	1.03418	1.03747
36.000	1.01046	1.01205	1.01353	1.01676
39.000	0.99019	0.99177	0.99324	0.99648
42.000	0.97027	0.97185	0.97334	0.97659
45.000	0.95073	0.95233	0.95383	0.95710
50.000	0.91962	0.92122	0.92274	0.92604
52.148	0.90603	0.90764	0.90917	0.91247

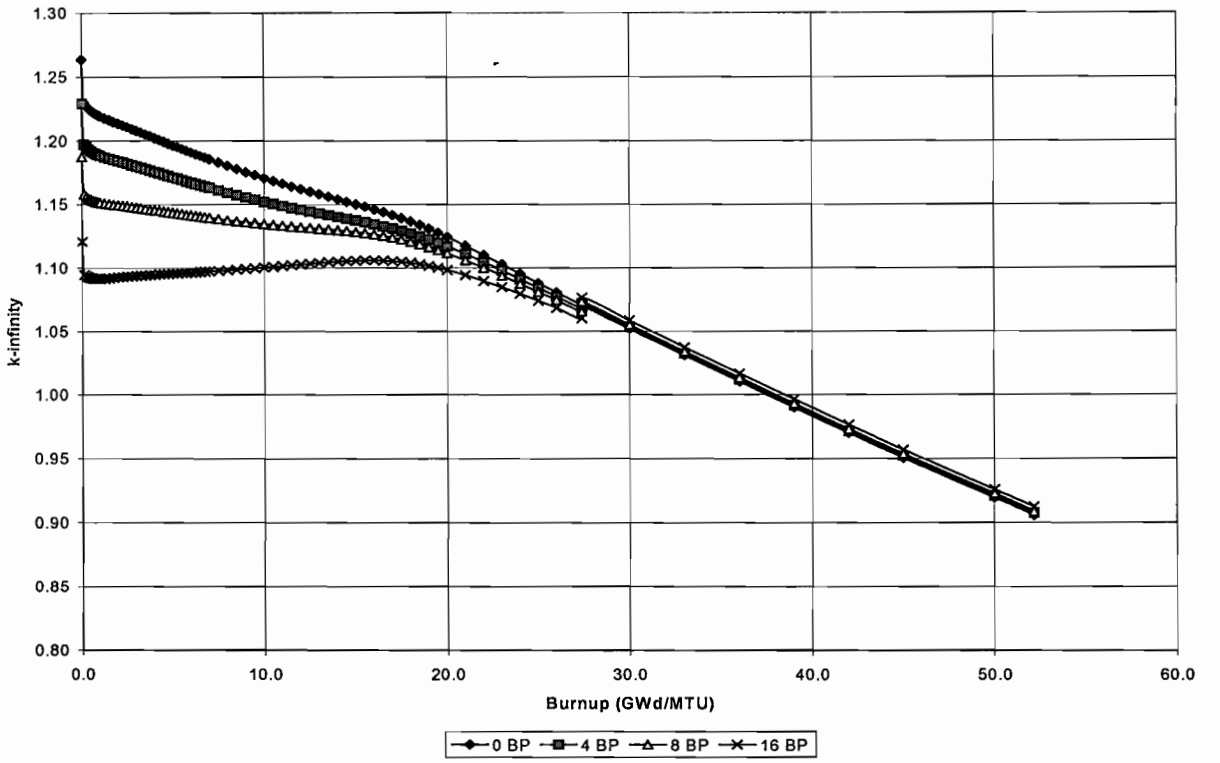

Figure A-65. k-infinity Vs Burnup for Various BP Loading (Figures 33-36)

Table A-11. k-infinity Vs Burnup for Various BP Loading (Figures 37-40)

Std UO_2 = 4.96 wt % ^{235}U, Gd_2O_3-UO_2 = 6.08 wt % - 3.40 wt % ^{235}U, B_4C= 2.6 wt %, 8 Gd rods

Burnup	k-infinity Vs Burnup			
GWd/mtU	0 BP rods	4 BP rods	8 BP rods	16 BP rods
0.000	1.25995	1.22838	1.19217	1.13154
0.125	1.22646	1.19648	1.16216	1.10451
0.250	1.22392	1.19419	1.16021	1.10308
0.375	1.22193	1.19243	1.15875	1.10207
0.500	1.22030	1.19101	1.15762	1.10135
0.625	1.21896	1.18985	1.15672	1.10085
0.750	1.21783	1.18890	1.15603	1.10051
0.875	1.21687	1.18810	1.15543	1.10030
1.000	1.21600	1.18740	1.15500	1.10018
1.250	1.21450	1.18618	1.15422	1.09998
1.500	1.21312	1.18511	1.15360	1.09999
1.750	1.21183	1.18411	1.15305	1.10004
2.000	1.21054	1.18311	1.15249	1.10009
2.250	1.20926	1.18212	1.15193	1.10014
2.500	1.20797	1.18111	1.15136	1.10015
2.750	1.20654	1.17998	1.15066	1.10016
3.000	1.20523	1.17896	1.15006	1.10005
3.250	1.20391	1.17791	1.14944	1.10002
3.500	1.20257	1.17686	1.14880	1.09997
3.750	1.20122	1.17579	1.14816	1.09990
4.000	1.19987	1.17471	1.14750	1.09983
4.250	1.19852	1.17364	1.14684	1.09974
4.500	1.19717	1.17256	1.14618	1.09965
4.750	1.19583	1.17150	1.14552	1.09956
5.000	1.19456	1.17043	1.14486	1.09946
5.250	1.19323	1.16943	1.14427	1.09938
5.500	1.19188	1.16838	1.14361	1.09934
5.750	1.19055	1.16732	1.14296	1.09927
6.000	1.18925	1.16627	1.14233	1.09918
6.250	1.18798	1.16526	1.14171	1.09910
6.500	1.18673	1.16428	1.14112	1.09905
6.750	1.18550	1.16331	1.14054	1.09902
7.000	1.18428	1.16235	1.13998	1.09899
7.500	1.18183	1.16047	1.13885	1.09897
8.000	1.17946	1.15858	1.13777	1.09898
8.500	1.17719	1.15684	1.13674	1.09899

Table A-11. k-infinity Vs Burnup for Various BP Loading (Figures 37-40), Cont.

Burnup	k-infinity Vs Burnup			
GWd/mtU	0 BP rods	4 BP rods	8 BP rods	16 BP rods
9.000	1.17498	1.15515	1.13580	1.09910
9.500	1.17282	1.15351	1.13489	1.09920
10.000	1.17072	1.15189	1.13402	1.09937
10.500	1.16871	1.15036	1.13319	1.09954
11.000	1.16678	1.14892	1.13245	1.09976
11.500	1.16489	1.14753	1.13175	1.10003
12.000	1.16304	1.14619	1.13105	1.10033
12.500	1.16122	1.14486	1.13038	1.10064
13.000	1.15943	1.14356	1.12973	1.10091
13.500	1.15766	1.14229	1.12907	1.10120
14.000	1.15589	1.14101	1.12841	1.10147
14.500	1.15413	1.13975	1.12771	1.10171
15.000	1.15232	1.13847	1.12698	1.10192
15.500	1.15038	1.13714	1.12617	1.10209
16.000	1.14831	1.13569	1.12524	1.10219
16.500	1.14607	1.13408	1.12417	1.10216
17.000	1.14364	1.13232	1.12287	1.10199
17.500	1.14095	1.13030	1.12141	1.10167
18.000	1.13814	1.12815	1.11971	1.10114
18.500	1.13505	1.12574	1.11780	1.10032
19.000	1.13185	1.12316	1.11569	1.09935
19.500	1.12845	1.12036	1.11333	1.09808
20.000	1.12493	1.11739	1.11085	1.09665
21.000	1.11760	1.11105	1.10530	1.09296
22.000	1.11019	1.10449	1.09946	1.08871
23.000	1.10274	1.09777	1.09340	1.08398
24.000	1.09532	1.09099	1.08719	1.07893
25.000	1.08794	1.08417	1.08085	1.07361
26.000	1.08061	1.07735	1.07443	1.06808
27.391	1.07052	1.06785	1.06543	1.06014
27.392	1.07050	1.07202	1.07345	1.07652
30.000	1.05194	1.05359	1.05518	1.05859
33.000	1.03096	1.03257	1.03410	1.03741
36.000	1.01034	1.01193	1.01344	1.01669
39.000	0.99007	0.99165	0.99315	0.99639
42.000	0.97015	0.97174	0.97324	0.97650
45.000	0.95062	0.95221	0.95373	0.95701
50.000	0.91952	0.92112	0.92265	0.92594
52.148	0.90593	0.90754	0.90908	0.91237

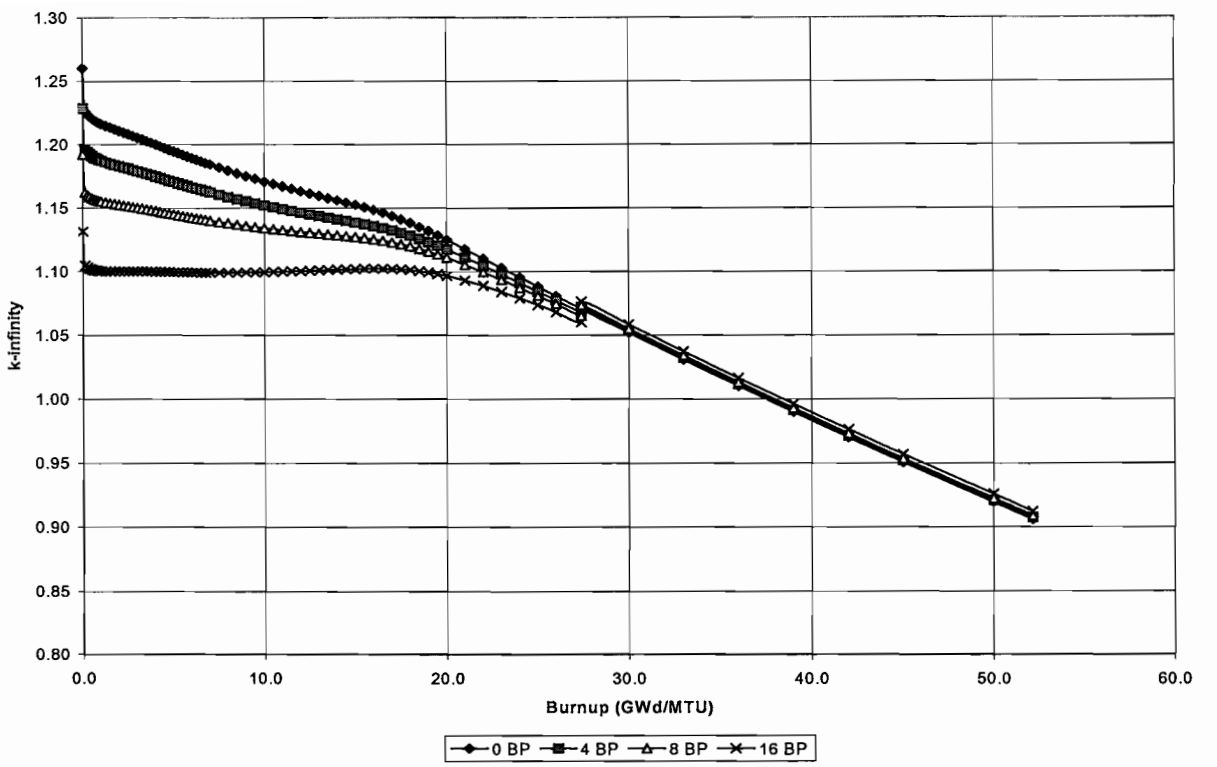

Figure A-66. k-infinity Vs Burnup for Various BP Loading (Figures 37-40)

Table A-12. k-infinity Vs Burnup for Various BP Loading (Figures 41-44)

Std UO_2 = 4.79 wt % ^{235}U, Gd_2O_3-UO_2 = 3.01 wt % - 3.99 wt % ^{235}U, B_4C= 2.1 wt %, 12 Gd rods

Burnup	k-infinity Vs Burnup			
GWd/mtU	0 BP rods	4 BP rods	8 BP rods	16 BP rods
0.000	1.22107	1.19102	1.16996	1.11677
0.125	1.18979	1.16130	1.14118	1.09061
0.250	1.18793	1.15976	1.13973	1.08955
0.375	1.18669	1.15877	1.13880	1.08900
0.500	1.18583	1.15816	1.13821	1.08875
0.625	1.18526	1.15780	1.13788	1.08876
0.750	1.18492	1.15766	1.13775	1.08892
0.875	1.18473	1.15767	1.13775	1.08921
1.000	1.18452	1.15765	1.13787	1.08958
1.250	1.18478	1.15824	1.13828	1.09048
1.500	1.18504	1.15884	1.13884	1.09138
1.750	1.18540	1.15953	1.13947	1.09265
2.000	1.18582	1.16025	1.14013	1.09377
2.250	1.18625	1.16100	1.14080	1.09489
2.500	1.18671	1.16176	1.14148	1.09601
2.750	1.18720	1.16255	1.14217	1.09713
3.000	1.18768	1.16331	1.14286	1.09825
3.250	1.18820	1.16412	1.14354	1.09936
3.500	1.18875	1.16495	1.14423	1.10044
3.750	1.18932	1.16579	1.14496	1.10156
4.000	1.18990	1.16665	1.14570	1.10268
4.250	1.19051	1.16754	1.14644	1.10382
4.500	1.19116	1.16845	1.14719	1.10496
4.750	1.19182	1.16937	1.14797	1.10611
5.000	1.19249	1.17031	1.14878	1.10728
5.250	1.19320	1.17128	1.14959	1.10847
5.500	1.19392	1.17226	1.15039	1.10966
5.750	1.19466	1.17325	1.15125	1.11086
6.000	1.19541	1.17425	1.15212	1.11210
6.250	1.19614	1.17523	1.15300	1.11334
6.500	1.19683	1.17617	1.15388	1.11459
6.750	1.19752	1.17712	1.15473	1.11581
7.000	1.19815	1.17802	1.15561	1.11707
7.500	1.19897	1.17932	1.15706	1.11935
8.000	1.19948	1.18038	1.15852	1.12174
8.500	1.19936	1.18086	1.15967	1.12395

Table A-12. k-infinity Vs Burnup for Various BP Loading (Figures 41-44), Cont.

Burnup	k-infinity Vs Burnup			
GWd/mtU	0 BP rods	4 BP rods	8 BP rods	16 BP rods
9.000	1.19851	1.18068	1.16036	1.12587
9.500	1.19703	1.17991	1.16056	1.12740
10.000	1.19495	1.17855	1.16022	1.12852
10.500	1.19233	1.17666	1.15942	1.12917
11.000	1.18925	1.17431	1.15820	1.12941
11.500	1.18580	1.17160	1.15656	1.12927
12.000	1.18207	1.16860	1.15456	1.12876
12.500	1.17817	1.16542	1.15228	1.12790
13.000	1.17416	1.16208	1.14979	1.12677
13.500	1.17011	1.15869	1.14713	1.12539
14.000	1.16595	1.15519	1.14433	1.12382
14.500	1.16184	1.15164	1.14149	1.12209
15.000	1.15768	1.14810	1.13851	1.12029
15.500	1.15355	1.14449	1.13553	1.11830
16.000	1.14945	1.14093	1.13246	1.11625
16.500	1.14536	1.13734	1.12940	1.11409
17.000	1.14131	1.13376	1.12629	1.11189
17.500	1.13727	1.13018	1.12319	1.10960
18.000	1.13327	1.12661	1.12004	1.10727
18.500	1.12929	1.12303	1.11688	1.10486
19.000	1.12534	1.11947	1.11370	1.10240
19.500	1.12140	1.11590	1.11050	1.09987
20.000	1.11750	1.11233	1.10728	1.09730
21.000	1.10971	1.10520	1.10077	1.09195
22.000	1.10205	1.09809	1.09423	1.08644
23.000	1.09445	1.09099	1.08761	1.08075
24.000	1.08693	1.08390	1.08093	1.07488
25.000	1.07948	1.07683	1.07422	1.06886
26.000	1.07207	1.06975	1.06747	1.06273
27.391	1.06188	1.05996	1.05806	1.05406
27.392	1.06186	1.06333	1.06473	1.06774
30.000	1.04315	1.04476	1.04629	1.04960
33.000	1.02203	1.02358	1.02506	1.02826
36.000	1.00128	1.00280	1.00425	1.00740
39.000	0.98090	0.98242	0.98385	0.98697
42.000	0.96090	0.96242	0.96385	0.96697
45.000	0.94129	0.94281	0.94425	0.94738
50.000	0.91024	0.91176	0.91319	0.91631
52.148	0.89670	0.89821	0.89965	0.90276

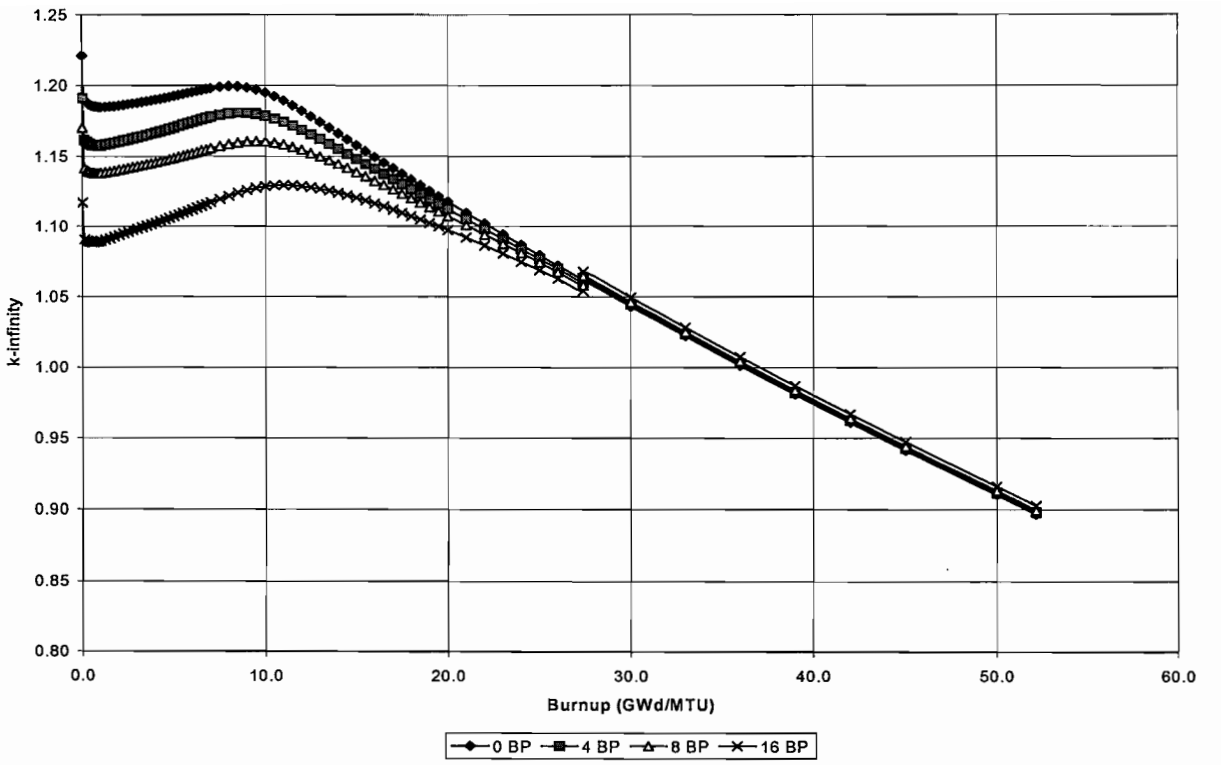

Figure A-67. k-infinity Vs Burnup for Various BP Loading (Figures 41-44)

Table A-13. k-infinity Vs Burnup for Various BP Loading (Figures 45-48)

Std UO_2 = 4.79 wt % ^{235}U, Gd_2O_3-UO_2 = 3.01 wt % - 3.99 wt % ^{235}U, B_4C= 2.1 wt %, 12 Gd rods

Burnup	k-infinity Vs Burnup			
GWd/mtU	0 BP rods	4 BP rods	8 BP rods	16 BP rods
0.000	1.22508	1.19876	1.16062	1.11153
0.125	1.19365	1.16856	1.13263	1.08584
0.250	1.19173	1.16686	1.13140	1.08492
0.375	1.19042	1.16572	1.13068	1.08450
0.500	1.18948	1.16494	1.13029	1.08437
0.625	1.18885	1.16443	1.13016	1.08449
0.750	1.18843	1.16414	1.13023	1.08477
0.875	1.18817	1.16399	1.13042	1.08518
1.000	1.18803	1.16395	1.13074	1.08567
1.250	1.18798	1.16408	1.13153	1.08680
1.500	1.18807	1.16435	1.13247	1.08790
1.750	1.18825	1.16470	1.13348	1.08939
2.000	1.18848	1.16508	1.13454	1.09072
2.250	1.18873	1.16547	1.13560	1.09206
2.500	1.18899	1.16588	1.13668	1.09339
2.750	1.18927	1.16629	1.13776	1.09471
3.000	1.18956	1.16672	1.13885	1.09603
3.250	1.18983	1.16712	1.13990	1.09734
3.500	1.19015	1.16755	1.14100	1.09863
3.750	1.19050	1.16800	1.14211	1.09994
4.000	1.19086	1.16847	1.14323	1.10126
4.250	1.19122	1.16894	1.14434	1.10259
4.500	1.19161	1.16944	1.14548	1.10391
4.750	1.19203	1.16995	1.14665	1.10524
5.000	1.19246	1.17049	1.14781	1.10659
5.250	1.19290	1.17103	1.14897	1.10795
5.500	1.19336	1.17159	1.15016	1.10931
5.750	1.19384	1.17217	1.15136	1.11069
6.000	1.19434	1.17277	1.15257	1.11208
6.250	1.19484	1.17338	1.15377	1.11348
6.500	1.19533	1.17399	1.15493	1.11487
6.750	1.19578	1.17457	1.15608	1.11623
7.000	1.19621	1.17514	1.15723	1.11762
7.500	1.19679	1.17604	1.15913	1.12013
8.000	1.19720	1.17691	1.16090	1.12270
8.500	1.19715	1.17743	1.16221	1.12504

Table A-13. k-infinity Vs Burnup for Various BP Loading (Figures 45-48), Cont.

Burnup	k-infinity Vs Burnup			
GWd/mtU	0 BP rods	4 BP rods	8 BP rods	16 BP rods
9.000	1.19651	1.17749	1.16290	1.12704
9.500	1.19525	1.17701	1.16301	1.12859
10.000	1.19343	1.17603	1.16255	1.12968
10.500	1.19111	1.17455	1.16158	1.13031
11.000	1.18832	1.17263	1.16014	1.13051
11.500	1.18513	1.17031	1.15829	1.13030
12.000	1.18163	1.16764	1.15610	1.12972
12.500	1.17790	1.16472	1.15365	1.12880
13.000	1.17400	1.16157	1.15102	1.12760
13.500	1.17001	1.15828	1.14824	1.12617
14.000	1.16597	1.15490	1.14538	1.12455
14.500	1.16189	1.15148	1.14244	1.12280
15.000	1.15776	1.14793	1.13941	1.12092
15.500	1.15366	1.14442	1.13636	1.11893
16.000	1.14955	1.14084	1.13326	1.11684
16.500	1.14548	1.13729	1.13014	1.11466
17.000	1.14142	1.13372	1.12701	1.11243
17.500	1.13740	1.13016	1.12385	1.11012
18.000	1.13339	1.12659	1.12067	1.10775
18.500	1.12941	1.12303	1.11746	1.10532
19.000	1.12545	1.11947	1.11424	1.10283
19.500	1.12152	1.11590	1.11101	1.10028
20.000	1.11760	1.11235	1.10776	1.09768
21.000	1.10982	1.10522	1.10118	1.09229
22.000	1.10217	1.09814	1.09457	1.08675
23.000	1.09457	1.09107	1.08790	1.08100
24.000	1.08704	1.08399	1.08119	1.07509
25.000	1.07959	1.07691	1.07444	1.06905
26.000	1.07218	1.06984	1.06766	1.06290
27.391	1.06199	1.06005	1.05820	1.05420
27.392	1.06196	1.06344	1.06482	1.06784
30.000	1.04325	1.04486	1.04638	1.04970
33.000	1.02212	1.02368	1.02515	1.02835
36.000	1.00136	1.00289	1.00433	1.00749
39.000	0.98098	0.98250	0.98393	0.98705
42.000	0.96098	0.96249	0.96393	0.96705
45.000	0.94136	0.94288	0.94433	0.94746
50.000	0.91030	0.91181	0.91326	0.91638
52.148	0.89676	0.89826	0.89972	0.90283

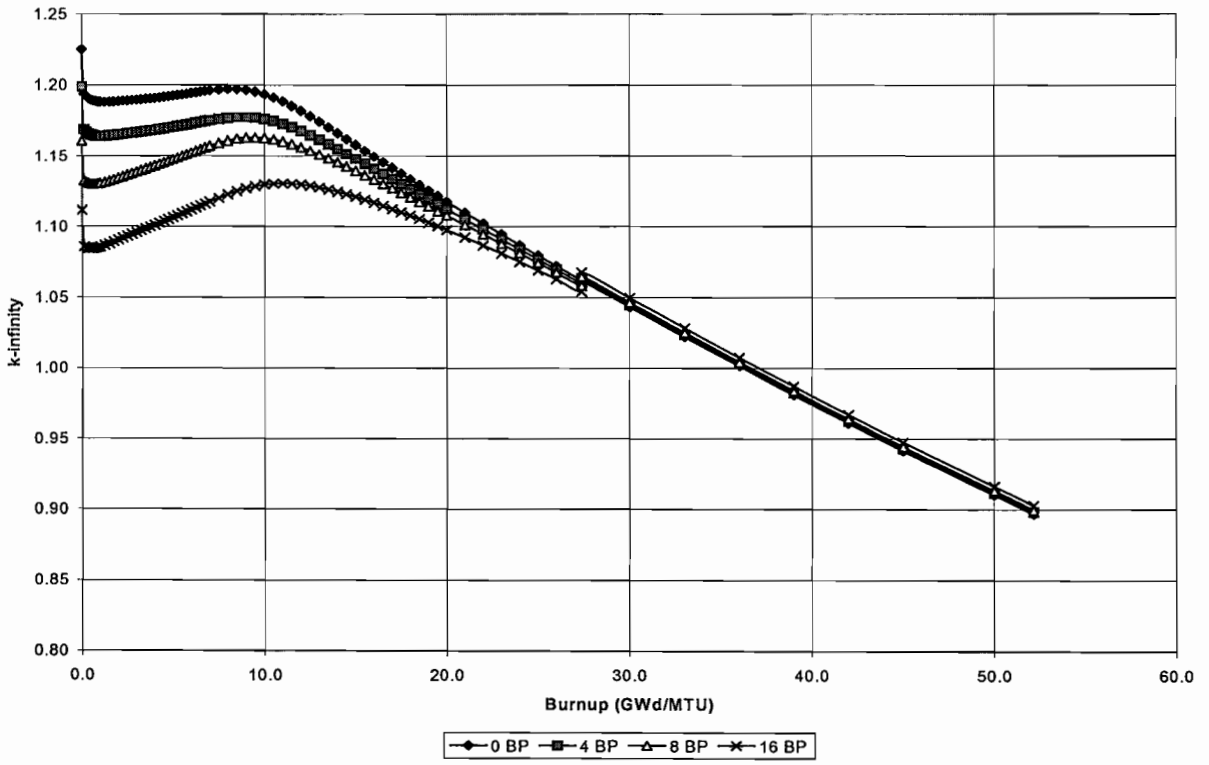

Figure A-68. k-infinity Vs Burnup for Various BP Loading (Figures 45-48)

Table A-14. k-infinity Vs Burnup for Various BP Loading (Figures 49-52)

Std UO_2 = 4.79 wt % ^{235}U, Gd_2O_3-UO_2 = 3.01 wt % - 3.99 wt % ^{235}U, B_4C= 2.1 wt %, 8 Gd rods, and Gd_2O_3-UO_2 = 8.17 wt % - 2.87 wt % ^{235}U, 8 Gd rods

Burnup	k-infinity Vs Burnup			
GWd/mtU	0 BP rods	4 BP rods	8 BP rods	16 BP rods
0.000	1.16674	1.14183	1.11207	1.06364
0.125	1.13795	1.11425	1.08597	1.03990
0.250	1.13626	1.11283	1.08480	1.03914
0.375	1.13517	1.11195	1.08414	1.03887
0.500	1.13443	1.11141	1.08379	1.03889
0.625	1.13395	1.11112	1.08368	1.03914
0.750	1.13368	1.11103	1.08374	1.03953
0.875	1.13354	1.11106	1.08393	1.04003
1.000	1.13342	1.11110	1.08422	1.04062
1.250	1.13365	1.11166	1.08493	1.04191
1.500	1.13392	1.11224	1.08578	1.04333
1.750	1.13423	1.11288	1.08665	1.04478
2.000	1.13460	1.11355	1.08757	1.04624
2.250	1.13495	1.11422	1.08846	1.04770
2.500	1.13533	1.11489	1.08936	1.04914
2.750	1.13568	1.11557	1.09025	1.05057
3.000	1.13605	1.11622	1.09114	1.05199
3.250	1.13629	1.11689	1.09189	1.05337
3.500	1.13668	1.11749	1.09278	1.05469
3.750	1.13708	1.11818	1.09366	1.05610
4.000	1.13747	1.11886	1.09455	1.05749
4.250	1.13788	1.11956	1.09543	1.05889
4.500	1.13830	1.12029	1.09632	1.06028
4.750	1.13875	1.12101	1.09723	1.06170
5.000	1.13919	1.12173	1.09815	1.06311
5.250	1.13965	1.12248	1.09907	1.06451
5.500	1.14013	1.12323	1.10001	1.06594
5.750	1.14063	1.12400	1.10096	1.06737
6.000	1.14113	1.12477	1.10193	1.06880
6.250	1.14164	1.12552	1.10290	1.07024
6.500	1.14214	1.12625	1.10389	1.07165
6.750	1.14260	1.12695	1.10482	1.07306
7.000	1.14304	1.12768	1.10575	1.07452
7.500	1.14369	1.12869	1.10745	1.07700
8.000	1.14421	1.12957	1.10914	1.07955
8.500	1.14437	1.13004	1.11058	1.08186

Table A-14. k-infinity Vs Burnup for Various BP Loading (Figures 49-52), Cont.

Burnup	k-infinity Vs Burnup			
GWd/mtU	0 BP rods	4 BP rods	8 BP rods	16 BP rods
9.000	1.14410	1.13006	1.11169	1.08381
9.500	1.14347	1.12968	1.11246	1.08539
10.000	1.14252	1.12896	1.11295	1.08662
10.500	1.14123	1.12797	1.11311	1.08762
11.000	1.13970	1.12670	1.11300	1.08831
11.500	1.13800	1.12525	1.11270	1.08872
12.000	1.13617	1.12370	1.11221	1.08895
12.500	1.13420	1.12207	1.11153	1.08908
13.000	1.13229	1.12037	1.11080	1.08906
13.500	1.13031	1.11873	1.11002	1.08891
14.000	1.12837	1.11701	1.10913	1.08875
14.500	1.12638	1.11537	1.10824	1.08858
15.000	1.12437	1.11369	1.10718	1.08823
15.500	1.12242	1.11196	1.10618	1.08785
16.000	1.12048	1.11032	1.10513	1.08743
16.500	1.11861	1.10867	1.10412	1.08689
17.000	1.11678	1.10706	1.10308	1.08639
17.500	1.11494	1.10550	1.10201	1.08586
18.000	1.11310	1.10392	1.10089	1.08526
18.500	1.11123	1.10235	1.09971	1.08463
19.000	1.10926	1.10074	1.09841	1.08395
19.500	1.10722	1.09907	1.09698	1.08317
20.000	1.10502	1.09732	1.09544	1.08229
21.000	1.09989	1.09312	1.09147	1.07981
22.000	1.09424	1.08861	1.08690	1.07690
23.000	1.08787	1.08336	1.08145	1.07318
24.000	1.08093	1.07739	1.07530	1.06860
25.000	1.07370	1.07084	1.06876	1.06321
26.000	1.06639	1.06399	1.06204	1.05732
27.391	1.05624	1.05431	1.05263	1.04872
27.392	1.05621	1.05776	1.05920	1.06233
30.000	1.03757	1.03926	1.04081	1.04427
33.000	1.01648	1.01811	1.01961	1.02295
36.000	0.99576	0.99736	0.99883	1.00210
39.000	0.97543	0.97700	0.97846	0.98170
42.000	0.95548	0.95705	0.95852	0.96174
45.000	0.93594	0.93751	0.93898	0.94220
50.000	0.90504	0.90659	0.90806	0.91125
52.148	0.89156	0.89310	0.89458	0.89776

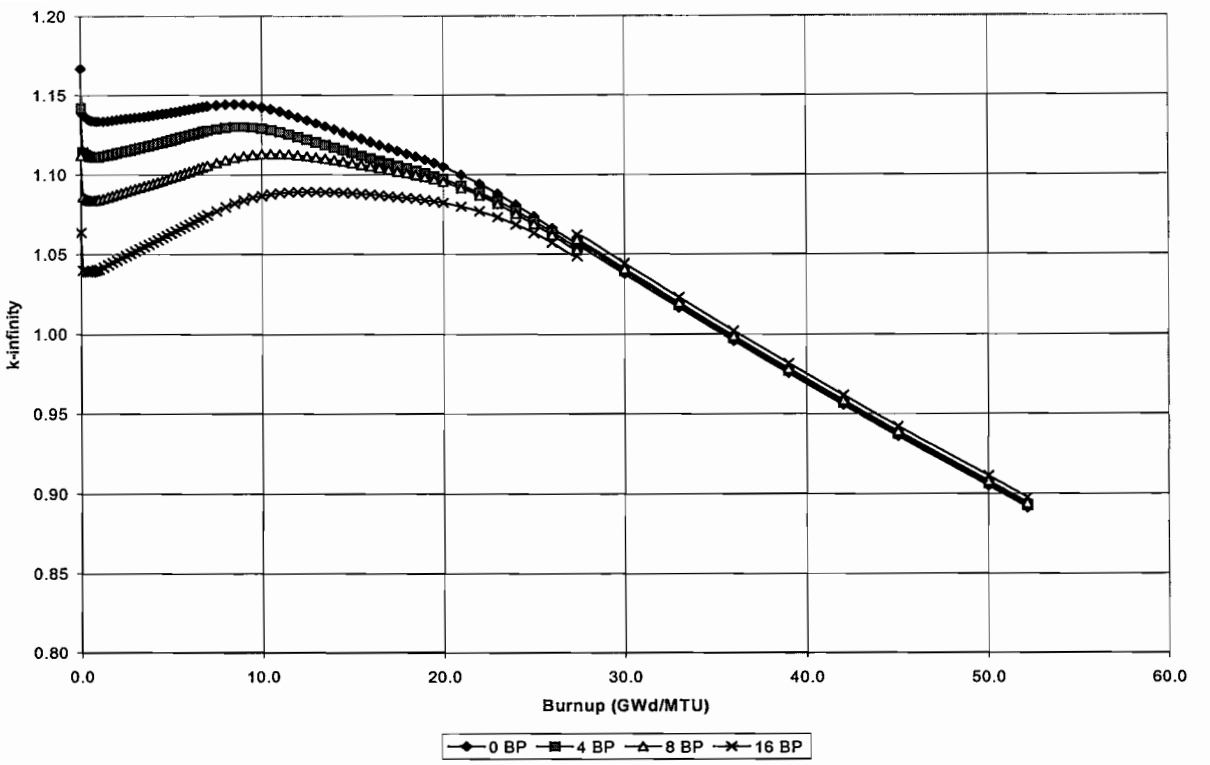

Figure A-69. k-infinity Vs Burnup for Various BP Loading (Figures 49-52)

Table A-15. k-infinity Vs Burnup for Various BP Loading (Figures 53-56)

Std UO_2 = 4.79 wt % ^{235}U, Gd_2O_3-UO_2 = 3.01 wt % - 3.99 wt % ^{235}U, B_4C= 2.1 wt %, 8 Gd rods, and Gd_2O_3-UO_2 = 8.17 wt % - 2.87 wt % ^{235}U, 8 Gd rods

Burnup	k-infinity Vs Burnup			
GWd/mtU	0 BP rods	4 BP rods	8 BP rods	16 BP rods
0.000	1.16832	1.14283	1.10915	1.06098
0.125	1.13948	1.11519	1.08336	1.03745
0.250	1.13779	1.11377	1.08230	1.03673
0.375	1.13670	1.11286	1.08172	1.03649
0.500	1.13596	1.11230	1.08148	1.03654
0.625	1.13548	1.11198	1.08146	1.03680
0.750	1.13520	1.11185	1.08163	1.03722
0.875	1.13506	1.11185	1.08191	1.03774
1.000	1.13494	1.11187	1.08220	1.03834
1.250	1.13517	1.11234	1.08320	1.03965
1.500	1.13543	1.11285	1.08425	1.04109
1.750	1.13575	1.11340	1.08534	1.04255
2.000	1.13611	1.11399	1.08646	1.04402
2.250	1.13647	1.11457	1.08757	1.04547
2.500	1.13684	1.11516	1.08868	1.04692
2.750	1.13721	1.11573	1.08978	1.04834
3.000	1.13757	1.11631	1.09087	1.04976
3.250	1.13794	1.11686	1.09187	1.05105
3.500	1.13824	1.11736	1.09299	1.05244
3.750	1.13864	1.11795	1.09409	1.05383
4.000	1.13904	1.11855	1.09519	1.05522
4.250	1.13946	1.11914	1.09630	1.05661
4.500	1.13990	1.11977	1.09743	1.05799
4.750	1.14035	1.12040	1.09857	1.05939
5.000	1.14080	1.12104	1.09969	1.06079
5.250	1.14127	1.12169	1.10084	1.06220
5.500	1.14176	1.12236	1.10200	1.06362
5.750	1.14227	1.12304	1.10317	1.06504
6.000	1.14278	1.12373	1.10433	1.06648
6.250	1.14329	1.12442	1.10549	1.06791
6.500	1.14376	1.12509	1.10660	1.06934
6.750	1.14423	1.12574	1.10776	1.07079
7.000	1.14470	1.12643	1.10882	1.07219
7.500	1.14527	1.12743	1.11065	1.07481
8.000	1.14569	1.12836	1.11235	1.07750
8.500	1.14573	1.12896	1.11368	1.08000

Table A-15. k-infinity Vs Burnup for Various BP Loading (Figures 53-56), Cont.

Burnup	k-infinity Vs Burnup			
GWd/mtU	0 BP rods	4 BP rods	8 BP rods	16 BP rods
9.000	1.14532	1.12918	1.11456	1.08222
9.500	1.14449	1.12897	1.11500	1.08409
10.000	1.14335	1.12846	1.11513	1.08572
10.500	1.14193	1.12767	1.11495	1.08707
11.000	1.14018	1.12657	1.11445	1.08808
11.500	1.13824	1.12526	1.11373	1.08886
12.000	1.13625	1.12383	1.11292	1.08945
12.500	1.13417	1.12232	1.11200	1.08984
13.000	1.13198	1.12070	1.11095	1.09002
13.500	1.12983	1.11907	1.10988	1.09010
14.000	1.12779	1.11747	1.10883	1.09018
14.500	1.12564	1.11582	1.10772	1.09010
15.000	1.12349	1.11415	1.10650	1.08989
15.500	1.12139	1.11245	1.10532	1.08961
16.000	1.11924	1.11076	1.10404	1.08922
16.500	1.11720	1.10909	1.10283	1.08882
17.000	1.11521	1.10745	1.10162	1.08839
17.500	1.11320	1.10583	1.10037	1.08788
18.000	1.11124	1.10420	1.09909	1.08732
18.500	1.10929	1.10257	1.09781	1.08669
19.000	1.10731	1.10089	1.09645	1.08597
19.500	1.10528	1.09919	1.09503	1.08513
20.000	1.10316	1.09739	1.09349	1.08415
21.000	1.09835	1.09323	1.08976	1.08145
22.000	1.09313	1.08871	1.08556	1.07817
23.000	1.08725	1.08351	1.08065	1.07407
24.000	1.08070	1.07758	1.07499	1.06917
25.000	1.07367	1.07105	1.06873	1.06358
26.000	1.06645	1.06419	1.06212	1.05758
27.391	1.05637	1.05450	1.05274	1.04892
27.392	1.05634	1.05787	1.05930	1.06242
30.000	1.03770	1.03936	1.04093	1.04434
33.000	1.01661	1.01822	1.01973	1.02303
36.000	0.99589	0.99747	0.99896	1.00219
39.000	0.97555	0.97711	0.97859	0.98179
42.000	0.95560	0.95716	0.95864	0.96184
45.000	0.93606	0.93761	0.93910	0.94230
50.000	0.90514	0.90669	0.90817	0.91135
52.148	0.89166	0.89320	0.89468	0.89786

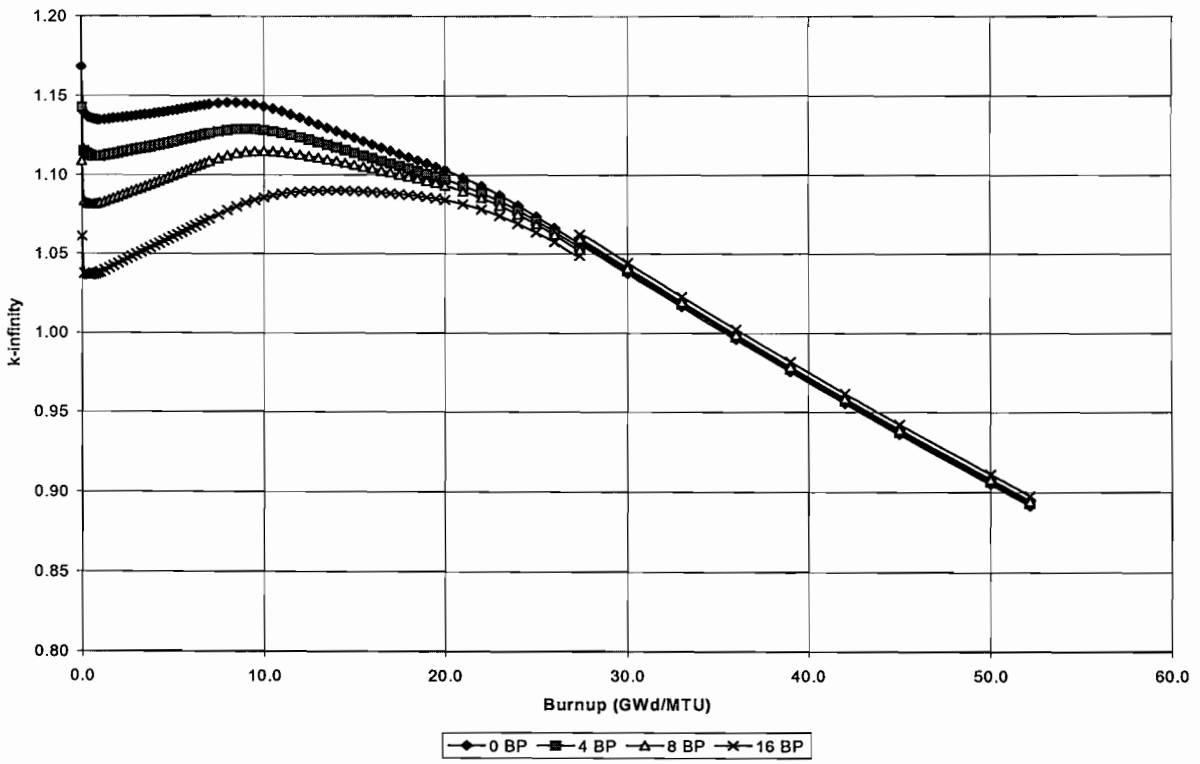

Figure A-70. k-infinity Vs Burnup for Various BP Loading (Figures 53-56)

Table A-16. Sample of Results (Number Density Vs Burnup)

BURNUP GWd/mtU	NUCLIDE 64155 Gd-155 at/barn-cm	NUCLIDE 45103 Rh-103 at/barn-cm	NUCLIDE 60143 Nd-143 at/barn-cm	NUCLIDE 60145 Nd-145 at/barn-cm	NUCLIDE 62147 Sm-147 at/barn-cm	NUCLIDE 62149 Sm-149 at/barn-cm	NUCLIDE 62150 Sm-150 at/barn-cm	NUCLIDE 62151 Sm-151 at/barn-cm	NUCLIDE 62152 Sm-152 at/barn-cm
0	0	0	0	0	0	0	0	0	0
0.125	2.74E-13	2.80E-08	5.30E-08	3.54E-08	2.92E-11	3.85E-09	4.90E-10	4.17E-09	2.51E-09
0.250	1.06E-12	5.60E-08	1.06E-07	7.07E-08	1.16E-10	1.00E-08	2.75E-09	8.19E-09	5.17E-09
0.375	2.29E-12	8.40E-08	1.59E-07	1.06E-07	2.61E-10	1.55E-08	6.93E-09	1.21E-08	7.98E-09
0.500	3.93E-12	1.12E-07	2.11E-07	1.41E-07	4.63E-10	1.98E-08	1.27E-08	1.58E-08	1.09E-08
0.625	5.93E-12	1.40E-07	2.64E-07	1.76E-07	7.20E-10	2.30E-08	1.96E-08	1.94E-08	1.40E-08
0.750	8.26E-12	1.68E-07	3.16E-07	2.11E-07	1.03E-09	2.54E-08	2.73E-08	2.29E-08	1.72E-08
0.875	1.09E-11	1.96E-07	3.68E-07	2.46E-07	1.40E-09	2.72E-08	3.58E-08	2.63E-08	2.05E-08
1.000	1.38E-11	2.24E-07	4.21E-07	2.81E-07	1.83E-09	2.85E-08	4.47E-08	2.96E-08	2.39E-08
1.250	2.02E-11	2.80E-07	5.24E-07	3.51E-07	2.83E-09	3.03E-08	6.34E-08	3.58E-08	3.11E-08
1.500	2.74E-11	3.36E-07	6.28E-07	4.21E-07	4.06E-09	3.14E-08	8.30E-08	4.17E-08	3.87E-08
1.750	3.53E-11	3.91E-07	7.31E-07	4.90E-07	5.48E-09	3.21E-08	1.03E-07	4.71E-08	4.66E-08
2.000	4.36E-11	4.47E-07	8.33E-07	5.59E-07	7.12E-09	3.27E-08	1.23E-07	5.23E-08	5.49E-08
2.250	5.23E-11	5.03E-07	9.36E-07	6.28E-07	8.95E-09	3.31E-08	1.44E-07	5.71E-08	6.35E-08
2.500	6.14E-11	5.59E-07	1.04E-06	6.97E-07	1.10E-08	3.34E-08	1.65E-07	6.17E-08	7.23E-08
2.750	7.07E-11	6.14E-07	1.14E-06	7.65E-07	1.32E-08	3.37E-08	1.86E-07	6.60E-08	8.14E-08
3.000	8.02E-11	6.70E-07	1.24E-06	8.33E-07	1.56E-08	3.39E-08	2.07E-07	7.00E-08	9.07E-08
3.250	8.98E-11	7.26E-07	1.34E-06	9.01E-07	1.82E-08	3.42E-08	2.28E-07	7.39E-08	1.00E-07
3.500	9.96E-11	7.81E-07	1.44E-06	9.69E-07	2.10E-08	3.44E-08	2.50E-07	7.75E-08	1.10E-07
3.750	1.10E-10	8.36E-07	1.54E-06	1.04E-06	2.39E-08	3.46E-08	2.71E-07	8.09E-08	1.20E-07
4.000	1.20E-10	8.92E-07	1.64E-06	1.10E-06	2.70E-08	3.48E-08	2.93E-07	8.41E-08	1.30E-07
4.250	1.30E-10	9.47E-07	1.74E-06	1.17E-06	3.03E-08	3.50E-08	3.15E-07	8.72E-08	1.40E-07
4.500	1.40E-10	1.00E-06	1.84E-06	1.24E-06	3.38E-08	3.52E-08	3.37E-07	9.01E-08	1.50E-07
4.750	1.50E-10	1.06E-06	1.93E-06	1.31E-06	3.74E-08	3.53E-08	3.59E-07	9.29E-08	1.60E-07
5.000	1.60E-10	1.11E-06	2.03E-06	1.37E-06	4.12E-08	3.55E-08	3.81E-07	9.55E-08	1.71E-07
5.250	1.70E-10	1.17E-06	2.13E-06	1.44E-06	4.51E-08	3.57E-08	4.03E-07	9.80E-08	1.81E-07
5.500	1.80E-10	1.22E-06	2.22E-06	1.50E-06	4.92E-08	3.59E-08	4.25E-07	1.00E-07	1.92E-07
5.750	1.90E-10	1.28E-06	2.32E-06	1.57E-06	5.35E-08	3.60E-08	4.47E-07	1.03E-07	2.02E-07
6.000	2.01E-10	1.33E-06	2.42E-06	1.64E-06	5.79E-08	3.62E-08	4.70E-07	1.05E-07	2.13E-07
6.250	2.11E-10	1.39E-06	2.51E-06	1.70E-06	6.24E-08	3.63E-08	4.92E-07	1.07E-07	2.24E-07
6.500	2.21E-10	1.44E-06	2.61E-06	1.77E-06	6.71E-08	3.65E-08	5.15E-07	1.09E-07	2.34E-07
6.750	2.31E-10	1.49E-06	2.70E-06	1.83E-06	7.19E-08	3.67E-08	5.38E-07	1.11E-07	2.45E-07
7.000	2.42E-10	1.55E-06	2.80E-06	1.90E-06	7.68E-08	3.68E-08	5.60E-07	1.13E-07	2.56E-07
7.500	2.63E-10	1.66E-06	2.98E-06	2.03E-06	8.71E-08	3.71E-08	6.06E-07	1.16E-07	2.77E-07
8.000	2.83E-10	1.76E-06	3.17E-06	2.16E-06	9.79E-08	3.74E-08	6.52E-07	1.19E-07	2.99E-07
8.500	3.05E-10	1.87E-06	3.35E-06	2.29E-06	1.09E-07	3.76E-08	6.99E-07	1.22E-07	3.20E-07
9.000	3.26E-10	1.98E-06	3.54E-06	2.41E-06	1.21E-07	3.79E-08	7.45E-07	1.25E-07	3.42E-07
9.500	3.47E-10	2.08E-06	3.72E-06	2.54E-06	1.33E-07	3.81E-08	7.92E-07	1.27E-07	3.63E-07
10.000	3.69E-10	2.19E-06	3.90E-06	2.67E-06	1.46E-07	3.83E-08	8.40E-07	1.30E-07	3.84E-07
10.500	3.91E-10	2.30E-06	4.08E-06	2.79E-06	1.58E-07	3.85E-08	8.87E-07	1.32E-07	4.06E-07
11.000	4.13E-10	2.40E-06	4.25E-06	2.92E-06	1.72E-07	3.87E-08	9.35E-07	1.34E-07	4.27E-07
11.500	4.36E-10	2.50E-06	4.43E-06	3.04E-06	1.86E-07	3.89E-08	9.83E-07	1.36E-07	4.47E-07
12.000	4.59E-10	2.61E-06	4.60E-06	3.16E-06	2.00E-07	3.90E-08	1.03E-06	1.38E-07	4.68E-07
12.500	4.82E-10	2.71E-06	4.78E-06	3.29E-06	2.14E-07	3.92E-08	1.08E-06	1.40E-07	4.88E-07
13.000	5.06E-10	2.81E-06	4.95E-06	3.41E-06	2.29E-07	3.93E-08	1.13E-06	1.42E-07	5.09E-07
13.500	5.30E-10	2.92E-06	5.12E-06	3.53E-06	2.44E-07	3.94E-08	1.18E-06	1.44E-07	5.29E-07
14.000	5.55E-10	3.02E-06	5.29E-06	3.65E-06	2.59E-07	3.95E-08	1.23E-06	1.46E-07	5.49E-07
14.500	5.80E-10	3.12E-06	5.45E-06	3.77E-06	2.74E-07	3.96E-08	1.28E-06	1.47E-07	5.68E-07

Table A-16. Sample of Results (Number Density Vs Burnup), Cont.

BURNUP GWd/mtU	NUCLIDE 64155 Gd-155 at/barn-cm	NUCLIDE 45103 Rh-103 at/barn-cm	NUCLIDE 60143 Nd-143 at/barn-cm	NUCLIDE 60145 Nd-145 at/barn-cm	NUCLIDE 62147 Sm-147 at/barn-cm	NUCLIDE 62149 Sm-149 at/barn-cm	NUCLIDE 62150 Sm-150 at/barn-cm	NUCLIDE 62151 Sm-151 at/barn-cm	NUCLIDE 62152 Sm-152 at/barn-cm
15.000	6.06E-10	3.22E-06	5.62E-06	3.89E-06	2.90E-07	3.97E-08	1.32E-06	1.49E-07	5.88E-07
15.500	6.32E-10	3.32E-06	5.78E-06	4.01E-06	3.06E-07	3.98E-08	1.37E-06	1.50E-07	6.07E-07
16.000	6.58E-10	3.42E-06	5.95E-06	4.13E-06	3.22E-07	3.99E-08	1.42E-06	1.52E-07	6.26E-07
16.500	6.86E-10	3.52E-06	6.11E-06	4.25E-06	3.38E-07	4.00E-08	1.47E-06	1.53E-07	6.45E-07
17.000	7.13E-10	3.61E-06	6.27E-06	4.36E-06	3.55E-07	4.00E-08	1.52E-06	1.55E-07	6.64E-07
17.500	7.41E-10	3.71E-06	6.42E-06	4.48E-06	3.72E-07	4.01E-08	1.57E-06	1.56E-07	6.83E-07
18.000	7.70E-10	3.81E-06	6.58E-06	4.60E-06	3.89E-07	4.01E-08	1.62E-06	1.58E-07	7.01E-07
18.500	7.99E-10	3.90E-06	6.74E-06	4.71E-06	4.06E-07	4.01E-08	1.67E-06	1.59E-07	7.19E-07
19.000	8.28E-10	4.00E-06	6.89E-06	4.83E-06	4.23E-07	4.02E-08	1.72E-06	1.61E-07	7.37E-07
19.500	8.59E-10	4.09E-06	7.04E-06	4.94E-06	4.40E-07	4.02E-08	1.77E-06	1.62E-07	7.55E-07
20.000	8.89E-10	4.19E-06	7.20E-06	5.05E-06	4.57E-07	4.02E-08	1.82E-06	1.63E-07	7.72E-07
21.000	9.53E-10	4.38E-06	7.49E-06	5.28E-06	4.92E-07	4.03E-08	1.93E-06	1.66E-07	8.07E-07
22.000	1.02E-09	4.56E-06	7.79E-06	5.50E-06	5.28E-07	4.03E-08	2.03E-06	1.68E-07	8.41E-07
23.000	1.08E-09	4.74E-06	8.07E-06	5.72E-06	5.63E-07	4.02E-08	2.13E-06	1.71E-07	8.74E-07
24.000	1.15E-09	4.92E-06	8.36E-06	5.93E-06	5.99E-07	4.02E-08	2.23E-06	1.73E-07	9.06E-07
25.000	1.22E-09	5.10E-06	8.63E-06	6.15E-06	6.35E-07	4.01E-08	2.33E-06	1.75E-07	9.37E-07
26.000	1.29E-09	5.27E-06	8.90E-06	6.36E-06	6.71E-07	4.00E-08	2.43E-06	1.77E-07	9.68E-07
27.391	1.40E-09	5.51E-06	9.27E-06	6.65E-06	7.20E-07	3.99E-08	2.57E-06	1.81E-07	1.01E-06
30.000	1.56E-09	5.95E-06	9.92E-06	7.19E-06	8.14E-07	3.82E-08	2.84E-06	1.83E-07	1.09E-06
50.000	2.79E-09	8.62E-06	1.36E-05	1.07E-05	1.43E-06	3.33E-08	4.75E-06	2.09E-07	1.56E-06
52.148	2.81E-09	8.85E-06	1.38E-05	1.10E-05	1.48E-06	3.21E-08	4.94E-06	2.09E-07	1.61E-06

Table A-16. Sample of Results (Number Density Vs Burnup), Cont.

BURNUP	NUCLIDE 63153 Eu-153	NUCLIDE 63155 Eu-155	NUCLIDE 92234 U-234	NUCLIDE 92235 U-235	NUCLIDE 92236 U-236	NUCLIDE 92238 U-238	NUCLIDE 93237 Np-237	NUCLIDE 94238 Pu-238	NUCLIDE 94239 Pu-239
GWd/mtU	at/barn-cm	at/barn-cm	at/barn-cm	at/barn-cm	at/barn-cm	at/barn-cm	at/barn-cm	at/barn-cm	at/barn-cm
0.000	0	0	2.62E-06	3.26E-04	0	6.61E-03	0	0	0
0.125	1.59E-09	3.53E-10	2.61E-06	3.25E-04	2.09E-07	6.61E-03	2.86E-09	3.72E-12	1.87E-07
0.250	3.20E-09	7.05E-10	2.61E-06	3.24E-04	4.19E-07	6.61E-03	5.95E-09	1.55E-11	5.66E-07
0.375	4.83E-09	1.06E-09	2.61E-06	3.23E-04	6.28E-07	6.61E-03	9.16E-09	3.56E-11	1.00E-06
0.500	6.47E-09	1.41E-09	2.60E-06	3.22E-04	8.36E-07	6.60E-03	1.25E-08	6.45E-11	1.45E-06
0.625	8.14E-09	1.76E-09	2.60E-06	3.21E-04	1.04E-06	6.60E-03	1.60E-08	1.02E-10	1.90E-06
0.750	9.83E-09	2.11E-09	2.59E-06	3.20E-04	1.25E-06	6.60E-03	1.97E-08	1.50E-10	2.34E-06
0.875	1.15E-08	2.46E-09	2.59E-06	3.18E-04	1.45E-06	6.60E-03	2.34E-08	2.07E-10	2.78E-06
1.000	1.33E-08	2.80E-09	2.59E-06	3.17E-04	1.66E-06	6.60E-03	2.74E-08	2.74E-10	3.22E-06
1.250	1.68E-08	3.50E-09	2.58E-06	3.15E-04	2.06E-06	6.60E-03	3.56E-08	4.41E-10	4.08E-06
1.500	2.04E-08	4.20E-09	2.57E-06	3.13E-04	2.47E-06	6.60E-03	4.44E-08	6.52E-10	4.92E-06
1.750	2.41E-08	4.90E-09	2.56E-06	3.11E-04	2.87E-06	6.60E-03	5.38E-08	9.11E-10	5.75E-06
2.000	2.80E-08	5.60E-09	2.55E-06	3.09E-04	3.26E-06	6.60E-03	6.36E-08	1.22E-09	6.55E-06
2.250	3.19E-08	6.30E-09	2.54E-06	3.07E-04	3.65E-06	6.60E-03	7.39E-08	1.58E-09	7.34E-06
2.500	3.60E-08	6.99E-09	2.54E-06	3.05E-04	4.04E-06	6.60E-03	8.47E-08	1.99E-09	8.12E-06
2.750	4.01E-08	7.69E-09	2.53E-06	3.03E-04	4.43E-06	6.60E-03	9.59E-08	2.47E-09	8.87E-06
3.000	4.44E-08	8.39E-09	2.52E-06	3.01E-04	4.81E-06	6.59E-03	1.08E-07	2.99E-09	9.62E-06
3.250	4.88E-08	9.09E-09	2.51E-06	3.00E-04	5.19E-06	6.59E-03	1.20E-07	3.59E-09	1.03E-05
3.500	5.32E-08	9.79E-09	2.50E-06	2.98E-04	5.57E-06	6.59E-03	1.32E-07	4.24E-09	1.11E-05
3.750	5.79E-08	1.05E-08	2.50E-06	2.96E-04	5.94E-06	6.59E-03	1.45E-07	4.96E-09	1.18E-05
4.000	6.26E-08	1.12E-08	2.49E-06	2.94E-04	6.31E-06	6.59E-03	1.59E-07	5.74E-09	1.24E-05
4.250	6.74E-08	1.19E-08	2.48E-06	2.92E-04	6.68E-06	6.59E-03	1.72E-07	6.59E-09	1.31E-05
4.500	7.24E-08	1.26E-08	2.47E-06	2.90E-04	7.05E-06	6.59E-03	1.87E-07	7.52E-09	1.38E-05
4.750	7.75E-08	1.33E-08	2.46E-06	2.88E-04	7.41E-06	6.59E-03	2.01E-07	8.51E-09	1.44E-05
5.000	8.27E-08	1.40E-08	2.46E-06	2.86E-04	7.77E-06	6.59E-03	2.16E-07	9.59E-09	1.50E-05
5.250	8.80E-08	1.48E-08	2.45E-06	2.84E-04	8.13E-06	6.58E-03	2.32E-07	1.07E-08	1.56E-05
5.500	9.34E-08	1.55E-08	2.44E-06	2.83E-04	8.48E-06	6.58E-03	2.48E-07	1.20E-08	1.62E-05
5.750	9.90E-08	1.62E-08	2.43E-06	2.81E-04	8.84E-06	6.58E-03	2.64E-07	1.33E-08	1.68E-05
6.000	1.05E-07	1.69E-08	2.43E-06	2.79E-04	9.19E-06	6.58E-03	2.80E-07	1.47E-08	1.74E-05
6.250	1.10E-07	1.77E-08	2.42E-06	2.77E-04	9.53E-06	6.58E-03	2.97E-07	1.61E-08	1.80E-05
6.500	1.16E-07	1.84E-08	2.41E-06	2.75E-04	9.88E-06	6.58E-03	3.14E-07	1.77E-08	1.86E-05
6.750	1.22E-07	1.92E-08	2.40E-06	2.74E-04	1.02E-05	6.58E-03	3.32E-07	1.93E-08	1.91E-05
7.000	1.29E-07	1.99E-08	2.39E-06	2.72E-04	1.06E-05	6.58E-03	3.50E-07	2.11E-08	1.96E-05
7.500	1.41E-07	2.14E-08	2.38E-06	2.68E-04	1.12E-05	6.57E-03	3.86E-07	2.48E-08	2.07E-05
8.000	1.54E-07	2.30E-08	2.36E-06	2.65E-04	1.19E-05	6.57E-03	4.24E-07	2.89E-08	2.17E-05
8.500	1.68E-07	2.46E-08	2.35E-06	2.61E-04	1.26E-05	6.57E-03	4.62E-07	3.34E-08	2.27E-05
9.000	1.82E-07	2.62E-08	2.33E-06	2.58E-04	1.32E-05	6.57E-03	5.02E-07	3.82E-08	2.36E-05
9.500	1.96E-07	2.78E-08	2.32E-06	2.55E-04	1.38E-05	6.57E-03	5.42E-07	4.35E-08	2.45E-05
10.000	2.11E-07	2.95E-08	2.30E-06	2.51E-04	1.45E-05	6.56E-03	5.84E-07	4.92E-08	2.53E-05
10.500	2.26E-07	3.12E-08	2.29E-06	2.48E-04	1.51E-05	6.56E-03	6.27E-07	5.53E-08	2.62E-05
11.000	2.41E-07	3.30E-08	2.27E-06	2.45E-04	1.57E-05	6.56E-03	6.71E-07	6.19E-08	2.70E-05
11.500	2.57E-07	3.48E-08	2.26E-06	2.41E-04	1.63E-05	6.56E-03	7.15E-07	6.89E-08	2.78E-05
12.000	2.74E-07	3.67E-08	2.24E-06	2.38E-04	1.69E-05	6.56E-03	7.61E-07	7.63E-08	2.85E-05
12.500	2.90E-07	3.86E-08	2.23E-06	2.35E-04	1.75E-05	6.55E-03	8.07E-07	8.42E-08	2.92E-05
13.000	3.07E-07	4.06E-08	2.21E-06	2.32E-04	1.81E-05	6.55E-03	8.54E-07	9.26E-08	2.99E-05
13.500	3.25E-07	4.26E-08	2.20E-06	2.29E-04	1.86E-05	6.55E-03	9.02E-07	1.02E-07	3.06E-05
14.000	3.42E-07	4.47E-08	2.19E-06	2.26E-04	1.92E-05	6.55E-03	9.51E-07	1.11E-07	3.12E-05
14.500	3.60E-07	4.69E-08	2.17E-06	2.23E-04	1.98E-05	6.54E-03	1.00E-06	1.21E-07	3.18E-05

Table A-16. Sample of Results (Number Density Vs Burnup), Cont.

BURNUP	NUCLIDE 63153	NUCLIDE 63155	NUCLIDE 92234	NUCLIDE 92235	NUCLIDE 92236	NUCLIDE 92238	NUCLIDE 93237	NUCLIDE 94238	NUCLIDE 94239
	Eu-153	Eu-155	U-234	U-235	U-236	U-238	Np-237	Pu-238	Pu-239
GWd/mtU	at/barn-cm	at/barn-cm	at/barn-cm	at/barn-cm	at/barn-cm	at/barn-cm	at/barn-cm	at/barn-cm	at/barn-cm
15.000	3.79E-07	4.91E-08	2.16E-06	2.20E-04	2.03E-05	6.54E-03	1.05E-06	1.31E-07	3.24E-05
15.500	3.97E-07	5.14E-08	2.14E-06	2.17E-04	2.09E-05	6.54E-03	1.10E-06	1.42E-07	3.30E-05
16.000	4.16E-07	5.37E-08	2.13E-06	2.14E-04	2.14E-05	6.54E-03	1.15E-06	1.54E-07	3.35E-05
16.500	4.35E-07	5.61E-08	2.11E-06	2.11E-04	2.19E-05	6.54E-03	1.21E-06	1.66E-07	3.41E-05
17.000	4.55E-07	5.86E-08	2.10E-06	2.08E-04	2.24E-05	6.53E-03	1.26E-06	1.78E-07	3.46E-05
17.500	4.74E-07	6.11E-08	2.09E-06	2.05E-04	2.29E-05	6.53E-03	1.31E-06	1.91E-07	3.51E-05
18.000	4.94E-07	6.37E-08	2.07E-06	2.02E-04	2.35E-05	6.53E-03	1.37E-06	2.05E-07	3.55E-05
18.500	5.14E-07	6.64E-08	2.06E-06	2.00E-04	2.40E-05	6.53E-03	1.42E-06	2.19E-07	3.60E-05
19.000	5.34E-07	6.91E-08	2.04E-06	1.97E-04	2.44E-05	6.52E-03	1.48E-06	2.34E-07	3.64E-05
19.500	5.55E-07	7.19E-08	2.03E-06	1.94E-04	2.49E-05	6.52E-03	1.54E-06	2.50E-07	3.68E-05
20.000	5.76E-07	7.48E-08	2.02E-06	1.91E-04	2.54E-05	6.52E-03	1.59E-06	2.66E-07	3.72E-05
21.000	6.18E-07	8.08E-08	1.99E-06	1.86E-04	2.64E-05	6.52E-03	1.71E-06	3.00E-07	3.80E-05
22.000	6.60E-07	8.71E-08	1.96E-06	1.81E-04	2.73E-05	6.51E-03	1.83E-06	3.37E-07	3.87E-05
23.000	7.04E-07	9.37E-08	1.93E-06	1.75E-04	2.81E-05	6.51E-03	1.94E-06	3.76E-07	3.93E-05
24.000	7.48E-07	1.01E-07	1.91E-06	1.70E-04	2.90E-05	6.50E-03	2.07E-06	4.18E-07	3.99E-05
25.000	7.92E-07	1.08E-07	1.88E-06	1.65E-04	2.98E-05	6.50E-03	2.19E-06	4.63E-07	4.05E-05
26.000	8.37E-07	1.15E-07	1.85E-06	1.61E-04	3.07E-05	6.49E-03	2.31E-06	5.10E-07	4.10E-05
27.391	9.00E-07	1.26E-07	1.82E-06	1.54E-04	3.17E-05	6.49E-03	2.49E-06	5.81E-07	4.16E-05
30.000	1.02E-06	1.47E-07	1.75E-06	1.42E-04	3.36E-05	6.47E-03	2.82E-06	7.24E-07	4.22E-05
50.000	1.90E-06	3.36E-07	1.28E-06	7.00E-05	4.34E-05	6.37E-03	5.38E-06	2.43E-06	4.27E-05
52.148	1.99E-06	3.57E-07	1.23E-06	6.41E-05	4.40E-05	6.36E-03	5.63E-06	2.67E-06	4.24E-05

Table A-16. Sample of Results (Number Density Vs Burnup), Cont.

BURNUP	NUCLIDE 94240	NUCLIDE 94241	NUCLIDE 94242	NUCLIDE 95241	NUCLIDE 95242	NUCLIDE 95243	NUCLIDE 47109	NUCLIDE 7300	NUCLIDE 7301
	Pu-240	Pu-241	Pu-242	Am-241	Am-242m	Am-243	Ag-109	Gd	Gd
GWd/mtU	at/barn-cm	at/barn-cm	at/barn-cm	at/barn-cm	at/barn-cm	at/barn-cm	at/barn-cm	at/barn-cm	at/barn-cm
0.000	0	0	0	0	0	0	0	1.20E-06	0
0.125	2.78E-10	1.22E-12	6.13E-16	1.33E-16	2.04E-20	2.59E-19	4.19E-10	1.16E-06	0
0.250	1.80E-09	1.69E-11	1.75E-14	3.79E-15	1.19E-18	1.54E-17	8.65E-10	1.12E-06	0
0.375	4.99E-09	7.25E-11	1.15E-13	2.50E-14	1.19E-17	1.55E-16	1.34E-09	1.08E-06	0
0.500	9.94E-09	1.97E-10	4.27E-13	9.23E-14	5.93E-17	7.79E-16	1.85E-09	1.04E-06	0
0.625	1.66E-08	4.21E-10	1.15E-12	2.50E-13	2.02E-16	2.67E-15	2.40E-09	1.01E-06	0
0.750	2.50E-08	7.72E-10	2.57E-12	5.56E-13	5.40E-16	7.22E-15	2.98E-09	9.70E-07	0
0.875	3.51E-08	1.28E-09	5.02E-12	1.09E-12	1.23E-15	1.66E-14	3.60E-09	9.34E-07	0
1.000	4.68E-08	1.96E-09	8.89E-12	1.92E-12	2.49E-15	3.39E-14	4.25E-09	8.99E-07	0
1.250	7.47E-08	3.98E-09	2.28E-11	4.94E-12	7.98E-15	1.10E-13	5.65E-09	8.31E-07	0
1.500	1.08E-07	6.99E-09	4.87E-11	1.05E-11	2.03E-14	2.85E-13	7.18E-09	7.64E-07	0
1.750	1.48E-07	1.12E-08	9.15E-11	1.98E-11	4.43E-14	6.32E-13	8.84E-09	7.01E-07	0
2.000	1.92E-07	1.67E-08	1.57E-10	3.40E-11	8.61E-14	1.25E-12	1.06E-08	6.40E-07	0
2.250	2.41E-07	2.36E-08	2.52E-10	5.44E-11	1.54E-13	2.27E-12	1.25E-08	5.83E-07	0
2.500	2.94E-07	3.20E-08	3.83E-10	8.26E-11	2.57E-13	3.86E-12	1.45E-08	5.28E-07	0
2.750	3.52E-07	4.21E-08	5.57E-10	1.20E-10	4.07E-13	6.21E-12	1.66E-08	4.76E-07	0
3.000	4.13E-07	5.39E-08	7.82E-10	1.68E-10	6.17E-13	9.57E-12	1.89E-08	4.27E-07	0
3.250	4.78E-07	6.75E-08	1.07E-09	2.29E-10	9.02E-13	1.42E-11	2.12E-08	3.82E-07	0
3.500	5.47E-07	8.29E-08	1.42E-09	3.04E-10	1.28E-12	2.04E-11	2.36E-08	3.39E-07	0
3.750	6.18E-07	1.00E-07	1.84E-09	3.95E-10	1.76E-12	2.86E-11	2.62E-08	3.00E-07	0
4.000	6.93E-07	1.19E-07	2.35E-09	5.04E-10	2.37E-12	3.91E-11	2.88E-08	2.63E-07	0
4.250	7.70E-07	1.40E-07	2.95E-09	6.32E-10	3.12E-12	5.24E-11	3.15E-08	2.30E-07	0
4.500	8.51E-07	1.63E-07	3.65E-09	7.81E-10	4.04E-12	6.89E-11	3.43E-08	1.99E-07	0
4.750	9.33E-07	1.88E-07	4.46E-09	9.53E-10	5.15E-12	8.92E-11	3.72E-08	1.72E-07	0
5.000	1.02E-06	2.15E-07	5.39E-09	1.15E-09	6.47E-12	1.14E-10	4.03E-08	1.47E-07	0
5.250	1.11E-06	2.44E-07	6.44E-09	1.37E-09	8.03E-12	1.43E-10	4.33E-08	1.25E-07	0
5.500	1.19E-06	2.75E-07	7.63E-09	1.62E-09	9.85E-12	1.79E-10	4.65E-08	1.06E-07	0
5.750	1.29E-06	3.07E-07	8.96E-09	1.90E-09	1.19E-11	2.20E-10	4.98E-08	8.86E-08	0
6.000	1.38E-06	3.42E-07	1.04E-08	2.21E-09	1.44E-11	2.68E-10	5.31E-08	7.38E-08	0
6.250	1.47E-06	3.78E-07	1.21E-08	2.55E-09	1.71E-11	3.24E-10	5.66E-08	6.09E-08	0
6.500	1.57E-06	4.16E-07	1.39E-08	2.93E-09	2.02E-11	3.89E-10	6.01E-08	4.99E-08	0
6.750	1.67E-06	4.56E-07	1.59E-08	3.34E-09	2.37E-11	4.63E-10	6.37E-08	4.05E-08	0
7.000	1.77E-06	4.98E-07	1.80E-08	3.79E-09	2.76E-11	5.48E-10	6.73E-08	3.24E-08	0
7.500	1.97E-06	5.88E-07	2.29E-08	4.80E-09	3.67E-11	7.51E-10	7.49E-08	2.05E-08	0
8.000	2.18E-06	6.83E-07	2.86E-08	5.97E-09	4.77E-11	1.01E-09	8.28E-08	1.20E-08	0
8.500	2.39E-06	7.85E-07	3.52E-08	7.31E-09	6.09E-11	1.32E-09	9.09E-08	6.55E-09	0
9.000	2.61E-06	8.93E-07	4.27E-08	8.83E-09	7.64E-11	1.71E-09	9.93E-08	3.19E-09	0
9.500	2.83E-06	1.01E-06	5.12E-08	1.05E-08	9.43E-11	2.17E-09	1.08E-07	1.36E-09	0
10.000	3.05E-06	1.13E-06	6.07E-08	1.24E-08	1.15E-10	2.73E-09	1.17E-07	4.95E-10	0
10.500	3.28E-06	1.25E-06	7.12E-08	1.45E-08	1.38E-10	3.38E-09	1.26E-07	1.41E-10	0
11.000	3.51E-06	1.38E-06	8.29E-08	1.68E-08	1.65E-10	4.14E-09	1.36E-07	2.98E-11	0
11.500	3.74E-06	1.51E-06	9.57E-08	1.93E-08	1.94E-10	5.02E-09	1.45E-07	4.50E-12	0
12.000	3.97E-06	1.65E-06	1.10E-07	2.20E-08	2.27E-10	6.04E-09	1.55E-07	4.84E-13	0
12.500	4.20E-06	1.79E-06	1.25E-07	2.48E-08	2.63E-10	7.19E-09	1.66E-07	3.87E-14	0
13.000	4.44E-06	1.94E-06	1.41E-07	2.79E-08	3.02E-10	8.50E-09	1.76E-07	2.46E-15	0
13.500	4.68E-06	2.09E-06	1.59E-07	3.13E-08	3.45E-10	9.98E-09	1.87E-07	1.33E-16	0
14.000	4.92E-06	2.24E-06	1.78E-07	3.48E-08	3.91E-10	1.16E-08	1.98E-07	6.49E-18	0
14.500	5.16E-06	2.40E-06	1.98E-07	3.85E-08	4.40E-10	1.35E-08	2.09E-07	2.81E-19	0

Table A-16. Sample of Results (Number Density Vs Burnup), Cont.

BURNUP	NUCLIDE 94240	NUCLIDE 94241	NUCLIDE 94242	NUCLIDE 95241	NUCLIDE 95242	NUCLIDE 95243	NUCLIDE 47109	NUCLIDE 7300	NUCLIDE 7301
	Pu-240	Pu-241	Pu-242	Am-241	Am-242m	Am-243	Ag-109	Gd	Gd
GWd/mtU	at/barn-cm	at/barn-cm	at/barn-cm	at/barn-cm	at/barn-cm	at/barn-cm	at/barn-cm	at/barn-cm	at/barn-cm
15.000	5.40E-06	2.55E-06	2.20E-07	4.24E-08	4.94E-10	1.55E-08	2.20E-07	1.03E-20	0
15.500	5.64E-06	2.71E-06	2.43E-07	4.66E-08	5.50E-10	1.78E-08	2.31E-07	3.95E-22	0
16.000	5.88E-06	2.88E-06	2.67E-07	5.09E-08	6.11E-10	2.03E-08	2.43E-07	1.38E-23	0
16.500	6.13E-06	3.04E-06	2.93E-07	5.54E-08	6.75E-10	2.30E-08	2.55E-07	4.85E-25	0
17.000	6.37E-06	3.20E-06	3.20E-07	6.01E-08	7.42E-10	2.60E-08	2.67E-07	1.64E-26	0
17.500	6.61E-06	3.37E-06	3.48E-07	6.51E-08	8.13E-10	2.93E-08	2.79E-07	5.42E-28	0
18.000	6.85E-06	3.54E-06	3.78E-07	7.02E-08	8.87E-10	3.28E-08	2.92E-07	1.78E-29	0
18.500	7.10E-06	3.71E-06	4.10E-07	7.54E-08	9.65E-10	3.67E-08	3.04E-07	5.55E-31	0
19.000	7.34E-06	3.88E-06	4.42E-07	8.09E-08	1.05E-09	4.08E-08	3.17E-07	1.73E-32	0
19.500	7.58E-06	4.05E-06	4.77E-07	8.65E-08	1.13E-09	4.53E-08	3.30E-07	5.98E-33	0
20.000	7.83E-06	4.22E-06	5.12E-07	9.23E-08	1.22E-09	5.00E-08	3.43E-07	5.98E-33	0
21.000	8.30E-06	4.57E-06	5.88E-07	1.04E-07	1.40E-09	6.07E-08	3.69E-07	5.98E-33	0
22.000	8.79E-06	4.91E-06	6.69E-07	1.17E-07	1.60E-09	7.28E-08	3.96E-07	5.98E-33	0
23.000	9.26E-06	5.26E-06	7.57E-07	1.30E-07	1.81E-09	8.65E-08	4.24E-07	5.98E-33	0
24.000	9.74E-06	5.60E-06	8.49E-07	1.44E-07	2.03E-09	1.02E-07	4.52E-07	5.98E-33	0
25.000	1.02E-05	5.94E-06	9.48E-07	1.58E-07	2.25E-09	1.19E-07	4.81E-07	5.98E-33	0
26.000	1.07E-05	6.28E-06	1.05E-06	1.73E-07	2.49E-09	1.38E-07	5.10E-07	5.98E-33	0
27.391	1.13E-05	6.75E-06	1.21E-06	1.93E-07	2.83E-09	1.68E-07	5.51E-07	5.98E-33	0
30.000	1.25E-05	7.56E-06	1.53E-06	2.34E-07	3.43E-09	2.33E-07	6.31E-07	5.98E-33	0
50.000	1.94E-05	1.22E-05	4.95E-06	4.97E-07	7.74E-09	1.31E-06	1.27E-06	5.98E-33	0
52.148	2.00E-05	1.24E-05	5.39E-06	5.14E-07	7.97E-09	1.49E-06	1.33E-06	5.98E-33	0

REFERENCES

Punatar, M.K. 2001. *Summary Report of Commercial Reactor Criticality Data for Crystal River Unit 3.* TDR-UDC-NU-000001 REV 02. Las Vegas, Nevada: Bechtel SAIC Company. ACC: MOL.20010702.0087.

Wimmer, L.B. 2001. *Summary Report of Commercial Reactor Criticality Data for Three Mile Island Unit 1.* TDR-UDC-NU-000004 REV 01. Las Vegas, Nevada: Bechtel SAIC Company. ACC: MOL.20010921.0047.

MO0204SPAIRB04.013. Integral and Removable Burnable Absorber Study. Submittal date: 04/19/2002.

INTENTIONALLY LEFT BLANK